

DISS. ETH NO. 25587

**DISSECTION OF AN INDUCIBLE DEFENSE OF MULTICELLULAR
FUNGI AGAINST ANIMAL PREDATORS AND BACTERIAL
COMPETITORS**

A thesis submitted to attain the degree of DOCTOR OF SCIENCES
of ETH ZURICH
(Dr. sc. ETH Zurich)

presented by
Annageldi Tayyrov
MSc, King Abdullah University of Science and Technology

born on 07.02.1991
citizen of Türkmenistan

accepted on the recommendation of
Prof. Dr. Markus Aebi
Prof. Dr. Markus Künzler
Prof. Dr. Julia Vorholt
Prof. Dr. Robin A. Ohm

2018

Acknowledgments

Many people have contributed to the development and completion of this doctoral thesis. First of all, I would like to thank my supervisors Prof. Dr. Markus Künzler and Prof. Dr. Markus Aebi for giving me an opportunity to perform this Ph.D. work in a stimulating and inspiring scientific environment. I am deeply grateful for their continued support and invaluable advice throughout all stages of this thesis.

I want to express my sincere gratitude to Dr. Stefanie Schmieder for introducing me into the fungal world and teaching me many techniques during the first year of my Ph.D.

I am truly thankful to my Ph.D. committee, Prof. Dr. Julia Vorholt and Prof. Dr. Robin A. Ohm for their helpful advice and fruitful discussions during my Ph.D.

I was fortunate to supervise three excellent Master students during my Ph.D. I want to thank Aleksandr Goryachkin and Philipp Schächle for doing a great job during their semester thesis. I am especially grateful to Sophie Azevedo for her enthusiastic and fruitful work during her Master's thesis.

Furthermore, I would like to thank our scientific collaborators, in particular, Dr. Claire Stanley from Agroscope, Prof. Dr. Peter Lüthy from the Institute of Microbiology (ETHZ), Chunyue Wei and Prof. Dr. Laura Nyström from Department of Health Sciences and Technology (ETHZ), Robert Herzog and Dr. Florian Hennicke from Senckenberg Biodiversity and Climate Research Centre (SBiK-F) and Prof. Dr. Ute Krengel from the University of Oslo for their contributions to my PhD projects.

I am also grateful to the past and present members of the Aebi Lab for creating a friendly and supportive environment inside and outside of the lab.

I want to thank Prof. Dr. Nikolaus Amrhein for his stimulating scientific and non-scientific discussions during my last four years at the Institute of Microbiology.

Finally, my deepest gratitude goes to my parents, sisters, and fiancée for their constant support and love.

TABLE OF CONTENTS

Summary.....	i
Zusammenfassung.....	iii
Chapter 1.....	1
Introduction	
Chapter 2.....	25
Combining microfluidics and RNA-sequencing to assess the inducible defensome of a mushroom against nematodes	
Chapter 3.....	59
Inducible cytoplasmic lipases - as a novel class of fungal defense proteins against Nematodes	
Chapter 4.....	89
Functional characterization of ageritin, a novel type of ribotoxin from the mushroom <i>Agrocybe aegerita</i>	
Chapter 5.....	127
Toxicity of potential fungal defense proteins towards the fungivorous nematodes <i>Aphelenchus avenae</i> and <i>Bursaphelenchus okinawaensis</i>	
Chapter 6.....	153
Induction of antibacterial proteins and peptides in the coprophilous mushroom <i>Coprinopsis cinerea</i> in response to bacteria	
Chapter 7.....	199
Concluding remarks and future perspectives	
Curriculum Vitae.....	209

Summary

Fungi produce a variety of toxic proteins to protect themselves against predation and nutrient competition of antagonistic organisms. The aim of this doctoral thesis was to expand our current understanding of the different aspects of the fungal defense system with a special focus on the identification and characterization of novel defense proteins from multicellular fungi.

Chapter 1 reviews already known fungal and bacterial defense proteins with a focus on three different classes: lipase toxins, pore-forming toxins, and ribotoxins.

Chapter 2 presents the RNA-seq-based overall defense response of the dung-inhabiting basidiomycete *Coprinopsis cinerea* towards the fungivorous nematode *Aphelenchus avenae*. A microfluidics device was used as a novel approach to perform the fungal-nematode challenge in a confined confrontation area. With the help of this device, the induced part of the mycelia was precisely extracted from the confrontation zone. One of the genes that was found to be significantly upregulated in the mycelia of *C. cinerea* upon nematode feeding was expressed in *Escherichia coli*, and its toxicity was assessed against six different nematode species. In addition, the microbiome of *A. avenae* was profiled using targeted 16S rRNA deep sequencing.

Chapter 3 characterizes two of the nematode-induced genes coding for proteins with lipase domains that were identified in the transcriptomics study described in chapter two. Namely, the CLT1 and CLT2 proteins were heterologously expressed in *E. coli*, and their toxicity spectrum was assessed against several nematode species, as well as *Aedes aegypti* larvae. The *in vitro* lipase activities of the toxic proteins were demonstrated using synthetic lipid substrates. Through site-directed mutagenesis of the predicted catalytic sites, the importance of a functional lipase domain for the toxicity of CLT1 and CLT2 was proven.

In Chapter 4, a novel type of ribotoxin called ageritin was studied. This ribotoxin was identified in the edible mushroom *Agrocybe aegerita* based on its published N-terminal sequence and exclusive access to the *A. aegerita* genome sequence. Its sequence has no homology with the sequences of the previously known ribotoxins. Ageritin was expressed in *E. coli*, and its insecticidal activity against *A. aegypti* mosquito larvae and Sf21 insect cells was demonstrated. Further, ageritin was purified on Ni-NTA columns, and its ribonucleolytic activity against ribosomes in rabbit reticulocyte lysate was demonstrated. By introducing point mutations in conserved residues, the correlation between the *in vivo* insecticidal activity and *in vitro* ribonucleolytic activity of ageritin was confirmed.

Chapter 5 describes a novel system for the heterologous expression of potential fungal defense proteins. This expression system makes it possible to test the toxicity of a fungal protein against

fungivorous nematodes. The filamentous yeast *Ashbya gossypii* was established as a host fungus to individually express fungal toxins and test their activities against the fungivorous nematodes *A. avenae* and *Bursaphelenchus okinawaensis*. The results indicated that *A. gossypii* is an excellent host for the expression of toxic proteins. The toxicity results obtained for the fungivorous nematodes were similar to the previously obtained toxicity results for toxins tested against bacterivorous nematodes; this indicates conservation of the target sites of these toxins across different feeding groups of nematodes.

In Chapter 6, transcriptomics analysis of *C. cinerea* mycelium challenged with either *Bacillus subtilis* or *E. coli* was performed. A family of induced lysozymes and defensin-like proteins (DLPs) were more closely investigated. In addition, an inducible paralog (CCP2) of copsin, an antibacterial protein, was discovered. The antibacterial activity of CCP2 and induced lysozymes against a range of gram-positive bacteria was demonstrated.

The final chapter presents the conclusions of the thesis and outlines potential lines of future research on the protein-based defense system of fungi.

Zusammenfassung

Pilze produzieren eine Vielzahl von toxischen Proteinen, um sich gegen die Prädation und die Nährstoffkonkurrenz von antagonistischen Organismen zu schützen. Ziel dieser Doktorarbeit war es, unser Verständnis der verschiedenen Aspekte des Pilzabwehrsystems zu erweitern. Die Arbeit konzentrierte sich dabei auf die Identifizierung und Charakterisierung neuartiger Abwehrproteine aus multizellulären Pilzen.

In Kapitel eins werden die bereits bekannten pilzlichen und bakteriellen Abwehrproteine mit Fokus auf drei verschiedene Klassen beschrieben: Lipase-Toxine, porenbildende Toxine und Ribotoxine. Die in dieser Arbeit identifizierten und charakterisierten Abwehrproteine gehören zu diesen Typen.

Im zweiten Kapitel wird die RNA-seq-basierte Abwehrreaktion des Dung-bewohnenden Basidiomyceten *Coprinopsis cinerea* gegen den pilzfressenden Nematoden *Aphelenchus avenae* vorgestellt. Eine mikrofluidische Vorrichtung wurde dabei als ein neuer Ansatz zur Konfrontation des Pilzes mit den Nematoden verwendet. Mit Hilfe dieses Ansatzes wurde nur der induzierte Teil der Mycelien aus der Konfrontationszone extrahiert. Eines der Gene, dass in den Mycelien von *C. cinerea* nach Nematodenfütterung signifikant hochreguliert war, wurde in *Escherichia coli* exprimiert, und seine Toxizität gegen sechs verschiedene Nematodenarten ermittelt. Zusätzlich wurde das Mikrobiom von *A. avenae* unter Verwendung von 16S-rRNA-Sequenzierung aufgeklärt.

In Kapitel drei werden zwei der Nematoden-induzierten Gene mit für Lipase-Domänen kodierenden Sequenzen charakterisiert, die in der in Kapitel zwei beschriebenen Transkriptom-Studie identifiziert wurden. Die CLT1- und CLT2-Proteine wurden in *E. coli* heterolog exprimiert und ihr Toxizitätsspektrum wurde gegen verschiedene Nematodenarten sowie gegen *Aedes aegypti*-Larven ermittelt. Die *in-vitro*-Lipaseaktivitäten der toxischen Proteine wurden unter Verwendung synthetischer Lipidsubstrate demonstriert. Durch zielgerichtete Mutagenese der vorhergesagten katalytischen Stellen wurde die Bedeutung einer funktionellen Lipase-Domäne für die Toxizität von CLT1 und CLT2 nachgewiesen.

Eine neue Art von Ribotoxin namens Ageritin wurde im vierten Kapitel untersucht. Dieses Ribotoxin wurde in dem essbaren Pilz *Agrocybe aegerita* identifiziert und seine Sequenz weist keine Homologie mit den Sequenzen der früher bekannten Ribotoxine auf. Ageritin wurde in *E. coli* exprimiert und seine insektizide Aktivität gegen *A. aegypti*-Mückenlarven und Sf21-Insektenzellen demonstriert. Ferner wurde Ageritin an Ni-NTA-Säulen aufgereinigt und seine ribonukleolytische Aktivität gegen Ribosomen in Kaninchen-Retikulozyten-Lysat demonstriert. Durch Einführung von Punktmutationen in konservierten Resten wurde die Korrelation zwischen der *in-vivo*-insektiziden und der *in-vitro*-ribonukleolytischen Aktivität von Ageritin bestätigt.

Das fünfte Kapitel beschreibt ein neues System für die heterologe Expression von potentiellen Pilzabwehrproteinen. Dieses Expressionssystem ermöglicht es, die Toxizität eines Pilzproteins gegen fungivore Nematoden zu testen. Die filamentöse Hefe *Ashbya gossypii* wurde als Wirtspilz etabliert, um Pilzgifte individuell zu exprimieren und ihre Aktivitäten gegen die fungivoren Nematoden *A. avenae* und *Bursaphelenchus okinawaensis* zu testen. Die Ergebnisse zeigten, dass *A. gossypii* ein ausgezeichneter Wirt für die Expression von toxischen Proteinen ist. Die für die fungivoren Nematoden ermittelten Toxizitätsergebnisse waren ähnlich den zuvor erhaltenen Toxizitätsergebnissen gegen bakteriovore Nematoden; dies weist auf eine mögliche Konservierung der Zielstrukturen dieser Toxine in beiden Nematodengruppen hin.

In Kapitel sechs wurde eine Transkriptomanalyse von *C. cinerea*-Myzel durchgeführt, das entweder mit *Bacillus subtilis* oder *E. coli* konfrontiert wurde. Eine Familie von Lysozymen und defensinähnlichen Proteinen (DLPs) wurde genauer untersucht. Außerdem wurde ein induzierbares Paralog (CCP2) von Copsin, einem antibakteriellen Protein, entdeckt. Die antibakterielle Aktivität von CCP2 und induzierten Lysozymen gegen eine Reihe von Gram-positiven Bakterien wurde demonstriert.

Das abschließende Kapitel stellt die Schlussfolgerungen der Arbeit vor und skizziert mögliche zukünftige Stossrichtungen zur Erforschung des proteinbasierten Abwehrsystems von Pilzen.

Chapter 1

Introduction

Chapter 1

1. Fungi and their environment

The kingdom Fungi comprises a diverse group of unicellular and multicellular eukaryotic organisms including mushrooms, molds, yeasts, and lichens [1]. These heterotrophic organisms are found in almost all habitats [2]. The omnipresence of fungi implies that they are exposed to predators, competitors, pathogens, and symbionts through a diverse spectrum of interactions ranging from mutualistic to antagonistic interactions [3, 4]. Mycorrhiza and lichen are two well-known examples of fungal mutualists that live in symbiosis with plants and algae, respectively [5, 6]. The main topic of this thesis is fungal antagonistic interactions, particularly the interactions of fungi with their predators and competitors, which belong to the animal and eubacteria kingdoms, respectively [7].

Higher fungi, i.e., ascomycetes and basidiomycetes, are composed of two major structures called the fruiting body and the vegetative mycelium. The fruiting body is the short-living sexual reproductive part of a fungus. On account of its high importance for the propagation of a fungus, it contains rich reservoirs of constitutively expressed fungal defense proteins [8-10]. On the other hand, the fungal vegetative mycelium is consisting network of filaments called hyphae. Via this network, fungi secrete digestive enzymes and absorb digested products from the environment [11, 12]. The lack of motility, the large area of their habitats and a high content of valuable nutrients such as nitrogen and phosphate [3] make fungal mycelium attractive for a wide spectrum of fungivorous soil microorganisms such as nematodes, insects, and mites [13, 14].

Fungi have three main defense mechanisms to protect themselves against their antagonists. Physical barriers such as the cell wall [15] and the melanized outer layer [16] constitute the first line of defense against both biotic and abiotic stresses. Secondary metabolites such as penicillin, aflatoxins, gliotoxins are the second line of the fungal defense system [17]. Fungal secondary metabolites have been extensively reviewed previously [18-23]. This thesis deals with the third line of fungal defense strategy, comprising fungal defense proteins and peptides [7, 10]. This introduction is limited to three types of toxins (lipase toxins, pore-forming toxins, and ribotoxins), as the defense proteins studied in this thesis are of these three types. For information about the other types of fungal defense proteins, such as biotin-binding proteins [24], protease inhibitors [10, 25], antibacterial proteins [26], and lectins [27], readers may use the cited articles.

Chapter 1

1.1. Lipase toxins

Lipids are biological molecules with amphipathic to hydrophobic properties that make them exclusively soluble in organic solvents [28]. Together with carbohydrates, nucleic acids, and proteins, they make up the main component of living cells. The two main classical roles of lipids are their structural role in biological membranes and energy storage. However, recent studies have shown a multitude of other essential functions of lipids in cellular signaling [29, 30], membrane trafficking [31], and interaction with other organisms [32]. This diversity of essential functions makes lipids an ideal target for pathogens. In fact, lipids play numerous important roles at various stages of host-pathogen interaction, from the recognition to the propagation of pathogens [33]. Due to technical limitations in the analysis of the complexity of the lipidome, the field of lipidology had been advancing slowly until very recently. With recent developments in mass spectrometry-based techniques, it has become easier to perform lipidomic analysis at the individual lipid species level [34]. Such technological developments will greatly aid in understanding the alterations in the fatty acid composition of host cell lipids, as well as the specific roles of individual lipid species [35].

Lipases are esterase enzymes that hydrolyze acyl ester bond-containing lipid substrates, and as a result, liberate one or more fatty acids from an alcohol backbone [36]. Until recently, lipases had received attention for their industrial applications, as they are the most widely used class of enzymes in biotechnological applications in the food industry, oil industry, textile industry, detergent industry, cosmetics industry and more [37]. It is beyond the scope of this thesis to describe the details of the industrial applications of lipases, but this topic is covered by many review articles [38-46].

The focus of this thesis is on the role of lipases as an effector protein in host-pathogen interactions. As a number of studies have shown, pathogenic microorganisms tackle the lipidome in their hosts with the help of lipases [32, 47]. There are several ways by which pathogens can modify the lipid composition of host cells. One way is to modulate the uptake of fatty acids in host cells from the environment, as observed in the case of the enteropathogenic *E. coli* [48]. The second way by which pathogens use lipases to attack host cells is by modifying the lipid composition of host cells via altering the expression of specific enzymes that are involved in fatty acid synthesis. For example, it has been shown that a certain amount of the host cell's acetyl-CoA carboxylase is required for *Mycobacterium fortuitum* infection [49]. Further, inhibition of fatty acid synthesis enzymes of a host cell inhibits the replication of several viral particles [50]. Finally, the third and the most common way for pathogens to modulate the lipid composition of host cells is through the direct action of their lipolytic enzymes, i.e., phospholipases and lipases, on the lipidome of host cells [47, 51-53].

Chapter 1

Phospholipases, a lipase subclass, cleave one or more ester bonds in glycerophospholipid molecules to release a variety of molecules including free fatty acids (FFA), phosphatidic acid, phosphoinositides and secondary messengers such as lysophospholipids (LPL) and diacylglycerols (DAG) [54]. Hence, phospholipases are involved in several cellular processes, including modification of cellular membranes and cell signaling pathways. Phospholipases are classified into five subclasses, A (PLA), A2 (PLA2), B (PLB), C (PLC), and D (PLD), based on the position at which they act within phospholipids (Figure 1). Several bacterial and viral phospholipases have been shown to play an essential role in pathogenic infection by modifying the fatty acid composition of the host cell to their advantage [47]. The main role of phospholipase in host-pathogen interactions is to facilitate the entry of the pathogens into the host by causing damage to the host cell membrane. Pathogenic bacteria and viruses also secrete phospholipases that are involved in the acquisition of fatty acids for energy production or complex lipid synthesis and in the regulation of host immune response by modifying certain factors in immune signaling pathways [55-57]. For instance, many pathogens cannot synthesize sphingolipids themselves and often utilize host sphingolipids for their metabolism [58, 59].

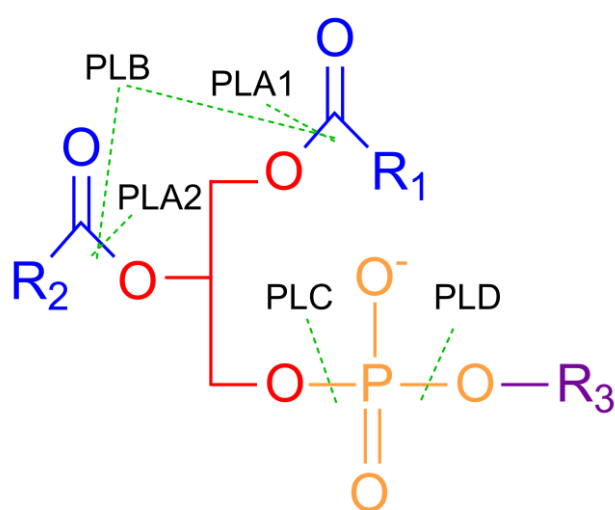


Figure 1. Nomenclature of phospholipases based on their cleavage sites

Phospholipase A1 (PLA1) and phospholipase A2 (PLA2) hydrolyze the carboxylester bonds at the sn-1 and sn-2 positions, respectively, releasing FFA and LPL. A phospholipase that has both PLA1 and PLA2 activities is called phospholipase B (PLB). In contrast, phospholipase C (PLC) and phospholipase D (PLD) act on the glycerol-oriented and the alcohol-oriented phosphoester linkages, respectively. R1 and R2: fatty acid residues, R3: alcohol residue.

Exotoxin U (ExoU), an effector protein of *Pseudomonas aeruginosa*, is one of the best-studied examples of phospholipases that aid the invasion of pathogens into host cells [56, 60]. ExoU is a cytotoxic protein with phospholipase A2 (PLA2) activity that is directly delivered into the host cell cytosol via the type-III secretion system (T3SS) and induces acute cell death via destroying cellular lipid membranes [61]. In addition to bacteria and viruses, the protozoan parasites *Cryptosporidium parvum* [62] and *Toxoplasma gondii* [63, 64] also secrete PLA2 effectors to facilitate host cell invasion.

Lipolytic enzymes have been postulated to contribute to the virulence of pathogenic fungi. For example, the roles of lipases and phospholipases have been extensively studied in the virulence of

Candida albicans [65, 66]. In a number of studies, these enzymes have shown to facilitate morphological transition, colonization, and penetration of *C. albicans* into the host. *Cryptococcus neoformans*, another opportunist pathogenic fungus, secretes phospholipase B in order to breach and invade human epithelial cells [67]. The possible roles of the microbial lipolytic enzymes are given in Figure 2.

Thus, lipases have been mainly studied as virulence factors promoting survival and reproduction of pathogenic microorganisms rather than as defense proteins of this organism to protect them from predators. However, in plants, lipid acyl hydrolase (LAH) has been reported to be a part of their inducible defense system against microbial attacks [68]. In Chapter 3, inducible fungal defense proteins with functional lipase domain are proposed as a novel type of fungal defense proteins.

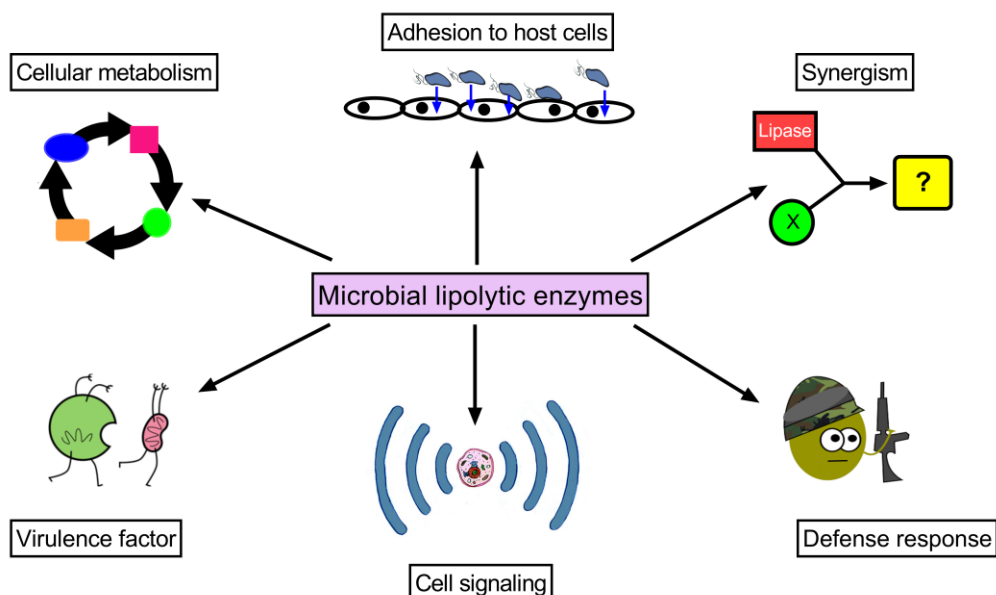


Figure 2: Roles of microbial lipolytic enzymes

Cellular metabolism: Lipases perform several essential functions in the growth and survival of microorganisms. **Adhesion:** Lipolytic enzymes release free fatty acids that could support the interactions of a pathogenic microorganism with their host cells. **Synergism:** Lipases co-operate with other cellular enzymes or molecules to promote or redirect the original function of these molecules. **Defense response:** Microorganisms secrete lipolytic enzymes to defend themselves against their antagonists. **Cell signaling:** Lipolytic enzymes and their enzymatic products modulate several cellular signaling pathways, particularly in the immune system, to coordinate processes such as inflammatory responses. **Virulence:** Several pathogenic microorganisms excrete lipases as a virulence factor to promote their infection and dissemination within host cells. Modified from [69].

1.2 Pore-forming toxins

Pore-forming toxins (PFTs) constitute a major class of pore-forming proteins (PFPs) expressed by many pathogenic microorganisms as a virulence factor [70]. PFPs form a very ancient protein family that is conserved among the three kingdoms of life [71]. PFTs form transmembrane pores in their target cell membranes, thus altering cell membrane permeability, and eventually leading to the malfunction and death of the target cells [72]. Pore formation occurs through the following steps: (a) secretion of the toxic protein as water-soluble monomers, (b) binding of the protein to target cells via specific membrane receptors, (c) assembly of monomers either on the surface or within the target plasma membrane, and (d) insertion of the oligomerized pore-complex into the target membrane (Figure 3) [71]. The most common classification of PFTs is based on the secondary structure of their membrane-spanning elements: α -PFTs use alpha helices to form pores, and β -PFTs are rich in beta sheets and form β -barrel pores [73, 74].

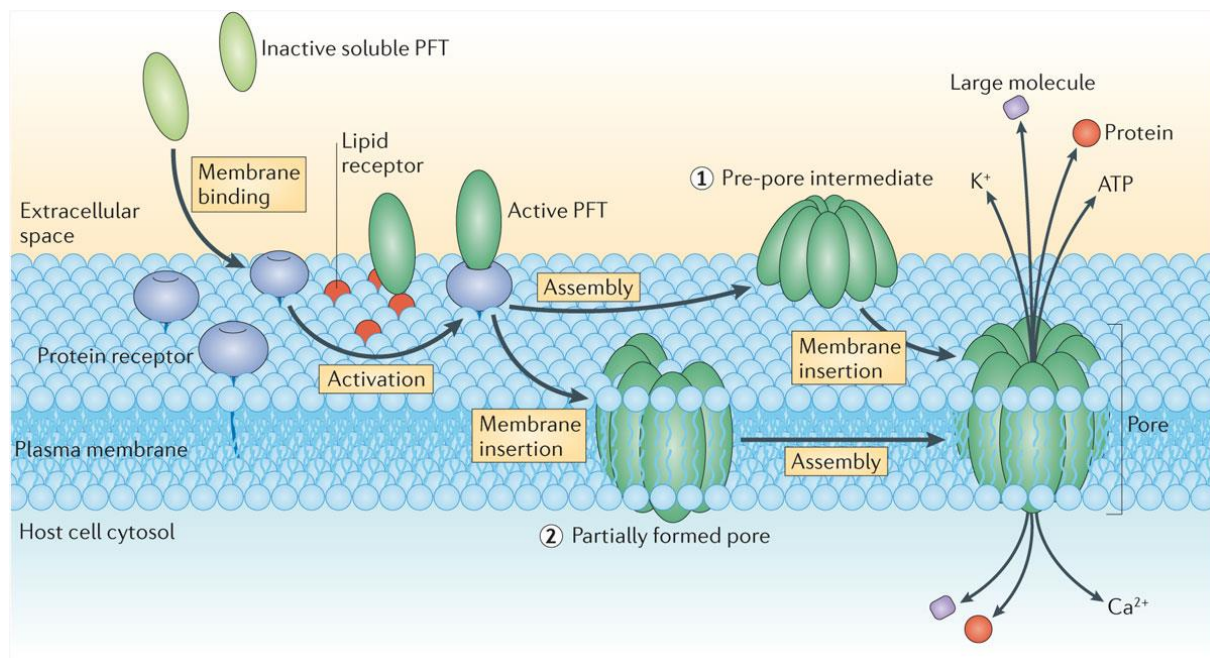


Figure 3: Molecular mechanisms of pore formation by PFTs

In the first step, soluble PFTs bind to the host membrane via toxin-specific receptors. Upon membrane binding, individual toxin monomers are activated and start to concentrate and form an oligomer. In the case of β -PFTs, assembly of monomers happens at the membrane surface, producing an intermediate pre-pore structure (pathway 1). This structure undergoes conformational rearrangements to form a fully functional membrane pore. In contrast, many α -PFT monomers are directly inserted into the membrane sequentially, forming an active transmembrane pore (pathway 2). Taken from [71].

Chapter 1

1.2.1 α -PFTs

α -PFTs are grouped into three subclasses: colicins, cytolsin A (ClyA) and actinoporins.

1.2.1.1 Colicins

The first member of the colicin family was discovered in *E. coli*, and this is also the reason why it was named colicin [75]. Many studies have demonstrated the importance of colicins in the self-defense mechanism of bacteria against other bacterial competitors and their contribution to bacterial growth and colonization [76]. Pore-forming colicins create nonspecific voltage-gated channels by inserting their hydrophobic α -helical hairpin into the target membrane. These pores modify cellular behavior by membrane depolarization, ion imbalance and ATP outflow, leading to death of the target cell [77]. Several other pore-forming toxins with the colicin fold have been discovered. For example, the diphtheria toxin secreted by *Corynebacterium diphtheriae* has a colicin fold in its translocation domain to translocate the toxin across the target membrane [78]. Furthermore, the pore-forming Cry toxins produced by *Bacillus thuringiensis* also have the colicin fold to facilitate their membrane translocation [79].

1.2.1.2 Cytolsin A

The second subclass of α -PFTs is the ClyA family. The toxins of this family are produced by certain strains of the bacterial species *E. coli*, *Salmonella enterica*, *Shigella flexneri* and *Bacillus cereus* [80]. ClyA has a fully elucidated structure of both the soluble and transmembrane form [81]. The structure exhibits unique conformational changes that occur during the pore-formation process of the ClyA family of PFTs. The toxin monomers are bound and inserted into the membrane until a fully functional oligomer containing 12 monomer units is formed [82, 83].

1.2.1.3 Actinoporins

In contrast to the previous two groups of PFTs that are mainly produced by bacteria, actinoporins are primarily produced by eukaryotic organisms called sea anemones as part of their venom [84]. Actinoporins aid in both preying by paralyzing prey and defending the anemones from predators. The radiographic structures of several actinoporins have been shown, including equinatoxin-II of *Actinia equina* [85], sticholysin-II of *Stichodactyla helianthus* [86] and fragaceatoxin-C of *Actinia fragacea* [87]. The structures reveal that actinoporins are composed of a β -sandwich flanked by two α -helices, and

Chapter 1

that the N-terminal helix is responsible for insertion into the target membrane [84]. This insertion is dependent on the enrichment of certain lipid species in the target membranes, such as sphingomyelins [88]. These lipids are believed to be involved in the arrangement and assembly of monomers in the formation of the actinoporin pores. The fully functional pores can form oligomers of four (equinatoxin-II and sticholysin-II) [86, 89] or nine monomers (fragaceatoxin-C) [87]. Lectins with actinoporin-like domains are also found in fungi [90-92].

1.2.2 β -PFTs

β -PFTs form a very broad group of PFTs, and the members of this group are mainly categorized as hemolysins and aerolysins.

1.2.2.1 Hemolysins

Hemolysins were initially discovered and named for their ability to lyse erythrocytes [93, 94]. Subsequent studies showed that they exhibited lysing activity also against nucleated cells [95]. The human pathogen *Staphylococcus aureus* produces several PFTs of the hemolysin family, including α -hemolysin (Hla), γ -hemolysin AB (HlgAB), leukocidin ED (LukED), leukocidin AB (LukAB) and Panton-Valentine leukocidin (PVL) [96]. These toxins have different but mostly overlapping functions that help *S. aureus* to target host immune cells and disrupt epithelial barriers to facilitate bacterial dissemination.

Leukocidins were initially discovered for their ability to lyse leukocytes. They are usually composed of two individual subunits (bi-component toxin) [97]. The two subunits together form a ring, which inserts itself into the target membrane to create a functional pore. The pore destroys the ion balance of the target cells and inevitably leads to apoptosis or necrosis of the affected cell [98]. Leukocidins can be chromosomally encoded as the LukG and LukH subunit, or phage encoded. In the latter case, they are called Pantone-Valentine leukocidins [99]. A single strain of *S. aureus* can express up to five different types of leukocidins [96].

The opportunistic human pathogen *Vibrio cholera* is an other well-known bacterium that produces hemolysin toxins known as *Vibrio cholera* cytolytic (VCC) [100]. VCC is an important virulence factor that is secreted by most pathogenic *V. cholera* strains. VCC has hemolytic activity in that it induces lysis of the target cells by forming large β -barrel pores in their membranes [101]. Recently, VCC was shown to have toxicity against nematodes such as *C. elegans* [102].

Chapter 1

In contrast to the bacterial hemolysins, there is not too much information about fungal hemolysins [103]. Some examples of already characterized fungal hemolysins are ostreolysins [104], asp-hemolysins [105] and aegerolysins [106]. The aegerolysins represent the largest group of fungal hemolysins. The function of hemolysins in fungi is still not clear. It has been suggested that opportunistic fungal pathogens use hemolysins to promote their infection [107]. In addition, it has been reported that hemolysins aid fungi in establishing their ecological niche by protecting them against competitors and predators. For instance, hemolysins produced by numerous basidiomycetous fungi have proven to have insecticidal activity [108].

While all the bacterial hemolysins discovered so far are extracellular, there is evidence for the intracellular expression of hemolysins in fungal species [109].

1.2.2 Aerolysins

Aerolysin is a cytotoxic β -pore-forming toxin produced by many pathogenic microorganisms as a major virulence factor [110]. Aerolysin produced by the pathogenic bacterium *Aeromonas hydrophila* is the first described member of this family [111]. Other bacterial aerolysins include α -toxin from *Clostridium septicum* [112], ϵ -toxin from *Clostridium perfringens* [113], monalysin from *Pseudomonas entomophila* [114] and parasporsins from *B. thuringiensis* [79]. Aerolysin-like toxins are also found in some eukaryotic organisms, such as hydralysins [115] from Cnidaria species and enterolobin [116] from the seeds of the Brazilian tree *Enterolobium contortisiliquum*. Bacterial aerolysins are secreted as a protoxin through a type II secretion system (T2SS) and are proteolytically activated either before or upon binding to the glycosylphosphatidylinositol (GPI)-anchored protein receptors in the target membrane [117, 118]. Upon binding to the receptors, activated toxin monomers form heptameric oligomers, which then form ring-like structured pores that impair membrane permeability and lead to cell death due to osmotic lysis [119, 120].

1.2.3 Cell surface receptors of PFTs

Each of the PFTs target different cells for different purposes. Therefore, they recognize and bind to specific receptors on the surface of their target membranes (Figure 4). PFT-binding receptors have broad diversity in term of their structure and composition. The binding epitope is mainly composed of glycans, lipids or proteins [71]. Many PFTs show a preference for certain glycan molecules in the target membrane. For example, certain lectin domain-containing members of the aerolysin and cholesterol-

Chapter 1

dependent cytolysins (CDCs) families recognize N-linked glycans [118] and glycosylphosphatidylinositol-anchored proteins [121], respectively.

Several members of both α -PFTs and β -PFTs bind to the lipid epitopes in their target membranes: actinoporins bind to sphingolipids, several members of CDCs bind to the lipid rafts composed of cholesterol, and some colicins and α -hemolysin (Hla) families bind to the cardiolipin and phosphocholine epitopes, respectively [122]. Two members of β -PFTs, Hla and CDC, have also been reported to bind to protein-composed epitopes in the target membranes. Hla recognizes disintegrin [123], while CDCs have a high affinity for CD59-based receptors [124].

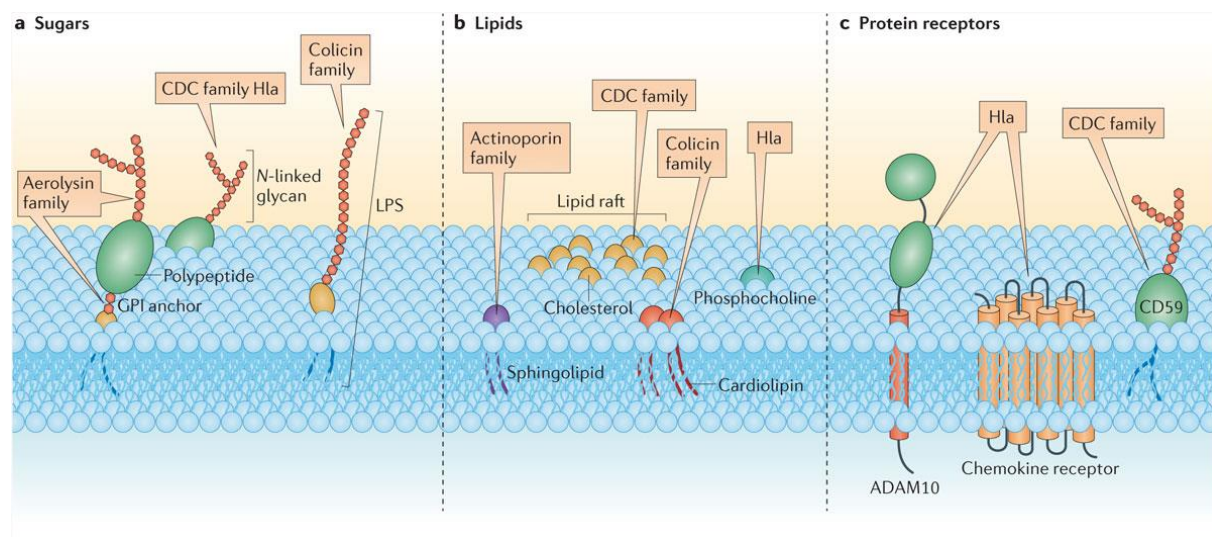


Figure 4: Cell surface receptors of PFTs

PFTs bind their target cells by recognizing specific membrane receptors, which could be glycans, lipids or proteins. **(a)** β -PFTs strongly interact with sugars in the target membrane. For example, α -hemolysin (Hla) and some of the cholesterol-dependent cytolysins (CDCs) bind to the glycan moieties that are covalently attached to the membrane proteins. Likewise, aerolysin targets sugar epitopes on glycosylphosphatidylaminositol anchors. Some *E. coli*-produced colicins bind to the lipopolysaccharides in the outer bacterial membrane. **(b)** Both α -PFTs and β -PFTs bind to the lipid moieties in their target membranes. For instance, some actinoporins bind to sphingomyelin, and some colicins recognize cardiolipins. Two β -PFTs, i.e., Hla and some CDCs, show affinity for phosphocholines and cholesterol, respectively. **(c)** Several β -PFTs bind to protein epitopes in their receptors. Hla can recognize disintegrin, and CDCs bind to CD59 receptors. Taken from [71].

1.3 Ribonucleolytic proteins

Ribosomes are an essential molecular machinery present in all living cells. They are responsible for protein biosynthesis, which is required for the growth and proper functioning of cells. All ribosomes are composed of small and large subunits, each of which are composed of ribosomal proteins and ribosomal RNAs. These subunits recognize and read messenger RNA and assemble the corresponding amino acids to form polypeptide chains [125, 126].

Toxins interfere with vital physiological functions of cells. Thus, ribosomes are ideal targets for toxins due to their critical functions [127]. There are two major classes of toxins that act directly on ribosomal RNAs: ribosome-inactivating proteins (RIPs) and ribotoxins.

1.3.1 Ribosome-inactivating proteins

RIPs are highly potent toxins with *N*-glycosidase [EC 3.2.2.22] activity [128]. These toxins induce the release of a specific adenine nucleobase from a highly conserved site of the large ribosomal subunit called the sarcin-ricin loop (SRL) [129]. The depurination of the adenine in the conserved loop disrupts the anchoring of elongation factor (EF) G and EF2 during mRNA translation, thus leading to the inhibition of protein synthesis, and subsequently, the death of the target cell [130-132]. Based on the number of polypeptide chains and receptor recognition, RIPs are classified into type 1, type 2 and type 3 (Figure 5) [133, 134].

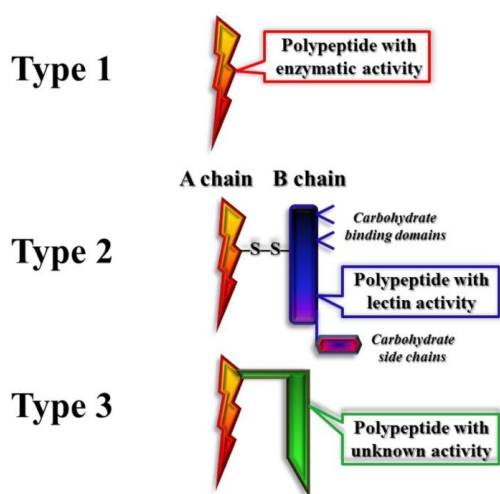


Figure 5. Schematic representation of the three types of RIPs

Type 1 RIPs, also known as holo-RIPs, consist of only a single RNA *N*-glycosidase domain. The other two types are chimera RIPs: they contain other domains such as a lectin domain (type 2 RIPs) or a domain with unknown function (type 3 RIPs), in addition to their A-chain *N*-glycosidase domain. Taken from [135].

The first toxin of the RIP family, named ricin, was discovered from the seeds of the castor oil plant *Ricinus communis* [136]. Ricin is a heterodimeric protein consisting of a glycan-binding lectin domain (B chain) and a toxic domain (A chain), and it is therefore a type 2 RIP [137]. Its two domains are linked via a disulfide bond. The B chain is responsible for recognizing and binding to high-mannose

Chapter 1

glycoproteins on the cell surface. Upon binding to the receptor, the toxin is taken up by cells via endocytosis, and the toxic domain, chain A, is translocated into the cytosol to irreversibly inhibit protein synthesis by cleaving of the adenine base of the SRL loop [138-140]. Due to its very high potency, ricin has been studied as a potential therapeutic agent in the treatment of cancer and viral infections, via linking of its active domain to cell-specific antibodies and thereby targeting cancer or infected cells [141].

Although RIPs are mainly found in plants, they are broadly distributed among fungi, algae and bacteria too. Shiga toxin (Stx) is one of the best-studied bacterial RIPs produced by *Shigella dysenteriae* 1 and some strains of *E. coli* [142-144]. Stx is a type 2 RIP; i.e., it has both a glycan-binding and an *N*-glycosidase domain. Similar to its plant counterparts, Stx acts by removing the adenine residue from the 28S rRNA of the large ribosomal subunit, which inhibits protein synthesis by the affected ribosomes [139]. RIPs are believed to play essential roles in plants, algae, and fungi as a defense protein against predators and pathogens, on account of their antiviral, antifungal and insecticidal activity [128, 133, 145, 146]. Bacterial RIPs have been suggested to promote the dissemination and survival of pathogenic bacteria within their host cells [147].

1.3.2 Ribotoxins

In contrast to RIPs, which tend to be larger proteins (30–60 kDa) and have RNA *N*-glycosidase activity, ribotoxins are small proteins (10–20 kDa) with a highly specific ribonuclease activity [148]. While RIPs depurinate adenine, ribotoxins cleave the phosphodiester bond between guanine and adenine residues at the universally conserved GAGA tetraloop of the large ribosomal subunit (Figure 6) [149]. The cleavage releases a small rRNA fragment comprising 300–400 nucleotides (depending on the ribosome source) called the α -fragment (Figure 7) [150]. The GAGA tetraloop is essential for the binding of elongation factors, and therefore, any damage to it halts protein synthesis and leads to apoptosis of the affected cell [151].

Unlike RIPs, the ribotoxins that have been characterized so far are exclusively from kingdom Fungi [152]. The first ribotoxin, named α -sarcin, was discovered in 1956 from *Aspergillus giganteus* as an antitumor agent [153, 154]. Similar to ricin, α -sarcin also acts on the SRL of ribosomes [155]. In fact, this is the origin of the name “sarcin-ricin loop.” Later on, two other proteins, mitogillin and restrictocin, were discovered in an antitumor screening process from another mold, *Aspergillus restrictus* [156-159]. Some other well-studied examples are hirsutellin A (HtA) [160] and anisoplin [161, 162] produced by *Hirsutella thompsonii* and *Metarrhizium anisopliae*, respectively. The primary sequences and certain core structures of these ribotoxins seem to be conserved across species. In fact,

the first 20 identified members had 85% sequence similarity [152]. However, recently, more diverse members of ribotoxins, with only 25% sequence similarity, have been described [161, 163].

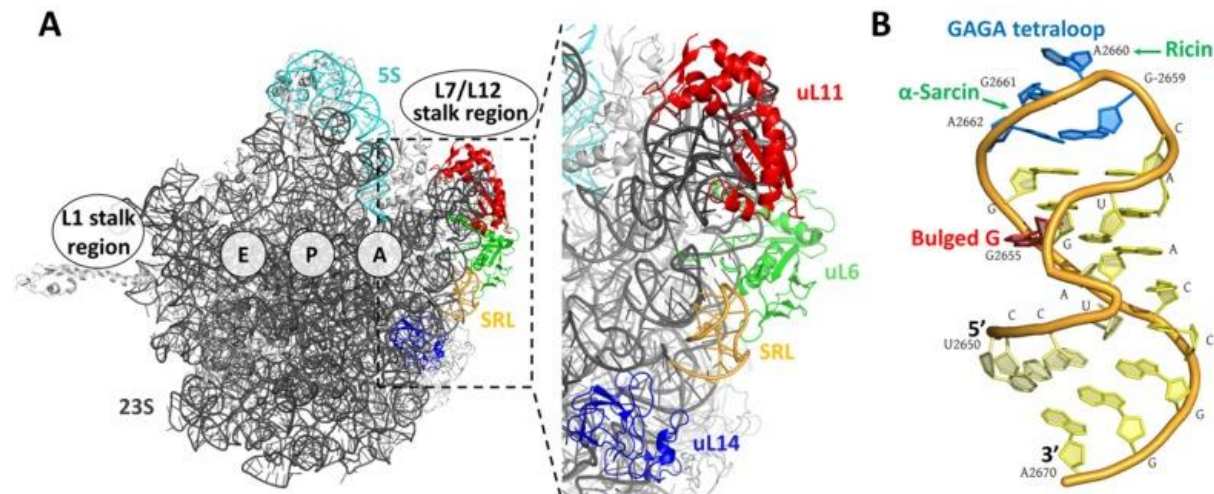


Figure 6: Ribotoxin and RIP targets within the SRL loop of ribosomes

(A) 3D structure of the large ribosomal subunit of *E. coli*. The location of the E (exit), P (peptidyl) and A (acceptor) sites and the ribosomal proteins uL6, uL11, uL14 around the SRL are indicated. (B) Sarcin-ricin loop structure. The bulged G, the conserved GAGA tetraloop, the phosphodiester bond cleaved by ribotoxins such as α -sarcin, and the adenine depurinated by RPs, such as ricin, are labeled. Adapted from [149].

All the ribotoxins characterized so far are produced by members of Ascomycota, with one exception: ageritin is a very recently discovered ribotoxin that is produced by the basidiomycete *Agrocybe aegerita* [164]. More information about ageritin can be found in the fourth chapter of this thesis.

1.3.2.1 Entry of ribotoxins into target cells

To date, no specific receptors have reported for the recognition or binding of ribotoxins to their target cells [165]. As ribotoxins are highly positively charged molecules, it is believed the high amount of positively charged residues in ribotoxins is important for their binding to negatively charged target membranes [166-168]. The binding and subsequent diffusion of ribotoxins through the plasma membrane are hypothesized to be determining factors in the susceptibility of cells to ribotoxins. Thus, the permeability and composition of the target cell membrane play an important role in the effect of ribotoxins. For instance, the susceptibility of insect cells to ribotoxins is believed to be due to their thinner and more fluidic plasma membrane structure, facilitating the diffusion of ribotoxins through

Chapter 1

the membrane [169-171]. Further, studies have shown that virus-infected [172] or phospholipase-treated cells [173] are more sensitive to ribotoxins due to the permeability of the cell membrane.

The importance of the positively charged residues in ribotoxins has been proven through experiments on RNase U2 from *Ustilago sphaerogenes* [174]. RNase U2 is a small extracellular endonuclease with high sequence similarity to ribotoxins. However, unlike ribotoxins, RNase U2 is a highly acidic protein, which makes it difficult for it to bind to the negatively charged phospholipids in the cell membrane and negatively charged ribosomal RNA molecules.

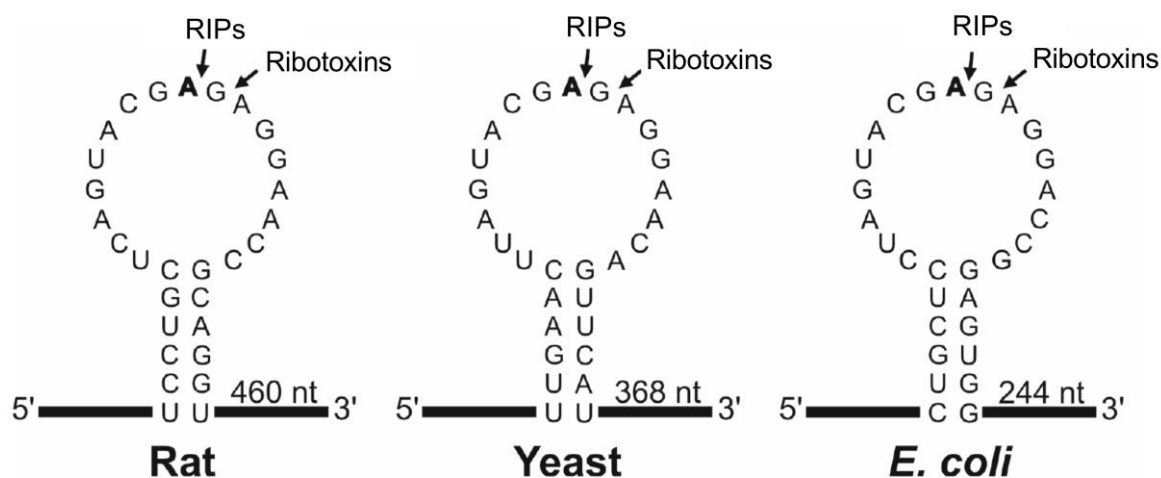


Figure 7: Sequence of the sarcin-ricin loop of rat, yeast and bacteria (*E. coli*) ribosomes

The phosphodiester bond cleaved by ribotoxins and the adenine nucleotide depurinated by RIPs are indicated. The size of the expected alpha fragments of the ribosomes of each species is indicated. Modified from [150].

The GAGA tetraloop, where both RIPs and ribotoxins act, is universally conserved throughout all known ribosomes (Figure 7), making every ribosome potentially susceptible [150]. Hence, one obvious question that needs to be addressed is how fungi that secrete such toxins are protected from the toxicity of their own ribotoxins. Several studies have suggested that fungi avoid self-toxicity by synthesizing ribotoxins as precursors inside their membrane compartments [175]. Further, mutational analysis has shown that mutating the signaling sequences of the ribotoxins results in lower transcriptional expression of the toxin and cellular lysis [176]. This question of self-protection has become even more intriguing after the discovery of the first ribotoxin expressed in the cytoplasm (see Chapter 4).

References

1. Stajich JE, Berbee ML, Blackwell M, Hibbett DS, James TY, Spatafora JW, Taylor JW: **The Fungi**. *Current Biology* 2009, **19**(18):R840-R845.
2. Treseder KK, Lennon JT: **Fungal Traits That Drive Ecosystem Dynamics on Land**. *Microbiol Mol Biol R* 2015, **79**(2):243-262.
3. Ruess L, Lussenhop J: **Trophic interactions of Fungi and Animals**. In: *The Fungal Community: Its Organization and Role in the Ecosystems*. Edited by J. D, White JF, Oudemans P. Boca Raton: CRC Press; 2005: 581–598.
4. Boddy L, Jones TH: **Interactions between Basidiomycota and Invertebrates**. *Br Mycol Sy* 2008, **28**:155-179.
5. Bonfante P, Genre A: **Mechanisms underlying beneficial plant-fungus interactions in mycorrhizal symbiosis**. *Nat Commun* 2010, **1**.
6. Hawksworth DL: **The Variety of Fungal Algal Symbioses, Their Evolutionary Significance, and the Nature of Lichens**. *Bot J Linn Soc* 1988, **96**(1):3-20.
7. Kunzler M: **How fungi defend themselves against microbial competitors and animal predators**. *PLoS Pathog* 2018, **14**(9):e1007184.
8. Wang M, Trigueros V, Paquereau L, Chavant L, Fournier D: **Proteins as active compounds involved in insecticidal activity of mushroom fruitbodies**. *J Econ Entomol* 2002, **95**(3):603-607.
9. Yao QZ, Yu MM, Ooi LSM, Ng TB, Chang ST, Sun SSM, Ooi VEC: **Isolation and characterization of a type 1 ribosome-inactivating protein from fruiting bodies of the edible mushroom (*Volvariella volvacea*)**. *J Agr Food Chem* 1998, **46**(2):788-792.
10. Sabotic J, Ohm RA, Kunzler M: **Entomotoxic and nematotoxic lectins and protease inhibitors from fungal fruiting bodies**. *Appl Microbiol Biot* 2016, **100**(1):91-111.
11. Rousk J, Baath E: **Growth of saprotrophic fungi and bacteria in soil**. *Fems Microbiol Ecol* 2011, **78**(1):17-30.
12. Boddy L, Watkinson SC: **Wood Decomposition, Higher Fungi, and Their Role in Nutrient Redistribution**. *Can J Bot* 1995, **73**:S1377-S1383.
13. Hanski I: **Fungivory: fungi, insects and ecology**: Academic Press, London; 1988.
14. Omoto C, McCoy CW: **Toxicity of purified fungal toxin hirsutellin A to the citrus rust mite *Phyllocoptrus oleivora* (Ash.)**. *Journal of Invertebrate Pathology* 1998, **72**(3):319-322.
15. Latge JP: **The cell wall: a carbohydrate armour for the fungal cell**. *Molecular microbiology* 2007, **66**(2):279-290.
16. Gomez BL, Nosanchuk JD: **Melanin and fungi**. *Curr Opin Infect Dis* 2003, **16**(2):91-96.
17. Kempken F, Rohlf M: **Fungal secondary metabolite biosynthesis - a chemical defence strategy against antagonistic animals?** *Fungal Ecology* 2010, **3**(3):107-114.
18. Demain A, Fang A: **The Natural Functions of Secondary Metabolites**. In: *History of Modern Biotechnology I*. Edited by Fiechter A, vol. 69: Springer Berlin Heidelberg; 2000: 1-39.
19. Macheleidt J, Mattern DJ, Fischer J, Netzker T, Weber J, Schroekh V, Valiante V, Brakhage AA: **Regulation and Role of Fungal Secondary Metabolites**. *Annu Rev Genet* 2016, **50**:371-392.
20. Netzker T, Fischer J, Weber J, Mattern DJ, Konig CC, Valiante V, Schroekh V, Brakhage AA: **Microbial communication leading to the activation of silent fungal secondary metabolite gene clusters**. *Front Microbiol* 2015, **6**:299.

Chapter 1

21. Rohlfs M, Albert M, Keller NP, Kempken F: **Secondary chemicals protect mould from fungivory.** *Biology Letters* 2007, **3**(5):523-525.
22. Rohlfs M, Churchill ACL: **Fungal secondary metabolites as modulators of interactions with insects and other arthropods.** *Fungal Genet Biol* 2011, **48**(1):23-34.
23. Stadler M, Sterner O: **Production of bioactive secondary metabolites in the fruit bodies of macrofungi as a response to injury.** *Phytochemistry* 1998, **49**(4):1013-1019.
24. Bleuler-Martinez S, Schmieder S, Aebi M, Kunzler M: **Biotin-Binding Proteins in the Defense of Mushrooms against Predators and Parasites.** *Appl Environ Microb* 2012, **78**(23):8485-8487.
25. Sabotić J, Bleuler-Martinez S, Renko M, Avanzo Caglić P, Kallert S, Štrukelj B, Turk D, Aebi M, Kos J, Künzler M: **Structural Basis of Trypsin Inhibition and Entomotoxicity of Cospin, Serine Protease Inhibitor Involved in Defense of Coprinopsis cinerea Fruiting Bodies.** *J Biol Chem* 2012, **287**(6):3898-3907.
26. Essig A, Hofmann D, Munch D, Gayathri S, Kunzler M, Kallio PT, Sahl HG, Wider G, Schneider T, Aebi M: **Copsin, a novel peptide-based fungal antibiotic interfering with the peptidoglycan synthesis.** *J Biol Chem* 2014, **289**(50):34953-34964.
27. Bleuler-Martínez S, Butschi A, Garbani M, Wilti MA, Wohlschlager T, Potthoff E, Sabotia J, Pohleven J, Lüthy P, Hengartner MO et al: **A lectin-mediated resistance of higher fungi against predators and parasites.** 2011, **20**:3056-3070.
28. Fahy E, Subramaniam S, Brown HA, Glass CK, Merrill Jr AH, Murphy RC, Raetz CRH, Russell DW, Seyama Y, Shaw W et al: **A comprehensive classification system for lipids.** *J Lipid Res* 2005, **46**(5):839-861.
29. Helms JB, Zurzolo C: **Lipids as targeting signals: Lipid rafts and intracellular trafficking.** *Traffic* 2004, **5**(4):247-254.
30. Berridge MJ, Irvine RF: **Inositol phosphates and cell signalling.** *Nature* 1989, **341**(6239):197-205.
31. Haucke V, Di Paolo G: **Lipids and lipid modifications in the regulation of membrane traffic.** *Curr Opin Cell Biol* 2007, **19**(4):426-435.
32. Wenk MR: **Lipidomics of host-pathogen interactions.** *Febs Lett* 2006, **580**(23):5541-5551.
33. Helms B: **Host-pathogen interactions: Lipids grease the way.** *European Journal of Lipid Science and Technology* 2006, **108**(11):895-897.
34. Dennis EA: **Lipidomics joins the omics evolution.** *P Natl Acad Sci USA* 2009, **106**(7):2089-2090.
35. Wenk MR: **The emerging field of lipidomics.** *Nature Reviews Drug Discovery* 2005, **4**(7):594-610.
36. Akoh CC, Lee GC, Liaw YC, Huang TH, Shaw JF: **GDSL family of serine esterases/lipases.** *Prog Lipid Res* 2004, **43**(6):534-552.
37. Jaeger KE, Reetz MT: **Microbial lipases form versatile tools for biotechnology.** *Trends Biotechnol* 1998, **16**(9):396-403.
38. Anuradha P, Rani DJ, Vijayalakshmi K, Pasha SA, Kamakshi S: **Microbial Lipases : A Potential Tool for Industrial Applications.** *J Pure Appl Microbiol* 2009, **3**(1):301-306.
39. Guerrand D: **Lipases industrial applications: focus on food and agroindustries.** *Ocl Oils Fat Crop Li* 2017, **24**(4).
40. Hasan F, Shah AA, Hameed A: **Industrial applications of microbial lipases.** *Enzyme Microb Tech* 2006, **39**(2):235-251.
41. Houde A, Kademi A, Leblanc D: **Lipases and their industrial applications - An overview.** *Applied Biochemistry and Biotechnology* 2004, **118**(1-3):155-170.

Chapter 1

42. Machida H, Higashi T, Kokusho Y: **Industrial-Production and Application of Microbial Lipases.** *J Agr Chem Soc Jpn* 1984, **58**(8):799-804.
43. Nielsen T: **Industrial Application Possibilities for Lipase.** *Fett Wiss Technol* 1985, **87**(1):15-19.
44. Sarmah N, Revathi D, Sheelu G, Rani KY, Sridhar S, Mehtab V, Sumana C: **Recent advances on sources and industrial applications of lipases.** *Biotechnol Progr* 2018, **34**(1):5-28.
45. Schmidt-Dannert C, Pleiss J, Schmid RD: **A toolbox of recombinant lipases for industrial applications.** *Ann Ny Acad Sci* 1998, **864**:14-22.
46. Seitz EW: **Industrial Application of Microbial Lipases - Review.** *J Am Oil Chem Soc* 1974, **51**(2):12-16.
47. Schmiel DH, Miller VL: **Bacterial phospholipases and pathogenesis.** *Microbes Infect* 1999, **1**(13):1103-1112.
48. Borthakur A, Gill RK, Hodges K, Ramaswamy K, Hecht G, Dudeja PK: **Enteropathogenic Escherichia coli inhibits butyrate uptake in Caco-2 cells by altering the apical membrane MCT1 level.** *American Journal of Physiology - Gastrointestinal and Liver Physiology* 2006, **290**(1):G30-G35.
49. Agaisse H, Burrack LS, Philips JA, Rubin EJ, Perrimon N, Higgins DE: **Genome-wide RNAi screen for host factors required for intracellular bacterial infection.** *Science* 2005, **309**(5738):1248-1251.
50. Su AI, Pezacki JP, Wodicka L, Brideau AD, Supekova L, Thimme R, Wieland S, Bukh J, Purcell RH, Schultz PG *et al*: **Genomic analysis of the host response to hepatitis C virus infection.** *P Natl Acad Sci USA* 2002, **99**(24):15669-15674.
51. Ghannoum MA: **Potential role of phospholipases in virulence and fungal pathogenesis.** *Clinical Microbiology Reviews* 2000, **13**(1):122-143.
52. Belaunzarán ML, Lammel EM, De Isola ELD: **Phospholipases A in trypanosomatids.** *Enzyme Research* 2011, **2011**(1).
53. Heffernan BJ, Thomason B, Herring-Palmer A, Shaughnessy L, McDonald R, Fisher N, Huffnagle GB, Hanna P: **Bacillus anthracis phospholipases C facilitate macrophage-associated growth and contribute to virulence in a murine model of inhalation anthrax.** *Infect Immun* 2006, **74**(7):3756-3764.
54. Aloulou A, Ben Ali Y, Bezzine S, Gargouri Y, Gelb MH: **Phospholipases: An Overview.** *Methods Mol Biol* 2012, **861**:63-85.
55. Sitkiewicz I, Stockbauer KE, Musser JM: **Secreted bacterial phospholipase A2 enzymes: better living through phospholipolysis.** *Trends in Microbiology* 2007, **15**(2):63-69.
56. Sato H, Frank DW: **ExoU is a potent intracellular phospholipase.** *Molecular microbiology* 2004, **53**(5):1279-1290.
57. Flieger A, Gong S, Faigle M, Mayer HA, Kehrer U, Mußotter J, Bartmann P, Neumeister B: **Phospholipase A secreted by Legionella pneumophila destroys alveolar surfactant phospholipids.** *FEMS Microbiology Letters* 2000, **188**(2):129-133.
58. Heung LJ, Luberto C, Del Poeta M: **Role of sphingolipids in microbial pathogenesis.** *Infect Immun* 2006, **74**(1):28-39.
59. Hanada K: **Sphingolipids in infectious diseases.** *Japanese Journal of Infectious Diseases* 2005, **58**(3):131-148.
60. Sato H, Frank DW, Hillard CJ, Feix JB, Pankhaniya RR, Moriyama K, Finck-Barbancon V, Buchaklian A, Lei M, Long RM *et al*: **The mechanism of action of the Pseudomonas aeruginosa-encoded type III cytotoxin, ExoU.** *Embo J* 2003, **22**(12):2959-2969.

Chapter 1

61. Phillips RM, Six DA, Dennis EA, Ghosh P: **In Vivo Phospholipase Activity of the *Pseudomonas aeruginosa* Cytotoxin ExoU and Protection of Mammalian Cells with Phospholipase A2 Inhibitors.** *J Biol Chem* 2003, **278**(42):41326-41332.
62. Pollok RCG, McDonald V, Kelly P, Farthing MJG: **The role of *Cryptosporidium parvum*-derived phospholipase in intestinal epithelial cell invasion.** *Parasitol Res* 2003, **90**(3):181-186.
63. Cassaing S, Fauvel J, Bessières MH, Guy S, Séguéla JP, Chap H: **Toxoplasma gondii secretes a calcium-independent phospholipase A2.** *Int J Parasitol* 2000, **30**(11):1137-1142.
64. Saffer LD, Long Krug SA, Schwartzman JD: **The role of phospholipase in host cell penetration by *Toxoplasma gondii*.** *American Journal of Tropical Medicine and Hygiene* 1989, **40**(2):145-149.
65. Leidich SD, Ibrahim AS, Fu Y, Koul A, Jessup C, Vitullo J, Fonzi W, Mirbod F, Nakashima S, Nozawa Y et al: **Cloning and disruption of caPLB1, a phospholipase B gene involved in the pathogenicity of *Candida albicans*.** *J Biol Chem* 1998, **273**(40):26078-26086.
66. McLain N, Dolan JW: **Phospholipase D activity is required for dimorphic transition in *Candida albicans*.** *Microbiology* 1997, **143**(11):3521-3526.
67. Ganendren R, Carter E, Sorrell T, Widmer F, Wright L: **Phospholipase B activity enhances adhesion of *Cryptococcus neoformans* to a human lung epithelial cell line.** *Microbes Infect* 2006, **8**(4):1006-1015.
68. Grienberger E, Geoffroy P, Mutterer J, Legrand M, Heitz T: **The interplay of lipid acyl hydrolases in inducible plant defense.** *Plant Signal Behav* 2010, **5**(10):1181-1186.
69. Stehr F, Kretschmar M, Kroger C, Huber B, Schafer W: **Microbial lipases as virulence factors.** *J Mol Catal B-Enzym* 2003, **22**(5-6):347-355.
70. Alouf JE: **Pore-forming bacterial protein toxins.** *Pore Forming Toxins* 2001:1-14.
71. Dal Peraro M, van der Goot FG: **Pore-forming toxins: ancient, but never really out of fashion.** *Nature Reviews Microbiology* 2016, **14**(2):77-92.
72. Parker MW, Feil SC: **Pore-forming protein toxins: From structure to function.** *Progress in Biophysics and Molecular Biology* 2005, **88**(1):91-142.
73. Lesieur C, Vécsey-Semjén B, Abrami L, Fivaz M, Gisou Van Der Goot F: **Membrane insertion: The strategies of toxins (Review).** *Molecular Membrane Biology* 1997, **14**(2):45-64.
74. Iacovache I, Bischofberger M, van der Goot FG: **Structure and assembly of pore-forming proteins.** *Current Opinion in Structural Biology* 2010, **20**(2):241-246.
75. Lakey JH, Slatin SL: **Pore-forming colicins and their relatives.** *Pore-Forming Toxins* 2001, **257**:131-161.
76. Lakey JH, Gisou van der Goot F, Pattus F: **All in the family: the toxic activity of pore-forming colicins.** *Toxicology* 1994, **87**(1-3):85-108.
77. Cascales E, Buchanan SK, Duché D, Kleanthous C, Lloubès R, Postle K, Riley M, Slatin S, Cavard D: **Colicin biology.** *Microbiol Mol Biol R* 2007, **71**(1):158-229.
78. Choe S, Bennett MJ, Fujii G, Curmi PMG, Kantardjieff KA, Collier RJ, Eisenberg D: **The crystal structure of diphtheria toxin.** *Nature* 1992, **357**(6375):216-222.
79. Xu C, Wang BC, Yu Z, Sun M: **Structural insights into *Bacillus thuringiensis* Cry, Cyt and parasporin toxins.** *Toxins* 2014, **6**(9):2732-2770.
80. Hunt S, Green J, Artymiuk PJ: **Hemolysin e (HlyE, ClyA, SheA) and related toxins.** In: *Advances in Experimental Medicine and Biology*. vol. 677; 2010: 116-126.
81. Wallace AJ, Stillman TJ, Atkins A, Jamieson SJ, Bullough PA, Green J, Artymiuk PJ: ***E. coli* hemolysin E (Hlye, ClyA, SheA): X-ray crystal structure of the toxin and observation of membrane pores by electron microscopy.** *Cell* 2000, **100**(2):265-276.

Chapter 1

82. Vaidyanathan MS, Sathyanarayana P, Maiti PK, Visweswariah SS, Ayappa KG: **Lysis dynamics and membrane oligomerization pathways for Cytolysin A (ClyA) pore-forming toxin.** *RSC Advances* 2014, **4**(10):4930-4942.
83. Fahie M, Romano FB, Chisholm C, Heuck AP, Zbinden M, Chen M: **A non-classical assembly pathway of Escherichia coli pore-forming toxin Cytolysin A.** *J Biol Chem* 2013, **288**(43):31042-31051.
84. Črnigoj Kristan K, Viero G, Dalla Serra M, Maček P, Anderluh G: **Molecular mechanism of pore formation by actinoporins.** *Toxicon* 2009, **54**(8):1125-1134.
85. Athanasiadis A, Anderluh G, Maček P, Turk D: **Crystal structure of the soluble form of equinatoxin II, a pore-forming toxin from the sea anemone Actinia equina.** *Structure* 2001, **9**(4):341-346.
86. Mancheño JM, Martín-Benito J, Martínez-Ripoll M, Gavilanes JG, Hermoso JA: **Crystal and electron microscopy structures of sticholysin II actinoporin reveal insights into the mechanism of membrane pore formation.** *Structure* 2003, **11**(11):1319-1328.
87. Mechaly AE, Bellomio A, Gil-Cartón D, Morante K, Valle M, González-Mañas JM, Guérin DMA: **Structural insights into the oligomerization and architecture of eukaryotic membrane pore-forming toxins.** *Structure* 2011, **19**(2):181-191.
88. Barlič A, Gutiérrez-Aguirre I, Caaveiro JMM, Cruz A, Ruiz-Argüello MB, Pérez-Gil J, González-Mañas JM: **Lipid phase coexistence favors membrane insertion of equinatoxin-II, a pore-forming toxin from Actinia equina.** *J Biol Chem* 2004, **279**(33):34209-34216.
89. Baker MAB, Rojko N, Cronin B, Anderluh G, Wallace MI: **Photobleaching reveals heterogeneous stoichiometry for equinatoxin II oligomers.** *ChemBioChem* 2014, **16**(17):2139-2145.
90. Carrizo ME, Capaldi S, Perduca M, Irazoqui FJ, Nores GA, Monaco HL: **The antineoplastic lectin of the common edible mushroom (*Agaricus bisporus*) has two binding sites, each specific for a different configuration at a single epimeric hydroxyl.** *J Biol Chem* 2005, **280**(11):10614-10623.
91. Birck C, Damian L, Marty-Detraves C, Lougarre A, Schulze-Briese C, Koehl P, Fournier D, Paquereau L, Samama JP: **A new lectin family with structure similarity to actinoporins revealed by the crystal structure of Xerocomus chrysenteron lectin XCL.** *Journal of Molecular Biology* 2004, **344**(5):1409-1420.
92. Nowrouzian M, Cebula P: **The gene for a lectin-like protein is transcriptionally activated during sexual development, but is not essential for fruiting body formation in the filamentous fungus *Sordaria macrospora*.** *BMC microbiology* 2005, **5**.
93. Coelho A, Andrade JRC, Vicente ACP, Dirita VJ: **Cytotoxic cell vacuolating activity from *Vibrio cholerae* hemolysin.** *Infect Immun* 2000, **68**(3):1700-1705.
94. Menestrina G, Serra MD, Prevost G: **Mode of action of beta-barrel pore-forming toxins of the staphylococcal alpha-hemolysin family.** *Toxicon* 2001, **39**(11):1661-1672.
95. Woodin AM: **The extrusion of protein from the rabbit polymorphonuclear leucocyte treated with staphylococcal leucocidin.** *Biochem J* 1962, **82**:9-15.
96. Prevost G, Mourey L, Colin DA, Menestrina G: **Staphylococcal pore-forming toxins.** *Curr Top Microbiol Immunol* 2001, **257**:53-83.
97. Miles G, Movileanu L, Bayley H: **Subunit composition of a bicomponent toxin: Staphylococcal leukocidin forms an octameric transmembrane pore.** *Protein Sci* 2002, **11**(4):894-902.
98. Alonzo F, Torres VJ: **The Bicomponent Pore-Forming Leucocidins of *Staphylococcus aureus*.** *Microbiol Mol Biol R* 2014, **78**(2):199-230.

Chapter 1

99. Labandeira-Rey M, Couzon F, Boisset S, Brown EL, Bes M, Benito Y, Barbu EM, Vazquez V, Höök M, Etienne J *et al*: **Staphylococcus aureus Panton-Valentine leukocidin causes necrotizing pneumonia.** *Science* 2007, **315**(5815):1130-1133.
100. Harris JR, Bhakdi S, Meissner U, Scheffler D, Bittman R, Li G, Zitzer A, Palmer M: **Interaction of the Vibrio cholerae cytolysin (VCC) with cholesterol, some cholesterol esters, and cholesterol derivatives: A TEM study.** *Journal of Structural Biology* 2002, **139**(2):122-135.
101. Olson R, Gouaux E: **Crystal structure of the Vibrio cholerae cytolysin (VCC) pro-toxin and its assembly into a heptameric transmembrane pore.** *Journal of Molecular Biology* 2005, **350**(5):997-1016.
102. Cinar HN, Kothary M, Datta AR, Tall BD, Sprando R, Bilecen K, Yildiz F, McCardell B: **Vibrio cholerae Hemolysin Is Required for Lethality, Developmental Delay, and Intestinal Vacuolation in Caenorhabditis elegans.** *Plos One* 2010, **5**(7).
103. Nayak AP, Green BJ, Beezhold DH: **Fungal hemolysins.** *Medical Mycology* 2013, **51**(1):1-16.
104. Sepcic K, Berne S, Rebolj K, Batista UK, Plemenitas A, Sentjurc M, Macek P: **Ostreolysin, a pore-forming protein from the oyster mushroom, interacts specifically with membrane cholesterol-rich lipid domains.** *Febs Lett* 2004, **575**(1-3):81-85.
105. Ebina K, Sakagami H, Yokota K, Kondo H: **Cloning and Nucleotide-Sequence of Cdna-Encoding Asp-Hemolysin from Aspergillus-Fumigatus.** *Bba-Gene Struct Expr* 1994, **1219**(1):148-150.
106. Berne S, Lah L, Sepcic K: **Aegerolysins: structure, function, and putative biological role.** *Protein Sci* 2009, **18**(4):694-706.
107. Ebina K, Ishizuka Y, Yokota K, Sakaguchi O: **Role of Asp-Hemolysin on Experimental Aspergillus Infection for Mice.** *Jpn J Med Sci Biol* 1982, **35**(3):140-141.
108. Wang M, Trigueros V, Paquereau L, Chavant L, Fournier D: **Proteins as active compounds involved in insecticidal activity of mushroom fruitbodies.** *J Econ Entomol* 2002, **95**(3):603-607.
109. Medina ML, Haynes PA, Breci L, Francisco WA: **Analysis of secreted proteins from Aspergillus flavus.** *Proteomics* 2005, **5**(12):3153-3161.
110. Rossjohn J, Feil SC, McKinstry WJ, Tsernoglou D, Van Der Goot G, Buckley JT, Parker MW: **Aerolysin - A paradigm for membrane insertion of beta-sheet protein toxins?** *Journal of Structural Biology* 1998, **121**(2):92-100.
111. Howard SP, Garland WJ, Green MJ, Buckley JT: **Nucleotide sequence of the gene for the hole-forming toxin aerolysin of Aeromonas hydrophila.** *Journal of Bacteriology* 1987, **169**(6):2869-2871.
112. Ballard J, Sokolov Y, Yuan WL, Kagan BL, Tweten RK: **Activation and mechanism of Clostridium septicum alpha toxin.** *Molecular microbiology* 1993, **10**(3):627-634.
113. Alves GG, de Ávila RAM, Chávez-Olórtegui CD, Lobato FCF: **Clostridium perfringens epsilon toxin: The third most potent bacterial toxin known.** *Anaerobe* 2014, **30**:102-107.
114. Opota O, Vallet-Gély I, Vincentelli R, Kellenberger C, Iacovache I, Gonzalez MR, Roussel A, van der Goot FG, Lemaitre B: **Monalysin, a novel β-pore-forming toxin from the drosophila pathogen pseudomonas entomophila, contributes to host intestinal damage and lethality.** *PLoS Pathogens* 2011, **7**(9).
115. Sher D, Fishman Y, Zhang M, Lebendiker M, Gaathon A, Mancheño JM, Zlotkin E: **Hydralysins, a new category of β-pore-forming toxins in cnidaria.** *J Biol Chem* 2005, **280**(24):22847-22855.
116. Sousa MV, Richardson M, Fontes W, Morhy L: **Homology between the seed cytolysin enterolobin and bacterial aerolysins.** *Journal of Protein Chemistry* 1994, **13**(8):659-667.

Chapter 1

117. Abrami L, Fivaz M, Decroly E, Seidah NG, Jean F, Thomas G, Leppla SH, Buckley JT, Van Der Goot FG: **The pore-forming toxin proaerolysin is activated by furin.** *J Biol Chem* 1998, **273**(49):32656-32661.
118. Hong Y, Ohishi K, Inoue N, Kang JY, Shime H, Horiguchi Y, Van der Goot FG, Sugimoto N, Kinoshita T: **Requirement of N-glycan on GPI-anchored proteins for efficient binding of aerolysin but not Clostridium septicum α -toxin.** *Embo J* 2002, **21**(19):5047-5056.
119. Wilmsen HU, Leonard KR, Tichelaar W, Buckley JT, Pattus F: **The aerolysin membrane channel is formed by heptamerization of the monomer.** *Embo J* 1992, **11**(7):2457-2463.
120. van der Goot FG, Pattus F, Wong KR, Buckley JT: **Oligomerization of the Channel-Forming Toxin Aerolysin Precedes Insertion into Lipid Bilayers.** *Biochemistry-US* 1993, **32**(10):2636-2642.
121. Shewell LK, Harvey RM, Higgins MA, Day CJ, Hartley-Tassell LE, Chen AY, Gillen CM, James DBA, Alonzo F, Torres VJ et al: **The cholesterol-dependent cytolsins pneumolysin and streptolysin O require binding to red blood cell glycans for hemolytic activity.** *P Natl Acad Sci USA* 2014, **111**(49):E5312-E5320.
122. Fivaz M, Abrami L, Van der Goot FG: **Landing on lipid rafts [2].** *Trends in Cell Biology* 1999, **9**(6):212-213.
123. Wilke GA, Wardenburg JB: **Role of a disintegrin and metalloprotease 10 in Staphylococcus aureus α -hemolysin - Mediated cellular injury.** *P Natl Acad Sci USA* 2010, **107**(30):13473-13478.
124. Giddings KS, Zhao J, Sims PJ, Tweten RK: **Human CD59 is a receptor for the cholesterol-dependent cytolsin intermedilysin.** *Nature Structural and Molecular Biology* 2004, **11**(12):1173-1178.
125. Woolford Jr JL, Baserga SJ: **Ribosome biogenesis in the yeast Saccharomyces cerevisiae.** *Genetics* 2013, **195**(3):643-681.
126. Ramakrishnan V, Moore PB: **Atomic structures at last: The ribosome in 2000.** *Current Opinion in Structural Biology* 2001, **11**(2):144-154.
127. Bottger EC: **The ribosome as a drug target.** *Trends Biotechnol* 2006, **24**(4):145-147.
128. Schrot J, Weng A, Melzig MF: **Ribosome-inactivating and related proteins.** *Toxins (Basel)* 2015, **7**(5):1556-1615.
129. Endo Y, Mitsui K, Motizuki M, Tsurugi K: **The mechanism of action of ricin and related toxic lectins on eukaryotic ribosomes. The site and the characteristics of the modification in 28 S ribosomal RNA caused by the toxins.** *J Biol Chem* 1987, **262**(12):5908-5912.
130. Brigotti M, Rambelli F, Zamboni M, Montanaro L, Sperti S: **Effect of Alpha-Sarcin and Ribosome-Inactivating Proteins on the Interaction of Elongation-Factors with Ribosomes.** *Biochem J* 1989, **257**(3):723-727.
131. Correll CC, Munishkin A, Chan YL, Ren Z, Wool IG, Steitz TA: **Crystal structure of the ribosomal RNA domain essential for binding elongation factors.** *P Natl Acad Sci USA* 1998, **95**(23):13436-13441.
132. Nilsson J, Nissen P: **Elongation factors on the ribosome.** *Current Opinion in Structural Biology* 2005, **15**(3 SPEC. ISS.):349-354.
133. Girbés T, Ferreras JM, Arias FJ, Stirpe F: **Description, distribution, activity and phylogenetic relationship of ribosome-inactivating proteins in plants, fungi and bacteria.** *Mini-Reviews in Medicinal Chemistry* 2004, **4**(5):461-476.
134. Mundy J, Leah R, Boston R, Endo Y, Stirpe F: **Genes encoding ribosome-inactivating proteins.** *Plant Molecular Biology Reporter* 1994, **12**(2):S60-S62.

Chapter 1

135. Domashevskiy AV, Goss DJ: **Pokeweed Antiviral Protein, a Ribosome Inactivating Protein: Activity, Inhibition and Prospects.** *Toxins* 2015, **7**(2):274-298.
136. Craig HL, Alderks OH, Corwin AH, Dieke SH, Karel CL: **Preparation of toxic ricin.** U.S. Patent 3,060 1962:165.
137. Rutenber E, Katzin BJ, Ernst S, Collins EJ, Mlsna D, Ready MP, Robertus JD: *Proteins: Structure, Function, and Bioinformatics* 1991, **10**(3):240-250.
138. Chen XY, Link TM, Schramm VL: **Ricin A-chain: Kinetics, mechanism, and RNA stem-loop inhibitors.** *Biochemistry-US* 1998, **37**(33):11605-11613.
139. Turner NE, Li XP: **Interaction of ricin and Shiga toxins with ribosomes.** In: *Current Topics in Microbiology and Immunology.* vol. 357; 2012: 1-18.
140. Sandvig K, van Deurs B: **Endocytosis and intracellular sorting of ricin and Shiga toxin.** *Febs Lett* 1994, **346**(1):99-102.
141. O'Toole JE, Esseltine D, Lynch TJ, Lambert JM, Grossbard ML: **Clinical trials with blocked ricin immunotoxins.** In: *Current Topics in Microbiology and Immunology.* vol. 234; 1998: 35-56.
142. Brown J, Ussery MA, Leppla SH, Rothman SW: **Inhibition of protein synthesis by Shiga toxin: Activation of the toxin and inhibition of peptide elongation.** *Febs Lett* 1980, **117**(1-2):84-88.
143. Bergan J, Dyve Lingelab AB, Simm R, Skotland T, Sandvig K: **Shiga toxins.** *Toxicon* 2012, **60**(6):1085-1107.
144. Melton-Celsa AR: **Shiga toxin (Stx) classification, structure, and function.** *Microbiology Spectrum* 2014, **2**(4).
145. Barbieri L, Battelli MG, Stirpe F: **Ribosome-inactivating proteins from plants.** *BBA - Reviews on Biomembranes* 1993, **1154**(3-4):237-282.
146. Bolognesi A, Bortolotti M, Maiello S, Battelli MG, Polito L: **Ribosome-Inactivating Proteins from Plants: A Historical Overview.** *Molecules* 2016, **21**(12).
147. Reyes AG, Anne J, Mejia A: **Ribosome-inactivating proteins with an emphasis on bacterial RIPs and their potential medical applications.** *Future Microbiol* 2012, **7**(6):705-717.
148. Herrero-Galán E, Álvarez-García E, Carreras-Sangrà N, Lacadena J, Alegre-Cebollada J, Martínez del Pozo Á, Oñaderra M, Gavilanes JG: **Fungal ribotoxins: structure, function and evolution.** In: *Microbial Toxins: Current Research and Future Trends.* 2009: 167-187.
149. Olombrada M, Lázaro-Gorines R, López-Rodríguez J, Martínez-del-Pozo Á, Oñaderra M, Maestro-López M, Lacadena J, Gavilanes J, García-Ortega L: **Fungal Ribotoxins: A Review of Potential Biotechnological Applications.** *Toxins* 2017, **9**:71.
150. Iglesias R, Cidores L, Ferreras JM: **Ribosomal RNA N-glycosylase activity assay of ribosome-inactivating proteins.** *Bio Protoc* 2017, **7**:e2180.
151. Olmo N, Turnay J, Gonzalez de Buitrago G, Lopez de Silanes I, Gavilanes JG, Lizarbe MA: **Cytotoxic mechanism of the ribotoxin alpha-sarcin. Induction of cell death via apoptosis.** *Eur J Biochem* 2001, **268**(7):2113-2123.
152. Martínez-Ruiz A, Kao R, Davies J, Martínez del Pozo A: **Ribotoxins are a more widespread group of proteins within the filamentous fungi than previously believed.** *Toxicon* 1999, **37**(11):1549-1563.
153. Jennings JC, Olson BH, Roga V, Junek AJ, Schuurmans DM: **ALPHA SARCI, A NEW ANTITUMOR AGENT. II. FERMENTATION AND ANTITUMOR SPECTRUM.** *Applied microbiology* 1965, **13**:322-326.

Chapter 1

154. Olson BH, Goerner GL: **ALPHA SARCIN, A NEW ANTITUMOR AGENT. I. ISOLATION, PURIFICATION, CHEMICAL COMPOSITION, AND THE IDENTITY OF A NEW AMINO ACID.** *Applied microbiology* 1965, **13**:314-321.
155. Endo Y, Wool IG: **The site of action of alpha-sarcin on eukaryotic ribosomes. The sequence at the alpha-sarcin cleavage site in 28 S ribosomal ribonucleic acid.** *J Biol Chem* 1982, **257**(15):9054-9060.
156. Roga V, Hedeman LP, Olson BH: **Evaluation of mitogillin (NSC-69529) in the treatment of naturally occurring canine neoplasms.** *Cancer chemotherapy reports Part 1* 1971, **55**(2):101-113.
157. Rodriguez R, Lopez-Otin C, Barber D, Fernandez-Luna JL, Gonzalez G, Mendez E: **Amino acid sequence homologies in alfa-sarcin, restrictocin and mitogillin.** *Biochemical and Biophysical Research Communications* 1982, **108**(1):315-321.
158. Fernandez-Luna JL, Lopez-Otin C, Soriano F, Mendez E: **Complete Amino Acid Sequence of the Aspergillus Cytotoxin Mitogillin.** *Biochemistry-US* 1985, **24**(4):861-867.
159. Kao R, Martínez-Ruiz A, Del Pozo AM, Crameri R, Davies J: **Mitogillin and related fungal ribotoxins.** In: *Methods in Enzymology*. vol. 341; 2001: 324-335.
160. Mazet I, Vey A: **Hirsutellin A, a toxic protein produced in vitro by Hirsutella thompsonii.** *Microbiology* 1995, **141**(6):1343-1348.
161. Olombrada M, Medina P, Budia F, Gavilanes JG, Martínez-Del-Pozo A, García-Ortega L: **Characterization of a new toxin from the entomopathogenic fungus Metarhizium anisopliae: The ribotoxin anisoplin.** *Biological Chemistry* 2017, **398**(1):135-142.
162. Herrero-Galán E, Lacadena J, Del Pozo ÁM, Boucias DG, Olmo N, Oñaderra M, Gavilanes JG: **The insecticidal protein hirsutellin A from the mite fungal pathogen Hirsutella thompsonii is a ribotoxin.** *Proteins: Structure, Function and Genetics* 2008, **72**(1):217-228.
163. Maimala S, Tartar A, Boucias D, Chandrapatya A: **Detection of the toxin Hirsutellin A from Hirsutella thompsonii.** *Journal of Invertebrate Pathology* 2002, **80**(2):112-126.
164. Landi N, Pacifico S, Ragucci S, Iglesias R, Piccolella S, Amici A, Di Giuseppe AMA, Di Maro A: **Purification, characterization and cytotoxicity assessment of Ageritin: The first ribotoxin from the basidiomycete mushroom Agrocybe aegerita.** *Biochimica et Biophysica Acta - General Subjects* 2017, **1861**:1113-1121.
165. Gasset M, Mancheño JM, Lacadena J, Turnay J, Olmo N, Lizarbe MA, Martínez Del Pozo A, Oñaderra M, Gavilanes JG: **α -Sarcin, a ribosome-inactivating protein that translocates across the membrane of phospholipid vesicles.** *Curr Top Pept Protein Res* 1994, **1**:99-104.
166. Korenykh AV, Piccirilli JA, Correll CC: **The electrostatic character of the ribosomal surface enables extraordinarily rapid target location by ribotoxins.** *Nat Struct Mol Biol* 2006, **13**(5):436-443.
167. García-Mayoral MF, Martínez Del Pozo Á, Campos-Olivas R, Gavilanes JG, Santoro J, Rico M, Laurents DV, Bruix M: **pH-dependent conformational stability of the ribotoxin α -sarcin and four active site charge substitution variants.** *Biochemistry-US* 2006, **45**(46):13705-13718.
168. Viegas A, Herrero-Galán E, Oñaderra M, MacEdo AL, Bruix M: **Solution structure of hirsutellin A - New insights into the active site and interacting interfaces of ribotoxins.** *FEBS Journal* 2009, **276**(8):2381-2390.
169. Olombrada M, Herrero-Galán E, Tello D, Oñaderra M, Gavilanes JG, Martínez-Del-Pozo Á, García-Ortega L: **Fungal extracellular ribotoxins as insecticidal agents.** 2013.
170. Olombrada M, Martínez-Del-Pozo Á, Medina P, Budia F, Gavilanes JG, García-Ortega L: **Fungal ribotoxins: Natural protein-based weapons against insects.** *Toxicon* 2014, **83**:69-74.

Chapter 1

171. Marheineke K, Grünwald S, Christie W, Reilander H: **Lipid composition of Spodoptera frugiperda (Sf9) and Trichoplusia ni (Tn) insect cells used for baculovirus infection.** *Febs Lett* 1998, **441**(1):49-52.
172. Fernández-Puentes C, Carrasco L: **Viral infection permeabilizes mammalian cells to protein toxins.** *Cell* 1980, **20**(3):769-775.
173. Otero MJ, Carrasco L: **Exogenous phospholipase C permeabilizes mammalian cells to proteins.** *Experimental Cell Research* 1988, **177**(1):154-161.
174. Martínez-Ruiz A, García-Ortega L, Kao R, Lacadena J, Oñaderra M, Mancheño JM, Davies J, Martínez del Pozo A, Gavilanes JG: **RNase U2 and α -sarcin: A study of relationships.** In: *Methods in Enzymology*. vol. 341; 2001: 335-351.
175. Endo Y, Oka T, Tsurugi K, Natori Y: **The biosynthesis of a cytotoxic protein, alpha-sarcin, in a mold Aspergillus giganteus. I. Synthesis of prepro- and pro-alpha-sarcin in vitro.** *Tokushima Journal of Experimental Medicine* 1993, **40**(1-2):1-6.
176. Brandhorst T, Kenealy WR: **Effects of leader sequences upon the heterologous expression of restrictocin in Aspergillus nidulans and Aspergillus niger.** *Canadian Journal of Microbiology* 1995, **41**(7):601-611.

Chapter 2

Combining microfluidics and RNA-sequencing to assess the inducible defensome of a mushroom against nematodes

Annageldi Tayyrov¹, Claire E. Stanley², Sophie Azevedo¹, Markus Künzler^{1*}

¹Institute of Microbiology, Department of Biology, ETH Zürich, Vladimir-Prelog-Weg 4, CH-8093 Zürich, Switzerland

²Agroecology and Environment Research Division, Agroscope, Reckenholzstrasse 191, CH-8046 Zürich, Switzerland

* Correspondence: mkuenzle@ethz.ch

Manuscript submitted to BMC Genomics.

Contributions:

- Sample preparation for RNA-sequencing and 16s rRNA sequencing
- Transcriptome and microbiome data analysis
- Identification, cloning and expression of P450139
- Part of the toxicity assays

Chapter 2

Abstract:

Background: Fungi are an attractive source of nutrients for predators. As part of their defense, some fungi are able to induce the production of anti-predator protein toxins in response to predation. A previous study on the interaction of the model mushroom *Coprinopsis cinerea* by the fungivorous nematode *Aphelenchus avenae* on agar plates has shown that this fungal defense response is most pronounced in the part of the mycelium that is in direct contact with the nematode. Hence, we hypothesized that, for a comprehensive characterization of this defense response, an experimental setup that maximizes the zone of direct interaction between the fungal mycelium and the nematode, was needed.

Results: In this study, we conducted a transcriptome analysis of *C. cinerea* vegetative mycelium upon challenge with *A. avenae* using a tailor-made microfluidic device. The device was designed such that the interaction between the fungus and the nematode was confined to a specific area and that the mycelium could be retrieved from this area for analysis. We took samples from the confrontation area after different time periods and extracted and sequenced the poly(A)⁺ RNA thereof. The identification of 1229 differentially expressed genes (DEGs) shows that this setup profoundly improved sensitivity over co-cultivation on agar plates where only 37 DEGs had been identified. The product of one of the most highly upregulated genes shows predicted structural homology to bacterial pore-forming toxins, and revealed strong toxicity to various bacterivorous nematodes. In order to explain the overlap of the antinematode defensome with a previously defined antibacterial defensome of *C. cinerea*, bacteria associated with the fungivorous nematode *A. avenae* were profiled with 16S rRNA deep sequencing.

Conclusions:

The use of a novel experimental setup for the investigation of the defense response of a fungal mycelium to predation by fungivorous nematodes resulted in the identification of a comprehensive set of DEGs and the discovery of a novel type of fungal defense protein against nematodes. The bacteria found to be associated with the fungivorous nematode are a possible explanation for the induction of some antibacterial defense proteins upon nematode challenge.

Chapter 2

Introduction

In their ecological environment, fungi are exposed to a variety of organisms including predators that use fungi as a food source [1]. Significant predators of fungi include mollusks, insects, collembola and nematodes [1-3]. During evolution, fungi have developed several defense lines to protect themselves against these predators. These defense lines can be categorized into three groups; physical barriers [4, 5], secondary metabolites [6, 7] and peptides/proteins [8, 9]. Amongst defense proteins, biotin-binding proteins [10], protease inhibitors [11], pore-forming proteins [12], ribotoxins [13], and lectins [14] have been characterized. While defense proteins against competitors tend to be secreted, protein toxins against predators are usually stored in the cytoplasm [15].

Given the diversity of antagonists that fungi need to combat, the list of characterized fungal defense proteins is most likely not complete. Hence, determining the complete set of defense effectors (defensome) of a fungus would help to attain a clearer picture of the chemical defense capacity of these organisms. Earlier studies have shown that genes encoding for fungal defense effectors can be induced upon challenge of a fungus with its antagonists and, thus, it is possible to identify novel defense effectors on the basis of differential gene expression [16-19].

Previous studies on the antagonistic interaction between the coprophilous model basidiomycete *Coprinopsis cinerea* and the fungivorous nematode *Aphelenchus avenae* have shown that induction of fungal defense genes is limited to the part of the mycelium that is in direct contact with the worm (Schmieder et al. in revision). Hence, for the identification of the complete set of genes of a multicellular fungus that is differentially expressed upon challenge with this type of predator, it is crucial to use an experimental setup that maximizes the area of direct interaction between the mycelium and the nematode and allows retrieval of the fungus from that area. In this respect, previously used co-cultivation methods on agar plates are not ideal [19]. As a solution, a tailor-made microfluidic device, referred to as fungus-nematode interaction (FNI) device, that allows confrontation between the fungus and the fungivorous nematode in a confined area and retrieval of the organisms from this area for analysis was developed. We used this setup to identify the inducible defensome of *C. cinerea* against the fungivorous nematode *A. avenae* by RNA-sequencing. The induced defensome contained several putative defense proteins, including a previously undetected putative β-pore-forming toxin which showed strong nematotoxicity when heterologously expressed in *Escherichia coli* and tested for toxicity towards several bacterivorous nematodes. This result suggests that the bacterial cytolysin-like toxin of *Coprinopsis cinerea* may represent a novel type of fungal effector proteins against nematodes. Furthermore, we identified the composition of bacteria associated with the nematode *Aphelenchus avenae*. To the best of our knowledge, this is the first study to profile the microbiome of a fungivorous nematode.

2. Materials and Methods

2.1 Strains and cultivation conditions

Self-compatible AmutBmut strain of *Coprinopsis cinerea* was maintained on YMG (0.4% (w/v) yeast extract, 1% (w/v) malt extract, 0.4% (w/v) glucose, 1.5% (w/v) agar) at 37 °C in humid dark chambers. The nematode *Aphelenchus avenae* was propagated on a sporulation-deficient strain (BC-3) [20] of the ascomycetous mold *Botrytis cinerea* on malt extract agar medium (MEA) supplemented with additional 15 g/L agar and 100 µg/ml chloramphenicol at 20 °C. All organisms used in this study are listed in Table S1.

2.2 Challenge experiment setup and total RNA extraction

The fungus-nematode challenge was performed in tailor-made microfluidic device as previously described [21] with some modifications (Schmieder et al. in revision). Briefly, freshly prepared microfluidic devices were filled with 100 µl liquid YMG medium and inoculated with a small *C. cinerea* plug that was cut from precultivated mycelium on YMG agar plates at 37 °C for three days. The inoculated devices were incubated at 37 °C for 30 h in a humid dark chamber. The nematodes were harvested from *B. cinerea* plates by Baermann funneling [22] and purged by letting them crawl on water agar plates containing 50 µg/ml gentamycin, 50 µg/ml nystatin and 100 µg/ml ampicillin to eliminate potential fungal and bacterial contaminants. Around ten purged worms were added to the confrontation areas of the microfluidic devices at three different time points. Adding the nematodes at the different time points made it possible to harvest all samples at the same time having the fungus cultivated for the same but challenged for different time periods (Fig. S1). Cocultivations were performed in three biological replicates at 20 °C in the dark. Mycelium was retrieved from the confrontation area upon three different confrontation periods i.e. 2 h, 8 h and 20 h, in the presence and absence (i.e. controls) of the predator nematode, using a sterile pipette. RNA of all samples was extracted using the Norgen RNA extraction kit according to the manufacturer's protocol (Norgen Bioteck Corporation, Canada).

2.3 RNA-sequencing and bioinformatics analysis

The concentration and quality of the isolated RNA samples were determined using a Qubit® (1.0) Fluorometer (Life Technologies, California, USA) and a Bioanalyzer 2100 (Agilent, Waldbronn, Germany), respectively. Samples with a 260nm/280nm ratio between 1.8–2.1 and a 28S/18S ratio within 1.5–2 were further processed. Transcriptome library preparation was performed at the

Chapter 2

Functional Genomics Center Zurich (FGCZ) using the TruSeq RNA Sample Prep Kit v2 (Illumina Inc, California, USA) following the manufacturers' protocols. Briefly, total RNA samples (100-1000 ng) were enriched for poly(A)⁺ RNA and then reverse-transcribed into double-stranded cDNA. The cDNA sample was fragmented, end-repaired and polyadenylated before ligation of TruSeq adapters containing the index for multiplexing. Fragments containing TruSeq adapters on both ends were selectively enriched with PCR. The quality and quantity of the enriched libraries were validated using Qubit® (1.0) Fluorometer and the Caliper GX LabChip® GX (Caliper Life Sciences, Inc., USA). Sequencing was performed on the Illumina HiSeq 2000 single end 100 bp using the TruSeq SBS Kit v3-HS (Illumina, Inc, California, USA).

The data was analyzed using the SUSHI platform [23], which was developed at FGCZ and supports variety of open source 'omics' data analysis packages. In brief, reads were aligned with STAR aligner [24] with the additional options (--outFilterMatchNmin 30 --outFilterMismatchNmax 5 --outFilterMismatchNoverLmax 0.05 --outFilterMultimapNmax 50) which requires at least 30 bp matches, and at most 5 mismatches with less than overall 5% of mismatches were allowed. Reads with more than 50 multiple alignments with the genome were filtered out. The *C. cinerea* AmutBmut genome (2013-07-19) together with its latest annotation v1.0 (2016-09-12, filtered gene models) from the Joint Genome Institute (JGI) were used as a reference [25]. The Bioconductor featureCounts function were run to compute expression counts [26]. DESeq2 analysis package was used for differential expression analysis [27].

Genes were considered significantly differentially expressed if they had at least a four-fold change in nematode-treated samples compared to the control samples and a false discovery rate (FDR) of at most 0.05. In addition, 10 reads/locus were taken as a minimal threshold for gene expression. SignalP v4.1 [28], and TMHMM v.2.0 [29] were used for the detection of signal peptides and transmembrane domain of proteins, respectively. PFAM-A v31 [30] and Gene Ontology (GO) [31] databases were used for putative functional annotations. Visualization of the abundance of specific PFAM domain annotation terms was generated using Wordle [32].

2.4 Analysis of nematode-associated bacteria using 16S rRNA sequencing

A. avenae was cultured on MEA agar plates preseeded with *Botrytis cinerea* as food. After two weeks, nematodes were harvested by Baermann funneling [22] under sterile conditions. Nematodes were ground in liquid nitrogen using a pellet pestle in 1.5 ml sterile Eppendorf tubes. Thereafter, the total (nematode+bacteria) genomic DNA was isolated with E.Z.N.A. Mollusc DNA Kit (Norcross, OMEGA, USA) based on manufacturer's instruction.

Chapter 2

To sequence the V4 region of the bacterial 16S rRNA gene, two-step PCR libraries using the primer pair 515F (5'- GTG CCA GCM GCC GCG GTA A -3') and 806R (5'- GGA CTA CHV GGG TWT CTA AT -3') were created. Subsequently the Illumina MiSeq platform and a v2 nano 500 cycles kit were used to sequence the PCR libraries. The produced paired-end reads which passed Illumina's chastity filter were subject to de-multiplexing and trimming of Illumina adaptor residuals using Illumina's real time analysis software (no further refinement or selection). The quality of the reads was checked with the software FastQC version 0.11.5. The locus specific V34 adaptors were trimmed from the sequencing reads with the software cutadapt v1.14. Paired-end reads were discarded if the adaptor could not be trimmed. Trimmed forward and reverse reads of the paired-end reads were merged considering a minimum overlap of 15 bases using the software USEARCH version 10.0.240 [33]. Merged sequences were then quality filtered allowing a maximum of one expected error per merged read and also discarding those containing ambiguous bases. The remaining reads were denoised using the UNOISE algorithm implemented in USEARCH to form operational taxonomic units (OTUs) discarding singletons and chimeras in the process. OTUs were aligned against the reference sequences of the RDP 16S database [34] and taxonomies were predicted considering a minimum confidence threshold of 0.7 using the SINTAX algorithm implemented in USEARCH. Alpha diversity calculations and rarefaction analysis were performed with the software phyloseq v1.16.2 [35]. The libraries, sequencing and data analysis described in this section were performed by Microsynth AG (Balgach, Switzerland). Generated nucleotide sequences were deposited at NCBI SRA database under the accession number SRP152111.

2.5 Cloning and heterologous expression of P450139-encoding cDNA

First strand cDNA was synthesized from 1 µg total RNA of nematode-induced *C. cinerea* AmutBmut using Transcriptor first strand cDNA synthesis kit (Roche) following the manufacturer's protocol. The coding region of P450139 (JGI MycoCosm ProteinID) was amplified from first strand cDNA using the P450139forNdeI and P450139revNotI primer pair (Table S2). The PCR product was cloned into expression vector pET24b (Novagen) using *Not*I and *Nde*I restriction sites. The constructed plasmid was transformed into the chemo-competent *E. coli* DH5 α cells. The sequence of the plasmid was verified by DNA-sequencing and the plasmid was transformed into *E. coli* BL21 cells for expression. Colonies were cultured in LB medium containing 50 mg/l kanamycin at 37 °C until OD600 0.5 and induced with 0.5 mM isopropyl β-D-1-thiogalactopyranoside (IPTG) at 16 °C for 24 h. Expression and solubility of the protein were assessed as previously described [36].

Chapter 2

2.6 Toxicity of P450139 against nematodes and insects

To assess the toxicity of P450139 protein against nematodes, eggs were isolated from five species of bacterivorous nematodes (*Caenorhabditis elegans*, *Caenorhabditis briggsae*, *Caenorhabditis tropicalis*, *Halicephalobus gingivalis*, *Pristionchus pacificus*) (Table S1) based on wormbook guidelines [37]. The nematodes were precultivated on NGM plates (2.5 g/L peptone, 50 mM NaCl, 1.7% agar and 13 mM cholesterol) seeded with *E. coli* OP50. Eggs were isolated by bleaching gravid hermaphrodites and hatched on 1% water agar plates overnight at 20 °C. Synchronized L1 stage larvae were collected in PBS and adjusted to 10-15 nematodes/10 µl. *E. coli* BL21 containing plasmids directing the heterologous expression of P450139, CGL2 and “empty” vector (EV) were preinduced with IPTG as described above. The CGL2-expressing plasmid and EV were used as positive and negative controls, respectively. 20 µl of number-adjusted L1 nematodes were incubated in 100 µl of PBS adjusted to OD₆₀₀ 2.0 of preinduced *E. coli* BL21 cells in a 96 well plate as described before [36]. The plate was incubated for 48 h at 20 °C for all nematodes except for *H. gingivalis* (72 h). The percentage of nematodes that developed into L4 larvae or adulthood were counted. All treatments were performed in three biological replicates. Dunnett's multiple comparisons test was used for statistical analysis. Furthermore, toxicity of P450139 towards *Aedes aegypti* larvae was tested as previously described [36].

2.7 Tagging and purification of P450139

To perform the *in vitro* hemolytic activity assay, P450139 was tagged at N-terminus with 8 His-residues and purified on Ni-NTA columns as described previously [38]. In brief, the parental P450139-encoding pET-24b plasmid was amplified with P450139forHis8 and P450139revHis8 primers (Table S2). The PCR product was treated with DpnI to eliminate the methylated template plasmid. 5 µl of DpnI-treated PCR product was transformed into *E. coli* DH5a for plasmid purification and subsequent sequencing. The plasmid with expected sequence was transformed into *E. coli* BL21 for expression and purification. The protein was expressed as described above for the untagged variant of the protein. The bacterial cells were harvested by centrifugation and resuspended in cold lysis buffer (50 mM PBS, 20 mM imidazole, pH 8.5) before being lysed using French press. The cell lysate was spun at 16000 rpm for 30 min at 4 °C and the supernatant containing the soluble fraction was incubated with Ni-NTA beads (Macherey-Nagel) for 1 h at 4 °C. The protein bound to the beads was washed with lysis buffer and subsequently eluted with lysis buffer supplemented with 250 mM imidazole. The eluate was desalted and concentrated on PD10 column (GE healthcare).

Chapter 2

2.8 Hemolysis assay for P450139

Defibrinated horse blood (Thermo Fisher) was washed three times with PBS by spinning down for 15 minutes at 4500 g in between. Two different concentrations (2 and 0.2 mg/mL) of the purified P450139 protein was added to 100 µl of the washed blood. The hemolysis reaction was incubated for one hour at room temperature followed by centrifugation for 10 minutes at 2400 g. The supernatant was transferred to a clear bottom 96-well plate and absorbance was measured at room temperature using a microplate reader (SpectraMax Plus, Molecular Devices Corp.) at OD₄₅₀. Bovine serum albumin (Sigma-Aldrich[®]) and 10% triton™ X-100 (Sigma-Aldrich[®]) were used as negative and positive controls, respectively. All treatments were performed in triplicates.

3. Results

3.1 Differentially expressed genes (DEGs) of *C. cinerea* in response to cocultivation with *A. avenae* for different time periods

To determine the defensome of a fungus against a fungivorous nematode, we sequenced the transcriptome of *C. cinerea* challenged with *A. avenae* using the FNI device. In order to gain an insight into the dynamics of the fungal defense response, DEGs were analyzed after three different time periods of cocultivation of the fungal mycelium with the fungivorous nematode. Strand specific RNA-seq libraries were prepared for three biological replicates of each cocultivation period and sequenced using the Illumina HiSeq 2000 platform.

For every sample, over 30 million reads (100 bp) were generated, and 83-88% of all generated reads mapped to the 37.5 Mb genome of *C. cinerea* AmutBmut. The percentage of the genomic features with at least 10 mapped reads were around 80% for all samples (Table S3). The *C. cinerea* genome contains 14242 predicted protein-encoding genes according to the JGI MycoCosm (May 2018) [39]. Thus, the 80% roughly represent 11400 of the predicted protein-encoding genes. These genes were considered transcribed. The significance of differential gene expression of *C. cinerea* was assessed by comparing the DESeq2 normalized read values of the various samples. Upon nematode challenge of 2 h, 8 h and 20 h, 66, 897 and 673 genes were significantly differentially expressed ($FDR \leq 0.05$ AND $|Fold change| \geq 4$), respectively, when compared to the control. Most of the DEGs (1024 out of 1229) were upregulated while only 17% of the DEGs were downregulated in the presence of nematodes (Fig. 1a-c). Roughly, 50% of DEGs (549) could be assigned to a PFAM domain (Table S4 - available in the online version). The majority of the annotated genes were assigned as a DUF (domain of unknown function). Visualization of enriched annotations showed that proteins with a functional domain of such as cytochrome P450 [40], galbindlectin [41], phagelysozyme [42], ceratoplatanin [43], which are known to be involved in the defense response of fungi against biotic and abiotic stresses, were enriched in the set of upregulated genes (Fig. S2). In addition, the upregulated set of the genes included previously characterized cytoplasmic nematotoxic proteins CGL2, CCL2 and CCTX2 (Table S4 – available in the online version) [19, 38]. The transcriptomics data is available at the ArrayExpress database under the accession number E-MTAB-7005.

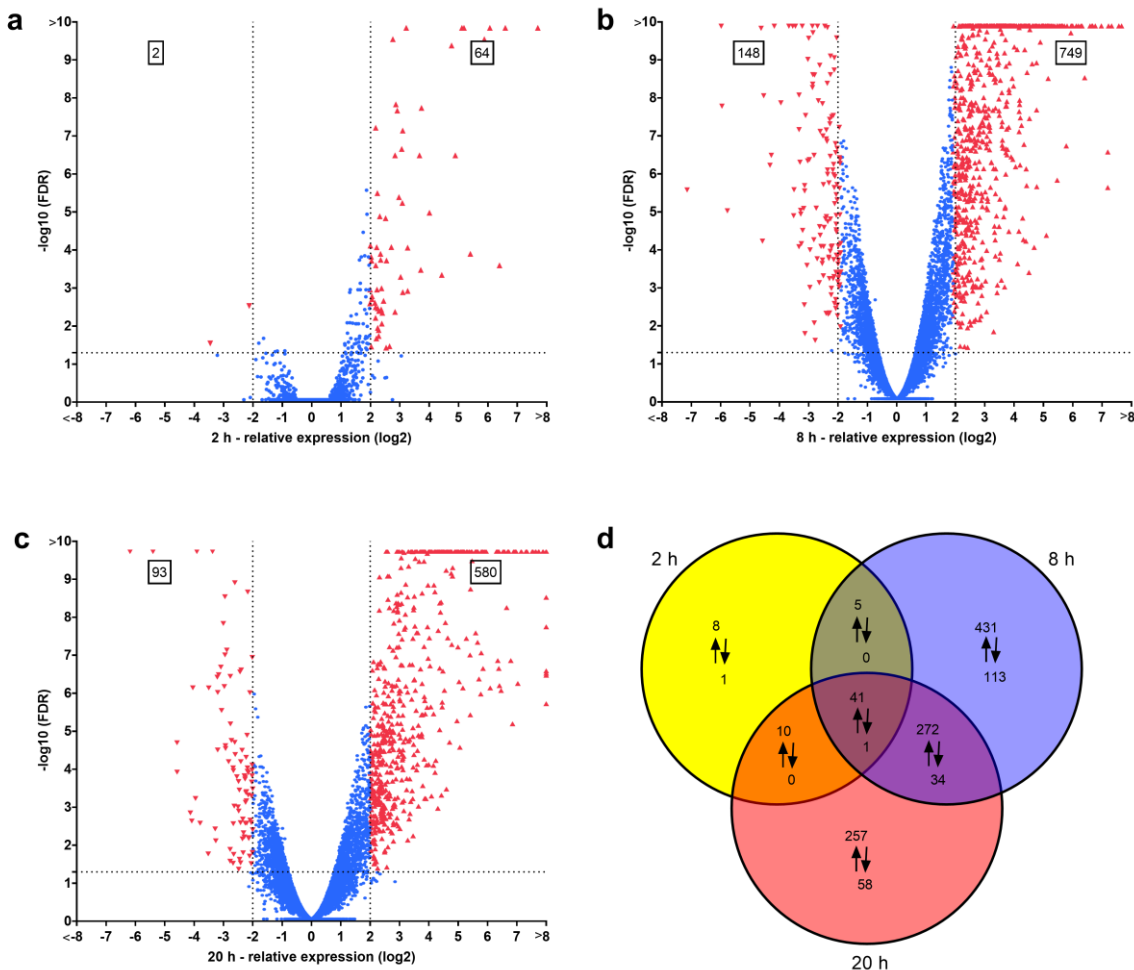


Figure 1: Differentially expressed genes (DEGs) of *C. cinerea* challenged by *A. avenae* for different time periods. Volcano plots showing DEGs in relation to FC (Fold change) and FDR (False discovery rate) for (a) 2 h nematode challenge vs. unchallenged control, (b) 8 h nematode challenge vs. unchallenged control, (c) 20 h nematode challenge vs. unchallenged control. Each gene is represented with a single data point. Genes with at least four fold change and FDR < 0.05 are colored red and considered significantly upregulated (upward triangles) or downregulated (downward triangles). (d) Venn diagram showing significantly upregulated (\uparrow) and downregulated (\downarrow) genes due to nematode challenge for each time point vs. unchallenged control. Overlapping areas represent DEGs common to different time points.

Chapter 2

3.2 Comparison between microfluidics- and agar-based challenges of *C. cinerea* with *A. avenae*

We hypothesized, based on a previous study (Schmieder et al., in revision), that performing the fungus-nematode challenge in the FNI device would allow us to collect and analyze samples from sections of the fungal mycelium that are highly induced. In agreement with this hypothesis, the transcriptome analysis of the microfluidics-based challenge yielded, in comparison to a previous agar-based challenge [19], a substantially higher number of differentially expressed genes (Fig. 2a). In addition, the fold change of almost all genes that had already been found to be differentially expressed on agar, was significantly higher when the confrontation was performed in the microfluidic device (Fig. 2b and 2c).

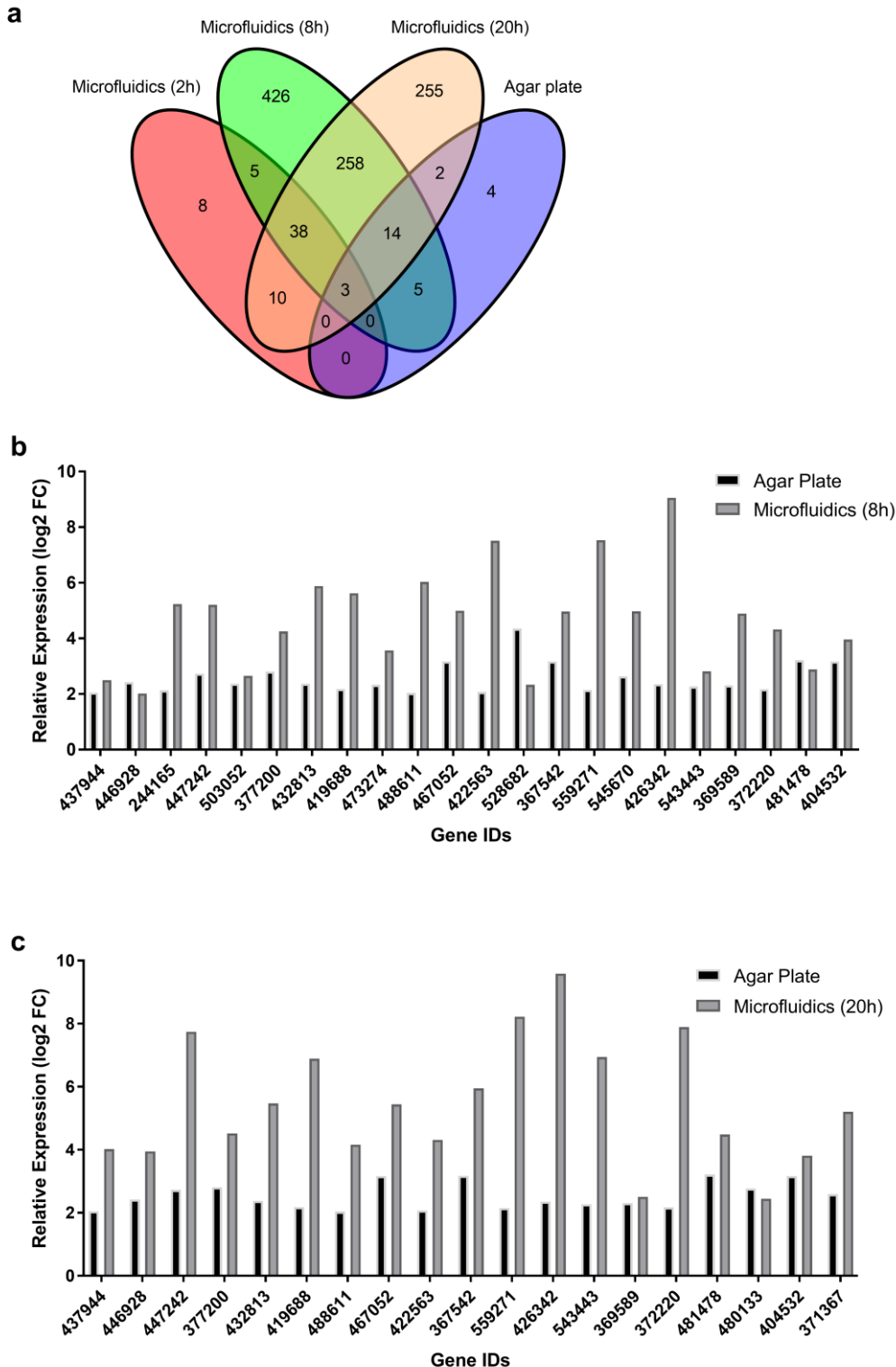


Figure 2: Comparison between microfluidics and agar-based confrontation of *C. cinerea* and *A. avenae*. (a) Venn diagram representing significantly upregulated genes for two different setups (microfluidic device and agar plate). (b) 20 out of 22 DEGs shared between microfluidics-8h and agar plate assay have higher relative expression in microfluidics compared to agar plate. (c) 18 of 19 DEGs shared between microfluidics-20h and agar plate assay reveal a higher relative expression in the microfluidic devic . Genes with fold change of ≥ 4 and FDR ≤ 0.05 considered as significantly induced.

Chapter 2

3.3 Diversity of *Aphelenchus avenae*-associated bacteria

The obtained 1229 DEGs of the current study were compared to our previous RNA-sequencing data (784 DEGs) of *C. cinerea* mycelium challenged with *E. coli* and *B. subtilis* [42]. More than half of the genes that were upregulated due to bacteria-challenge were also found to be upregulated in our current nematode-challenge dataset (Fig. 3a). Based on these findings, we analyzed the fungivorous nematode for naturally associated bacteria which could be responsible for the upregulation of antibacterial genes in *C. cinerea*. While there are several studies on associated bacteria of bacterivorous [44, 45], animal parasitic [46] and plant pathogenic nematodes [47-55], to our knowledge there is only one study on the diversity of bacteria associated with a fungivorous nematode *Aphelenchus* sp. [56]. However, in the latter study, only five OTUs could be detected.

In this study, we determined the diversity of the bacteria associated with *A. avenae* by high-throughput sequencing of their 16S rDNA. The nematodes were cultured on *Botrytis cinerea* for two weeks. Thereafter, the worms were isolated under sterile conditions and total DNA was extracted. The libraries were prepared from six biological replicates. Sequencing was performed on the Illumina MiSeq platform. The analyses yielded a total of 47672 high quality reads with an average of 7945 reads per sample. The reads were clustered into OTUs in USEARCH. The distributed numbers of identified OTUs ranged from 18 to 23 for six samples. 17 of the distributed OTUs were common for all samples while 21 OTUs were found in more than half of the samples (Fig. 3b). The rarefaction curves for all samples were flattened within the obtained sequencing depth (Fig. 3c), indicating that the sampling was reasonable and able to represent the majority of the bacterial community associated with the fungivorous nematode.

The generated OTUs were searched against reference sequences of the RDP 16S database, and predicted taxonomical units were assigned (Table S5). The biological replicates were generally consistent (Fig. S3). Bacteria associated with the fungivorous nematode were classified into four taxonomical phyla where the predominant phyla of all samples were Proteobacteria and Bacteroidetes (Fig. 3d). The Proteobacteria were mostly Gammaproteobacteria and Betaproteobacteria (Fig. 3e). At genus level, *Coxiella*, *Halomonas*, *Escherichia/Shigella*, *Herbaspirillum* altogether make up the majority of the assigned bacteria whereas the proportion of unassigned OTUs was 34% on average per sample at this taxonomic level (Fig. S3).

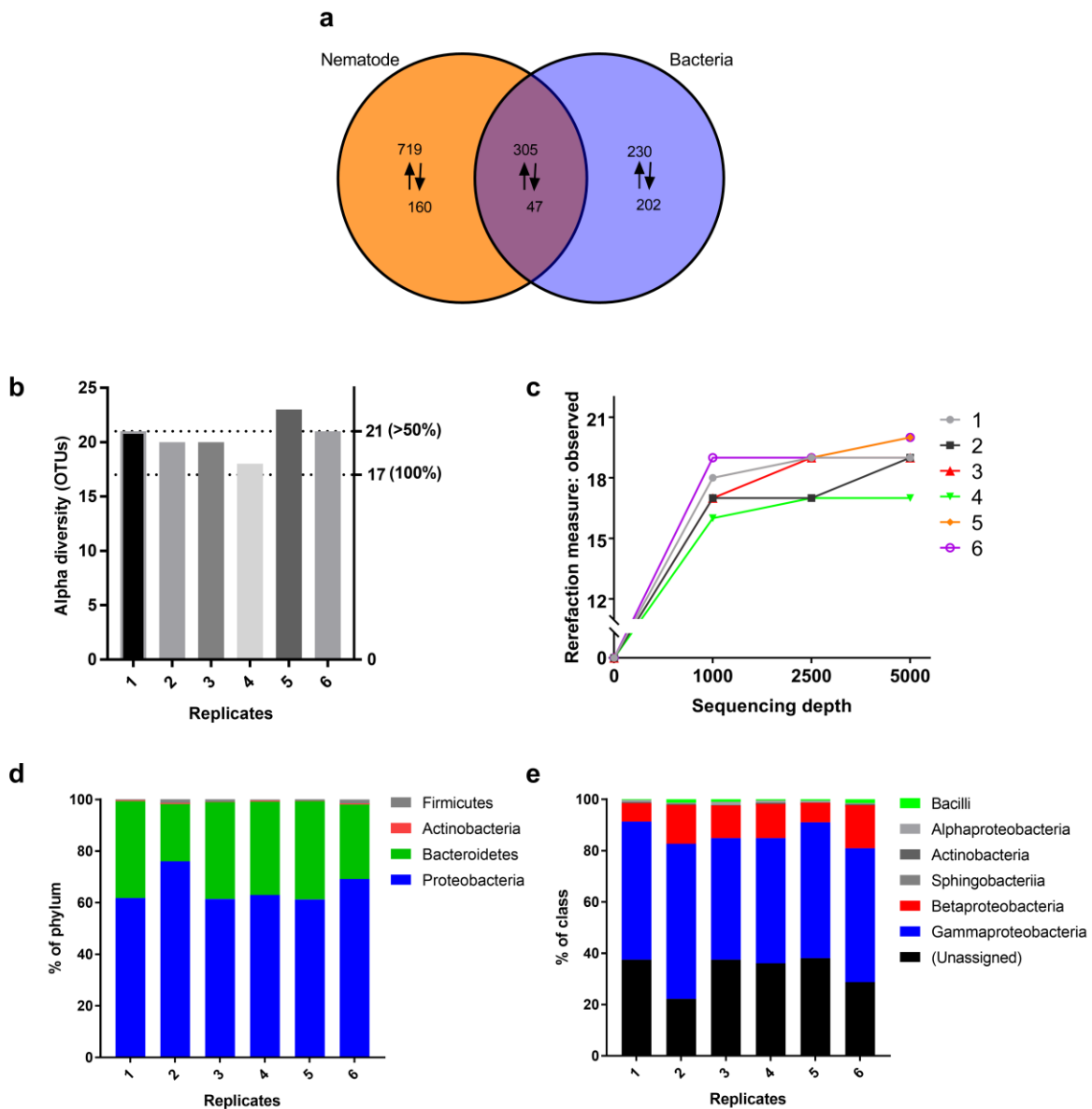


Figure 3: Associated bacteria of fungivorous nematode *A. avenae*. (a) Venn diagram showing significantly upregulated (\uparrow) and downregulated (\downarrow) genes of *C. cinerea* in response to nematode (present study) and bacteria (previous study) challenges. Genes with fold change of ≥ 4 and FDR ≤ 0.05 considered as significantly upregulated while genes with fold change of ≤ -4 and FDR ≤ 0.05 considered as significantly downregulated (b) Assigned OTU numbers for associated bacteria of *Aphelenchus avenae* for each biological replicate. (c) Rarefaction analysis of observed OTUs of nematode-associated bacteria. The relative abundance of the bacterial composition of the nematode at phylum (d) and class (e) levels.

Chapter 2

3.4 P450139 is a nematode-inducible nematotoxic protein with a putative hemolysin domain

The *C. cinerea* gene coding for the predicted protein P450139 showed a similar expression pattern as the previously characterized nematotoxic lectin CGL2 (Fig. 4a), suggesting that the gene products may have similar functions. Furthermore, a homology search at HHpred (Homology detection & structure prediction by HMM-HMM comparison) [57] indicated a similarity of the protein to bacterial β-pore-forming toxins, i.e. leukocidins (*Staphylococcus aureus*) [58] and hemolysin (*Vibrio cholera*) [59], as top hits with significantly high probabilities (Table 1). Based on this data, the cDNA of P450139 from *C. cinerea* was cloned and heterologously expressed in *E. coli* for further investigation. For the purification of the protein, an 8-histidine tag was introduced at the N-terminus of P450139. The heterologous expression and solubility of the untagged and tagged proteins were evaluated. Both protein variants were well expressed but their solubility was low (Fig. S4).

Table 1 The P450139 amino acid sequence was analyzed using HHpred server. Similarities were found for internal 75 amino acids (110-185).

#	Hit IDs	Annotation	Toxin type	Organism	Probability*	Template HMM
1	4IYA_A	S component leucocidin	Pore-forming toxin	<i>Staphylococcus aureus</i>	85.9	85-151 (292)
2	4Q7G_A	Leucotoxin LukDv	Pore-forming toxin	<i>Staphylococcus aureus</i>	71.8	104-173 (324)
3	4TW1_J	LUKG, LUKH; leukocidin;	Pore-forming toxin	<i>Staphylococcus aureus</i>	71.6	110-177 (324)
4	1XEZ_A	Hemolysin	Pore-forming toxin	<i>Vibrio cholerae</i>	70.5	258-332 (721)
5	7AHL_E	Alpha-hemolysin cytolytic protein	Pore-forming toxin	<i>Staphylococcus aureus</i>	66.1	83-154 (293)
6	4I0N_A	Necrotic enteritis toxin B	Pore-forming toxin	<i>Clostridium perfringens</i>	62.9	84-155 (289)

* Cut-off: > 50% probability

The soluble recombinant 8-histidine-tagged P450139 protein was purified over Nickel NTA. The purity of the purified protein was verified by SDS-PAGE and Coomassie blue staining (Fig. S4).

To check whether P450139 is toxic against nematodes, recombinant bacteria producing the protein were fed to five different species of bacterivorous nematodes. Impairment of nematode larval development was assessed after 48 h. *C. elegans*, *C. briggsae*, *C. tropicalis* and *P. pacificus* showed susceptibility to P450139 while the development of *H. gingivalis* larvae was not inhibited by the recombinant fungal protein (Fig. 4b, Fig. 4c).

Chapter 2

To test whether P450139 is active against insects, its toxicity was assessed by feeding the recombinant bacteria to *A. aegypti* larvae. The mosquito larvae were not impaired in their development by this food, indicating that the fungal protein does not have insecticidal activity (Fig. 4c).

Finally, the hemolytic activity of P450139 towards horse erythrocytes was assessed. For this purpose, the cells were incubated with different concentrations of the His8-tagged purified protein, pelleted and the OD₄₅₀ of the supernatant was measured. P450139 did not cause any apparent lysis of horse erythrocytes (Fig. S4).

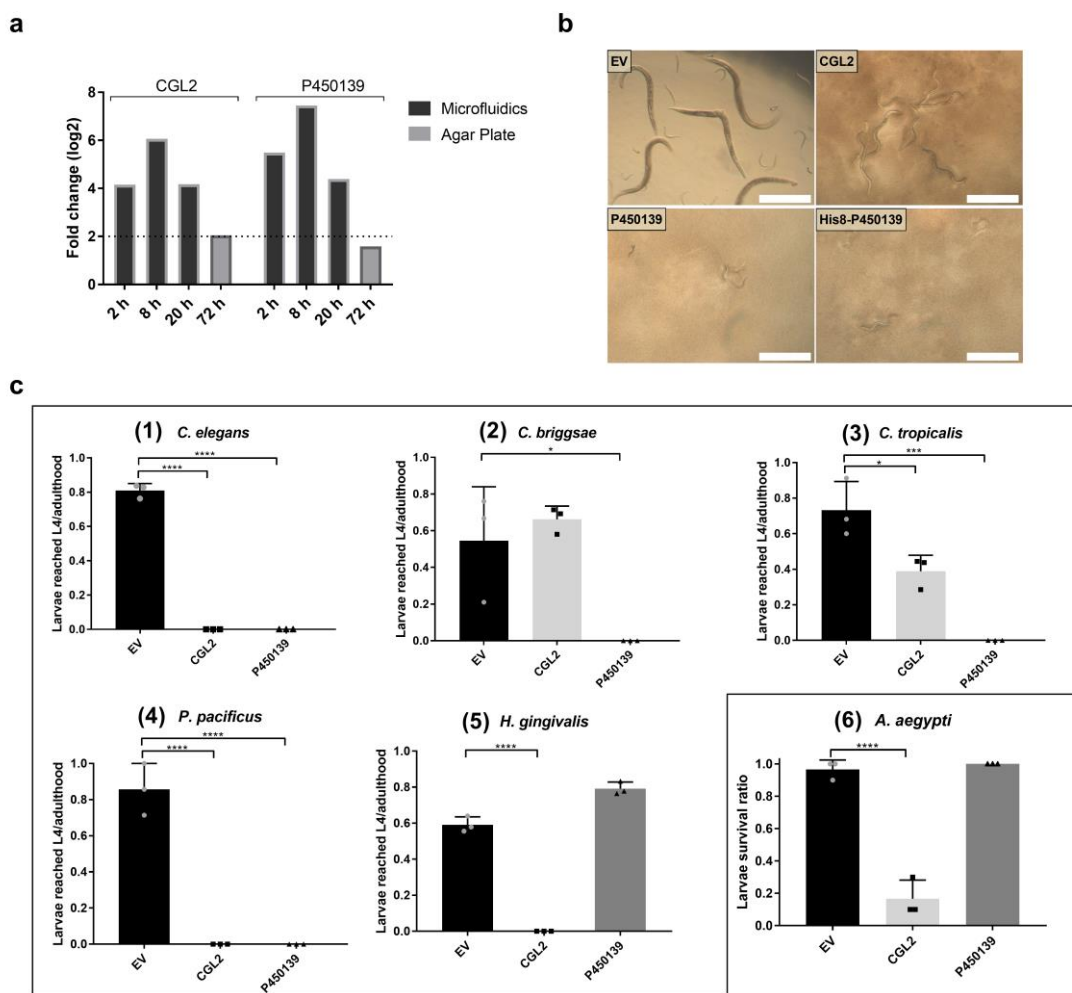


Figure 4: P450139 is an inducible nematotoxic protein with a putative hemolysin domain. (a) The *C. cinerea* gene coding for P450139 is significantly induced upon nematode challenge in the microfluidic setup in a similar manner to the previously identified nematotoxic lectin, CGL2. (b) Phase-contrast micrographs of *C. elegans* fed with IPTG-induced *E. coli* BL21 for 72 h, containing either an 'empty' vector (EV) or expressing CGL2, P450139 or P450139_8His. Scale bar = 500 μ m. (c) The toxicity of the P450139 protein was assessed against five different species of bacterivorous nematodes (1-5) and larvae of *Aedes aegypti* (6). IPTG-induced *E. coli* BL21 bearing either the previously characterized nematotoxic protein CGL2 or an empty vector (EV) were used as positive and negative controls, respectively. Dunnett's multiple comparisons test was used for statistical analysis. Error bars represent standard deviation of three biological replicates. ns: not significant, * $p < 0.05$, ** $p < 0.01$, *** $p < 0.001$, **** $p < 0.0001$ vs. EV.

Discussion

Here, we profiled the transcriptional response of the model fungus *C. cinerea* to the fungivorous nematode *A. avenae* using a microfluidics-based, tailor-made fungus-nematode interaction (FNI) device for the confrontation. In contrast to the previous challenge experiments [19] that were performed on agar plates, the microfluidic approach yielded a higher number of DEGs. In addition to the higher number of DEGs, the degree of differential expression of the DEGs that were found in both studies, was significantly higher in the microfluidic approach. This result is in accordance with the high expression level of the *cgl2p-dTomato* reporter gene in the fungal-nematode confrontation area of the fungal-nematode interaction (FNI) microfluidic device (Schmieder et al. in revision). Previously characterized cytoplasmic nematotoxic proteins (CGL1, CGL2, CCTX2) [19, 38] were also found to be significantly upregulated in the microfluidic setup, confirming the presence of an antagonist-inducible defense response of fungi against their antagonists [17] and its reproducibility in the FNI microfluidic device. Taken together, these results show that the microfluidic assay is highly sensitive and provides significant advantages over the agar-based assay for assessing nematode-inducible defense responses of fungi. It should be noted, however, that the previous fungal-nematode challenge studies were performed only at a single time-point [19]. Thus, the number and the level of induced defense genes might not have reached their maximum expression level in these previous studies.

A comparison between the *C. cinerea* DEGs identified during this study and the DEGs of a previous study where *C. cinerea* was confronted with bacteria under submerse conditions [42] revealed considerable overlap between the two datasets. The DEGs that were identified in both studies, include some genes coding for characterized antibacterial defense proteins such as phage-type lysozymes and copsis paralogs. Various precautions were taken to avoid bacterial contaminations in the experiments e.g. occasional bleaching of gravid nematodes and starting nematode cultures from fresh eggs, cultivation of the nematodes on fungal plates containing antibiotics and elimination of potential contaminants after Baermann funneling by allowing nematodes to crawl on agar plates containing an antibiotic cocktail. In fact, several antibacterial proteins were found to be upregulated in previously performed fungal-nematode confrontation studies on agar plates [19]. These findings suggested the possibility of the involvement of nematode-associated bacteria in fungal-nematode interactions. The importance of the bacterial community of nematodes for the fitness and virulence of parasites was previously suggested in several studies [47, 48, 50, 51, 54]. Although there are several studies that have analysed the bacteria associated with bacterivorous [44, 45], plant pathogenic [47, 52, 53, 55], and animal parasitic [46] nematodes, currently no data concerning the bacterial communities associated with fungivorous nematodes is available. Taken together, these findings directed us to look

Chapter 2

into the bacterial diversity of our model fungivorous nematode, *Aphelenchus avenae*, using 16S rDNA amplification and sequencing.

The analysis of the six 16S rDNA libraries showed good consistency among replicates. The observed small variations among the biological replicates are most likely due to the sampling process as it was previously suggested that even the technical replicates can show significant differences due to the inherently introduced errors in amplicon sequencing-based detection [60]. Results showed that Proteobacteria and Bacteroidetes were the most dominant phyla. Previous studies on bacterial- [44, 56, 61] and plant-feeding [53, 56] nematodes showed very similar results, suggesting that – at least at higher taxonomic levels – bacteria associated with nematodes within different feeding groups are conserved. However, at lower taxonomic levels, such as the genus level, the diversity of bacteria starts to change significantly. Many of the most commonly found groups of bacteria, such as Achromobacter [52, 53], Burkholderia [55], Herbaspirillum [61], Stenotrophomonas [62], Escherichia [63], Serratia [48] and Halomonas [53], were shown in previous studies to be present in bacteria- and/or plant-feeding nematodes. Additionally, in this study, one of the most predominant genera was Coxiella, which has not previously been shown to form part of a nematode's bacterial diversity. However, previous studies concerning bacteria associated with Arthropods showed that Coxiella are comprising 98% of the 16S rRNA sequences in both eggs and larvae of the cattle tick *Rhipicephalus microplus*, and the authors suggested that the bacteria provide a nutritional complement to the tick host [64]. In the same study, treatment of the tick with an antibiotic to kill its mutualistic symbionts resulted in developmental retardation of the tick. Very similar outcomes were observed for plant pathogenic nematodes when they were treated with antibiotics to eliminate their associated bacteria, albeit in this case different bacteria were involved [48]. Although the exact roles of these bacteria in nematodes remain largely unknown, they are, as suggested by previous studies [45, 54], likely to be important with regard to nematode fitness and might be involved in protecting the host against potential pathogens and enzymatic digestion of ingested food.

It is important to note that due to the surface sterilization treatments of the nematodes, we suspect that mainly the internal bacteria of the nematodes were detected. However, we cannot exclude that some bacteria might have originated from the surface of the nematodes. It has been previously shown that nematodes can carry bacteria in their eggs [46] and on their cuticle [65]. Since the entire nematode is used for DNA-extraction, we cannot make a statement in this regard. In future studies, it would be exciting to investigate the spatial distribution of the identified bacteria in the nematode.

Identification of a fungal defense proteins by challenge of the fungus with predatory nematodes and analysis of differential gene expression was one of the main goals of this study. As part of this process, we examined the genes of *C. cinerea* that were highly induced in an effort to identify novel nematotoxic

Chapter 2

defense proteins. One of these highly induced genes, coding for P450139, showed, in addition to its upregulation in the presence of the fungivorous nematode, overall expression dynamics that were similar to previously characterized inducible nematotoxic proteins. Furthermore, structural homology searches suggested significant similarity to β -pore-forming bacterial toxins, namely staphylococcal leukocidins [58] and *Vibrio cholera* cytolysin (VCC) [59]. Interestingly, VCC had been shown to be toxic against nematodes [66], supporting our hypothesis that P450139 was a nematotoxic protein. Heterologously expression of P450139 in *E. coli* and testing the toxicity of these bacteria towards nematodes and insects revealed a strong toxicity of the protein against four of the five tested nematode species (*C. elegans*, *C. briggsae*, *C. tropicalis* and *P. pacificus*) whereas *H. gingivalis* was resistant. Interestingly, the four P450139-susceptible nematode species are phylogenetically more closely related to each other than to *H. gingivalis* [67]. This observation suggests the existence of a conserved target for P450139 in the closely related species, while this target is apparently lacking or not accessible in the resistant nematode species. Interestingly, the susceptibility pattern was different for the CGL2 lectin, suggesting that the distribution of targets of protein toxins does not always correlate with phylogeny of the organisms.

Other bacterial pore-forming proteins that are structurally similar to P450139 lyse different blood cell types. *Vibrio cholera* cytolysin and staphylococcal leukocidin (LeukS-PV) lyse erythrocytes [68] and human leukocytes [69], respectively. The observed lack of lysis of the tested erythrocytes by P450139 under the applied assay conditions may be due to the lack of cofactors or activators. In fact, the bacterial homologue VCC undergoes activation with proteolytic cleavage prior to being able to assemble the pore forming structure [70]. Therefore, the lack of hemolytic activity could be due to the absence of the specific receptors, missing activating co-factors or a lack of prior activation. Nevertheless, the observed nematotoxic effects strongly support that P450139 is an inducible protein involved in the chemical defense of *C. cinerea* against nematodes. Interestingly, we couldn't find any sequence homologous to P450139 within the NCBI non-redundant database or the JGI MycoCosm, suggesting that this protein toxin is so far unique to *C. cinerea*.

Chapter 2

Conclusion:

In this study, we analyzed the genome-wide transcriptional response of a fungus upon challenge with a fungivorous nematode using a tailor-made microfluidic setup. Our results indicate that the current setup significantly improves the sensitivity of the analysis in comparison to standard agar-based confrontations.

The presence of a considerable diversity of bacteria associated with fungivorous nematodes and the induction of antibacterial defense genes in the fungus upon nematode predation suggest that nematode predation of a fungus is a tripartite rather than a bipartite interaction. Similar to plant defense against plant pathogenic nematodes, the induction of antibacterial defense genes might allow the fungus to defend itself against nematode predators in part by interfering with the microbiome of the nematode.

One of the identified nematode-induced *C. cinerea* genes, coding for P450139, was previously missed most likely due to the limited sensitivity of agar plate-based assays. This protein, having a predicted structural homology comparable to that of bacterial pore forming toxins, showed strong toxicity against four of the five bacterivorous nematodes tested, suggesting that P450139 is a part of the inducible armory of *C. cinerea* against predatory nematodes. The different specificities of the nematotoxins P450139 and CGL2 with regard to nematode species are probably a consequence of the different modes of action of these protein toxins and implies that the various nematotoxins of a specific fungus have complementary specificities, ensuring an efficient defense against a large number of different predators. We propose P450139 as a novel type of pore-forming protein toxins of *C. cinerea* based on its structural similarity to the well-studied *Staphylococcus aureus* and *Vibrio cholera* pore-forming toxins. The self-protection mechanism of the fungus towards this cytoplasmic protein toxin and its mode of action in nematodes remain to be elucidated.

Chapter 2

Declarations

Ethics approval and consent to participate

Not applicable

Consent for publication

Not applicable

Availability of data and materials

The transcriptomics data are available in the ArrayExpress repository under the accession numbers E-MTAB-7005 (<http://www.ebi.ac.uk/arrayexpress/>).

16S rDNA nucleotide sequences were deposited at NCBI SRA database under the accession numbers SRR7472378-SRR7472383.

Competing interests

The authors declare that they have no competing interests.

Funding

This work was supported by the Swiss National Science Foundation (Grant No: 31003A-173097) and ETH Zurich.

Authors' contributions

AT prepared samples for RNA-seq and 16s rRNA sequencing, analyzed transcriptome and microbiome data, cloned and expressed P450139, and wrote initial manuscript draft.

CS prepared microfluidic devices, proofread the manuscript.

SA performed biotoxicity and cell lysis assays.

MK started and coordinated the project and critically revised the manuscript.

Acknowledgements

We thank Markus Aebi for fruitful discussions, Pie Müller (Swiss Tropical and Public Health Institute, Basel, Switzerland) for supplying *Aedes aegypti* eggs and Robin Ohm (Utrecht University, Utrecht, The Netherlands) for critically reading of the manuscript.

References

1. Ruess L, Lussenhop J: **Trophic Interactions of Fungi and Animals.** 2005, **20050554**:581-598.
2. Boddy L, Jones TH: **Interactions between Basidiomycota and Invertebrates.** *Br Mycol Sy* 2008, **28**:155-179.
3. Doll K, Chatterjee S, Scheu S, Karlovsky P, Rohlfs M: **Fungal metabolic plasticity and sexual development mediate induced resistance to arthropod fungivory.** *Proc Biol Sci* 2013, **280**(1771):20131219.
4. Gomez BL, Nosanchuk JD: **Melanin and fungi.** *Current Opinion in Infectious Diseases* 2003, **16**(2):91-96.
5. Latge JP: **The cell wall: a carbohydrate armour for the fungal cell.** *Mol Microbiol* 2007, **66**(2):279-290.
6. Kempken F, Rohlfs M: **Fungal secondary metabolite biosynthesis - a chemical defence strategy against antagonistic animals?** *Fungal Ecology* 2009, **3**:107-114.
7. Rohlfs M, Churchill ACL: **Fungal secondary metabolites as modulators of interactions with insects and other arthropods.** In., vol. 48; 2011: 23-34.
8. Sabotic J, Ohm RA, Kunzler M: **Entomotoxic and nematotoxic lectins and protease inhibitors from fungal fruiting bodies.** *Appl Microbiol Biot* 2016, **100**(1):91-111.
9. Walton JD, Hallen-Adams HE, Luo H: **Ribosomal biosynthesis of the cyclic peptide toxins of Amanita mushrooms.** *Biopolymers* 2010, **94**(5):659-664.
10. Bleuler-Martinez S, Schmieder S, Aebi M, Kunzler M: **Biotin-Binding Proteins in the Defense of Mushrooms against Predators and Parasites.** *Appl Environ Microb* 2012, **78**(23):8485-8487.
11. Renko M, Sabotic J, Mihelic M, Brzin J, Kos J, Turk D: **Versatile Loops in Mycocypins Inhibit Three Protease Families.** *J Biol Chem* 2010, **285**(1):308-316.
12. Mancheno JM, Tateno H, Sher D, Goldstein IJ: **Laetiporus sulphureus Lectin and Aerolysin Protein Family.** *Adv Exp Med Biol* 2010, **677**:67-80.
13. Lacadena J, Alvarez-Garcia E, Carreras-Sangra N, Herrero-Galan E, Alegre-Cebollada J, Garcia-Ortega L, Onaderra M, Gavilanes JG, del Pozo AM: **Fungal ribotoxins: molecular dissection of a family of natural killers.** *Fems Microbiol Rev* 2007, **31**(2):212-237.
14. Bleuler-Martinez S, Butschi A, Garbani M, Walti MA, Wohlschlager T, Potthoff E, Sabotic J, Pohleven J, Luthy P, Hengartner MO *et al:* **A lectin-mediated resistance of higher fungi against predators and parasites.** *Mol Ecol* 2011, **20**(14):3056-3070.
15. Kunzler M: **Hitting the sweet spot-glycans as targets of fungal defense effector proteins.** *Molecules* 2015, **20**(5):8144-8167.
16. Mathioni SM, Patel N, Riddick B, Sweigard JA, Czymmek KJ, Caplan JL, Kunjeti SG, Kunjeti S, Raman V, Hillman BI *et al:* **Transcriptomics of the Rice Blast Fungus Magnaporthe oryzae in Response to the Bacterial Antagonist Lysobacter enzymogenes Reveals Candidate Fungal Defense Response Genes.** *Plos One* 2013, **8**(10).
17. Ortiz SC, Trienens M, Rohlfs M: **Induced Fungal Resistance to Insect Grazing: Reciprocal Fitness Consequences and Fungal Gene Expression in the Drosophila-Aspergillus Model System.** *Plos One* 2013, **8**(8).
18. Schroechk V, Scherlach K, Nutzmann HW, Shelest E, Schmidt-Heck W, Schuemann J, Martin K, Hertweck C, Brakhage AA: **Intimate bacterial-fungal interaction triggers biosynthesis of archetypal polyketides in Aspergillus nidulans.** *P Natl Acad Sci USA* 2009, **106**(34):14558-14563.

Chapter 2

19. Plaza DF, Schmieder SS, Lipzen A, Lindquist E, Künzler M: **Identification of a Novel Nematotoxic Protein by Challenging the Model Mushroom Coprinopsis cinerea with a Fungivorous Nematode.** *Genes/Genomes/Genetics* 2016, **6**:87-98.
20. Shinya R, Hasegawa K, Chen A, Kanzaki N, Sternberg PW: **Evidence of Hermaphroditism and Sex Ratio Distortion in the Fungal Feeding Nematode Bursaphelenchus okinawaensis.** *G3 (Bethesda, Md)* 2014, **4**:1907-1917.
21. Stanley CE, Stö M, Swaay DV, Sabotič J, Kallio PT, Kü M, Demello AJ, Aebi M: **Probing bacterial-fungal interactions at the single cell level.** *Integr Biol Integr Biol* 2014, **6**:935-945.
22. Staniland LN: **A Modification of the Baermann Funnel Technique for the Collection of Nematodes from Plant Material.** 1954, **28**:115-118.
23. Hatakeyama M, Opitz L, Russo G, Qi W, Schlapbach R, Rehrauer H: **SUSHI: an exquisite recipe for fully documented, reproducible and reusable NGS data analysis.** *BMC Bioinformatics* 2016, **17**(1):228.
24. Dobin A, Davis CA, Schlesinger F, Drenkow J, Zaleski C, Jha S, Batut P, Chaisson M, Gingeras TR: **STAR: ultrafast universal RNA-seq aligner.** *Bioinformatics* 2013, **29**(1):15-21.
25. Muraguchi H, Umezawa K, Niikura M, Yoshida M, Kozaki T, Ishii K, Sakai K, Shimizu M, Nakahori K, Sakamoto Y *et al*: **Strand-Specific RNA-Seq Analyses of Fruiting Body Development in Coprinopsis cinerea.** *Plos One* 2015, **10**(10).
26. Liao Y, Smyth GK, Shi W: **featureCounts: an efficient general purpose program for assigning sequence reads to genomic features.** *Bioinformatics* 2014, **30**(7):923-930.
27. Love MI, Huber W, Anders S: **Moderated estimation of fold change and dispersion for RNA-seq data with DESeq2.** *Genome Biol* 2014, **15**(12):550.
28. Petersen TN, Brunak S, von Heijne G, Nielsen H: **SignalP 4.0: discriminating signal peptides from transmembrane regions.** *Nat Methods* 2011, **8**(10):785-786.
29. Krogh A, Larsson B, von Heijne G, Sonnhammer EL: **Predicting transmembrane protein topology with a hidden Markov model: application to complete genomes.** *J Mol Biol* 2001, **305**(3):567-580.
30. Finn RD, Coggill P, Eberhardt RY, Eddy SR, Mistry J, Mitchell AL, Potter SC, Punta M, Qureshi M, Sangrador-Vegas A *et al*: **The Pfam protein families database: towards a more sustainable future.** *Nucleic Acids Res* 2016, **44**(D1):D279-285.
31. Ashburner M, Ball CA, Blake JA, Botstein D, Butler H, Cherry JM, Davis AP, Dolinski K, Dwight SS, Eppig JT *et al*: **Gene ontology: tool for the unification of biology. The Gene Ontology Consortium.** *Nat Genet* 2000, **25**(1):25-29.
32. Viegas FB, Wattenberg M, Feinberg J: **Participatory Visualization with Wordle.** *Ieee T Vis Comput Gr* 2009, **15**(6):1137-1144.
33. Edgar RC: **Search and clustering orders of magnitude faster than BLAST.** *Bioinformatics* 2010, **26**(19):2460-2461.
34. Cole JR, Wang Q, Fish JA, Chai BL, McGarrell DM, Sun YN, Brown CT, Porras-Alfaro A, Kuske CR, Tiedje JM: **Ribosomal Database Project: data and tools for high throughput rRNA analysis.** *Nucleic Acids Research* 2014, **42**(D1):D633-D642.
35. McMurdie PJ, Holmes S: **phyloseq: An R Package for Reproducible Interactive Analysis and Graphics of Microbiome Census Data.** *Plos One* 2013, **8**(4).
36. Künzler M, Bleuler-Martinez S, Butschi A, Garbani M, Lüthy P, Hengartner MO, Aebi M: **Biotoxicity assays for fruiting body lectins and other cytoplasmic proteins.** 2010, **480**:141-150.

Chapter 2

37. Stiernagle T: **Maintenance of *C. elegans*.** *The C elegans Research Community, WormBook*, doi/101895/wormbook11011, <http://wwwwormbookorg> 2006.
38. Bleuler-Martínez S, Butschi A, Garbani M, Wilti MA, Wohlschlager T, Potthoff E, Sabotia J, Pohleven J, Lüthy P, Hengartner MO et al: **A lectin-mediated resistance of higher fungi against predators and parasites.** 2011, **20**:3056-3070.
39. Grigoriev IV, Nikitin R, Haridas S, Kuo A, Ohm R, Otillar R, Riley R, Salamov A, Zhao XL, Korzeniewski F et al: **MycoCosm portal: gearing up for 1000 fungal genomes.** *Nucleic Acids Res* 2014, **42**(D1):D699-D704.
40. Anzenbacher P, Anzenbacherova E: **Cytochromes P450 and metabolism of xenobiotics.** *Cell Mol Life Sci* 2001, **58**(5-6):737-747.
41. Butschi A, Titz A, Walti MA, Olieric V, Paschinger K, Nobauer K, Guo X, Seeberger PH, Wilson IB, Aebi M et al: **Caenorhabditis elegans N-glycan core beta-galactoside confers sensitivity towards nematotoxic fungal galectin CGL2.** *PLoS Pathog* 2010, **6**(1):e1000717.
42. Kombrink A, Tayyrov A, Essig A, Stöckli M, Micheller S, Hintze J, Heuvel YV, Dürig N, Lin CW, Kallio PT et al: **Induction of antibacterial proteins and peptides in the coprophilous mushroom Coprinopsis cinerea in response to bacteria.** *ISME J* in press.
43. Gaderer R, Bonazza K, Seidl-Seiboth V: **Cerato-platanins: a fungal protein family with intriguing properties and application potential.** *Appl Microbiol Biot* 2014, **98**(11):4795-4803.
44. Zhang F, Berg M, Dierking K, Felix MA, Shapira M, Samuel BS, Schulenburg H: **Caenorhabditis elegans as a Model for Microbiome Research.** *Front Microbiol* 2017, **8**:485.
45. Baquiran JP, Thater B, Sedky S, De Ley P, Crowley D, Orwin PM: **Culture-Independent Investigation of the Microbiome Associated with the Nematode Acrobeloides maximus.** *Plos One* 2013, **8**(7).
46. Sinnathamby G, Henderson G, Umair S, Janssen P, Bland R, Simpson H: **The bacterial community associated with the sheep gastrointestinal nematode parasite Haemonchus contortus.** *Plos One* 2018, **13**(2):e0192164.
47. Han ZM, Hong YD, Zhao BG: **A study on pathogenicity of bacteria carried by pine wood nematodes.** *Journal of Phytopathology* 2003, **151**:683-689.
48. Kwon HR, Choi GJ, Choi YH, Jang KS, Sung ND, Kang MS, Moon Y, Lee SK, Kim JC: **Suppression of pine wilt disease by an antibacterial agent, oxolinic acid.** *Pest Management Science* 2010, **66**:634-639.
49. Proença DN, Grass G, Morais PV: **Understanding pine wilt disease: roles of the pine endophytic bacteria and of the bacteria carried by the disease-causing pinewood nematode.** *MicrobiologyOpen* 2017, **6**:1-20.
50. Nascimento FX, Hasegawa K, Mota M, Vicente CSL: **Bacterial role in pine wilt disease development - review and future perspectives.** *Environmental Microbiology Reports* 2015, **7**:51-63.
51. Torres JP, Tianero MD, Robes JMD, Kwan JC, Biggs JS, Concepcion GP, Olivera BM, Haygood MG, Schmidta EW: **Stenotrophomonas-like bacteria are widespread symbionts in cone snail venom ducts.** *Appl Environ Microb* 2017, **83**:1-10.
52. Wu XQ, Yuan WM, Tian XJ, Fan B, Fang X, Ye JR, Ding XL: **Specific and functional diversity of endophytic bacteria from pine wood nematode bursaphelenchus xylophilus with different virulence.** *International Journal of Biological Sciences* 2012, **9**:34-44.
53. Xiang Y, Wu XQ, Zhou AD: **Bacterial diversity and community structure in the pine wood nematode bursaphelenchus xylophilus and B. mucronatus with different virulence by high-throughput sequencing of the 16S rDNA.** *Plos One* 2015, **10**:1-14.

Chapter 2

54. Zhao BG, Tao J, Ju YW, Wang PK, Ye JL: **The role of wood-inhabiting bacteria in pine wilt disease.** *J Nematol* 2011, **43**:129-134.
55. Palomares-Rius JE, Archidona-Yuste A, Cantalapiedra-Navarrete C, Prieto P, Castillo P: **Molecular diversity of bacterial endosymbionts associated with dagger nematodes of the genus Xiphinema (Nematoda: Longidoridae) reveals a high degree of phylogenetic congruence with their host.** *Mol Ecol* 2016, **25**(24):6225-6247.
56. Ladygina N, Johansson T, Canback B, Tunlid A, Hedlund K: **Diversity of bacteria associated with grassland soil nematodes of different feeding groups.** *Fems Microbiol Ecol* 2009, **69**(1):53-61.
57. Zimmermann L, Stephens A, Nam S-Z, Rau D, Kübler J, Lozajic M, Gabler F, Söding J, Lupas AN, Alva V: **A Completely Reimplemented MPI Bioinformatics Toolkit with a New HHpred Server at its Core.** *Journal of Molecular Biology* 2017.
58. Alonso F, Torres VJ: **The Bicomponent Pore-Forming Leucocidins of *Staphylococcus aureus*.** *Microbiol Mol Biol R* 2014, **78**(2):199-230.
59. Olson R, Gouaux E: **Crystal structure of the *Vibrio cholerae* cytolsin (VCC) pro-toxin and its assembly into a heptameric transmembrane pore.** *Journal of Molecular Biology* 2005, **350**(5):997-1016.
60. Zhou JZ, Wu LY, Deng Y, Zhi XY, Jiang YH, Tu QC, Xie JP, Van Nostrand JD, He ZL, Yang YF: **Reproducibility and quantitation of amplicon sequencing-based detection.** *Isme J* 2011, **5**(8):1303-1313.
61. Tian XL, Cheng XY, Mao ZC, Chen GH, Yang JR, Xie BY: **Composition of Bacterial Communities Associated with a Plant-Parasitic Nematode *Bursaphelenchus mucronatus*.** *Curr Microbiol* 2011, **62**(1):117-125.
62. He LX, Wu XQ, Xue Q, Qiu XW: **Effects of *Endobacterium (Stenotrophomonas maltophilia)* on Pathogenesis-Related Gene Expression of Pine Wood Nematode (*Bursaphelenchus xylophilus*) and Pine Wilt Disease.** *International journal of molecular sciences* 2016, **17**.
63. Zhao BG, Lin F, Guo DS, Li RG, Li SN, Kulnich O, Ryss A: **Pathogenic Roles of the Bacteria carried by *Bursaphelenchus mucronatus*.** *J Nematol* 2009, **41**(1):11-16.
64. Guizzo MG, Parizi LF, Nunes RD, Schama R, Albano RM, Tirloni L, Oldiges DP, Vieira RP, Oliveira WHC, Leite MD et al: **A *Coxiella* mutualist symbiont is essential to the development of *Rhipicephalus microplus*.** *Sci Rep-Uk* 2017, **7**.
65. Standing D, Knox OGG, Mullins CE, Killham KK, Wilson MJ: **Influence of nematodes on resource utilization by bacteria - an in vitro study.** *Microb Ecol* 2006, **52**(3):444-450.
66. Cinar HN, Kothary M, Datta AR, Tall BD, Sprando R, Bilecen K, Yildiz F, McCardell B: ***Vibrio cholerae* Hemolysin Is Required for Lethality, Developmental Delay, and Intestinal Vacuolation in *Caenorhabditis elegans*.** *Plos One* 2010, **5**(7).
67. Holovachov O, Camp L, Nadler SA: **Sensitivity of Ribosomal RNA Character Sampling in the Phylogeny of Rhabditida.** *J Nematol* 2015, **47**(4):337-355.
68. Krasilnikov OV, Muratkhanova JN, Zitzer AO: **The Mode of Action of *Vibrio-Cholerae* Cytolysin - the Influences on Both Erythrocytes and Planar Lipid Bilayers.** *Biochim Biophys Acta* 1992, **1111**(1):7-16.
69. Sugawara N, Tomita T, Sato T, Kamio Y: **Assembly of *Staphylococcus aureus* leukocidin into a pore-forming ring-shaped oligomer on human polymorphonuclear leukocytes and rabbit erythrocytes.** *Biosci Biotech Bioch* 1999, **63**(5):884-891.
70. Nagamune K, Yamamoto K, Naka A, Matsuyama J, Miwatani T, Honda T: **In vitro proteolytic processing and activation of the recombinant precursor of El Tor cytolsin/hemolysin (Pro-**

Chapter 2

HlyA) of Vibrio cholerae by soluble hemagglutinin/protease of V-cholerae, trypsin, and other proteases. *Infect Immun* 1996, **64**(11):4655-4658.

Chapter 2

Supplementary Information

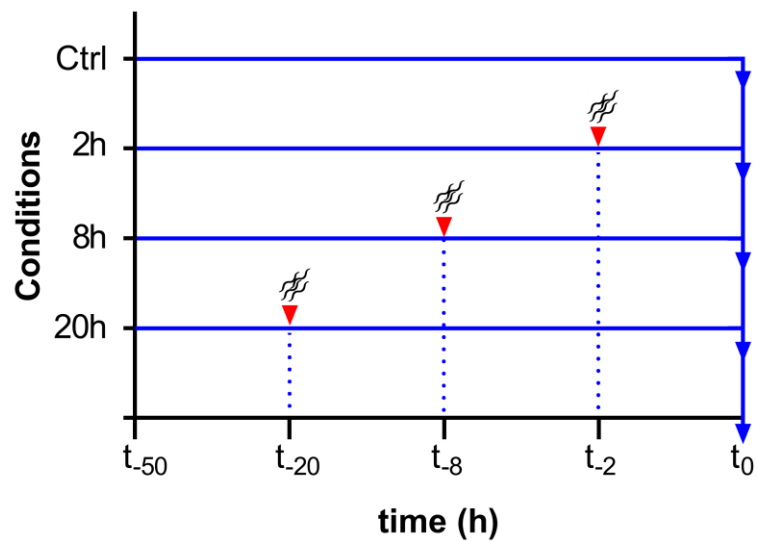


Figure S1: Nematode-fungus challenge experiment setup and RNA extraction. Microfluidic devices were inoculated with a small *C. cinerea* plug and incubated for 30 h. Around ten worms were added to the confrontation area of the microfluidic device at three different time points i.e. 2 h, 8 h and 20 h. The time point when nematodes were added are indicated with a red triangle. The control samples were incubated in the absence of the predator nematodes throughout. All samples were harvested at the same time point (t_0) and used for total RNA extraction. Each treatment was performed in three biological replicates.

Chapter 2

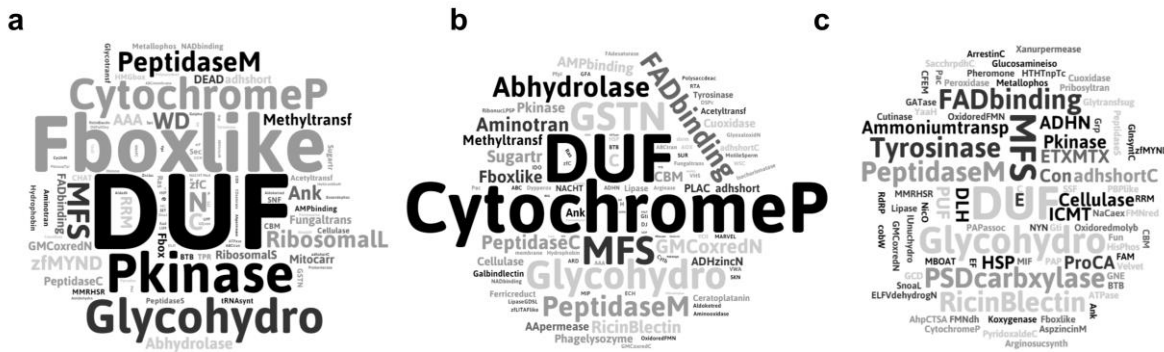


Figure S2: Overall visualization of *C. cinerea* DEGs annotations. Tag clouds were generated for all (a), upregulated (b) and downregulated (c) genes of *C. cinerea* using annotated PFAM domains as an input for Wordle.

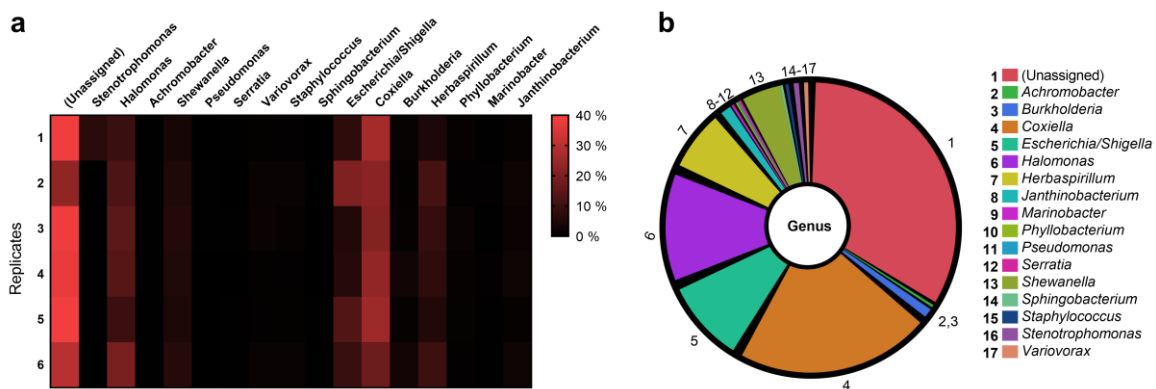


Figure S3: Analysis of 16 rRNA-based associated bacteria of *A. avenae* (a) Heat map showing 16S rDNA based profile of *A. avenae* associated bacteria for each of the six biological replicates. The figure legend represents the percentage of assigned OTUs to each genus of bacteria. (b) The pie chart represents the composition of nematode-associated bacteria at the genus level.

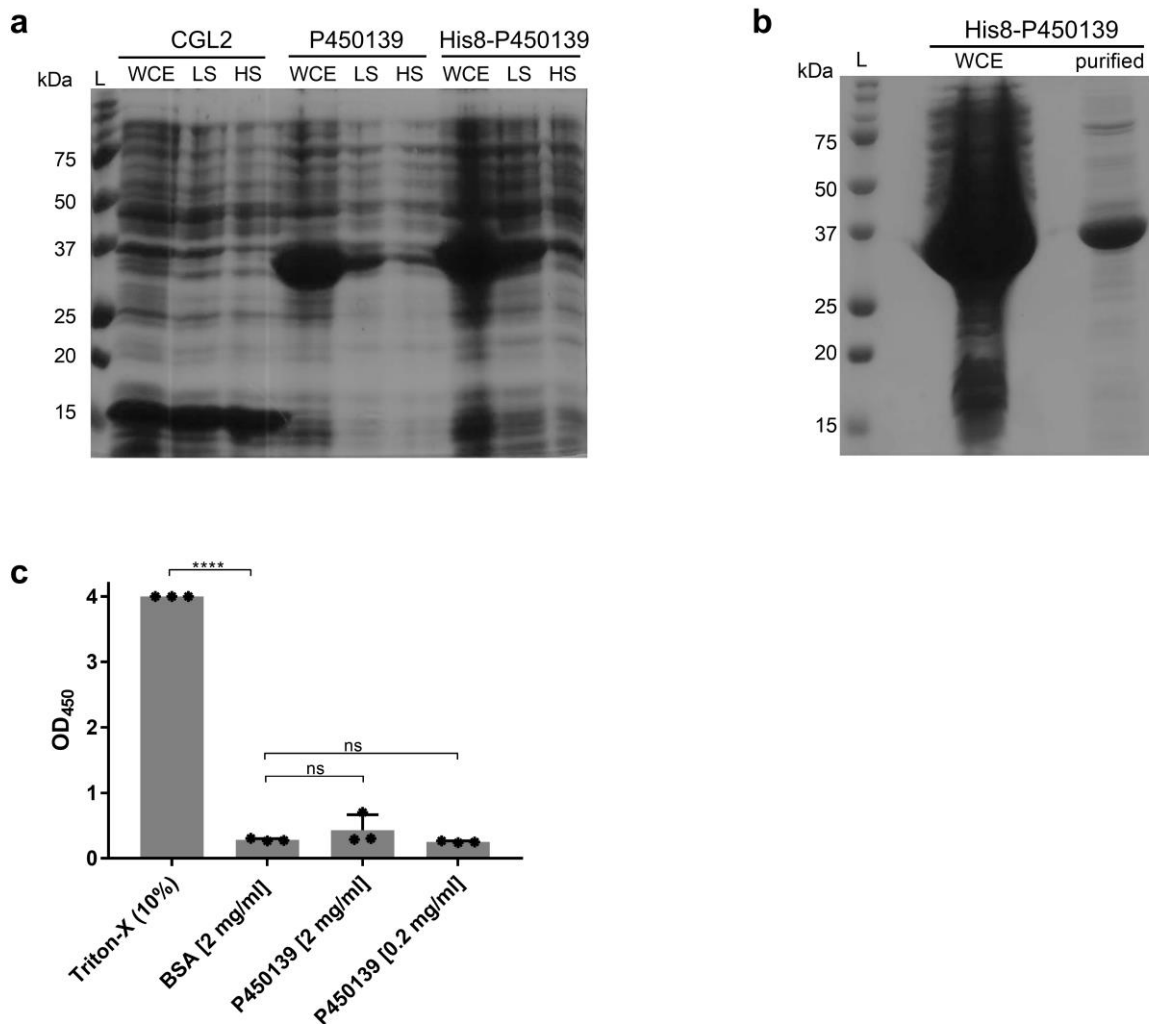


Figure S4: Expression and hemolytic activity of P450139. (a) Coomassie-stained SDS-PAGE showing heterologous expression and solubility of wild type and 8His-tagged constructs of the P450139 protein. 20 µl of whole cell extract (WCE), supernatants of low spin (LS; 5 min at 5000g) and high spin (HS; 30 min at 16000g) bacterial lysate were loaded on a gel. CGL2 was used as positive control for IPTG-induced expression and solubility. (b) The P450139-8His construct was produced in *E.coli* BL21 and 12 µg of Ni-NTA purified protein loaded onto the SDS-PAGE along with 20 µl of WCE. (c) Potential hemolytic activity of purified P450139 proteins was assayed with horse erythrocytes. Triton X-100 and BSA were used as positive and negative controls, respectively. Dunnett's multiple comparisons test was used for statistical analysis. Error bars represent standard deviation of three biological replicates.

Chapter 2

Table S1: Used organisms in this study.

Name	Strain	Source/Reference
<i>Caenorhabditis elegans</i>	N2	Caenorhabditis Genetics Center (CGC)
<i>Caenorhabditis briggsae</i>	AF16	Caenorhabditis Genetics Center (CGC)
<i>Caenorhabditis tropicalis</i>	JU1373	Caenorhabditis Genetics Center (CGC)
<i>Halicephalobus gingivalis</i>	Environmental isolate	Pamela Fonderie, Ghent University, Belgium
<i>Pristionchus pacificus</i>	PS312	Iain Wilson, BOKU, Vienna, Austria
<i>Aphelenchus avenae</i>	Standard lab strain	Richard Sikora, University of Bonn, Germany
<i>Aedes aegypti</i>	Rockefeller	Pie Müller, Swiss Tropical and Public Health Institute, Basel, Switzerland
<i>Coprinopsis cinerea</i>	AmutBmut	(Swamy et al., 1984)
<i>Botrytis cinerea</i>	BC-3	Paul W. Sternberg, California Institute of Technology, Pasadena, USA
<i>Escherichia coli</i>	DH5 α	
<i>Escherichia coli</i>	BL21(DE3)	Novagen
<i>Escherichia coli</i>	OP50	Hengartner laboratory (University of Zürich)

Table S2: Used primers in this study.

Name	Sequence (5'-3')
P450139forNdeI	GGCGCATATGCCAGAACACCAAGAACCTCTACGACAGCATC
P450139revNotI	AATGCGGCCGCTCATTCCGTCTTGGGGCGAG
P450139forHis8	CACCACCACCGAAGAACACCAAGAACCTCTACG
P450139revHis8	ATGATGATGATGTGGCATATGTATATCTCCTCT
515f	TCGTCGGCAGCGTCAGATGTGTATAAGAGACAGNNNNNTGCCAGCMGCCGGTAA
806r	GTCTCGTGGGCTCGGAGATGTGTATAAGAGACAGNNNNNGACTACHVGGGTWTCTAAT

Chapter 2

Table S3: RNA sequencing read counts and alignment statistics.

Samples	Total raw reads	Mapped reads	Mapped reads (%)	Genomic features (%) [*]
Ctrl_1	33,736,525	28,931,231	85.8	80.7
Ctrl_2	42,267,578	36,248,399	85.8	80.8
Ctrl_3	45,756,430	39,568,173	86.5	80.5
2h_1	31,160,742	27,255,939	87.5	79.7
2h_2	47,247,117	39,506,827	83.6	81.1
2h_3	36,702,592	31,494,884	85.8	80.3
8h_1	34,036,193	29,951,723	88.0	81.7
8h_2	30,921,637	26,427,852	85.5	81.2
8h_3	39,23,1376	33,172,543	84.6	81.5
20h_1	36,737,179	31,889,797	86.8	80.3
20h_2	53,957,132	45,826,904	84.9	81.4
20h_3	37,693,002	31,437,156	83.4	79.8

*Percentage of genes with reads above threshold 10.

The following supplementary table is available in the electronic version of this thesis:

Table S4: RNA-seq analysis of *C. cinerea* mycelium challenged by *A. avenae*

Description: The file includes all DEGs of the *C. cinerea* together with their relative and absolute expression values and PFAM and GO-term annotations.

Chapter 2

Table S5: OTU read numbers and taxonomic assignments

OTU_ID	R1	R2	R3	R4	R5	R6	Phylum	Class	Order	Family	Genus	OTU_reads	OUT (%)
OTU5	5.15	0	0	0.0708	0.033	0.0153	Proteobacteria	Gammaproteobacteria	Xanthomonadales	Xanthomonadaceae	Stenotrophomonas	1317.28	1.135
OTU13	1.45	0.0891	0	0	0	0	Proteobacteria	Gammaproteobacteria	Xanthomonadales	Xanthomonadaceae	Stenotrophomonas	110.35	0.095
OTU119	0.0121	0	0	0	0	0	Proteobacteria	Gammaproteobacteria	Xanthomonadales	Xanthomonadaceae	Stenotrophomonas	0.11	0
OTU4	0	0	0	0	0.0083	0	Bacteroidetes	Sphingobacteriia	Sphingobacteriales	Sphingobacteriaceae	Sphingobacterium	2.71	0.002
OTU7	22.9	16.3	22.3	22.3	25.4	19	Bacteroidetes					26793.8	23.088
OTU9	14.6	5.85	15.1	13.8	12.7	9.79	Bacteroidetes					8333.44	7.181
OTU14	0.339	1.43	1.07	0.478	0.569	1.55	Firmicutes	Bacilli	Bacillales	Staphylococcaceae	Staphylococcus	267.99	0.231
OTU17	0.823	0.431	1.31	0.956	0.693	0.383	Proteobacteria	Alphaproteobacteria	Rhizobiales	Phyllobacteriaceae	Phyllobacterium	88.24	0.076
OTU2	0.121	0.0297	0.0239	0.0531	0.198	0.199	Proteobacteria	Betaproteobacteria	Burkholderiales	Alcaligenaceae	Achromobacter	1268.14	1.093
OTU22	0.363	0.401	0.0955	0.407	0.14	0.429	Actinobacteria	Actinobacteria	Actinomycetales			15.09	0.013
OTU137	0	0	0	0	0.0083	0	Proteobacteria	Betaproteobacteria	Burkholderiales	Alcaligenaceae	Achromobacter	0.08	0
OTU20	0	0.0297	0.119	0	0	0	Proteobacteria	Gammaproteobacteria	Pseudomonadales	Pseudomonadaceae	Pseudomonas	1.38	0.001
OTU6	26.5	22.1	21.1	23.4	25.1	17.3	Proteobacteria	Gammaproteobacteria	Legionellales	Coxiellaceae	Coxiella	32791	28.255
OTU10	5.66	7.32	9.21	8.34	5.29	8.92	Proteobacteria	Gammaproteobacteria	Oceanospirillales	Halomonadaceae	Halomonas	5503.02	4.742
OTU12	3.63	4.83	5.08	5.14	4.03	9.76	Proteobacteria	Gammaproteobacteria	Oceanospirillales	Halomonadaceae	Halomonas	2724.23	2.347
OTU23	0	0	0.0716	0	0.033	0.505	Proteobacteria	Gammaproteobacteria	Oceanospirillales	Halomonadaceae	Halomonas	4.79	0.004
OTU21	0.0242	0.386	0.0716	0.407	0.066	0.046	Proteobacteria	Gammaproteobacteria	Alteromonadales	Alteromonadaceae	Marinobacter	9.04	0.008
OTU11	3.61	4.8	5.49	5.05	4.55	5.94	Proteobacteria	Gammaproteobacteria	Alteromonadales	Shewanellaceae	Shewanella	2840.96	2.448
OTU3	7.23	20.5	5.39	5.69	13.1	8.79	Proteobacteria	Gammaproteobacteria	Enterobacteriales	Enterobacteriaceae	Escherichia/Shigella	25979.6	22.386
OTU19	0.133	0	0.298	0	0.116	0.245	Proteobacteria	Gammaproteobacteria	Enterobacteriales	Enterobacteriaceae	Serratia	11.48	0.01
OTU24	0.375	0.386	0.525	0.691	0.495	0.49	Proteobacteria	Gammaproteobacteria	Enterobacteriales	Enterobacteriaceae		23.81	0.021
OTU8	4.4	11	8.25	7.31	5.29	9.65	Proteobacteria	Betaproteobacteria	Burkholderiales	Oxalobacteraceae	Herbaspirillum	6976.8	6.012
OTU15	0.907	1.99	1.64	2.57	0.916	2.53	Proteobacteria	Betaproteobacteria	Burkholderiales	Oxalobacteraceae	Janthinobacterium	370.41	0.319
OTU16	1.26	0.52	1.09	2.71	0.866	2.97	Proteobacteria	Betaproteobacteria	Burkholderiales	Burkholderiaceae	Burkholderia	333.33	0.287
OTU18	0.52	1.56	1.68	0.62	0.346	1.42	Proteobacteria	Betaproteobacteria	Burkholderiales	Comamonadaceae	Variovorax	128.45	0.111
OTU1	0	0.0149	0	0	0.0248	0.0306	Proteobacteria	Gammaproteobacteria	Xanthomonadales	Xanthomonadaceae	Stenotrophomonas	156.77	0.135

Chapter 3

Inducible cytoplasmic lipases - a novel class of fungal defense proteins against nematodes

Annageldi Tayyrov¹, Aleksandr Goryachkin¹, Philipp Schächle¹, Markus Künzler^{1*}

¹Institute of Microbiology, Department of Biology, ETH Zürich, Vladimir-Prelog-Weg 4, CH-8093 Zürich, Switzerland

*Correspondence: mkuenzle@ethz.ch

Manuscript to be submitted

Contributions:

- Isolation and cloning of *CLT1* and *CLT2*
- Heterologous expression and purification of Clt1 and Clt2 proteins
- *In vitro* lipases assays
- Creating and analyzing point mutations
- Part of the toxicity assays

Chapter 3

Abstract:

Fungi are an attractive food source of predators such as nematodes. Several fungal defense proteins and their protective mechanisms against nematodes have been described. Most of these proteins are lectins that are stored in the cytoplasm of the fungal cells and bind to specific glycan epitopes in the digestive tract of the nematode upon predation.

Here, we studied two novel nematotoxic proteins with lipase domains from the model mushroom *Coprinopsis cinerea*. These two cytoplasmically localized proteins were found to be induced in mycelia of *C. cinerea* upon feeding of fungivorous nematode *Aphelenchus avenae*, and showed nematotoxicity when heterologously expressed in *E. coli* and fed to several bacterivorous nematodes. Site-specific mutagenesis of predicted catalytic residues eliminated the *in vitro* lipase activity of the proteins and significantly reduced their nematotoxicity, indicating the importance of the lipase activity for the function of these proteins in the defense of the fungus against predatory nematodes. Our results suggest that cytoplasmic lipases constitute a novel class of fungal defense proteins against nematodes. Our findings improve our understanding of the fungal molecular defense mechanisms and may find applications in the control of parasitic nematodes in agriculture and animal diseases.

Chapter 3

Introduction

Due to their immobility and high nutrient content, fungi are an ideal food source for many predatory organisms [1, 2]. In order to protect themselves against predation, fungi have evolved various defense mechanisms [3]. In addition to physical defense [4, 5] or chemical defense by secondary metabolites [6, 7], fungi rely on chemical defense mediated by proteins and peptides [8, 9]. Several of such fungal defense proteins, i.e., biotin-binding proteins [10], lectins [11], protease inhibitors [12], pore-forming proteins [13] and ribotoxins [14] have been discovered and studied to some extent. Considering the high diversity of fungal predators and the specificity of many defense effectors with regard to target organisms, the diversity of fungal defense proteins must be huge. It has been shown that genes encoding for fungal defense proteins can be identified on the basis of their expression upon challenge of a fungus with its antagonists [15-18]. Hence, we previously conducted RNA seq-based genome-wide analysis of the model mushroom *Coprinopsis cinerea* challenged by the fungivorous nematode *Aphelenchus avenae* in a microfluidics device (Tayyrov et al. submitted).

Here, we report on the characterization of two highly induced *C. cinerea* genes encoding for P452912 and P430758 (JGI MycoCosm ProteinIDs), that were also showed expression dynamics that were similar to previously known nematotoxic proteins. These two proteins contain putative lipase domains, and showed toxicity towards the bacterivorous nematodes. Hereafter, to reflect the likely nature of their biological activity, we named P452912 and P430758 as Coprinopsis Lipase Toxin-1 (CLT1) and Coprinopsis Lipase Toxin-2 (CLT2), respectively. Site-specific mutagenesis of predicted catalytic residues significantly reduced the toxicity and abolished *in vitro* lipase activity of the proteins, suggesting the nematotoxicity effect of the toxins is dependent on a functional lipase domain.

Two main well-known roles of lipids are a structural role in biomembranes [19] and a role in energy storage [20]. In addition, lipids have a multitude of other functions in several essential biological processes such as cellular signaling [21], cellular organization [22] and membrane trafficking [23]. This multi-functionality and essentiality of lipids make them an ideal target for pathogens and competitors [24]. Microorganisms, especially bacteria were reported to use lipases as virulence factors [25], [26]. In fact, there are many secreted bacterial toxins that contain lipase domains [27, 28]. The type III secretory toxin, ExoU, as major virulence factor of *Pseudomonas aeruginosa* [29, 30] and the T6SS effector of *Vibrio cholera*, the lipase TseL [31], can be given as a well-studied examples of lipase toxins being used against its eukaryotic host cells and in self-protection against bacterial competitors, respectively. Protozoan parasites are also know to target host-lipidome to achieve a successful parasitism inside their host [32]. Furthermore, venoms of certain insects and reptiles are known to contain lipases [33].

Chapter 3

Our results suggest that proteins with functional lipase domains might be a novel class of fungal defense proteins against nematode predators.

2. Materials and Methods

2.1 Strains and cultivation conditions

E. coli DH5 α was used for cloning and plasmid amplification. Heterologous protein expression was performed in *E. coli* BL21 (DE3). *Coprinopsis cinerea* AmutBmut strain was maintained on YMG (0.4% (w/v) yeast extract, 1% (w/v) malt extract, 0.4% (w/v) glucose, 1.5% (w/v) agar) at 37 °C in a dark chamber. *Aphelenchus avenae* was propagated on pre-grown *Botrytis cinerea* (BC-3) [34] on MEA (Difco™ Malt Extract Agar) at 20 °C.

2.2 Validation of RNA-seq by qRT-PCR

To validate RNA-seq-based induction of CLT1 and CLT2, quantitative real-time PCR (qRT-PCR) was performed with three biological replicates of RNA. A small chunk of mycelium from *C. cinerea* AmutBmut was inoculated into microfluidic devices and cultivated for 30 h at 37 °C. Subsequently, roughly 10 fungivorous nematode *Aphelenchus avenae* were added to the interaction zones and the microfluidic devices were incubated for another 8 h at 20 °C. Thereafter, mycelia was extracted from the interaction zone for RNA extraction. RNA was extracted using Norgen RNA extraction kit according to the manufacturer's protocol (Norgen Biotek Corporation, Canada). For each sample, 15 ng of extracted RNA was reverse transcribed into cDNA using the Transcriptor Universal cDNA Master (Roche, Switzerland) following manufacturer's instructions. 20 μ l qRT-PCR reactions containing 2 μ l of cDNA, 10 μ l 2x FastStart Universal SYBR Green Master (Roche, Switzerland) and 900 nM of the respective primer pair were prepared. qRT-PCR was performed in a Rotor-Gene 3000 (Corbett Life Science, Australia) in quadruplicates for each biological replicate with following program: 95 °C for 15 min followed by denaturation at 95 °C for 15 s, annealing at 60 °C for 30 s and extension at 72 °C for 30 s (40 cycles). Specificity of amplification was confirmed with melting curve analysis. Differential gene expression ratios were calculated using the CT formula [35]. Primers were designed at Primer3Plus website [36] where at least one primer of each pair was designed to span exon-exon junctions. Samples that were not challenged with nematode were used as controls. The housekeeping gene tubulin (MycoCosm JGI protein ID: 357668) was used as an internal standard. qRT-PCR primers are listed in Table S2.

Chapter 3

2.3 Construction of expression plasmids harboring CLT1- and CLT2- encoding cDNAs

The cDNA synthesized from RNA of nematode-induced *C. cinerea* was used as a template for the amplification of the coding region of CLT1 and CLT2 by PCR. The primer pairs used for cloning of the coding regions are given in Table S2. The obtained PCR products were cloned into *E. coli* expression vector pET-24b (+) (Novagen, Germany) using *Nde*I/*Vsp*I and *Not*I restriction sites. The constructs were verified by Sanger sequencing (Microsynth, Switzerland), and transformed into *E. coli* BL21 for heterologous expression. Transformants were cultured in LB medium supplemented with 50 mg/l kanamycin at 37 °C. Cultures were induced with 0.5 mM isopropyl β-D-1-thiogalactopyranoside (IPTG) at OD₆₀₀=0.5 and cultivated over night at 18 °C. Heterologous expression and solubility for CLT1 and CLT2 were assessed as previously described [37].

2.4 Toxicity of CLT1 and CLT2 towards nematodes and insects

To assess nemato- and entomotoxicity of the heterologously expressed lipases, eight bacterivorous nematodes and omnivorous mosquito *Aedes aegypti* (see Table S1), respectively, were used. For nematotoxicity assays, nematode eggs were isolated and hatched to L1 larvae as described in the wormbook [38]. 20-30 freshly hatched, synchronized L1 stage-larvae were added to 100 µl of PBS containing preinduced *E. coli* BL21 cells adjusted to OD₆₀₀ 2.0. After 48 h (72 h for *H. gingivalis*) of incubation at 20°C, the percentage of nematodes that developed into L4 larvae or adulthood were assessed. Toxicity of CLT1 and CLT2 towards *Aedes aegypti* larvae was assayed as previously described [37]. *E. coli* BL21 cells expressing previously characterized, nemato- and entomotoxic lectin CGL2 was used as a positive control in all toxicity assays, and BL21 cells carrying 'empty' vector served as a negative control. All assays were performed in three or four biological replicates. Dunnett's multiple comparisons test was used for statistical analysis.

2.5 Tagging and purification of the proteins

To test the *in vitro* lipase activity of CLT1 and CLT2, the proteins were tagged at their N-termini with 8 His-residues and purified on Ni-NTA columns as described previously [39]. In brief, the parental expression plasmids encoding untagged CLT1 and CLT2 were PCR-amplified using 8-histidine tag-encoding primers (Table S2). After the PCR, the reaction products were treated with methylation dependent *Dpn*I endonuclease to eliminate the plasmid template. 5 µl of the treated PCR product was ligated and transformed into *E. coli* DH5α cells. The retrieved plasmids were verified with Sanger sequencing and transformed into *E. coli* BL21 for protein expression and purification . The proteins

Chapter 3

were expressed as described above for the untagged lipase proteins. The protein-expressing bacterial cells were centrifuged and resuspended in lysis buffer (50 mM Tris-HCl, 5 mM imidazole, pH 8.5) before being lysed using a French press. The bacterial lysate was spun at 16000 rpm for 30 min at 4 °C and the supernatant containing the soluble fraction was incubated with Ni-NTA beads (Macherey-Nagel, Germany) for overnight at 4 °C. The beads were washed with lysis buffer and subsequently eluted with elution buffer (50 mM Tris-HCl, 250 mM imidazole, pH 8.5). The final elute was desalting and concentrated on disposable PD-10 Desalting column (GE Healthcare Life Sciences™, USA).

2.6 Construction and expression of catalytic site mutants and truncated constructs

Mutations in the putative catalytic sites of CLT1 and CLT2 were introduced by PCR. The expression plasmids encoding His8-tagged CLT1 and CLT2 were amplified with mutagenic PCR primers carrying the respective mutations (Table S2). Likewise, the N- and C- termini of CLT1 and CLT2 were truncated by PCR using the specific primers listed in Table S2. Cloning of the plasmids and protein expression and purification were performed as described above.

2.7 *In vitro* lipase assays

In vitro lipase activities of CLT1 and CLT2 were assayed by measuring the rate of release of p-nitrophenol from p-nitrophenyl acetate (C2), p-nitrophenyl butyrate (C4) and p-nitrophenyl palmitate (C16) (all from Sigma) [40]. 2 µg of purified protein was mixed with each substrate (20mM) in 200 µl reaction buffer (100mM phosphate buffer, 150mM NaCl and 0.5% (v/v) Triton X -100, pH 7.2). The reaction was monitored in the microplate reader (Infinite 200 PRO; Tecan) at 25 °C by measuring the OD405 in time intervals of 3-150 min, depending on the activity of the lipases for the individual substrates. *Candida rugosa* lipase (Sigma) was used as a positive control.

3. Results

3.1 Identification of candidate nematotoxic proteins from *C. cinerea* based on differential gene expression

Previous sequencing of the *C. cinerea* transcriptome upon challenge with the fungivorous nematode *A. avenae* resulted in the identification of over one thousand nematode-induced *C. cinerea* genes (Tayyrov et al. submitted). Two of these genes, *clt1* and *clt2*, showed a similar expression pattern regarding the different cocultivation periods as some previously characterized nematotoxic proteins (Fig. 1A). To confirm the induction of these two genes upon nematode challenge, we performed qRT-PCR using RNA of *A. avenae*-induced mycelia of *C. cinerea*. Both, *clt1* and *clt2* revealed strong upregulation in nematode-challenged samples compared to non-challenged samples, confirming the previous RNA-seq results (Fig. 1B).

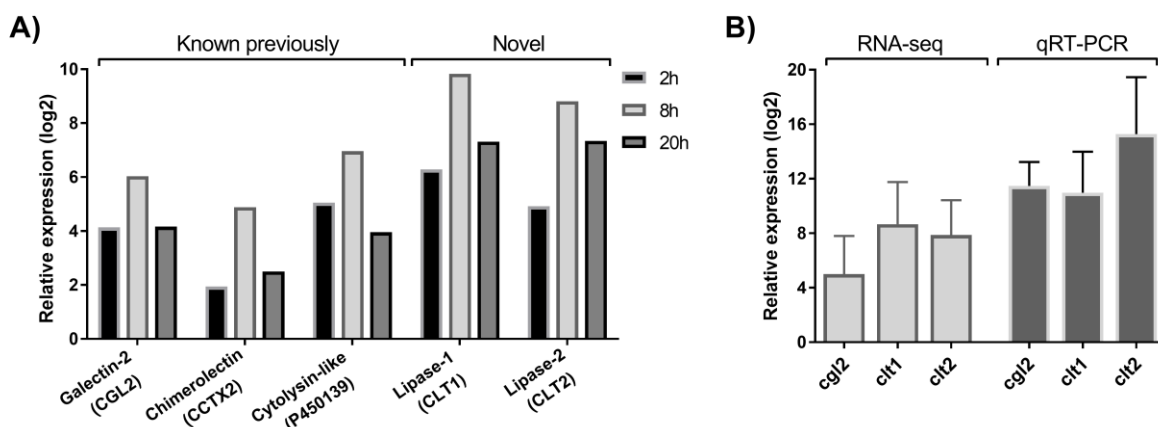


Figure 1: Nematode-inducible defense proteins of *C. cinerea*. **A)** RNA-seq based expression pattern of previously known and novel defense proteins of *C. cinerea* challenged by *A. avenae* at different time points. **B)** Expression of novel defense proteins together with CGL2 were validated with qRT-PCR. *C. cinerea* was challenged by *A. avenae* in microfluidic device for 8 hours. Error bars represent standard deviation of three biological replicates.

Chapter 3

3.2. CLT1 and CLT2 contain lipase domains

The predicted amino acid sequences of CLT1 and CLT2 were examined by SMART (Simple Modular Architecture Research Tool) [41] and *Phyre2* [42] web servers for characterized protein domains based on sequence and structural homologies, respectively. The search results indicated that CLT1 contains a putative lipase domain covering the region from residues 172 to 335 including conserved serine-aspartate residues forming a putative catalytic dyad for serine-dependent hydrolysis of ester bonds between fatty acids and glycerol [30, 43, 44] (Fig. 2A). Similarly, the CLT2 homology search predicted a putative (phospho)lipase domain in the region between residues 72 and 177. This predicted lipase domain contains conserved histidine-cysteine residues that are known to form the catalytic site for cysteine-dependent hydrolysis of (phosphor) glycerolipids [45] (Fig. 2B). Despite both proteins having a lipase domain, the amino acid sequences of CLT1 and CLT2 are vastly differ from one another without any significant similarity between them.

Chapter 3

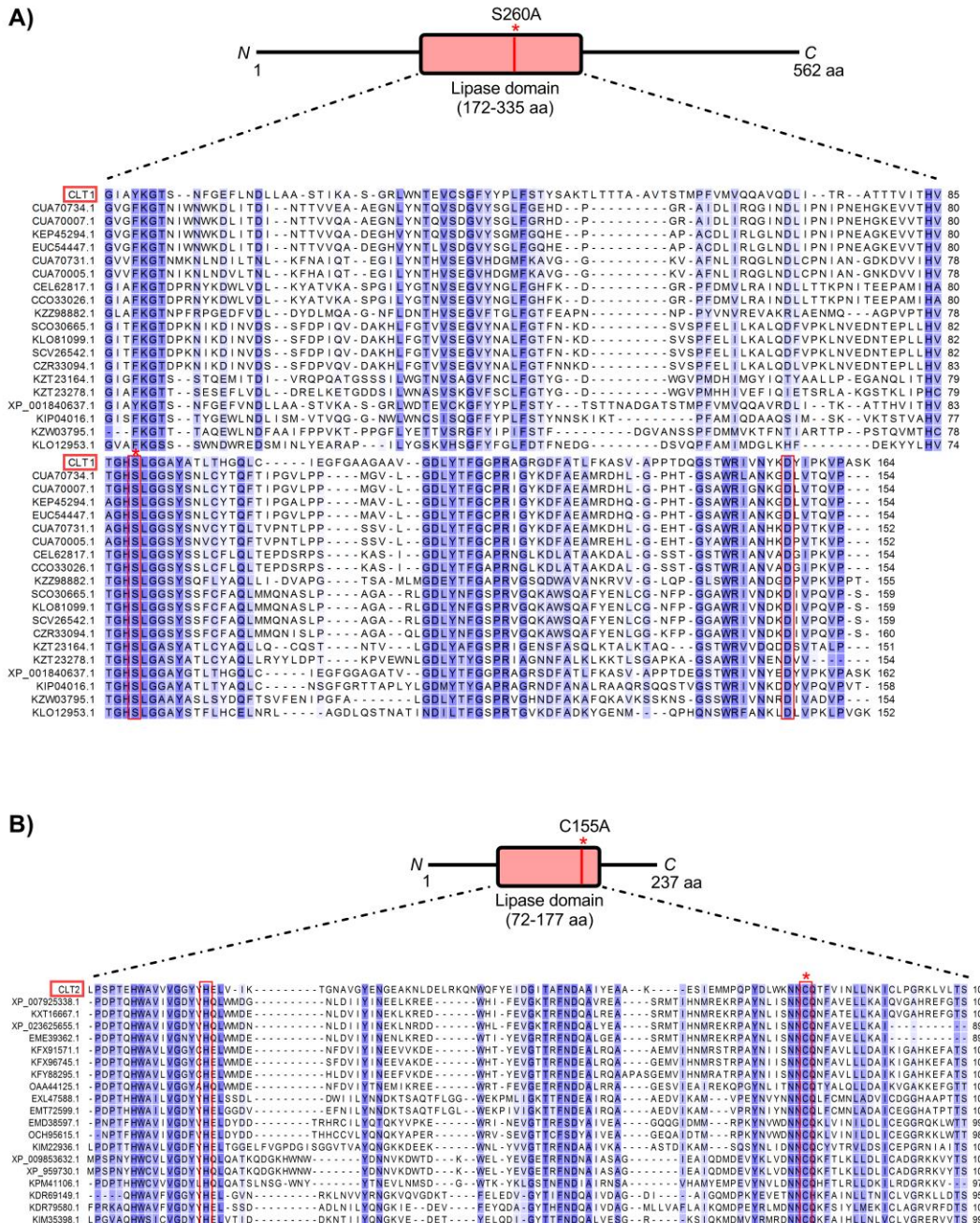


Figure 2: Sequence alignments of CLT1 and CLT2 lipase domains with sequences from NCBI. Amino acid sequences of CLT1 (A) and CLT2 (B) lipase domains were searched against NCBI database. Top 20 results were aligned. Blue shading indicates the degree of conservation from dark to light. Presumed catalytic dyads were denoted by red line boxes. Mutated catalytic sites, S266 for CLT1 and C155 for CLT2, were indicated with an asterisk. N– and C – termini are labeled with letters N and C, respectively. Length of whole genes and lipases domains are indicated with amino acid location numbers. The sequences were aligned using the ClustalW algorithm (v2.1). The amino acid sequences of the genes can be retrieved from NCBI non-redundant protein database by using the given accession numbers.

Chapter 3

3.3. Heterologous expression and nematotoxicity of CLT1 and CLT2

In order to functionally characterize CLT1 and CLT2, the untagged and His8-tagged version of the proteins were expressed in *E. coli*. Expression and solubility assays revealed high expression of the proteins in largely soluble form (Fig 3A). We tested a possible nematotoxicity of these proteins by feeding *C. elegans* N2 larvae with *E.coli* BL21 cells expressing the proteins of interest. After 48 hours of incubation, L4 larvae and adult nematodes were counted under the microscope. The results showed strong toxicity of CLT1 and CLT2 against the model bacterivorous nematode (Fig. 3B, 3C). Higher expression levels of His8-tagged CLT2 compared to the untagged form (Fig. 3A) correlated with higher nematotoxicity (Fig. 3B). In case of CLT1, the tagging decreased the solubility of the protein (Fig. 3A), and toxicity of 8his-tagged CLT1 was less severe than the wild type (Fig. 3B). The correlation between amount of the expressed protein and severity of the toxicity suggests that toxicity is dependent on the concentration of soluble protein as suggested earlier (Künzler et al., Methods Enzymol).

Chapter 3

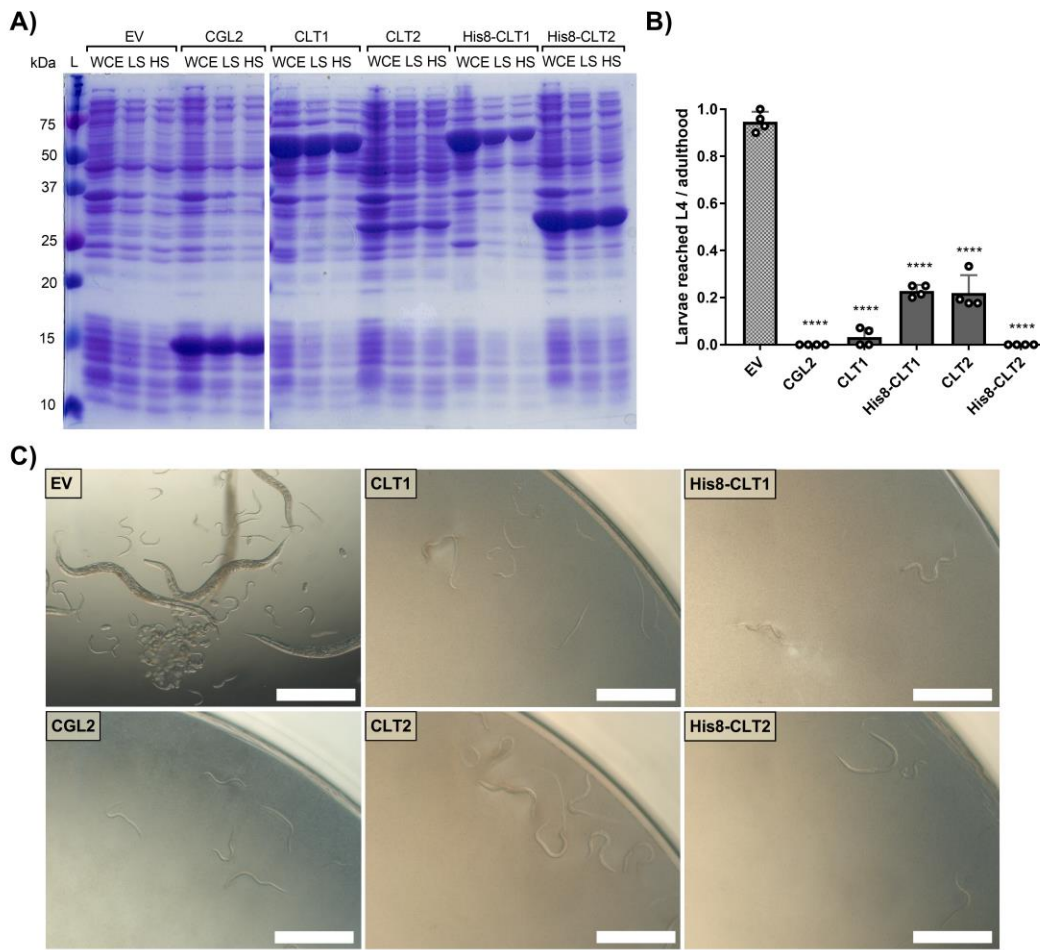


Figure 3: CLT1 and CLT2 are inducible novel nematotoxic proteins with putative cytolysin domain. **A)** Coomassie-stained SDS-PAGE showing heterologous expression and solubility of wild type and 8His-tagged constructs of CLT1 and CLT2 proteins. 20 μ l of whole cell extract (WCE), supernatants of low spin (LS; 5 min. at 5000g) and high spin (HS; 30 min. at 16000g) bacterial lysate were loaded on a gel. CGL2 was used as a positive control and 'empty' vector (EV) was used as a background control for IPTG-induced expression and solubility. **B)** Toxicity of CLT1 and CLT2 along with their 8His-tagged versions were assessed against *C. elegans* N2. IPTG-induced *E.coli* BL21 bearing previously characterized nematotoxic protein CGL2 and 'empty' vector (EV) were used as positive and negative controls, respectively. Dunnett's multiple comparisons test was used for statistical analysis. Error bars represent standard deviation of four biological replicates. * p < 0.05, ** p < 0.01, *** p < 0.001, **** p < 0.0001 vs. EV. **C)** Phase-contrast micrographs of *C. elegans* fed with IPTG-induced *E. coli* BL21 for 72 hr. expressing either of the labeled constructs. Scale bar = 500 μ m.

Chapter 3

3.4. *In vitro* lipase activity of CLT1 and CLT2 and analysis of the catalytic site mutant constructs

In order to confirm the predicted lipase activity of CLT1 and CLT2, we expressed and purified polyhistidine-tagged derivatives of wild type CLT1 and CLT2 from *E. coli* (Fig. 4C). The purified recombinant proteins were mixed with three different chromogenic ester substrates, and the lipase (esterase) activity of the proteins was determined by the release of p-nitrophenol from the substrates. In these assays, CLT2 showed lipase activity with para-nitrophenyl acetate (Fig. 4D) and para-nitrophenyl butyrate (Fig. 4E). Interestingly, we did not detect CLT2 activity against a longer carbon chain ester para-nitrophenyl palmitate (Fig. 4F). Conversely, CLT1 was neither active towards para-nitrophenyl acetate (Fig. 4D) nor towards para-nitrophenyl butyrate (Fig. 4E). The protein showed, however, weak activity towards para-nitrophenyl palmitate (Fig. 4F). As additional confirmation of these lipase activities, we introduced mutations in putative catalytic site residues of the toxins. Amino acid sequences of the predicted lipase domains of CLT1 and CLT2 were searched against NCBI non-redundant database. Alignment of the top 100 sequences revealed presumed serine-aspartate catalytic dyads [43] for CLT1. Both S260 and D326 amino acid residues were found to be conserved within 99% of the top 100 sequences. Similar analysis for CLT2 showed that putative catalytic dyads H89 and C155 [45] were conserved for 99 and 100 of the top 100 sequences, respectively. An alignment of the top 20 hits is shown in Fig. 2A and 2B.

Hereafter, CLT1(S260) and CLT2(C155) were mutated to alanine. A subsequent SDS-PAGE analysis demonstrated that both toxin variants were expressed in good amounts and soluble form in *E. coli* (Fig. 4A). *In vitro* lipase assays with the toxin variants revealed that the lipase activity of CLT2(C155A) was almost completely abolished against both substrates. The activity of CLT1 towards para-nitrophenyl palmitate was abolished by mutation of the predicted catalytic residue (S260A).

Nematotoxicity assays with *C. elegans* showed that the mutations of the predicted catalytic residues significantly reduced the toxicity for both CLT1 and CLT2 (Fig. 4B). Taken together, these data suggest that the lipase activity of CLT1 and CLT2 is required for their nematotoxicity.

Chapter 3

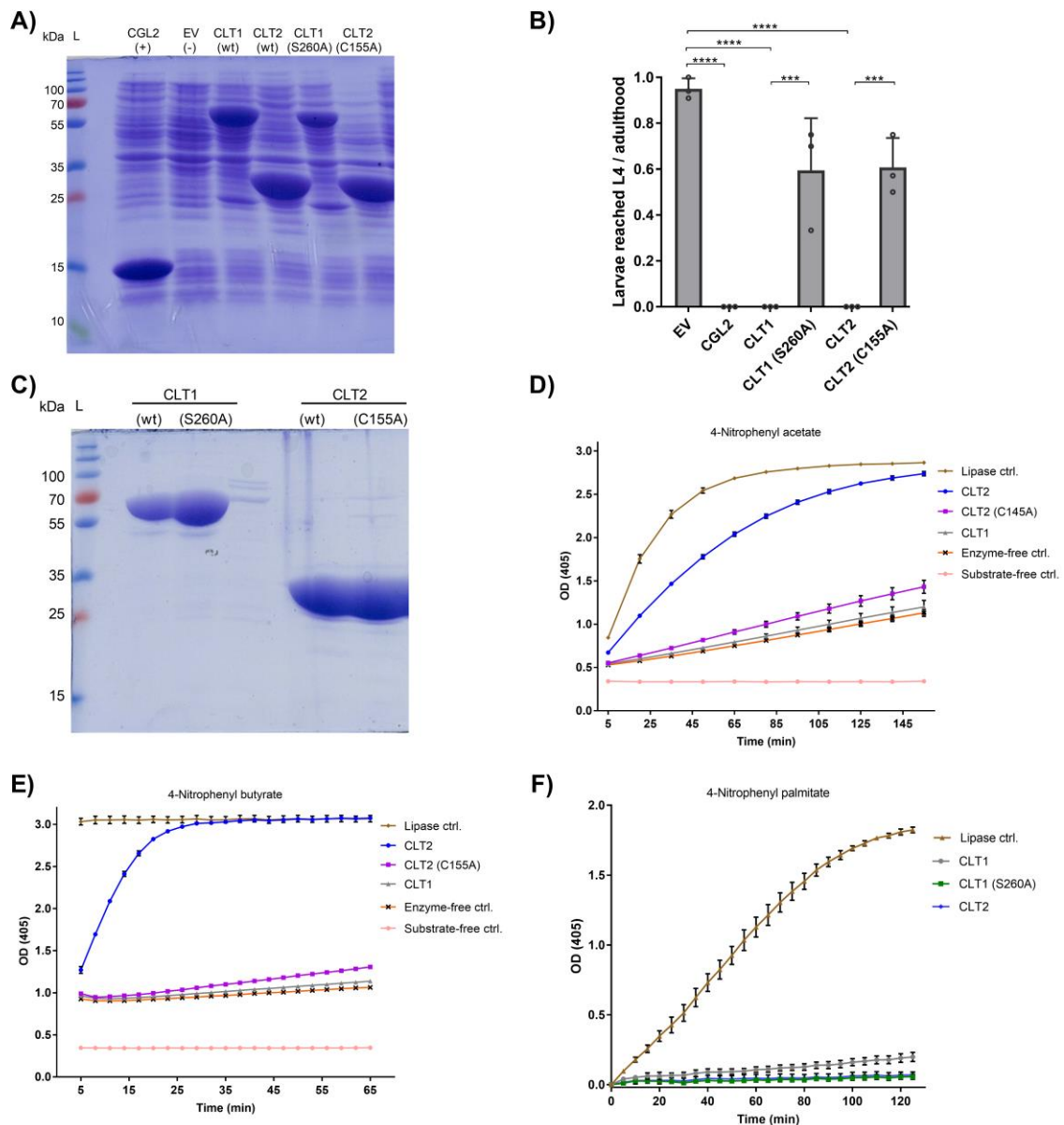


Figure 4: Analysis of catalytic site mutants and lipases assays with purified proteins. **A)** Heterologous expression of wild type and catalytic site mutants of CLT1 and CLT2 proteins. 20 μ l of bacterial lysate were loaded on polyacrylamide gel. CGL2 and 'empty' vector (EV) was used as positive and background controls for IPTG-induced expression, respectively. **B)** Effect of catalytic site mutations on toxicity of CLT1 and CLT2 against *C. elegans* N2. IPTG-induced *E.coli* BL21 carrying either previously characterized nematotoxic protein CGL2 or 'empty' vector (EV) were used as positive and negative controls, respectively. Dunnett's multiple comparisons test was used for statistical analysis. Error bars represent standard deviation of three biological replicates. * $p < 0.05$, ** $p < 0.01$, *** $p < 0.001$, **** $p < 0.0001$ vs. EV. **C)** The 8His-tagged proteins were purified over Ni-NTA beads and 10 μ l of final elute of each were analyzed on 12% SDS-PAGE gel, followed by Coomassie staining. The size of molecular markers are indicated. Lipase activity of the purified proteins were assessed towards p-nitrophenyl acetate (**D**), p-nitrophenyl butyrate (**E**), and p-nitrophenyl palmitate (**F**). Enzyme activity is shown as mean values \pm SD (n=4) for each time point. The error bars were not drawn if they are shorter than the height of the symbol. *Candida rugose* lipase (L1754, Sigma) was used as a positive control and labeled as 'Lipase ctrl'.

Chapter 3

3.5 Toxicity spectrum of CLT1 and CLT2

After confirming the toxicity of CLT1 and CLT2 towards the model organism *C. elegans*, we tested their toxicity against other six different bacterivorous nematode species and one omnivorous insect in order to assess the toxicity spectrum of these lipase toxins. All toxicity results are summarized in Fig. 5A. In contrast to the previously characterized lectin CGL2, neither CLT1 nor CLT2 showed toxicity against *A. aegypti* larvae (Fig. 5B). Interestingly, CLT1 and CLT2 showed different toxicity against two of the tested bacterivorous nematodes; while CLT1 was toxic towards *Distolabrellus veechi*, CLT2 was ineffective towards the same nematode species. The toxicity of CLT1 against *D. veechi* was weaker than the toxicity of CGL2 (Fig. 5C). We also found a different susceptibility of the facultative parasitic nematode *Helicephalobus gingivalis* towards the two lipase toxins. In this case, CLT2 was toxic whereas no toxicity of CLT1 towards the same nematode was detected, (Fig. 5C). These results suggest a difference in the target(s) of these toxins between the different nematode species.

Chapter 3

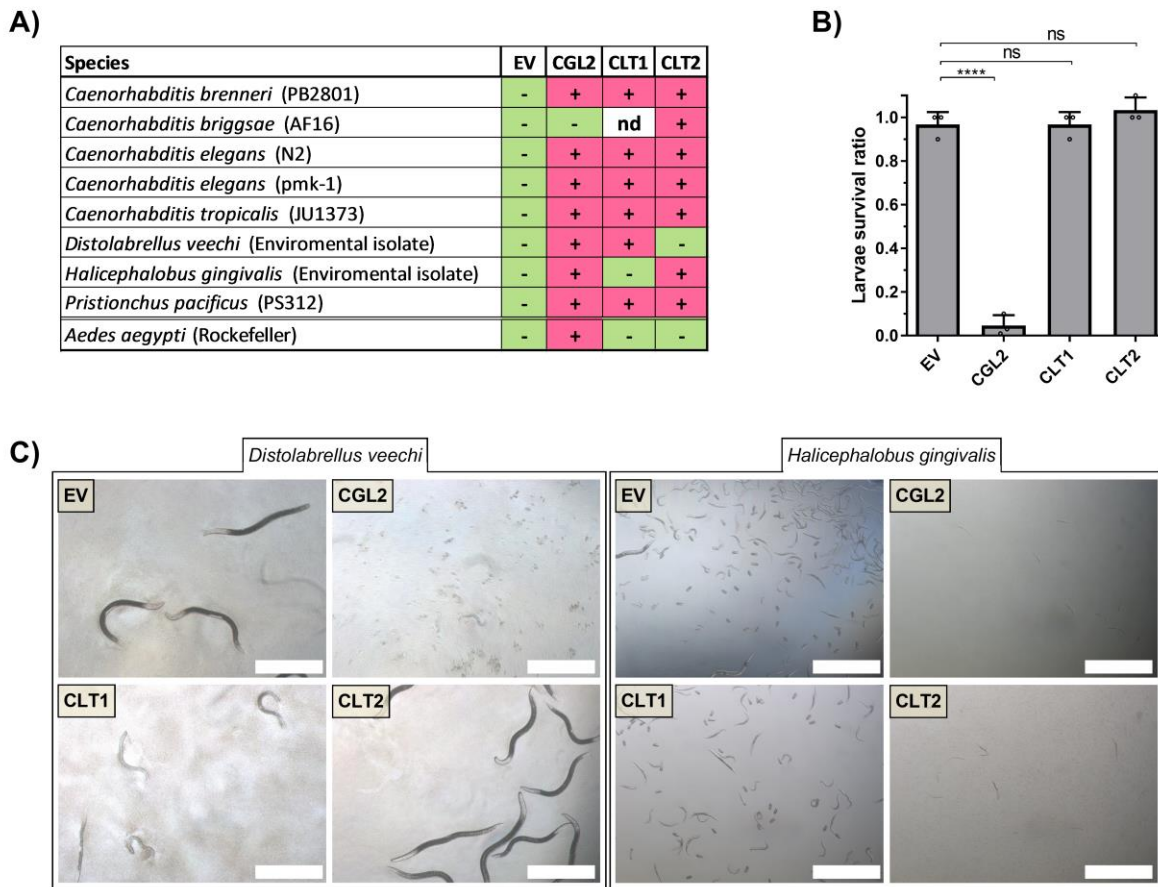


Figure 5: Toxicity of CLT1 and CLT2 against bacterivorous nematodes and omnivorous insect. **A)** Toxicity spectrum of CLT1 and CLT2 proteins was assessed against seven different species of bacterivorous nematodes and larvae of *Aedes aegypti*. Minus (-): lack of toxicity, plus (+): presence of toxicity, nd: not determined. **B)** Toxicity of CLT1 and CLT2 against *A. aegypti* larvae was quantified by counting number of survived larvae after four days of feeding on IPTG-induced *E.coli* BL21 bearing CLT1 or CLT2. *E.coli* BL21 expressing either previously characterized nematotoxic protein CGL2 or carrying 'empty' vector (EV) were used as positive and negative controls, respectively. Dunnett's multiple comparisons test was used for statistical analysis. Error bars represent standard deviation of three biological replicates. *** $p < 0.001$, **** $p < 0.0001$ vs. EV. **C)** Differential susceptibility of *D. veechi* and *H. gingivalis* against two lipases when they fed with IPTG-induced *E. coli* BL21 for 72 hr. containing either 'empty' vector (EV), or expressing CGL2 or CLT1 or CLT2. Scale bar = 500 μ m.

3.6 Comparison between CLT1 and its paralog

BLASTing of the CLT1 amino acid sequence against *C. cinerea* genome identified a predicted protein (P252116-JGI MycoCosm ProteinID) that is 78% identical to CLT1. This identity is even higher (87%) between the predicted lipase domains of the two proteins (Fig. S1-A). However, the differential expression of this paralog is considerably lower than of the CLT1 in the nematode-confronted mycelia of *C. cinerea* (Fig. S1-B). We wanted to know whether the two genes, which encoded by highly similar proteins but showed a different expression pattern upon nematode challenge, would have a similar toxicity. For this purpose, we cloned and expressed the cDNA encoding the CLT1 paralog in the same way as CLT1 (Fig. S1-C) and tested the toxicity of the respective recombinant bacteria against *C. elegans* and *A. aegypti*. Interestingly, unlike CLT1, the CLT1 paralog was not active against *C. elegans* (Fig. S1-D). On the other hand, the CLT1-paralog did, similar to CLT1, not show any sign of toxicity towards *A. aegypti* larvae (Fig. S1-E).

Chapter 3

Discussion

In this study, we report two novel fungal nematotoxic proteins, CLT1 and CLT2, with predicted lipase domains from the multicellular fungus *C. cinerea*. The genes coding for these fungal proteins were upregulated upon nematode predation, which indicates the involvement of these proteins in the defense response of the fungus against nematodes [15, 16, 18].

The results of mutation studies indicate that the nematotoxicity of *C. cinerea* is dependent on the lipase activity of the two identified proteins (CLT1 and CLT2), and that residues S260 and C155 are part of the catalytic site of CLT1 and CLT2, respectively. Similarly, Sato et al. showed that mutating the predicted active site residue (S142) of the *P. aeruginosa* lipase toxin ExoU inhibits its cytotoxicity and reduces the release of palmitic acid through *in vivo* assays [29, 30]. Another study showed that mutating the cysteine residue in the catalytic dyad of the cytotoxic tumor suppressor protein H-Rev107 eliminates its phospholipase activity along with its cytotoxicity [45, 46].

In addition to the *C. elegans* toxicity assay, we tested CLT1 and CLT2 toxicity against seven other species, including mosquito larvae, in order to determine the activity spectrum of these toxins. In contrast to the positive control CGL2, neither CLT1 nor CLT2 was active against *A. aegypti* larvae; this could mean that this insect does not contain any target molecules for these toxins or that they were not accessible to the toxins. Interestingly, we also observed a difference between the specificity of CLT1 and CLT2 against two of the eight tested species. Even though both are lipase domain-containing toxins, only CLT1 was toxic against the free-living bacterivorous nematode *D. veechi* and only CLT2 was toxic against the parasitic nematode *H. gingivalis*. These findings are indicative of the existence of different targets for these toxins. These two nematodes, *D. veechi* and *H. gingivalis*, are phylogenetically more distantly related to the rest of the tested nematodes [47]. This observation indicates the presence of conserved lipid targets among closely related species and the absence or inaccessibility of this target in resistant species. Several studies have shown different lipid compositions within different nematode species and proposed the identification of organisms based on their unique lipid profiles [48, 49]. These findings, taken together with the substrate specificity of the fungal lipase toxins, may explain the specific toxicity of lipases against certain species.

One of the main questions that remained unanswered is the self-protection mechanism of the producer fungus against its cytoplasmic lipase toxins. There are mainly three ways that producers overcome self-intoxication by their toxins; (a) they co-express a specific antitoxin along with a toxin [50, 51], (b) they express the toxin in inactive form that requires host-specific cofactors to activate toxin activity [52-54], (c) the toxin target molecule is lacking or inaccessible in the producer [55]. Several studies have shown that purified recombinant lipase toxins fail to show *in vitro* lipase activity;

Chapter 3

this is indicative of post-translational activation by the host. However, in the current study, we were able to detect lipase activity against synthetic lipid substrates (esters), especially in the case of CLT2. The activity of CLT1 was feeble, which might mean that it needed to be activated for its toxic effects. Lipidomics studies have revealed the unique composition of fatty acids for different nematode species [56]. Hence, targeting lipid molecules that are specific to the antagonist could be a self-protection strategy of producers and would shed some light on substrate specificity-based mechanisms of action of the lipase toxins. Interestingly, the CLT1 and CLT2 proteins can be expressed in the cytoplasm of *E. coli* in soluble form without any sign of toxicity against the expressing bacteria; this indicates that these lipase toxins have pronounced substrate specificity. The observed differences in the activities of CLT1 and CLT2 against different substrates in our *in vitro* lipase assays support the substrate specificity of these lipase toxins.

Unlike CLT2, CLT1 has a paralog gene in the *C. cinerea* genome. However, this paralog gene is not induced as strongly as CLT1 in the mycelia of *C. cinerea* upon nematode challenge; this might mean that it has a different function from CLT1. Indeed, our biotoxicity results show that the CLT1 paralog is not active against either of the tested species. This means that the toxicity of CLT1 is not limited to its lipase domain, and that regions outside of the lipase domains are probably also necessary for the toxicity of CLT1. These outside regions have lower similarity than the lipase domains between the amino acid sequences of CLT1 and its paralog.

Outside of the predicted lipase domains, CLT1 and CLT2 lack significant homology with known lipase proteins; this indicates that these toxins may represent a previously uncharacterized type of lipase superfamily. As seen in Figure 2, the predicted lipase domain is roughly one-third of the whole protein sequence of both CLT1 and CLT2. Therefore, we wanted to investigate the importance of regions outside of this predicted lipase domain for nematotoxicity and the *in vitro* lipase activity of CLT1 and CLT2. In the case of other lipase toxins, their C- and N-terminal regions may be involved in activation of the lipase activity of the toxin upon binding of a host factor, proteolytic cleavage, or subcellular localization of the toxin [30, 46]. Therefore, we truncated either the C- or the N-terminal of CLT1 and CLT2 and cloned them into *E. coli* BL21 for expression and subsequent studies. Unfortunately, these constructs (CLT1 Δ C, CLT1 Δ N, CLT2 Δ C, and CLT2 Δ N) were either insoluble or toxic to the *E. coli* after induction of their expression (Fig. S2A-C). Therefore, we could not proceed with the study, and the roles of the N- and C-terminal regions of CLT1 and CLT2 remain to be elucidated, perhaps with the help of a different expression system, in the future.

Nematodes are responsible for several human [57] and animal diseases [58] and are one of the prominent pests in agriculture [59, 60]. There are few agents that can be used for the bio-control of nematodes [61, 62]. Hence, our current findings may be useful with regard to the development of

Chapter 3

potential applications to control nematode populations in the context of nematode-borne diseases and agriculture. Although our current toxicity findings are specific to bacterivorous nematodes, the potential toxicity of our novel toxins against nematodes pathogenic to plants and animals should not be excluded and will be the topic of future studies.

Chapter 3

Competing interests

The authors declare that they have no competing interests.

Funding

This work was supported by the Swiss National Science Foundation (Grant No: 31003A-173097) and ETH Zurich.

Authors' contributions

AT prepared RNA samples for qRT-PCR, cloned and expressed CLT1 and CLT2, purified the proteins and performed lipases and biotoxicity assays, and wrote initial manuscript draft.

AG constructed 8His tagged CLT1 and CLT2 versions and performed toxicity assays with the tagged constructs.

PS created and analyzed part of the truncated constructs.

MK conceived and coordinated the project and critically revised the manuscript.

Acknowledgements

We thank Markus Aebei for fruitful discussions, P. Müller (Swiss Tropical and Public Health Institute, Basel, Switzerland) for supplying *Aedes aegypti* eggs. We also thank Chunyue Wei and Prof. Dr. Laura Nyström (Department of Health Sciences and Technology - ETHZ) for their suggestions to improve the *in vitro* lipase assays.

References

1. Boddy L, Jones TH: **Interactions between Basidiomycota and Invertebrates.** *Br Mycol Sy* 2008, **28**:155-179.
2. Doll K, Chatterjee S, Scheu S, Karlovsky P, Rohlfs M: **Fungal metabolic plasticity and sexual development mediate induced resistance to arthropod fungivory.** *Proc Biol Sci* 2013, **280**(1771):20131219.
3. Kunzler M: **How fungi defend themselves against microbial competitors and animal predators.** *PLoS Pathog* 2018, **14**(9):e1007184.
4. Gomez BL, Nosanchuk JD: **Melanin and fungi.** *Curr Opin Infect Dis* 2003, **16**(2):91-96.
5. Latge JP: **The cell wall: a carbohydrate armour for the fungal cell.** *Molecular microbiology* 2007, **66**(2):279-290.
6. Kempken F, Rohlfs M: **Fungal secondary metabolite biosynthesis - a chemical defence strategy against antagonistic animals?** *Fungal Ecology* 2009, **3**:107-114.
7. Rohlfs M, Churchill ACL: **Fungal secondary metabolites as modulators of interactions with insects and other arthropods.** In., vol. 48; 2011: 23-34.
8. Sabotic J, Ohm RA, Kunzler M: **Entomotoxic and nematotoxic lectins and protease inhibitors from fungal fruiting bodies.** *Appl Microbiol Biotechnol* 2016, **100**(1):91-111.
9. Kunzler M: **Hitting the sweet spot-glycans as targets of fungal defense effector proteins.** *Molecules* 2015, **20**(5):8144-8167.
10. Bleuler-Martinez S, Schmieder S, Aebi M, Kunzler M: **Biotin-Binding Proteins in the Defense of Mushrooms against Predators and Parasites.** *Appl Environ Microb* 2012, **78**(23):8485-8487.
11. Bleuler-Martinez S, Butschi A, Garbani M, Walti MA, Wohlschlager T, Potthoff E, Sabotic J, Pohleven J, Luthy P, Hengartner MO *et al*: **A lectin-mediated resistance of higher fungi against predators and parasites.** *Mol Ecol* 2011, **20**(14):3056-3070.
12. Renko M, Sabotic J, Mihelic M, Brzin J, Kos J, Turk D: **Versatile Loops in Mycocypins Inhibit Three Protease Families.** *J Biol Chem* 2010, **285**(1):308-316.
13. Mancheno JM, Tateno H, Sher D, Goldstein IJ: **Laetiporus sulphureus Lectin and Aerolysin Protein Family.** *Adv Exp Med Biol* 2010, **677**:67-80.
14. Lacadena J, Alvarez-Garcia E, Carreras-Sangra N, Herrero-Galan E, Alegre-Cebollada J, Garcia-Ortega L, Onaderra M, Gavilanes JG, del Pozo AM: **Fungal ribotoxins: molecular dissection of a family of natural killers.** *Fems Microbiol Rev* 2007, **31**(2):212-237.
15. Plaza DF, Schmieder SS, Lipzen A, Lindquist E, Künzler M: **Identification of a Novel Nematotoxic Protein by Challenging the Model Mushroom Coprinopsis cinerea with a Fungivorous Nematode.** *Genes/Genomes/Genetics* 2016, **6**:87-98.
16. Mathioni SM, Patel N, Riddick B, Sweigard JA, Czymmek KJ, Caplan JL, Kunjeti SG, Kunjeti S, Raman V, Hillman BI *et al*: **Transcriptomics of the Rice Blast Fungus Magnaporthe oryzae in Response to the Bacterial Antagonist Lysobacter enzymogenes Reveals Candidate Fungal Defense Response Genes.** *Plos One* 2013, **8**(10).
17. Schroechk V, Scherlach K, Nutzmann HW, Shelest E, Schmidt-Heck W, Schuemann J, Martin K, Hertweck C, Brakhage AA: **Intimate bacterial-fungal interaction triggers biosynthesis of archetypal polyketides in Aspergillus nidulans.** *P Natl Acad Sci USA* 2009, **106**(34):14558-14563.
18. Ortiz SC, Trienens M, Rohlfs M: **Induced Fungal Resistance to Insect Grazing: Reciprocal Fitness Consequences and Fungal Gene Expression in the Drosophila-Aspergillus Model System.** *Plos One* 2013, **8**(8).

Chapter 3

19. Davey J: **Biomembranes - Molecular-Structure and Function - Gennis,Rb.** *Nature* 1989, **339**(6226):591-591.
20. Murphy DJ: **The biogenesis and functions of lipid bodies in animals, plants and microorganisms.** *Prog Lipid Res* 2001, **40**(5):325-438.
21. Berridge MJ, Irvine RF: **Inositol phosphates and cell signalling.** *Nature* 1989, **341**(6239):197-205.
22. Simons K, Ikonen E: **Cell biology - How cells handle cholesterol.** *Science* 2000, **290**(5497):1721-1726.
23. Haucke V, Di Paolo G: **Lipids and lipid modifications in the regulation of membrane traffic.** *Curr Opin Cell Biol* 2007, **19**(4):426-435.
24. van der Meer-Janssen YPM, van Galen J, Batenburg JJ, Helms JB: **Lipids in host-pathogen interactions: Pathogens exploit the complexity of the host cell lipidome.** *Prog Lipid Res* 2010, **49**(1):1-26.
25. Saising J, Singdam S, Ongsakul M, Voravuthikunchai SP: **Lipase, protease, and biofilm as the major virulence factors in staphylococci isolated from acne lesions.** *Biosci Trends* 2012, **6**(4):160-164.
26. Singh VK, Srivastava M, Dasgupta A, Singh MP, Srivastava R, Srivastava BS: **Increased virulence of Mycobacterium tuberculosis H37Rv overexpressing LipY in a murine model.** *Tuberculosis (Edinb)* 2014, **94**(3):252-261.
27. Russell AB, LeRoux M, Hathazi K, Agnello DM, Ishikawa T, Wiggins PA, Wai SN, Mougous JD: **Diverse type VI secretion phospholipases are functionally plastic antibacterial effectors.** *Nature* 2013, **496**(7446):508-+.
28. Schmiel DH, Miller VL: **Bacterial phospholipases and pathogenesis.** *Microbes Infect* 1999, **1**(13):1103-1112.
29. Sato H, Frank DW: **ExoU is a potent intracellular phospholipase.** *Molecular microbiology* 2004, **53**(5):1279-1290.
30. Sato H, Frank DW, Hillard CJ, Feix JB, Pankhaniya RR, Moriyama K, Finck-Barbancon V, Buchaklian A, Lei M, Long RM *et al*: **The mechanism of action of the Pseudomonas aeruginosa-encoded type III cytotoxin, ExoU.** *Embo J* 2003, **22**(12):2959-2969.
31. Dong TG, Ho BT, Yoder-Himes DR, Mekalanos JJ: **Identification of T6SS-dependent effector and immunity proteins by Tn-seq in Vibrio cholerae.** *P Natl Acad Sci USA* 2013, **110**(7):2623-2628.
32. Rub A, Arish M, Husain SA, Ahmed N, Akhter Y: **Host-lipidome as a potential target of protozoan parasites.** *Microbes Infect* 2013, **15**(10-11):649-660.
33. Aloulou A, Ben Ali Y, Bezzine S, Gargouri Y, Gelb MH: **Phospholipases: An Overview.** *Methods Mol Biol* 2012, **861**:63-85.
34. Shinya R, Hasegawa K, Chen A, Kanzaki N, Sternberg PW: **Evidence of Hermaphroditism and Sex Ratio Distortion in the Fungal Feeding Nematode Bursaphelenchus okinawaensis.** *G3 (Bethesda, Md)* 2014, **4**:1907-1917.
35. Scheife JH, Lehmann KE, Buschmann IR, Unger T, Funke-Kaiser H: **Quantitative real-time RT-PCR data analysis: current concepts and the novel "gene expression's C-T difference" formula.** *J Mol Med* 2006, **84**(11):901-910.
36. Untergasser A, Nijveen H, Rao X, Bisseling T, Geurts R, Leunissen JAM: **Primer3Plus, an enhanced web interface to Primer3.** *Nucleic Acids Research* 2007, **35**:W71-W74.

Chapter 3

37. Künzler M, Bleuler-Martinez S, Butschi A, Garbani M, Lüthy P, Hengartner MO, Aeby M: **Biotoxicity assays for fruiting body lectins and other cytoplasmic proteins.** 2010, **480**:141-150.
38. Stiernagle T: **Maintenance of *C. elegans*.** *The C elegans Research Community, WormBook*, doi/101895/wormbook11011, <http://wwwwormbookorg> 2006.
39. Bleuler-Martínez S, Butschi A, Garbani M, Wilti MA, Wohlschlager T, Potthoff E, Sabotia J, Pohleven J, Lüthy P, Hengartner MO et al: **A lectin-mediated resistance of higher fungi against predators and parasites.** 2011, **20**:3056-3070.
40. Glogauer A, Martini VP, Faoro H, Couto GH, Muller-Santos M, Monteiro RA, Mitchell DA, de Souza EM, Pedrosa FO, Krieger N: **Identification and characterization of a new true lipase isolated through metagenomic approach.** *Microb Cell Fact* 2011, **10**.
41. Letunic I, Bork P: **20 years of the SMART protein domain annotation resource.** *Nucleic Acids Research* 2018, **46**(D1):D493-D496.
42. Kelley LA, Mezulis S, Yates CM, Wass MN, Sternberg MJE: **The Phyre2 web portal for protein modeling, prediction and analysis.** *Nat Protoc* 2015, **10**(6):845-858.
43. Simon GM, Cravatt BF: **Activity-based Proteomics of Enzyme Superfamilies: Serine Hydrolases as a Case Study.** *J Biol Chem* 2010, **285**(15):11051-11055.
44. Agarwal S, Kim H, Chan RB, Agarwal S, Williamson R, Cho W, Paolo GD, Satchell KJF: **Autophagy and endosomal trafficking inhibition by Vibrio cholerae MARTX toxin phosphatidylinositol-3-phosphate-specific phospholipase A1 activity.** *Nat Commun* 2015, **6**.
45. Uyama T, Morishita J, Jin XH, Okamoto Y, Tsuboi K, Ueda N: **The tumor suppressor gene H-Rev107 functions as a novel Ca(2+)-independent cytosolic phospholipase A(1/2) of the thiol hydrolase type.** *J Lipid Res* 2009, **50**(4):685-693.
46. Wei HJ, Wang L, Ren XB, Yu WY, Lin J, Jin CW, Xia B: **Structural and functional characterization of tumor suppressors TIG3 and H-REV107.** *Febs Lett* 2015, **589**(11):1179-1186.
47. Holovachov O, Camp L, Nadler SA: **Sensitivity of Ribosomal RNA Character Sampling in the Phylogeny of Rhabditida.** *Journal of Nematology* 2015, **47**(4):337-355.
48. Kuhn J, Richter A, Kahl T, Bauhus J, Schonning I, Ruess L: **Community level lipid profiling of consumers as a tool for soil food web diagnostics.** *Methods Ecol Evol* 2018, **9**(5):1265-1275.
49. Sekora NS, Lawrence KS, Agudelo P, van Santen E, McInroy JA: **Using FAME Analysis to Compare, Differentiate, and Identify Multiple Nematode Species.** *Journal of Nematology* 2009, **41**(3):163-173.
50. Campos PC, de Melo LA, Dias GLF, Fortes-Dias CL: **Endogenous phospholipase A(2) inhibitors in snakes: a brief overview.** *J Venom Anim Toxins* 2016, **22**.
51. Muñoz-Gómez AJ, Lemonnier M, Santos-Sierra S, Berzal-Herranz A, Díaz-Orejas R: **RNase/anti-RNase activities of the bacterial parD toxin-antitoxin system.** *Journal of Bacteriology* 2005, **187**(9):3151-3157.
52. Anderson DM, Feix JB, Frank DW: **Cross Kingdom Activators of Five Classes of Bacterial Effectors.** *Plos Pathogens* 2015, **11**(7).
53. Tyson GH, Hauser AR: **Phosphatidylinositol 4,5-Bisphosphate Is a Novel Coactivator of the *Pseudomonas aeruginosa* Cytotoxin ExoU.** *Infect Immun* 2013, **81**(8):2873-2881.
54. Christen M, Coyle LH, Hontz JS, LaRock DL, Pfuetzner RA, Megha, Miller SI: **Activation of a Bacterial Virulence Protein by the GTPase RhoA.** *Sci Signal* 2009, **2**(95).
55. Butschi A, Titz A, Walti MA, Olieric V, Paschinger K, Nobauer K, Guo XQ, Seeberger PH, Wilson IBH, Aeby M et al: **Caenorhabditis elegans N-glycan Core beta-galactoside Confers Sensitivity towards Nematotoxic Fungal Galectin CGL2.** *Plos Pathogens* 2010, **6**(1).

Chapter 3

56. Chen J, Ferris H, Scow KM, Graham KJ: **Fatty acid composition and dynamics of selected fungal-feeding nematodes and fungi.** *Comp Biochem Phys B* 2001, **130**(2):135-144.
57. L'Ollivier C, Piarroux R: **Diagnosis of human nematode infections.** *Expert Rev Anti-Infe* 2013, **11**(12):1363-1376.
58. Waller PJ: **The future of anthelmintics in sustainable parasite control programs for livestock.** *Helminthologia* 2003, **40**(2):97-102.
59. Engelbrecht G, Horak I, van Rensburg PJJ, Claassens S: **Bacillus-based bionematicides: development, modes of action and commercialisation.** *Biocontrol Sci Techn* 2018, **28**(7):629-653.
60. Quist CW, Smart G, Helder J: **Evolution of Plant Parasitism in the Phylum Nematoda.** *Annu Rev Phytopathol* 2015, **53**:289-310.
61. Kenney E, Eleftherianos I: **Entomopathogenic and plant pathogenic nematodes as opposing forces in agriculture.** *Int J Parasitol* 2016, **46**(1):13-19.
62. Witty MJ: **Current strategies in the search for novel antiparasitic agents.** *Int J Parasitol* 1999, **29**(1):95-103.

Chapter 3

Supplementary Information

Chapter 3

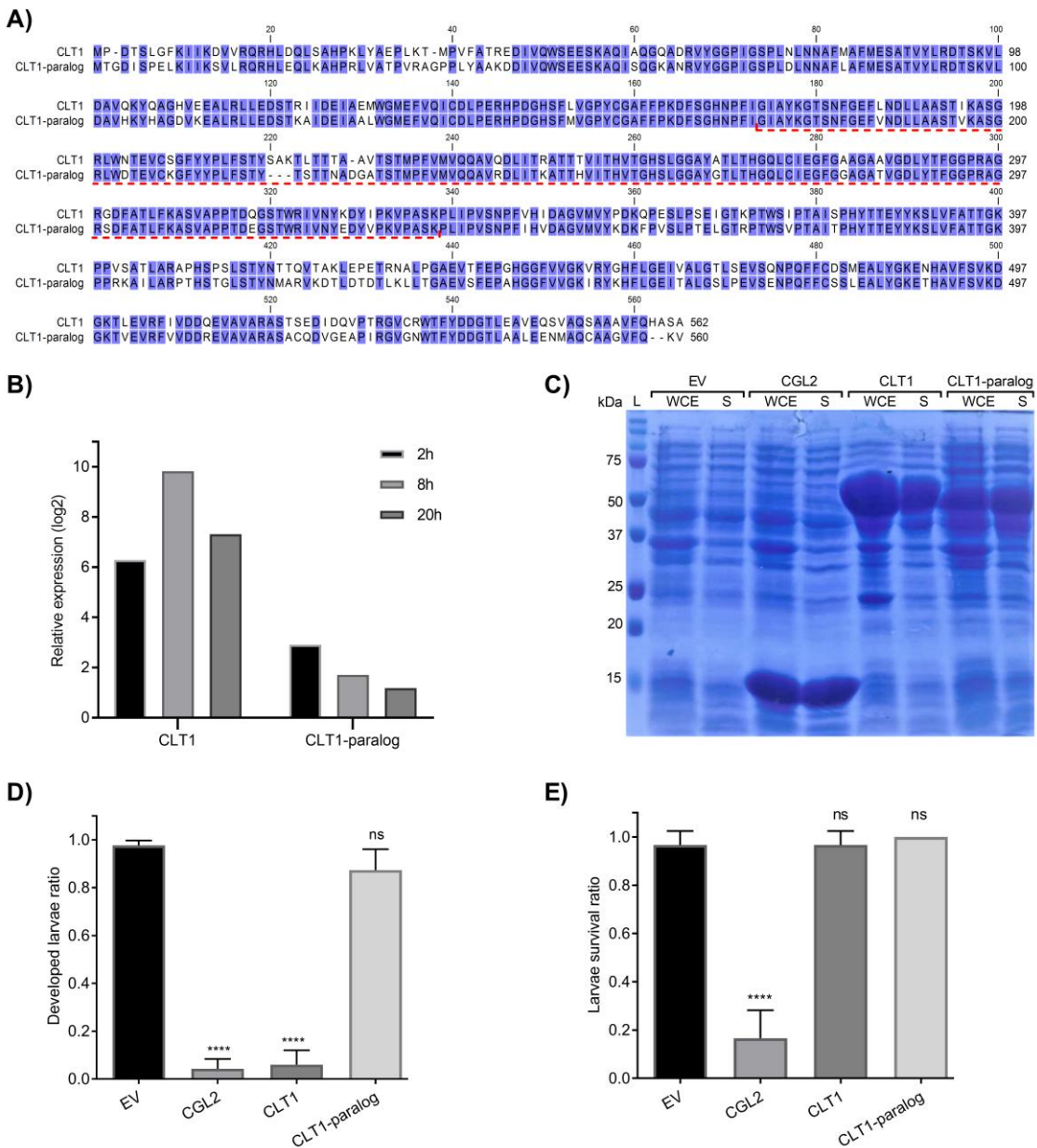


Figure S1: Comparison of CLT1 and its paralog. **A)** Amino acid sequences of CLT1 and its paralog were aligned using the ClustalW algorithm (v2.1). Dashed red line indicates predicted lipase domain. **B)** Relative expression of CLT1 and its paralog in mycelia of *C. cinerea* upon fungivorous nematode *A. avenae* challenge. **C)** Heterologous expression and solubility of CLT1 and its paralog in *E. coli* BL21. 20 μ l of bacterial whole cell extract (WCE) along with its supernatant (S) after 16,000g for 30 min were loaded on polyacrylamide gel. CGL2 and ‘empty’ vector (EV) was used as positive and background controls for IPTG-induced expression, respectively. **D)** Toxicity of CLT1 and its paralog against *C. elegans* larvae was assessed by counting number of developed larvae after two days of feeding on IPTG-induced *E. coli* BL21 bearing CLT1 or its paralog. **E)** Insecticidal effect of CLT-paralog along with CLT1 were tested against *A. aegypti* larvae by feeding the mosquito larvae with *E. coli* BL21 expressing proteins of interests for four days. *E. coli* expressing either previously characterized toxic protein CGL2 or carrying ‘empty’ vector (EV) were used as positive and negative controls, respectively. Dunnett’s multiple comparisons test was used for statistical analysis. Error bars represent standard deviation of three biological replicates. ns: not significant, *** $p < 0.0001$ vs. EV.

Chapter 3

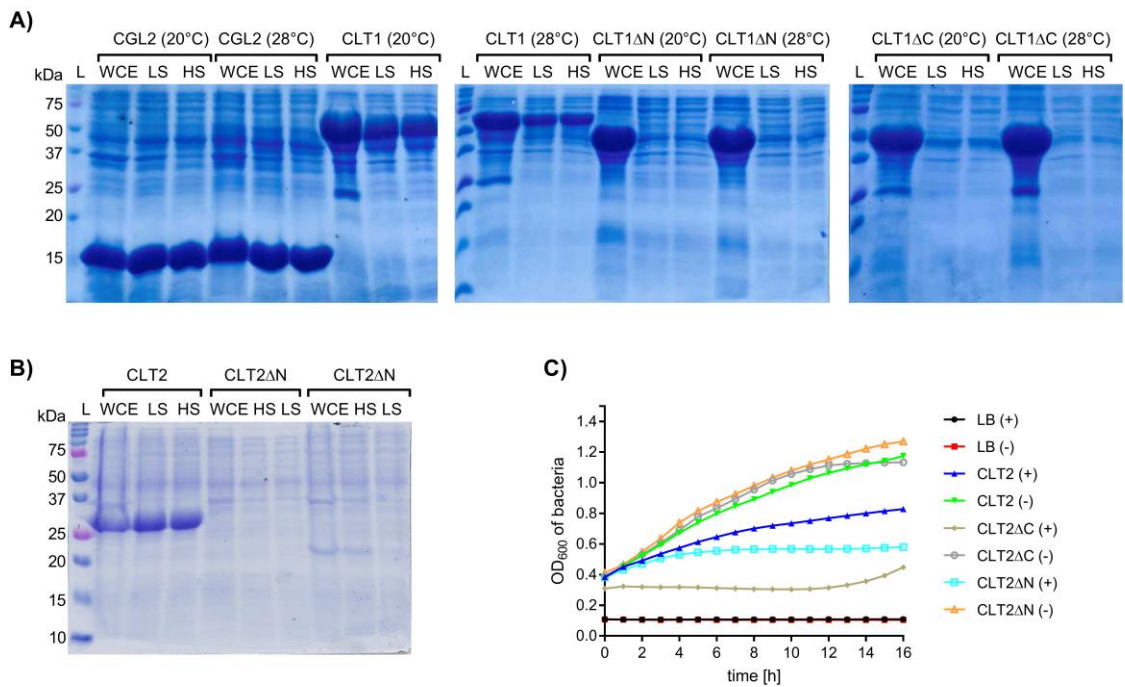


Figure S2: Truncated constructs of CLT1 and CLT2. **A)** Heterologous expression and solubility of CLT1 and its N- and C- termini truncated versions. 150 amino acids were truncated from either N-terminal or C terminal of CLT1 and the constructs were expressed in *E. coli* BL21 at two different temperatures. 20 μ l of bacterial whole cell extract (WCE) along with supernatants of low spin (LS; 5 min. at 5000g) and high spin (HS; 30 min. at 16000g) bacterial lysate were loaded on a SDS-PAGE. CGL2 was used as positive control for IPTG-induced expression and solubility. **B)** Likewise, 50 amino acids were truncated from either N-terminal or C terminal of CLT2 and the constructs were expressed in *E. coli* BL21 at 20°C. **C)** Bacterial growth effect of expressing the CLT2 truncated constructs were assessed in either IPTG induced (+) or non-induced *E. coli* BL21 cultures overnight at 20°C.

Chapter 3

Table S1: Organisms used in this study

Name	Strain	Source/Reference
<i>Caenorhabditis brenneri</i>	PB2801	Caenorhabditis Genetics Center (CGC)
<i>Caenorhabditis briggsae</i>	AF16	Caenorhabditis Genetics Center (CGC)
<i>Caenorhabditis elegans</i>	N2	Caenorhabditis Genetics Center (CGC)
<i>Caenorhabditis elegans</i>	pmk-1	Caenorhabditis Genetics Center (CGC)
<i>Caenorhabditis tropicalis</i>	JU1373	Caenorhabditis Genetics Center (CGC)
<i>Distolabrellus veechi</i>	environmental isolate	Luis Lugones, Utrecht university, Netherlands
<i>Halicephalobus gingivalis</i>	environmental isolate	Pamela Fonderie, Ghent University, Belgium
<i>Pristionchus pacificus</i>	PS312	Iain Wilson, BOKU, Vienna, Austria
<i>Aphelenchus avenae</i>	Standard lab strain	Richard Sikora, University of Bonn, Germany Pie Müller, Swiss Tropical and Public Health Institute, Basel, Switzerland
<i>Aedes aegypti</i>	Rockefeller	(Swamy et al., 1984)
<i>Coprinopsis cinerea</i>	AmutBmut	Paul W. Sternberg, California Institute of Technology, Pasadena, USA
<i>Botrytis cinerea</i>	BC-3	
<i>Escherichia coli</i>	DH5 α	
<i>Escherichia coli</i>	BL21(DE3)	Novagen
<i>Escherichia coli</i>	OP50	Hengartner laboratory, University of Zürich, Switzerland

Chapter 3

Table S2. Primers used in this study

Primer name	Sequence 5' - 3'
pF_CLT1	GGCGCATATGCCAGACACTCCCTCGGATTCAAGATTATCAAAG
pR_CLT1	AGTGC GGCCGCTTAAGCTGAAGCATGCTGAAAG
pF_CLT2	CCCCATTAATGACGTTGCGTCTCGCTCGGTCTTCTTCGAAT
pR_CLT2	GCTCGAGTGCGGCCGCTCACGCAGAGCCATCTCC
pF_CLT1_Paralog	GGCGCATATGACCGGCACATCTCCCCGAGC
pR_CLT1_Paralog	GTGCGGCCGCTCAGACCTCTGGAACACGCCGCT
pF_8His-CLT1	AATT CATATGCCACATCATCATCATCATCATGACACTCCCTCGGATTCAAGAT
pR_8His-CLT1	AGTGC GGCCGCTTAAGCTGAAGCATGCTGAAAG
pF_8His-CLT1ΔN	CTGGTAGGCCCTACTGTGGTGCATT
pR_8His-CLT1ΔN	ATGATGATGATGATGATGATGATGTGGCATA
pF_8His-CLT1ΔC	TTAAGCGGCCGCACTCGAGCAC
pR_8His-CLT1ΔC	CTCGCGAATGTGGCGCTCTG
pF_8His-CLT2	CTTATTAAATGACGCATCATCATCATCATCATCATCATT CGGTCTCGCTCCGGTCTTCTC
pR_8His-CLT2	GCTCGAGTGCGGCCGCTCACGCAGAGCCATCTT
pF_8His-CLT1(S260A)	CATGTC ACTGGTCATGC ACTCGGCCGTGCC
pR_8His-CLT1(S260A)	GGTGATGACCGTTGTAGTGGCCCTGGT
pF_8His-CLT2ΔN	ATCTTCCC AAGGGCACTCCATT
pR_8His-CLT2ΔN	ATGATGATGATGATGATGATGATGCG
pF_8His-CLT2ΔC	TGAGCGGCCGCACTCGAGCAC
pR_8His-CLT2ΔC	GTCGACGCCGTGTTCTCGCG
pF_8His-CLT2(C155A)	CTCTGGAAAGAACAAACGCCAGACATTGTCATC
pR_8His-CLT2(C155A)	GTCGTAAGGCTGTGGCATCATCTCGATGG
pF_CLT1_qRT-PCR	ATT CGCCGC ATTATACGACG
pR_CLT1_qRT-PCR	AGGCTCGAAGGTGACTTCAG
pF_CLT2_qRT-PCR	ACCTCTGGAAAGAACAACTGCC
pR_CLT2_qRT-PCR	TAAC TTGGCGAGCTCCTCG
pF_CGL2_qRT-PCR	AGCATCACTGTCATCGACCA
pR_CGL2_qRT-PCR	CCAGCGAGAACCTAAGCAG
pF_Tubulin_qRT-PCR	CAATCCATCGCTCACCTCTC
pR_Tubulin_qRT-PCR	GCGTAATGTCTGTGATGTC

Chapter 4

Functional characterization of ageritin, a novel type of ribotoxin highly expressed during fructification of the mushroom *Agrocybe aegerita*

Annageldi Tayyrov¹, Sophie Azevedo¹, Robert Herzog^{2,3}, Peter Lüthy¹, Pie Müller⁴, Simon Arzt⁵, Martin Rühl⁵, Florian Hennicke^{2,6*}, Markus Künzler^{1*}

¹Institute of Microbiology, Department of Biology, ETH Zürich, Vladimir-Prelog-Weg 4, CH-8093 Zürich, Switzerland

²Junior Research Group Genetics and Genomics of Fungi, Senckenberg Biodiversity and Climate Research Centre (SBiK-F), Georg-Voigt-Str. 14–16, 60325 Frankfurt/M, Germany

³Department of Environmental Biotechnology, TU Dresden, Markt 23, 02763 Zittau, Germany

⁴Swiss Tropical and Public Health Institute, Socinstrasse 57, CH-4002 Basel, Switzerland

⁵Institute of Food Chemistry and Food Biotechnology, Justus-Liebig-University Gießen, Heinrich-Buff-Ring 17, 35392 Gießen, Germany

⁶Institute of Ecology, Evolution and Diversity, Goethe-University, Max-von-Laue-Str. 13, 60438 Frankfurt/M, Germany

*Corresponding authors: florian.hennicke@senckenberg.de and mkuenzle@ethz.ch

Manuscript to be submitted.

Contributions:

- Cloning and expression of ageritin
- rRNA cleave activity assay
- Creating and analyzing point mutations
- Part of the toxicity assays

Chapter 4

Abstract:

Fungi are exposed to a large diversity of antagonists in their environment. To protect themselves, fungi mainly rely on chemical defense mediated by secondary metabolites, peptides and proteins. One type of defense proteins are toxic ribonucleases also called ribotoxins. These toxins are highly specific and cleave a single phosphodiester bond within the universally conserved sarcin-ricin loop (SRL) of ribosomes that is essential to the binding of translation elongation factors. Ribotoxin-mediated cleavage thus inhibits protein synthesis in the cells of antagonists exposed to the toxin. Here, we report on a ribotoxin from the edible mushroom *Agrocybe aegerita* referred to as ageritin, the first ribotoxin described from Basidiomycota. The amino acid sequence markedly differs from Ascomycota ribotoxins. It does not contain any signal peptide for classical secretion, which represents the first cytoplasmic ribotoxin found or discovered. Expression analysis of the ageritin-encoding gene *AaeAGT1* revealed a massive transcriptional induction during fruiting. *AaeAGT1*-cDNA was cloned and heterologously expressed in *E. coli* for further study. Toxicity assays with the ageritin-expressing bacterial cells, showed a strong insecticidal activity against *Aedes aegypti* larvae whereas no toxicity was found against five nematode species. The rRNase activity of the recombinant ageritin was confirmed *in vitro* using ribosomes of rabbit reticulocyte lysate. Treatment of the ribosomes with ageritin released a classical cleavage product of ribotoxins known as α -fragment. Site-specific mutagenesis of conserved residues showed correlation between *in vivo* and *in vitro* activities indicating that the entomotoxicity is mediated by the ribonucleolytic cleavage. The strong toxicity of ageritin against mosquito larvae makes it a potential candidate for the development of new biopesticides.

Chapter 4

Introduction

Fungi produce a variety of defense proteins to defend against antagonists [1-7]. They interfere with essential biological processes or structures within the target organisms. Ribosomes are essential molecular machineries present in all living cells, which make them ideal targets for defense proteins [8, 9]. Previous studies have revealed three main classes of proteins with ribonucleolytic activity towards ribosomal RNA. The first class comprises classical ribonucleases (RNases) that cleave any phosphodiester bond between ribonucleotides. These RNases have a rather low specificity for ribosomal RNAs and include non-toxic RNases [10, 11]. The second class of proteins is represented by ribosome inactivating proteins (RIPs) that act on ribosomes [12]. RIPs are *N*-glycosidases that depurinate a specific adenine residue located in the highly conserved sarcin-ricin loop (SRL) of the large subunit of the eukaryotic and prokaryotic ribosomes [13, 14]. The depurination of the adenine disrupts the binding of the translation elongation factors [15], inhibiting the protein synthesis and leading to the death of the targeted cells [16, 17]. High effectiveness and specificity makes RIPs a part of the defense systems of many organisms including bacteria [18], algae [19], fungi [20] and plants [21].

The third class of proteins with ribonucleolytic activity towards rRNA are called ribotoxins. They are small sized (10-20 kDa) and highly toxic [7, 22, 23]. Ribotoxins are highly specific fungal endonucleases that cleave a single phosphodiester bond at a universally conserved GAGA tetraloop of the SRL loop. Similar to RIPs, the damage of the loop inhibits binding of translation elongation factors and thus protein biosynthesis. Ultimately leading to the death of the target cells [24]. Until recently, characterized ribotoxins were all produced by members of the phylum Ascomycota. Two of the best-studied ribotoxins are α -sarcin [25] and restrictocin [26] produced by *Aspergillus giganteus* and *Aspergillus restrictus*, respectively. Hirsutellin A [27] from the fungal pathogen of mites, *Hirsutella thompsonii*, and anisoplin [28] from the entomopathogenic fungus *Metarrhizium anisopliae* are other, recently discovered ribotoxins. Lately, Landi et al. (2017) purified a protein, named ageritin, with ribonucleolytic activity towards rRNA from the commercially produced edible mushroom *Agrocybe aegerita*, a member of the phylum Basidiomycota [29]. In addition to the RNase activity, the authors demonstrated cytotoxicity and cell death promoting effects of ageritin towards certain human central nervous system (CNS) tumor cell lines.

In the present study, we identified the ageritin-encoding gene *AaeAGT1* and the neighboring gene *AaeAGT2* on the chromosomal *A. aegerita* DNA encoding a paralogous protein, from the recently published genome sequence of *A. aegerita* [30]. Transcriptional profiling of *AaeAGT1* revealed a massive induction of *AaeAGT1* expression during mushroom formation with a trend towards specificity to the developing mushroom cap. The predicted amino acid sequence of ageritin revealed marked differences with all other fungal ribotoxins described so far. Employing heterologous expression of

Chapter 4

ageritin in *E. coli*, we subsequently checked for insect and nematode toxicity as well as for *in vitro* ribonucleolytic activity of wild type and mutagenized ageritin. Finally, we functionally characterized the *AaeAGT2*-encoded ageritin paralog, which we identified based on its high sequence similarity to *AaeAgt1*. We performed sequence homology searches, revealing that homologs of ageritin are widespread among a variety of fungal species including several plant pathogenic fungi.

2. Materials and Methods

2.1 Strains and cultivation conditions

Cultivation and strain maintenance of *A. aegerita* AAE-3 was performed as described previously [31]. *Escherichia coli* strains DH5 α and BL21 (DE3) were used for cloning and protein expression, respectively. Other organisms including microorganisms used in this study are listed in Table S1.

2.2 Isolation of total RNA from *A. aegerita*

To sample vegetative mycelium and different fruiting body development stages of *A. aegerita* AAE-3, fruiting induction and sampling of fruiting stages was performed as described by Herzog et al. [31]. In brief, 1.5% w/v malt extract agar plates were inoculated centrally with a 0.5 cm diameter agar plug originating from the growing edge of an *A. aegerita* AAE-3 culture. The plates were incubated for 10 days at 25 °C in the dark and then exposed for fruiting body development (20 °C, 12 h/12 h light/dark cycle, saturated humidity, aeration).

Samples, consisting of at least three independent replicates, were taken (or isolated) from the following fruiting body development stages: I) vegetative mycelium before exposure to fruiting conditions (day 10 post inoculation); II) fruiting-primed mycelium 24 h to 48 h before emergence of fruiting body initials (day 14 post inoculation), III) fruiting body initials (day 15 to 16 post inoculation), IV) fruiting body primordia (day 17 to morning of day 19 post inoculation), V-VI) young fruiting bodies separated into stipe (V) and cap (VI) plectenchyme (day 19 to morning of day 21 post inoculation). Mature fruiting bodies exhibiting full cap expansion and a spore print emerging by morning of day 22 post inoculation were not sampled. Sample I) and II) were obtained by sampling the outermost 1 cm of mycelium from three replicate plates by gently scraping it off the agar with a sterile spatula. Samples were transferred immediately to a 2 mL microcentrifuge tube containing 1 mL of RNAlater® (product ID: R0901, Sigma Aldrich GmbH, Munich, Germany) which was transferred to 4 °C for a maximum of 3 days before freezing at -80 °C until total RNA extraction.

For total RNA extraction, NucleoSpin® RNA Plant kit (product ID: 740949, Macherey-Nagel GmbH & Co. KG, Düren, Germany) was used. Cell homogenization and lysis were modified. First, the RNAlater® was removed from each pooled sample and an appropriate amount of lysis Buffer RA1 added (350 µl per 100 mg fungal biomass). One 4 mm- and about ten 1 mm-diameter acetone-cleaned stainless-steel beads (product IDs: G40 and G10, respectively, KRS - Trading GmbH, Barchfeld-Immelborn, Germany) were then added to each tube. Homogenization was achieved using a mixer mill MM 200 (Retsch, Haan, Germany) set to 8 min at 25 Hz. Then, the protocol follows the manufacturer's recommendations

Chapter 4

for RNA-extraction from filamentous fungi, including a DNA digestion step with the kit's rDNase, beginning with the "filtrate lysate" step.

Total RNA extractions were eluted in nuclease-free water (product ID: T143, Carl Roth GmbH & Co. KG, Karlsruhe, Germany) and the RNA concentration was measured spectrophotometrically with a NanoDrop 2000c (Thermo Fisher Scientific, Waltham, USA). RNA quality was visually assessed by checking the integrity of the major rRNA bands in a Urea-PAGE. Per lane, 1 µg of total RNA was loaded onto pre-cast 6% TBE-Urea polyacrylamide gels (product ID: EC68652BOX, Thermo Fischer Scientific, Waltham, USA) and separated for 1 h at a constant voltage of 180V. For the detection SYBR™ Gold (product ID: S11494, Thermo Fisher Scientific) was used to stain the gel following the manufacturer's recommendations. Only if no degradation of the RNA was observed (major rRNA bands intact), the respective sample was further employed. Total RNAs were routinely stored at -80 °C.

2.3 Determination of suitable reference genes for quantitative real-time reverse transcription-PCR

Primer pairs for *A. aegerita* AAE-3 genes *AaeIMP1* (gene ID AAE3_02268), *AaeTIF1* (gene ID AAE3_07769) and *AaeARP1* (gene ID AAE3_11594) have been designed manually on basis of their genomic DNA ([30]; www.thines-lab.senckenberg.de/agrocybe_genome). In each case, the gene name was assigned in accordance with name of the kind of protein the gene putatively encodes according to the UniProt database (www.uniprot.org). Each primer pair (Table S2) spans a cDNA nucleotide region of 150 bp. Twelve reference samples were taken from vegetative mycelia grown for 10, 14, 18, 20, 22 and 27 days on agar plates, from primordia derived from 18 day old agar plate cultures, and from fruiting bodies before, during and after sporulation. The samples were stored in RNAlater (Qiagen, Venlo, Netherlands). Total RNA was extracted using TRIzol (Thermo Fischer Scientific) according to the manufacturer's protocol by the method of Chomczynski and Sacchi [32]. The RNA concentration was determined by the absorbance at 260 nm using a Pearl Nanophotometer (Implen, Munich, Germany). 2 µg total RNA of each sample was reverse transcribed applying the M-MLV reverse transcriptase kit according to the manufacturer's protocol (Thermo Fischer Scientific) using oligo-(dT)₃₀-Primer. The resulting cDNA sample was incubated for 20 min at 37 °C with 1 µL AMRESCO RNase A (VWR International, Radnor, PA, USA) instead of the RNase H described in the M-MLV reverse transcriptase kit protocol. Quantitative polymerase chain reaction (qPCR) was conducted in triplicates using the KAPA SYBR® FAST Universal Kit (Sigma Aldrich GmbH) according to the manufacturer's protocol with an annealing step at 60 °C for 30 sec, an elongation step at 72 °C for 10 sec in a total volume of 25 µL with a final concentration of 0.9 µM for each primer and 7 µL of cDNA sample applying an CFX connect Real-Time Detection System (Bio-Rad, Hercules, CA, USA).

Chapter 4

To test primer efficiency, cDNA samples were combined in equal parts. Six logarithmic dilution steps of the cDNA master mix were used for qPCR (see above). Cq-values of the dilutions were plotted versus the dilution factor and linear regression as well as the corresponding determination coefficient were calculated for each reference gene. The primer efficiency was calculated according to Pfaffl [33]. For validation of the reference genes, all 12 cDNA samples were used separately for a qPCR analysis with all three primer pairs. Cq-values were used for validation using the NormFinder [34] and geNorm [35] algorithm.

2.4 One-step quantitative real-time reverse transcription-PCR (qRT-PCR) using total RNA samples

Primers and qRT-PCR conditions were designed according to the general recommendations of the MIQE guidelines [36]. The software Geneious R11 (<https://www.geneious.com>, Kearse et al. [37]) was applied to design the primers for the genes encoding ageritin (*AaeAGT1*, gene ID AAE3_01767) and its paralog (*AaeAGT2*, gene ID AAE3_01768) as well as the two reference genes *AaeTIF1* (gene ID AAE3_07669) and *AaeIMP1* (gene ID AAE3_02268) from the *A. aegerita* AAE-3 genome sequence ([30]; www.thines-lab.senckenberg.de/agrocybe_genome). Primers for these genes are listed in Table S2. All qRT-PCRs were performed on an AriaMX Real-Time PCR System (Agilent Technologies, La Jolla, CA, USA) in optically clear 96-well plates with 8-cap strips using the Brilliant Ultra-Fast SYBR Green QRT-PCR Master Mix (Agilent Technologies). This one-step master mix included the reverse transcriptase (RT), reaction buffer, DNA polymerase and SYBR green. The RT-reaction was performed in each well before the qRT-PCR program was started. All samples were run in three biological replicates with 25 ng total RNA per reaction as template. Constant qRT-PCR reaction components across same-amplicon-PCRs were prepared in master mixes. The final concentration per primer was 250 nM. A melting curve analysis was done for each reaction at the end of the qRT-PCR to determine amplicon purity. See Table S3 for the qRT-PCR program.

2.5 Relative differential expression analysis

For data analysis the fluorescence readings were extracted from the raw run plots. The baseline correction and determination of the quantification cycle (Cq) and mean PCR efficiency (E) per amplicon was done according to Ruijter et al. [38] using the LinRegPCR program in version 2017.1. An evaluation of several established qPCR data analysis methods can be found in Ruijter et al. [39]. LinRegPCR computes PCR efficiencies by finding the best window-of-log-linearity (W-o-L) of each single PCR reaction kinetic and taking the rate change within this window as the PCR efficiency (E). All E values of

Chapter 4

the same amplicon were averaged and this “mean amplicon E” value was then used for further calculations.

To calculate relative expression ratios the software REST [40], in its REST2009 version, was used. It employs the ‘Pfaffl method’ [33] to calculate the E corrected relative gene expressions allowing the use of multiple reference genes at the same time for normalization based on Vandesompele et al. [35]. In addition, REST2009 performs iterative (here 2000 times) randomization tests to produce 95% confidence intervals around the calculated relative expressions. Foraging, vegetative mycelium that was not induced for fruiting (Sample I) was chosen as calibrator sample.

2.6 cDNA generation from *A. aegerita* RNA

To produce first strand cDNA from total RNA of fruiting-primed mycelium 24 to 48 h before emergence of fruiting body initials (day 14 post inoculation), the RevertAid first strand cDNA synthesis kit (product ID: K1621, Thermo Fisher Scientific) and an oligo(dT)₁₈ primer was used according to the manufacturer’s recommendations. First strand total-cDNA was then directly used as a template to produce specific cDNA of the ageritin-encoding gene *AaeAGT1* (gene ID AAE3_01767) with primer pair cds01767-f and cds01767-r (Table S2) in a standard 3-step PCR using Phusion polymerase (product ID: F530, Thermo Fischer Scientific) with a 62 °C annealing temperature. DNA sequence information for primer design was obtained from the genome sequence of *A. aegerita* AAE-3 ([30]; www.thines-lab.senckenberg.de/agrocybe_genome).

2.7 Construction of ageritin expression vectors

The coding sequence of ageritin was identified by BLASTing the published 25 N-terminal residues of ageritin against the predicted proteome of *Agrocybe aegerita* [30]. The sequence was amplified with the primer pair pAGT1-Nd and pAGT1-N (Table S2) from the *AaeAGT1*-cDNA and cloned into a pET-24b (+) expression vector. The sequence of the cloned cDNA was confirmed by DNA sequencing. The plasmid was transformed into *E. coli* BL21 cells. For expression of ageritin, BL21-transformants were pre-cultivated in Luria-Bertani (LB) medium supplemented with 50 mg/l kanamycin at 37 °C. At an OD₆₀₀ of around 0.5, the cells were induced with 0.5 mM isopropyl β-D-1-thiogalactopyranoside (IPTG) and cultivated over night at 16 °C. Expression and solubility checks of ageritin were performed as previously described [41].

Chapter 4

2.8 Toxicity against mosquito larvae and nematodes

Egg masses of the mosquito *Aedes aegypti* (strain Rockefeller) were provided on filter papers by the Swiss Tropical and Public Health Institute (Basel, Switzerland). To rear the mosquito larvae, small pieces of the filter paper, 2 cm² to 5 cm², depending on the density of the eggs were placed into glass petri dishes containing tap water at 28 °C. The larvae hatched within a few hours. They were fed with finely ground commercially available food for ornamental fish. The toxicity assays against the mosquito larvae were performed as described previously [41]. In brief larvae in their third stage (L3) were used for the toxicity assays. The food source was changed from fish food to *E. coli*, adjusted in all the bioassays to OD₆₀₀ of 0.4. The mosquito larvae fed readily on and were able to develop to the adult stage. The consumption of empty vector *E. coli* reduced the optical density. The bioassay was performed by transferring 10 L3 larvae to Schott bottles containing 99 mL of tap water. Suspensions of 1 ml of *E. coli* cells expressing the desired protein were added. The mosquito larvae were kept in the dark at 28 °C for 4 to 7 days. The toxicity was assessed by measuring the reduction optical density, and by recording larval mortality over a four day period. Adult mosquitoes which were able to develop from the larvae were counted after 7 days. Starvation controls were used to check whether the death of the larvae is due to toxicity or refrainment of the larvae from consuming the bacteria.

Nematotoxicity assays against five different species of nematodes were performed as described before [41, 42].

2.9 Tagging and purification of ageritin

For the purification of recombinant ageritin over Ni-NTA columns, the protein was tagged with a polyhistidine(8)-tag at its N-terminus. A respective expression plasmid was constructed by PCR using pF_8His-Ag and pR_8His-Ag primer pair listed in Table S2. His8-ageritin was expressed as described for untagged ageritin. Protein purification was performed as described previously [3]. In brief, IPTG induced *E. coli* BL21 cells expressing ageritin overnight at 16 °C were harvested at 8000 × g for 10 min at 4 °C. The bacterial pellet was resuspended in cold lysis buffer (50 mM PBS, 20 mM imidazole, pH 8.0) and homogenized in a French Press, followed by centrifugation for 30 minutes at 16000 × g. The supernatant containing the soluble protein fraction was incubated with Ni-NTA beads overnight on a turning wheel at 4 °C. The beads were then loaded onto a Protino® column and washed five times with the lysis buffer. The proteins were eluted from the beads using an elution buffer (50 mM PBS, 400 mM imidazole, pH 8.0). The proteins were concentrated on a 15 mL 30 kD cut-off Amicon® Ultra-4 centrifugal filter unit, and desalting using a PD-10 column (GE Healthcare). Protein concentration was

Chapter 4

determined with the Pierce BCA kit (Thermo Scientific). Purified proteins were run on a 14% SDS-PAGE along with whole cell extract (WCE) and stained with Coomassie Brilliant Blue G 250.

2.10 *In vitro* rRNA cleavage assay

To detect the rRNA cleavage activity, 20 µL of untreated rabbit reticulate lysate (Promega) was mixed with final concentration of 400 nM ageritin or with its mutant versions in the reaction buffer (15 mM Tris-HCl, 15 mM NaCl, 50 mM KCl, 2.5 mM EDTA. pH 7.6) to a final volume of 30 µL [43]. The reaction mixture was incubated for one hour at 30 °C, and stopped by adding 3 µL of 10% SDS. RNAs were isolated from the reaction mixture by chloroform-phenol extraction. The RNAs were mixed with 2x RNA loading dye (ThermoFisher) and denatured for 5 minutes at 65 °C, cooled on ice and run on 2% native agarose gel in cold TBE Buffer (Tris-borate-EDTA) for 30 minutes at 100 V. A-Sarcin (Axxora, USA) and PBS buffer were used as positive and negative controls, respectively.

2.11 Toxicity towards insect cells

Cytotoxicity of ageritin was tested against *Spodoptera frugiperda* Sf21 cells (IPLB-Sf21-AE). The insect cells were pre-cultivated in Sf-900™ II SFM medium (Invitrogen) supplemented with streptomycin (100 µg/mL) and penicillin (100 µg/mL). Cells were diluted to a final density of 0.29×10^6 /mL and 500 µL of the cell were added per well of 24-well plates. The insect cells were exposed to different concentrations of ageritin (0.1 µM, 1 µM and 10 µM) dissolved in PBS. The well plates were incubated for three days at 27 °C. The liquid medium was removed from the wells and the cells were stained with 15 µL of 0.4% Trypan Blue solution. The number of unstained (alive) cells was determined under a microscope. A-Sarcin (Axxora, USA) and 5% DMSO were used as positive controls whereas the PBS buffer served as a negative control. Dunnett's multiple comparisons test was used to assess the statistical differences between mean values of treatment and control groups.

2.12 Alignment and phylogenetic tree

The complete amino acid sequence of ageritin was BLASTed against Gene Catalog Proteins (GCP) database at JGI MycoCosm [44]. The hit regions of the top 10 sequences with highest homology were aligned using the ClustalW algorithm (v2.1) at CLC Genomics Workbench [45].

For the analysis of phylogenetic relationships among the top homologs of ageritin, the complete amino acid sequence of top 30 hits were aligned using ClustalW (v2.1) [45] and, based on the alignment, a

Chapter 4

phylogenetic tree was constructed with Maximum Likelihood algorithm [46]. The tree was depicted as a rooted circular cladogram. The hit with the lowest homology to ageritin among the 30 hits had an E-value of 7.2E-16. The more information about these 30 hits see Table S4.

2.13 Creation and expression of mutant versions

Based on the created alignment, six of the completely conserved residues (Y57, R87, D89, D91, H98 and K110) of ageritin were mutated individually to alanine using the site-specific primers listed in Table S2. The plasmid encoding His8-ageritin was used as template for construction of single-site mutants. Expression and purification of the mutant ageritin variants were done as for wild type His8-ageritin.

2.14 Expression of ageritin paralog

The coding sequence for the paralog of ageritin (63% sequence identity) was ordered from GenScript (Piscataway, NJ, USA). Expression and purification of the paralogous protein was done as described above for ageritin.

3. Results

3.1 Identification of the ageritin encoding gene from the *A. aegerita* genome sequence

By BLASTing the published 25 N-terminal residues of ageritin [29] against the predicted proteome of *A. aegerita*, we could identify the ageritin-encoding gene from the fungus' genome sequence. It is further referred as *AaeAGT1* (gene ID AAE3_01767, www.thines-lab.senckenberg.de/agrocybe_genome). In addition, we also spotted a neighboring gene encoding a paralogous protein, which is referred as *AaeAGT2* (gene ID AAE3_01768, www.thines-lab.senckenberg.de/agrocybe_genome). Interestingly, the comparison of the predicted amino acid sequence of *AaeAgt1* did not show any sequence similarity to known ascomycete ribotoxins and does not possess any known signal sequence. Thus, it is suggesting to be a novel type of ribotoxin.

3.2 Identification of reference genes for expression monitoring during *A. aegerita* mushroom formation

Based on a transcriptomic analysis of 15 different biological samples spanning the whole *A. aegerita* fructification process of *A. aegerita* AAE-3 (Hennicke, unpublished) three genes with a putative high expression stability (Fig. S1A) have been spotted within the genome sequence of this dikaryotic strain ([30]; www.thines-lab.senckenberg.de/agrocybe_genome): *AaeIMP1* (gene ID AAE3_02268), *AaeTIF1* (gene ID AAE3_07769) and *AaeARP1* (gene ID AAE3_11594). Blast search of the deduced amino acid sequences against the UniProt database (www.uniprot.org) revealed AAE3_02268 encoding a putative importin, AAE3_07669 coding for a putative translation initiation factor and AAE3_11594 encoding a putative autophagy related protein. The manually designed primer pairs for each putative reference gene showed efficiencies of 104%, 109% and 107% with a regression coefficient of 0.998, 0.996 and 0.998 for *AaeIMP1*, *AaeTIF1* and *AaeARP1*, respectively. Validation of the reference genes according to their Cq-values for 12 analyzed samples (Fig. S1B) with the NormFinder algorithm revealed values of 0.119, 0.126 and 0.167 for genes *AaeTIF1*, *AaeIMP1* and *AaeARP1*, respectively. geNorm showed a similar trend with values of 0.29 for *AaeTIF1* and *AaeIMP1* as well as 0.33 for *AaeARP1*. Overall, on the basis of the NormFinder and geNorm validation, reference genes *AaeTIF1* (gene ID AAE3_07769) and *AaeIMP1* (gene ID AAE3_02268) are the best combination for qPCR based transcription analyses of *A. aegerita* qPCR.

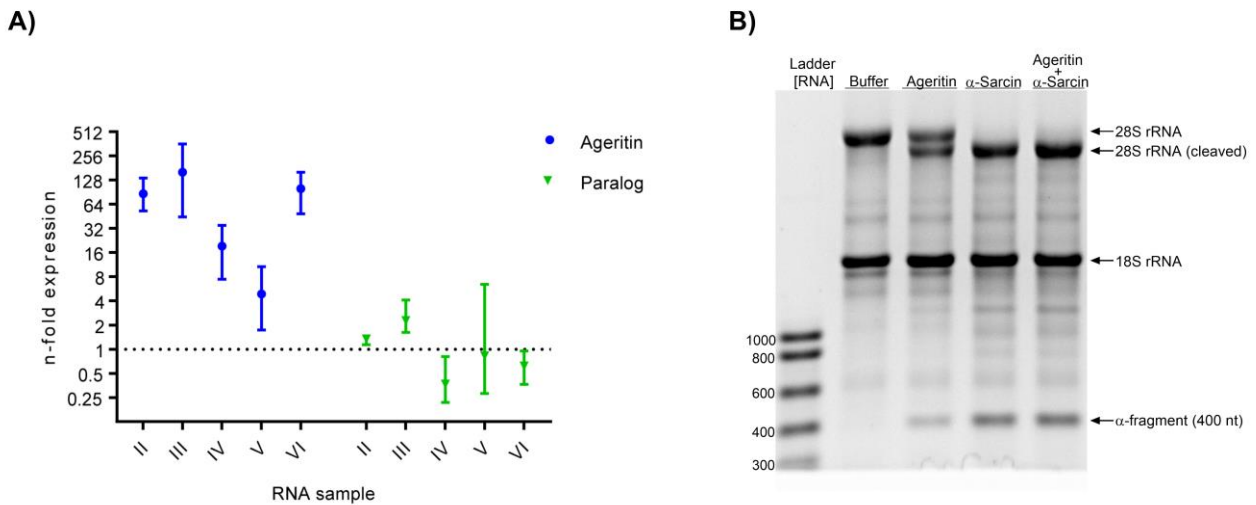


Figure 1: Differential expression and *in vitro* rRNA cleavage activity of ageritin. **A)** qRT-PCR results for *AaeAGT1* (encoding ageritin) and *AaeAGT2* (encoding ageritin-paralog) expression. The relative n-fold expression to the calibrator-sample (I, vegetative mycelium) is shown on a log 2 scale. The error bars represent the standard deviation of three biological replicates. The dotted horizontal line indicates the normalized expression level in sample I. Further samples are: II, fruiting primed mycelium 24 h to 48 h before emergence of visible fruiting body (FB) initials; III, FB initials; IV, entire FB primordia; V, young FB stipe; VI, young FB cap. **B)** Ribonucleolytic activity of ageritin was assayed with 400 nM of purified ageritin against ribosomes of rabbit reticulocyte lysate. Ribotoxin α -Sarcin and PBS buffer were used as positive and negative controls, respectively. Ribosomal RNAs and classical ribotoxin cleavage product, α -fragment, were indicated.

3.3 Expression of the ageritin gene during fruiting body formation of *A. aegerita*

In order to assess the expression of both the ageritin encoding gene *AaeAGT1* and the paralogous gene *AaeAGT2*, quantitative real-time reverse transcription PCR (qRT-PCR) analyses were carried out using RNA from different dikaryotic developmental stages of *A. aegerita* AAE-3. Using vegetative mycelium as a calibrator sample, a strong upregulation of *AaeAGT1* expression was detected throughout the fruiting body development of *A. aegerita* AAE-3, which was not the case regarding the expression of *AaeAGT2* (Fig. 1A). LinRegPCR-determined mean amplicon PCR efficiencies were on average derived from 4.8 separate reaction kinetics per amplicon and had in all cases a relative standard error $\leq 0.6\%$. The determined PCR efficiencies, as expressed by the mean amplicon E value, for *AaeAGT1* (gene ID AAE3_01767) and its paralog (*AaeAGT2*, gene ID AAE3_01768), were comparable to each other, likewise the reference genes *AaeTIF1* (gene ID AAE3_07769) and *AaeIMP1* (gene ID AAE3_02268). The distribution ranged within 11%. The baseline corrected Cq values and respective mean amplicon E values were fed into the REST2009 version of the REST software [40] and the results are shown in Fig. 1A as n-fold changes to the calibrator sample (I, vegetative mycelium). *AaeAGT1* expression is highly

Chapter 4

upregulated in an apparent switch-like manner in the ready-to-fruit mycelium (sample II; 87-fold), fruiting body initials (sample III; 160-fold) and young fruiting body caps (sample VI; 100-fold), to a lesser extend in whole primordia (sample IV; 19-fold) and in comparison, negligible in young fruiting body stipes (sample V; 5-fold). *AaeAGT2* showed no clear change in expression of the magnitudes of the *AaeAGT1* amplicon varying from 0.4 for sample IV to 2.3 for sample III. Both gene's Cq values in the calibrator sample were very similar with an average 25.55 for the *AaeAGT1* amplicon and an average 25.73 for its paralog *AaeAGT2* indicating comparable template amounts for a '1-fold' expression for the two genes in this cDNA pool.

3.4 Heterologous expression and purification of ageritin from *E. coli* cells

In contrast to all other ribotoxins, *AaeAgt1* does not contain a signal peptide for a classical secretion and is thus predicted to be localized in the cytoplasm. Based on the lack of a signal peptide in the predicted amino acid sequence of ageritin, we aimed at expressing the protein in the cytoplasm of *E. coli*. Expression and solubility tests confirmed that both untagged and N-terminally His8-tagged ageritin can be expressed in a fully soluble form in the bacterial cytoplasm (Fig. S2A). The solubility of the His8-tagged ageritin allowed us to purify the recombinant protein for the *in vitro* experiments (Fig. S2A). His8-ageritin was purified over Ni-NTA affinity columns to homogeneity (Fig. S2B). The purified ageritin protein was used for *in vitro* ribonucleolytic cleavage assay and for Sf21 insect cell line toxicity assay.

3.5 rRNA cleavage activity of recombinant ageritin

Ribonucleolytic activity of ageritin was assayed against ribosomes of a rabbit reticulocyte lysate. The results indicate that ageritin, same as α -Sarcin [47], acts on the 28S rRNA subunit of ribosomes and releases as classical ribotoxin cleavage product the α -fragment (Fig. 1B). We observed a similar pattern on a gel for the two samples that were either treated with only α -Sarcin or simultaneously with both α -Sarcin and ageritin, suggesting that the cleavage site for ageritin is the same or identical (Fig. 1B).

3.6 Entomo- and nematotoxicity of wild type and recombinant ageritin

The ageritin-expressing *E. coli* cells and its tagged version were tested for insecticidal activity against L3-larvae of *A. aegypti*. After four days, significant larval mortality was recorded (Fig. 2A). Concomitantly, feeding inhibition was measured with the change in OD₆₀₀. Larvae feeding on "empty

Chapter 4

"vector" cells reduced the bacterial concentration resulting in a drop of OD₆₀₀. In fact, the bacterial consumption was significantly reduced in the case of CciCgl2-, ageritin- or His8-ageritin-expressing bacteria (Fig. 2B).

The purified ageritin protein also showed toxicity against the Sf21 insect cell line in a concentration dependent manner (Fig. 2C).

After confirming the insecticidal activity of the ribotoxin, we tested its activity against five different bacterivorous nematode species (Table S1). Synchronized L1 larvae of the nematodes (*Caenorhabditis elegans*, *C. briggsae*, *C. tropicalis*, *Distolabrellus veechi* and *Pristionchus pacificus*) were fed with bacteria expressing ageritin, and their development was assessed after 2 days. Interestingly, ageritin was not active against any of the tested nematode species, pointing to specificity for certain organisms (Fig. S3).

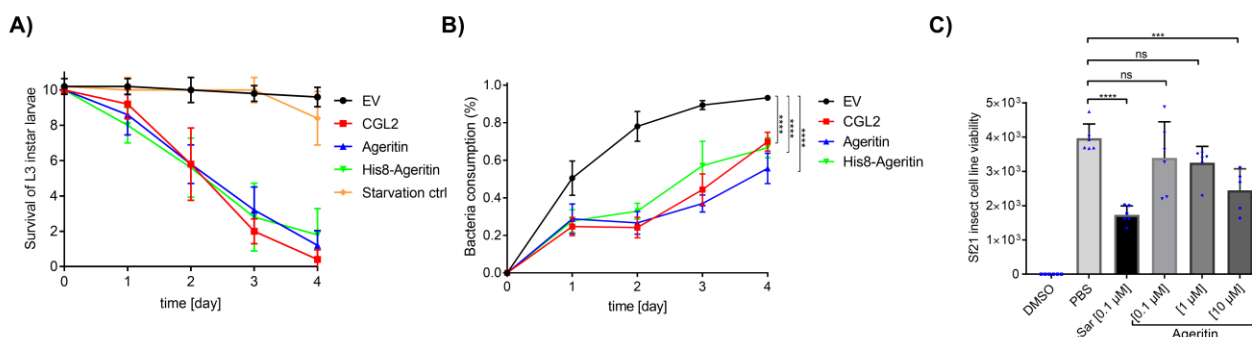


Figure 2: Toxicity of ageritin towards insect larvae and cells. Toxicity of ageritin and its tagged version were tested against *A. aegypti* larvae by counting number of survived larvae (A) and measuring OD₆₀₀-based bacteria consumption (B) every day for four days during which the larvae were feeding on IPTG-induced *E. coli* BL21 expressing proteins of interest. *E. coli* BL21 expressing either previously characterized insecticidal protein Cgl2 or carrying 'empty' vector (EV) were used as positive and negative controls, respectively. Statistical analysis was done using Dunnett's multiple comparisons test. Error bars represent standard deviation of five biological replicates. ***p < 0.0001 vs. EV. C) Ageritin toxicity was tested against insect Sf21 cell lines. Different concentration of purified ageritin was incubated with Sf21 cells for 72 h and number of viable cells were counted and plotted against its treatment condition. DMSO and ribotoxin α-Sarcin were used as positive controls, and PBS buffer was used as a negative control. Dunnett's multiple comparisons test was used for statistical analysis. Error bars represent standard deviation of six biological replicates. Symbols/abbreviations: ns: not significant, ***p < 0.001, ****p < 0.0001 vs. PBS.

3.7 Correlation between rRNA cleavage and toxicity

The gene sequence of ageritin was aligned against its top 10 homologs. Six conserved residues were chosen for mutation into alanine (Fig. 3A). All the mutants were expressible in a highly soluble manner in the cytoplasm of *E. coli* (Fig. S2C). To assess the importance of the mutated residues for the insecticidal activity of ageritin, we performed a toxicity assay against *A. aegypti* larvae. No toxicity was measured for three conserved-site mutants (R87A, D89A and H98A) while the other three mutants (Y57A, D91A and K110A) performed similar to the wild type ageritin (Fig. 3B). In a second approach we measured the change in OD₆₀₀ on a daily basis to check larval feeding inhibition. The toxic constructs inhibited feeding whereas the reduction in OD₆₀₀ by non-insecticidal bacterial strains was in line with the control. (Fig. 3C). In order to differentiate between the effect level of the three point mutations (R87A, D89A and H98A) that those showing were shown significant reduction in ageritin toxicity, the mosquito larvae exposed to bacteria expressing different constructs was monitored until adult mosquitoes had developed. The mutant construct D89A showed complete loss of toxicity. All larvae developed into imagines (Fig. 3D). An average of 40% of the larvae developed into adult mosquitoes when the other two conserved site mutants (R87A and H98A) were assayed. This indicates that partial toxicity in these two mutants is still present (Fig. 3D).

Ageritin single-site mutant constructs were produced in *E.coli* BL21 in a fully soluble manner and purified over Ni-NTA columns (Fig. S2D). Subsequently, ribonucleolytic activity of the purified proteins were assessed against ribosomes of rabbit reticulocyte lysate. Interestingly, all of the three single-site mutants which were non-toxic *in vivo* against *A. aegypti* larvae were also inactive in the ribosome cleavage assay (Fig 3E). The single site mutants that were still toxic *in vivo* performed similar to the wild type ageritin. This means that they all released the 400 nucleotide long ribotoxin cleavage product, the α -fragment (Fig. 3E). Combined with our insecticidal assay data, the *in vitro* results demonstrate that the insecticidal toxicity is based on ribonucleolytic activity of the ageritin.

Chapter 4

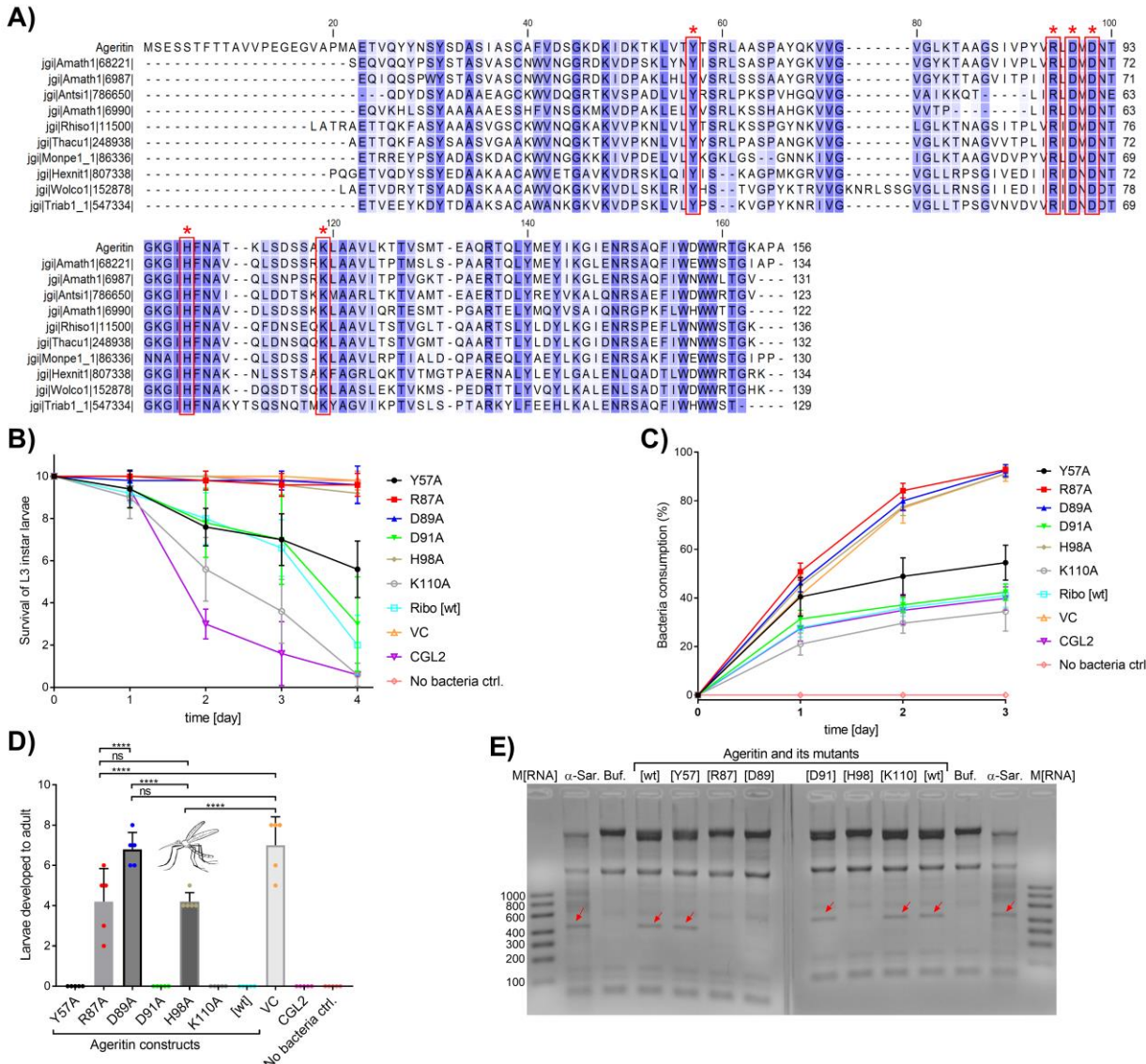


Figure 3: Effect of mutations in conserved residues on *in vivo* and *in vitro* activities of ageritin. A) The amino acid sequence of ageritin was searched against JGI MycoCosm fungal database. The hit regions of the top 10 sequences with highest homology were aligned using the ClustalW algorithm (v2.1). Blue shading indicates the degree of conservation from dark to light. Individually mutated conserved regions are indicated by red line boxes and asterisks. The numerical values, used datasets and origin of species of the genes used in these alignments are given in Table S4. Insecticidal activity of mutated ageritin versions was monitored by feeding *A. aegypti* larvae with *E. coli* BL21 cells expressing proteins of interest. **B-D)** Wild type and mutated ageritin toxicity was assessed by counting the number of surviving larvae (**B**), measuring OD₆₀₀-based bacteria consumption (**C**) every day for four days and counting number of larvae that reached to adulthood (**D**) by the end of day 7 of the larvae feeding on bacteria expressing one of the corresponding proteins. *E. coli* BL21 expressing either previously characterized insecticidal protein Cgl2 or carrying 'empty' vector (EV) were used as positive and negative controls, respectively. Statistical analysis was done using Dunnett's multiple comparisons test. Error bars represent standard deviation of five biological replicates. ****p < 0.0001 vs. EV **E)** Ribonucleolytic activity of ageritin mutants were assessed with 400 nM of purified proteins using ribosomes of rabbit reticulocyte lysate. α-Sarcin and PBS buffer were used as positive and negative controls, respectively. Ribosomal RNAs and ribotoxin cleavage product, α-fragment, were indicated.

Chapter 4

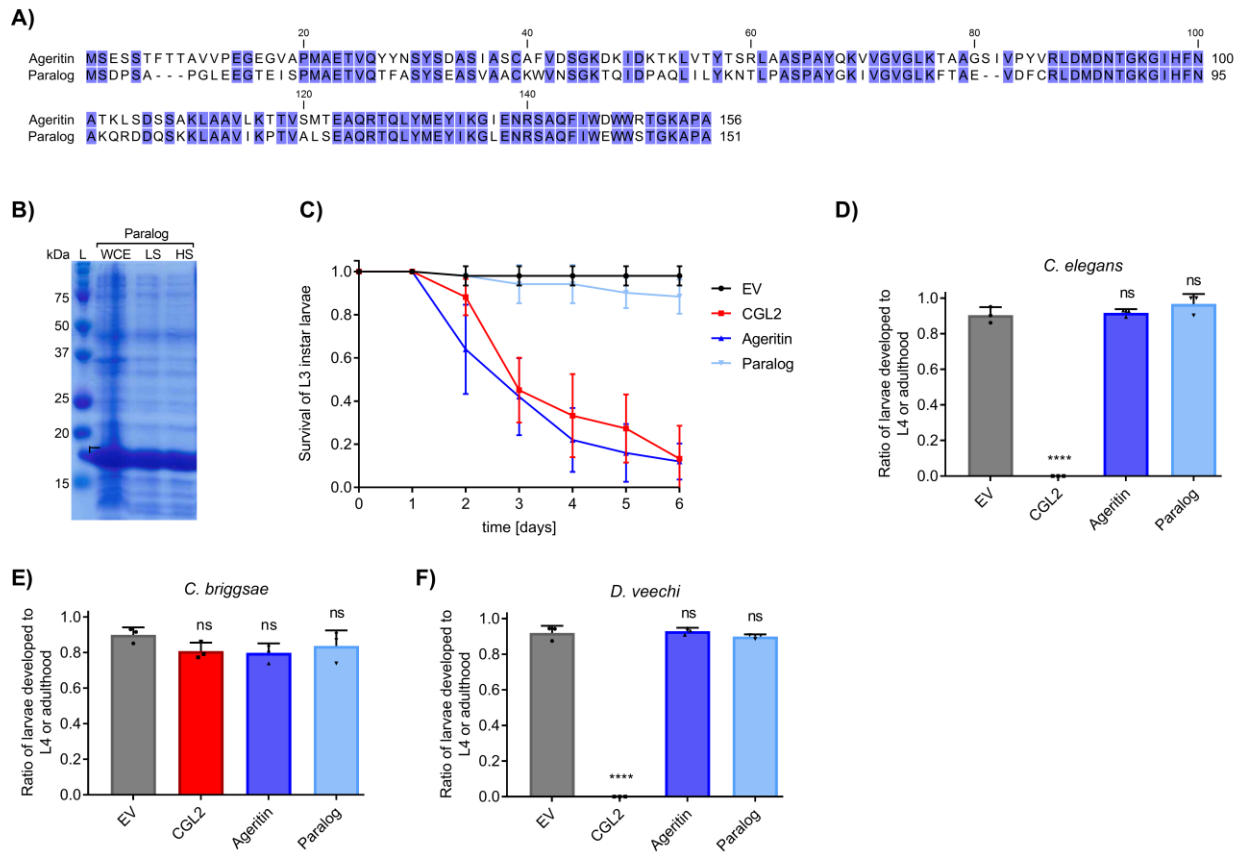


Figure 4: Ageritin paralog and its comparison with ageritin. **A)** Amino acid sequences of ageritin and its paralog were aligned using the ClustalW algorithm (v2.1). Blue shades indicate conservation of the residues. **B)** Heterologous expression and solubility of ageritin paralog in *E. coli* BL21. 20 µl of either bacterial whole cell extract (WCE), supernatants of WCE after low spin (LS; 5 min at 5000 × g) or high spin (HS; 30 min at 16000 × g) were loaded on a SDS-PAGE and stained with Coomassie brilliant blue. **E)** Insecticidal activity of the ageritin paralog along with ageritin was tested against *A. aegypti* larvae by feeding the L3 staged mosquito larvae with *E. coli* BL21 expressing proteins of interests. Nematotoxicity of ageritin paralog was assessed against *Caenorhabditis elegans* (**D**) *Caenorhabditis briggsae* (**E**) and *Distolabrellus veechi* (**F**) by counting number of developed larvae after two days of feeding on IPTG-induced *E. coli* BL21 expressing either previously characterized toxic protein Cgl2 or carrying 'empty' vector (EV) were used as positive and negative controls, respectively. Dunnett's multiple comparisons test was used for statistical analysis. Error bars represent standard deviation of three biological replicates. Symbols/abbreviations: ns: not significant, *p < 0.05, **p < 0.01, ***p < 0.001, ****p < 0.0001 vs. EV.

Chapter 4

3.8 Functional characterization of the ageritin paralog in comparison with ageritin

Adjacent to the ageritin-encoding *AaeAGT1* gene on the chromosomal DNA of *A. aegerita*, we spotted a paralogous gene, named *AaeAGT2*. Compared to ageritin, the deduced amino acid sequence of *AaeAgt2* displays a 63% sequence identity (Fig. 4A). Given the different expression dynamics of *AaeAGT2* and *AaeAGT1* throughout the different developmental stages of the fungus and the recorded bioactivity spectrum of *AaeAgt1*, we draw our attention to a potential bioactivity of *AaeAgt2*. Hence, we cloned and expressed *AaeAGT2* in *E. coli* BL21 cells in the same way as *AaeAGT1*, and tested it against *A. aegypti* and bacterivorous nematodes. The ageritin paralog was expressible and highly soluble in the cytoplasm of the bacteria (Fig 4B). Interestingly, unlike ageritin, its paralog was not active against *A. aegypti* larvae (Fig. 4C). Subsequently, we tested its toxicity against three different nematode species. Similar to ageritin, its paralog did not show any sign of toxicity neither against *C. elegans* (Fig. 4D), *C. briggsae* (Fig. 4E) nor *D. veechi* (Fig. 3F). This suggests a different biological function of the ageritin paralog.

3.9 Distribution of ageritin homologs in the fungal kingdom

Ageritin homologs were searched using JGI MycoCosm portal [44]. A high degree of sequence conservation was found among the ageritin homolog proteins of different fungal species. The top 30 hits were retrieved from the MycoCosm portal and their phylogenetic relationships were depicted using circular cladogram (Fig. 5). Within the 30 hits, all were members of Basidiomycota including several plant-pathogenic fungi such as *Rhizoctonia solani*, *Moniliophthora perniciosa*, *Rigidoporus microporus* and *Pleurotus eryngii*. Interestingly, despite ageritin being a cytoplasmic protein, several of its homologs possess known signal sequences, which resembles more closely to the secreted ribotoxins of ascomycetes.

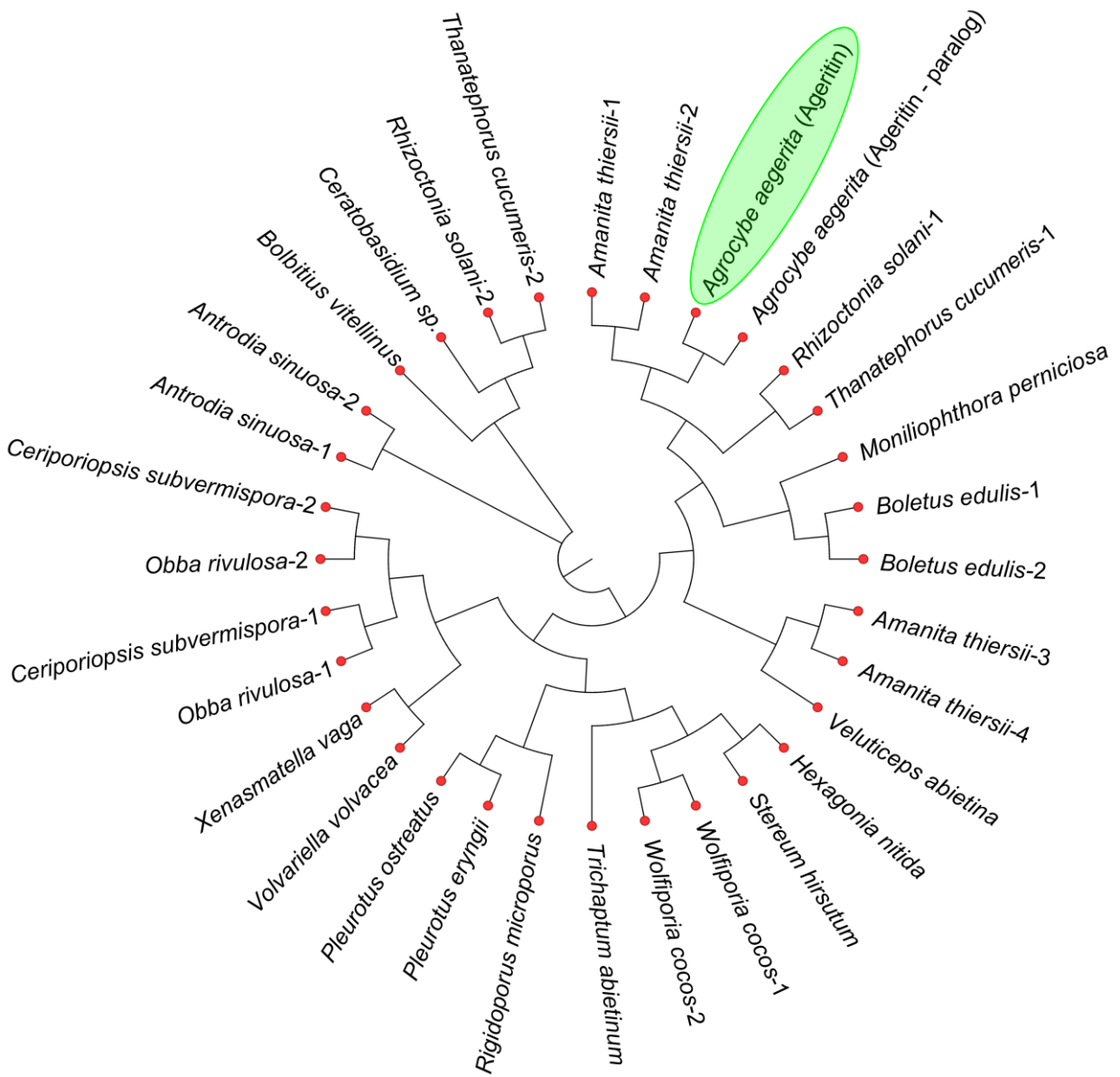


Figure 5: Rooted circular cladogram of putative ageritin homologs. Amino acid sequences of ageritin were searched against JGI MycoCosm fungal database. The complete amino acid sequence of top 30 hits were aligned using the ClustalW (v2.1), and phylogenetic relationships among the sequences were depicted with circular cladogram. The hit with the lowest homology to ageritin among those 30 hits had E-value of 7.2E⁻¹⁶, identity of 44.8% and subject coverage of 64.8%. The numerical values and used datasets for the genes used in these alignments can be found in Table S4. The branch lengths are relative and not to scale. Different ageritin homologs in the genome of a given species are labeled with numbers.

Discussion

Ribotoxins are suggested to be part of the fungal defense system against insect predators [23, 48, 49]. Here we describe a novel type of ribotoxin named ageritin from the edible mushroom *A. aegerita*. Ageritin is so far the first ribotoxin identified from the phylum Basidiomycota. Its sequence is very different from those of the well-known ribotoxins of Ascomycota. Furthermore, it is the first cytoplasmic ribotoxin discovered up to now. Yet, it was reported to release the same α -fragment, similar to other ribotoxins, when incubated with yeast lysate ribosomes [29]. Our results demonstrate high toxicity of ageritin against *A. aegypti* larvae, suggesting that it is likely to play an important role in the defense of *A. aegerita* against still unknown insect predators inhabiting the environment colonized by the mushroom. Insecticidal activity is a common feature of fungal ribotoxins [50]. Anisopilin [28] and hirsutellin A [27], two previously described ribotoxins had been shown to exert cytotoxicity against insect cell lines. Similarly, ageritin showed cytotoxicity against the insect Sf21 cell line, albeit at a higher concentration than the well-studied α -Sarcin, suggesting that ageritin is either less active than α -Sarcin or the reaction conditions are not optimal activity. *In vitro* ribonucleolytic assay with ribosomes of rabbit reticulocyte lysate indicates that the latter is likely to be true, since, the cleavage of 28S rRNA was slower for ageritin than α -Sarcin.

Next, we wanted to know if the insecticidal activity of ageritin is dependent on its ribonucleolytic activity. The putative catalytic residues of ageritin could not be identified by comparison with the previously characterized ribotoxins due to the lack of sequence homology. However, previous studies had shown that catalytic residues of ribotoxins mostly consist of acidic and basic residues [51]. The charged amino acids of ribotoxins had been found to support binding to the negatively charged rRNA facilitating interactions with target ribosomes [51, 52]. For instance, the active site of α -Sarcin consists of histidine and a glutamic acid (H50, E96 and H137) [25, 53]. Therefore, we mutated the conserved charged amino acid residues (R87, D89, D91, H98 and K110) and tyrosine (Y57) in the ageritin amino acid sequence. Tyrosine-48 [54] together with arginine-121 [55] and leucine-145 [56] were shown to contribute the biological activity of ageritin. Three (R87A, D89A and H98A) of the six mutations abolished both insecticidal activity and *in vitro* ribonucleolytic cleavage while the other three mutants (Y57A, D91A and K110A) did not affect neither *in vivo* nor *in vitro* activity of ageritin. The mutant studies indicate that the insecticidal activity of ageritin depends on the rRNA cleavage activity, and the residues R87, D89 and H98 are part of the catalytic site of ageritin.

Nematodes are one of the main fungal predators in the environment [57]. No activity of ribotoxins against nematodes has been reported so far. As ageritin differs from other ribotoxins in sequence and structure, we tested the susceptibility of five nematode species (*C. elegans*, *C. briggsae*, *C. tropicalis*, *D. veechi* and *P. pacificus*) against ageritin. However, nematotoxicity results show that ageritin is

Chapter 4

inactive against the five nematode species, suggesting the ribosomes are either resistant or not accessible for ageritin. These findings are in line with previous studies on the activity spectrum of ribotoxins where they exhibit specificity to insect cells due to the special structure and composition of insect cell membrane [23, 49]. So far, no specific receptors that facilitate the entry of ribotoxins into the target cell have been identified. Still, the small molecular weight and high number of positively charged residues were found to be crucial for binding of ribotoxins to the cell membrane of their target cells [58]. The binding capacity to different kinds of cell membranes together with diffusion efficiency of ribotoxins are hypothesized to be the main selective factors in susceptibility of cells to ribotoxins [59]. Thus, permeability and composition of the target cell membrane are decisive for susceptibility of cells to ribotoxins. The Insect cell membrane has a significant lower cholesterol/phospholipid ratio that makes it presumably thinner and more fluidic with higher permeability [50, 60]. Furthermore, they contain more acidic phospholipids which facilitates the binding of basic ribotoxins and their subsequent diffusion through the plasma membrane [58, 61]. Hence, it is suggested that ribotoxins are specific to insects and act as insecticides by the fungal producers [23, 27, 49].

Unlike ageritin, its paralog AaeAgt2 was not toxic to *A. aegypti* despite the 63% sequence identity with ageritin. Ageritin and its paralog differ in terms of their isoelectric point (pl) and their expression patterns during the life cycle of the mushrooms. Furthermore, it has been shown, that the positive charge of ribotoxins is crucial for the interaction with cell membranes and ribosomes [52, 62]. Ageritin has a pl of 8.6 that makes it a positively charged molecule in most of the intra- and extracellular matrix to facilitate cell entry and interaction with ribosomes. In contrast, its paralog has a pl value of 5.8, and the ineffectiveness of the paralog towards *A. aegypti* could be explained by its unfavorable electrostatic interactions with the cell membrane and ribosomes. In addition to the different pl of the two proteins, the regulation of gene expression appears very different between the ageritin-encoding gene *AaeAGT1* and its paralog *AaeAGT2*. Both genes are hardly expressed in the vegetative mycelium of *A. aegerita* AAE-3. This drastically changes after fruiting induction. In the case of *AaeAGT2* the expression level remains unchanged. On the other hand, *AaeAGT1* transcription increases continuously in a switch-like manner after the onset of fruiting, reaching a first peak with the starting of mushroom formation, i.e. the fruiting body initials. A second slightly lower expression maximum is reached within the cap of the already well-differentiated young fruiting bodies. The apparent drop in *AaeAGT1* expression increase within primordia could simply be explained by the applied sampling procedure: while RNA extraction in young fruiting bodies was performed from separately sampled caps and stipes, primordia were sampled and extracted in their entirety. Supporting this explanation is the n-fold expression of *AaeAGT1* in stipes (5-fold) of young fruiting bodies which was about 20-fold lower compared to n-fold expression of *AaeAGT1* in caps of young fruiting bodies (100-fold). Interestingly, n-

Chapter 4

fold expression of *AaeAGT1* in primordia (19-fold) is about five times lower than the one in caps of young fruiting bodies.

Both observations, i.e. the start of *AaeAGT1* expression by the onset of fruiting and with tissue specific expression (mushroom cap), certainly relate to the evolutionary survival strategy of mushrooms. Protection of the developing meiospores (basidiospores) from adverse biotic such as fungivores and abiotic factors like water loss are essential to reach maturity. This of course needs to involve the surrounding mushroom plectenchyme accommodating the meiospore producing hyphae. Abiotic stress by water loss for instance, as caused e.g. by a more dry climate, would put the developing mushroom at the risk of withering before the spores reach maturity and is counteracted by an evolutionary response of basidiomycete mushroom species called ‘gasteromycetation’ [63, 64]. Regarding a mushroom’s response to biotic stress by fungivores, it was accordingly pointed out that fungal defense proteins are highly expressed in the fruiting bodies due to the evolutionary importance of this sexual stage for the mushroom’s survival [3, 65, 66]. Argumentum e contrario, the inactivity of *AaeAgt2* against fungal antagonists and the absence transcriptional induction of *AaeAGT2* in fruiting-related structures implies that unlike ageritin, this paralog has a role outside the fruiting-associated fungal defense system.

Ribotoxins cleave the ribosomal RNA in the universally conserved GAGA tetra loop found in the sarcin-ricin loop of the large ribosomal subunit. Therefore, all known ribosomes are potentially susceptible and a ribotoxin producing fungus has to avoid autoimmunity. Previously described producers protect themselves by preventing the active ribotoxin to get in touch with ribosomes by compartmentalization and efficient secretion systems [67]. However, unlike all previously described ribotoxins, ageritin has no known signal peptide sequence and is thus either retained in the cytoplasm or secreted using a yet undiscovered unconventional secretion pathway in *A. aegerita* similar to the one described for Cts1 in the more basal basidiomycete *Ustilago maydis* [68]. Interestingly, we could express ageritin in a highly soluble manner in the cytoplasm of *E. coli*. This indicates that it is not active against its bacterial ribosomes. It could also be that ageritin has developed or generated a specificity to the ribosomes of the actual target organisms. Such a specificity would certainly help the fungus to gain protection against the cytoplasmic ageritin. *A. aegerita* could avoid self-poisoning by shielding the cleavage site in its ribosomes with a minor sequence variation in its SRL region. Furthermore, the ribosomal proteins in proximity of the SRL or a secondary structure modification in the region could make the GAGA tetra loop inaccessible for ageritin. However, the exact mechanism(s) of basidiomycete self-protection remain(s) to be elucidated.

Our results imply that ageritin homologs are widely distributed among different species of fungi including several plant pathogens such as *R. solani*, *M. perniciosa*, *R. microporus* and the King Oyster

Chapter 4

mushroom *P. eryngii*. It would be of interest to learn more about the function(s) of these putative homologs. For instance, a recent study by Kettles et al., describes the Zt6 protein from the wheat pathogenic fungus *Zymoseptoria tritici* as an effector with ribonuclease activity suggesting interactions between the host and the local microbial community [69, 70].

On the broader perspective, the high toxicity of ageritin against mosquito larvae makes ageritin a potential candidate for the development of new bio-insecticides. Novel mosquito control agents are needed since more and more insecticides are phased out. On the other hand mosquitoes as vectors of infectious diseases are expanding also in Europe. For examples *Ae. albopictus* has invaded large parts of southern Europe. This insect is an efficient vector viral diseases of dengue, chikungunya and zika virus [71].

Chapter 4

Competing interests

The authors declare that they have no competing interests.

Funding

This work was supported by the Swiss National Science Foundation (Grant No: 31003A-173097) and ETH Zurich. Furthermore, this work was funded by the Senckenberg Biodiversity and Climate Research Centre (SBiK-F) and the Landes-Offensive zur Entwicklung Wissenschaftlich-ökonomischer Exzellenz (LOEWE) by the State of Hesse's Ministry of Higher Education, Research and the Arts.

Acknowledgements

We thank Markus Aebi for fruitful discussions, P. Müller (Swiss Tropical and Public Health Institute, Basel, Switzerland) for supplying *Aedes aegypti* eggs.

References

1. Sabotic J, Ohm RA, Kunzler M: **Entomotoxic and nematotoxic lectins and protease inhibitors from fungal fruiting bodies.** *Appl Microbiol Biotechnol* 2016, **100**(1):91-111.
2. Kunzler M: **Hitting the sweet spot-glycans as targets of fungal defense effector proteins.** *Molecules* 2015, **20**(5):8144-8167.
3. Bleuler-Martínez S, Butschi A, Garbani M, Wälti MA, Wohlschlager T, Potthoff E, Sabotia J, Pohleven J, Lüthy P, Hengartner MO *et al*: **A lectin-mediated resistance of higher fungi against predators and parasites.** 2011, **20**:3056-3070.
4. Bleuler-Martinez S, Schmieder S, Aebi M, Kunzler M: **Biotin-Binding Proteins in the Defense of Mushrooms against Predators and Parasites.** *Appl Environ Microb* 2012, **78**(23):8485-8487.
5. Renko M, Sabotic J, Mihelic M, Brzin J, Kos J, Turk D: **Versatile Loops in Mycocypins Inhibit Three Protease Families.** *J Biol Chem* 2010, **285**(1):308-316.
6. Mancheno JM, Tateno H, Sher D, Goldstein IJ: **Laetiporus sulphureus Lectin and Aerolysin Protein Family.** *Adv Exp Med Biol* 2010, **677**:67-80.
7. Lacadena J, Alvarez-Garcia E, Carreras-Sangra N, Herrero-Galan E, Alegre-Cebollada J, Garcia-Ortega L, Onaderra M, Gavilanes JG, del Pozo AM: **Fungal ribotoxins: molecular dissection of a family of natural killers.** *Fems Microbiol Rev* 2007, **31**(2):212-237.
8. Ben-Shem A, Jenner L, Yusupova G, Yusupov M: **Crystal structure of the eukaryotic ribosome.** *Science* 2010, **330**(6008):1203-1209.
9. Bottger EC: **The ribosome as a drug target.** *Trends Biotechnol* 2006, **24**(4):145-147.
10. Deutscher MP, Li ZW: **Exoribonucleases and their multiple roles in RNA metabolism.** *Prog Nucleic Acid Re* 2001, **66**:67-105.
11. Loverix S, Steyaert J: **Deciphering the mechanism of RNase T1.** *Method Enzymol* 2001, **341**:305-323.
12. Shi WW, Mak ANS, Wong KB, Shaw PC: **Structures and ribosomal interaction of ribosome-inactivating proteins.** *Molecules* 2016, **21**.
13. Endo Y, Tsurugi K: **Rna N-Glycosidase Activity of Ricin a-Chain - Mechanism of Action of the Toxic Lectin Ricin on Eukaryotic Ribosomes.** *J Biol Chem* 1987, **262**(17):8128-8130.
14. Zhu F, Zhou YK, Ji ZL, Chen XR: **The Plant Ribosome-Inactivating Proteins Play Important Roles in Defense against Pathogens and Insect Pest Attacks.** *Front Plant Sci* 2018, **9**.
15. Brigotti M, Rambelli F, Zamboni M, Montanaro L, Sperti S: **Effect of Alpha-Sarcin and Ribosome-Inactivating Proteins on the Interaction of Elongation-Factors with Ribosomes.** *Biochem J* 1989, **257**(3):723-727.
16. Schrot J, Weng A, Melzig MF: **Ribosome-inactivating and related proteins.** *Toxins (Basel)* 2015, **7**(5):1556-1615.
17. Olmo N, Turnay J, Gonzalez de Buitrago G, Lopez de Silanes I, Gavilanes JG, Lizarbe MA: **Cytotoxic mechanism of the ribotoxin alpha-sarcin. Induction of cell death via apoptosis.** *Eur J Biochem* 2001, **268**(7):2113-2123.
18. Endo Y, Tsurugi K, Yutsudo T, Takeda Y, Ogasawara T, Igarashi K: **Site of action of a Vero toxin (VT2) from Escherichia coli O157:H7 and of Shiga toxin on eukaryotic ribosomes. RNA N-glycosidase activity of the toxins.** *Eur J Biochem* 1988, **171**(1-2):45-50.
19. Sawa T, Hamaoka S, Kinoshita M, Kainuma A, Naito Y, Akiyama K, Kato H: **Pseudomonas aeruginosa Type III Secretory Toxin ExoU and Its Predicted Homologs.** *Toxins* 2016, **8**(11).

Chapter 4

20. Yao QZ, Yu MM, Ooi LSM, Ng TB, Chang ST, Sun SSM, Ooi VEC: **Isolation and characterization of a type 1 ribosome-inactivating protein from fruiting bodies of the edible mushroom (*Volvariella volvacea*)**. *J Agr Food Chem* 1998, **46**(2):788-792.
21. Bolognesi A, Bortolotti M, Maiello S, Battelli MG, Polito L: **Ribosome-Inactivating Proteins from Plants: A Historical Overview**. *Molecules* 2016, **21**(12).
22. Herrero-Galán E, Álvarez-García E, Carreras-Sangrà N, Lacadena J, Alegre-Cebollada J, Martínez del Pozo Á, Oñaderra M, Gavilanes JG: **Fungal ribotoxins: structure, function and evolution**. In: *Microbial Toxins: Current Research and Future Trends*. 2009: 167-187.
23. Olombrada M, Herrero-Galán E, Tello D, Oñaderra M, Gavilanes JG, Martínez-Del-Pozo Á, García-Ortega L: **Fungal extracellular ribotoxins as insecticidal agents**. 2013.
24. Correll CC, Munishkin A, Chan YL, Ren Z, Wool IG, Steitz TA: **Crystal structure of the ribosomal RNA domain essential for binding elongation factors**. *P Natl Acad Sci USA* 1998, **95**(23):13436-13441.
25. Perez-Canadillas JM, Santoro J, Campos-Olivas R, Lacadena J, del Pozo AM, Gavilanes JG, Rico M, Bruix M: **The highly refined solution structure of the cytotoxic ribonuclease alpha-sarcin reveals the structural requirements for substrate recognition and ribonucleolytic activity**. *Journal of Molecular Biology* 2000, **299**(4):1061-1073.
26. Yang XJ, Moffat K: **Insights into specificity of cleavage and mechanism of cell entry from the crystal structure of the highly specific Aspergillus ribotoxin, restrictocin**. *Structure* 1996, **4**(7):837-852.
27. Herrero-Galan E, Lacadena J, del Pozo AM, Boucias DG, Olmo N, Onaderra M, Gavilanes JG: **The insecticidal protein hirsutellin A from the mite fungal pathogen Hirsutella thompsonii is a ribotoxin**. *Proteins* 2008, **72**(1):217-228.
28. Olombrada M, Medina P, Budia F, Gavilanes JG, Martinez-Del-Pozo A, Garcia-Ortega L: **Characterization of a new toxin from the entomopathogenic fungus Metarhizium anisopliae: the ribotoxin anisoplin**. *Biol Chem* 2017, **398**(1):135-142.
29. Landi N, Pacifico S, Ragucci S, Iglesias R, Piccolella S, Amici A, Di Giuseppe AMA, Di Maro A: **Purification, characterization and cytotoxicity assessment of Ageritin: The first ribotoxin from the basidiomycete mushroom Agrocybe aegerita**. *Biochimica et Biophysica Acta - General Subjects* 2017, **1861**:1113-1121.
30. Gupta DK, Rühl M, Mishra B, Kleofas V, Hofrichter M, Herzog R, Pecyna MJ, Sharma R, Kellner H, Hennicke F et al: **The genome sequence of the commercially cultivated mushroom Agrocybe aegerita reveals a conserved repertoire of fruiting-related genes and a versatile suite of biopolymer-degrading enzymes**. *Bmc Genomics* 2018, **19**.
31. Herzog R, Solovyeva I, Ruhl M, Thines M, Hennicke F: **Dikaryotic fruiting body development in a single dikaryon of Agrocybe aegerita and the spectrum of monokaryotic fruiting types in its monokaryotic progeny**. *Mycol Prog* 2016, **15**(9):947-957.
32. Chomczynski P, Sacchi N: **Single-Step Method of Rna Isolation by Acid Guanidinium Thiocyanate Phenol Chloroform Extraction**. *Anal Biochem* 1987, **162**(1):156-159.
33. Pfaffl MW: **A new mathematical model for relative quantification in real-time RT-PCR**. *Nucleic Acids Research* 2001, **29**(9).
34. Andersen CL, Jensen JL, Orntoft TF: **Normalization of real-time quantitative reverse transcription-PCR data: A model-based variance estimation approach to identify genes suited for normalization, applied to bladder and colon cancer data sets**. *Cancer Res* 2004, **64**(15):5245-5250.

Chapter 4

35. Vandesompele J, De Preter K, Pattyn F, Poppe B, Van Roy N, De Paepe A, Speleman F: **Accurate normalization of real-time quantitative RT-PCR data by geometric averaging of multiple internal control genes.** *Genome Biology* 2002, **3**(7).
36. Bustin SA, Benes V, Garson JA, Hellemans J, Huggett J, Kubista M, Mueller R, Nolan T, Pfaffl MW, Shipley GL *et al*: **The MIQE Guidelines: Minimum Information for Publication of Quantitative Real-Time PCR Experiments.** *Clin Chem* 2009, **55**(4):611-622.
37. Kearse M, Moir R, Wilson A, Stones-Havas S, Cheung M, Sturrock S, Buxton S, Cooper A, Markowitz S, Duran C *et al*: **Geneious Basic: An integrated and extendable desktop software platform for the organization and analysis of sequence data.** *Bioinformatics* 2012, **28**(12):1647-1649.
38. Ruijter JM, Ramakers C, Hoogaars WMH, Karlen Y, Bakker O, van den Hoff MJB, Moorman AFM: **Amplification efficiency: linking baseline and bias in the analysis of quantitative PCR data.** *Nucleic Acids Research* 2009, **37**(6).
39. Ruijter JM, Pfaffl MW, Zhao S, Spiess AN, Boggy G, Blom J, Rutledge RG, Sisti D, Lievens A, De Preter K *et al*: **Evaluation of qPCR curve analysis methods for reliable biomarker discovery: Bias, resolution, precision, and implications.** *Methods* 2013, **59**(1):32-46.
40. Pfaffl MW, Horgan GW, Dempfle L: **Relative expression software tool (REST (c)) for group-wise comparison and statistical analysis of relative expression results in real-time PCR.** *Nucleic Acids Research* 2002, **30**(9).
41. Künzler M, Bleuler-Martinez S, Butschi A, Garbani M, Lüthy P, Hengartner MO, Aeby M: **Biotoxicity assays for fruiting body lectins and other cytoplasmic proteins.** 2010, **480**:141-150.
42. Plaza DF, Schmieder SS, Lipzen A, Lindquist E, Künzler M: **Identification of a Novel Nematotoxic Protein by Challenging the Model Mushroom Coprinopsis cinerea with a Fungivorous Nematode.** *Genes/Genomes/Genetics* 2016, **6**:87-98.
43. Kao R, Martínez-Ruiz A, Del Pozo AM, Crameri R, Davies J: **Mitogillin and related fungal ribotoxins.** *Methods in Enzymology* 2001, **341**:324-335.
44. Grigoriev IV, Nikitin R, Haridas S, Kuo A, Ohm R, Otillar R, Riley R, Salamov A, Zhao XL, Korzeniewski F *et al*: **MycoCosm portal: gearing up for 1000 fungal genomes.** *Nucleic Acids Research* 2014, **42**(D1):D699-D704.
45. Chenna R, Sugawara H, Koike T, Lopez R, Gibson TJ, Higgins DG, Thompson JD: **Multiple sequence alignment with the Clustal series of programs.** *Nucleic Acids Research* 2003, **31**(13):3497-3500.
46. Aldrich J: **R. A. Fisher and the making of maximum likelihood 1912-1922.** *Stat Sci* 1997, **12**(3):162-176.
47. Chan YL, Endo Y, Wool IG: **The Sequence of the Nucleotides at the Alpha-Sarcin Cleavage Site in Rat 28-S Ribosomal Ribonucleic-Acid.** *J Biol Chem* 1983, **258**(21):2768-2770.
48. Olombrada M, Lázaro-Gorines R, López-Rodríguez J, Martínez-del-Pozo Á, Oñaderra M, Maestro-López M, Lacadena J, Gavilanes J, García-Ortega L: **Fungal Ribotoxins: A Review of Potential Biotechnological Applications.** *Toxins* 2017, **9**:71.
49. Olombrada M, Martínez-Del-Pozo Á, Medina P, Budia F, Gavilanes JG, García-Ortega L: **Fungal ribotoxins: Natural protein-based weapons against insects.** *Toxicon* 2014, **83**:69-74.
50. Herrero-Galán E, García-Ortega L, Olombrada M, Lacadena J, Del Pozo ÁM, Gavilanes JG, Oñaderra M: **Hirsutellin A: A Paradigmatic Example of the Insecticidal Function of Fungal Ribotoxins.** *Insects* 2013, **4**:339-356.

Chapter 4

51. Herrero-Galán E, García-Ortega L, Lacadena J, Martínez-Del-Pozo Á, Olmo N, Gavilanes JG, Oñaderra M: **Implication of an Asp residue in the ribonucleolytic activity of hirsutellin A reveals new electrostatic interactions at the active site of ribotoxins.** *Biochimie* 2012, **94**:427-433.
52. Korenykh AV, Piccirilli JA, Correll CC: **The electrostatic character of the ribosomal surface enables extraordinarily rapid target location by ribotoxins.** *Nat Struct Mol Biol* 2006, **13**(5):436-443.
53. Lacadena J, del Pozo AM, Martinez-Ruiz A, Perez-Canadillas JM, Bruix M, Mancheno JM, Onaderra M, Gavilanes CG: **Role of histidine-50, glutamic acid-96, and histidine-137 in the ribonucleolytic mechanism of the ribotoxin alpha-sarcin.** *Proteins-Structure Function and Genetics* 1999, **37**(3):474-484.
54. Alvarez-Garcia E, Garcia-Ortega L, Verdun Y, Bruix M, del Pozo AM, Gavilanes JG: **Tyr-48, a conserved residue in ribotoxins, is involved in the RNA-degrading activity of alpha-sarcin.** *Biological Chemistry* 2006, **387**(5):535-541.
55. Masip M, Lacadena J, Mancheno JM, Onaderra M, Martinez-Ruiz A, del Pozo AM, Gavilanes JG: **Arginine 121 is a crucial residue for the specific cytotoxic activity of the ribotoxin alpha-sarcin.** *European Journal of Biochemistry* 2001, **268**(23):6190-6196.
56. Masip M, Garcia-Ortega L, Olmo N, Garcia-Mayoral MF, Perez-Canadillas JM, Bruix M, Onaderra M, del Pozo AM, Gavilanes JG: **Leucine 145 of the ribotoxin alpha-sarcin plays a key role for determining the specificity of the ribosome-inactivating activity of the protein.** *Protein Sci* 2003, **12**(1):161-169.
57. Boddy L, Jones TH: **Interactions between Basidiomycota and Invertebrates.** *Br Mycol Sy* 2008, **28**:155-179.
58. Onaderra M, Mancheno JM, Lacadena J, de los Rios V, Martinez del Pozo A, Gavilanes JG: **Oligomerization of the cytotoxin alpha-sarcin associated with phospholipid membranes.** *Mol Membr Biol* 1998, **15**(3):141-144.
59. Onaderra M, Mancheno JM, Gasset M, Lacadena J, Schiavo G, Delpozo AM, Gavilanes JG: **Translocation of Alpha-Sarcin across the Lipid Bilayer of Asolectin Vesicles.** *Biochem J* 1993, **295**:221-225.
60. Marheineke K, Grünwald S, Christie W, Reilander H: **Lipid composition of Spodoptera frugiperda (Sf9) and Trichoplusia ni (Tn) insect cells used for baculovirus infection.** *Febs Lett* 1998, **441**(1):49-52.
61. Gasset M, Onaderra M, Goormaghtigh E, Gavilanes JG: **Acid Phospholipid-Vesicles Produce Conformational-Changes on the Antitumor Protein Alpha-Sarcin.** *Biochim Biophys Acta* 1991, **1080**(1):51-58.
62. Perez-Canadillas JM, Campos-Olivas R, Lacadena J, del Pozo AM, Gavilanes JG, Santoro J, Rico M, Bruix M: **Characterization of pK(a) values and titration shifts in the cytotoxic ribonuclease alpha-sarcin by NMR. Relationship between electrostatic interactions, structure, and catalytic function.** *Biochemistry-US* 1998, **37**(45):15865-15876.
63. Bruns TD, Fogel R, White TJ, Palmer JD: **Accelerated Evolution of a False-Truffle from a Mushroom Ancestor.** *Nature* 1989, **339**(6220):140-142.
64. Wilson AW, Binder M, Hibbett DS: **Effects of Gasteroid Fruiting Body Morphology on Diversification Rates in Three Independent Clades of Fungi Estimated Using Binary State Speciation and Extinction Analysis.** *Evolution* 2011, **65**(5):1305-1322.

Chapter 4

65. Plaza DF, Lin CW, Sebastiaan N, Van der Velden J, Aebi M, Kunzler M: **Comparative transcriptomics of the model mushroom *Coprinopsis cinerea* reveals tissue-specific armories and a conserved circuitry for sexual development.** *Bmc Genomics* 2014, **15**.
66. Doll K, Chatterjee S, Scheu S, Karlovsky P, Rohlfs M: **Fungal metabolic plasticity and sexual development mediate induced resistance to arthropod fungivory.** *P Roy Soc B-Biol Sci* 2013, **280**(1771).
67. Lamy B, Davies J: **Isolation and Nucleotide-Sequence of the Aspergillus-Restrictus Gene Coding for the Ribonucleolytic Toxin Restrictocin and Its Expression in Aspergillus-Nidulans - the Leader Sequence Protects Producing Strains from Suicide.** *Nucleic Acids Research* 1991, **19**(5):1001-1006.
68. Stock J, Sarkari P, Kreibich S, Brefort T, Feldbrugge M, Schipper K: **Applying unconventional secretion of the endochitinase Cts1 to export heterologous proteins in *Ustilago maydis*.** *J Biotechnol* 2012, **161**(2):80-91.
69. Kettles GJ, Bayon C, Sparks CA, Canning G, Kanyuka K, Rudd JJ: **Characterization of an antimicrobial and phytotoxic ribonuclease secreted by the fungal wheat pathogen *Zymoseptoria tritici*.** *New Phytol* 2018, **217**(1):320-331.
70. Snelders NC, Kettles GJ, Rudd JJ, Thomma BPHJ: **Plant pathogen effector proteins as manipulators of host microbiomes?** *Mol Plant Pathol* 2018, **19**(2):257-259.
71. Kampen H, Schuhbauer A, Walther D: **Emerging mosquito species in Germany-a synopsis after 6 years of mosquito monitoring (2011-2016).** *Parasitol Res* 2017, **116**(12):3253-3263.

Chapter 4

Supplementary Information

Chapter 4

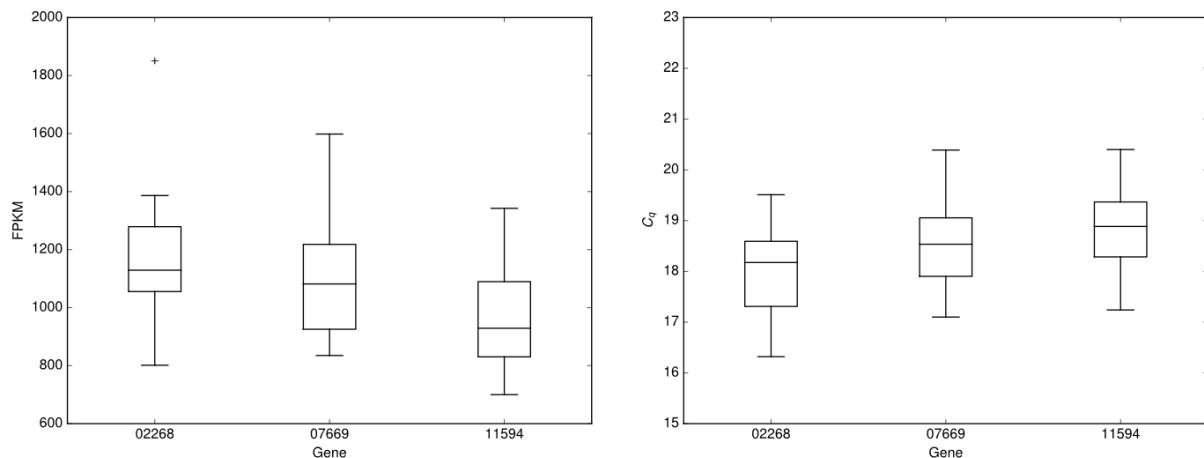


Figure S1: Boxplots of reference genes *AaeIMP1* (gene ID AAE3_02268), *AaeTIF1* (gene ID AAE3_07769) and *AaeARP1* (gene ID AAE3_11594) from the genome sequence of the dikaryon *A. aegerita* AAE-3 (www.thines-lab.senckenberg.de/agrocybe_genome) showing their (A) transcription level by means of their fragments per kilo base per million mapped reads (FPKM) as well as their (B) Cq-values derived from the qRT-PCR analysis. Outliers are marked as a +.

Chapter 4

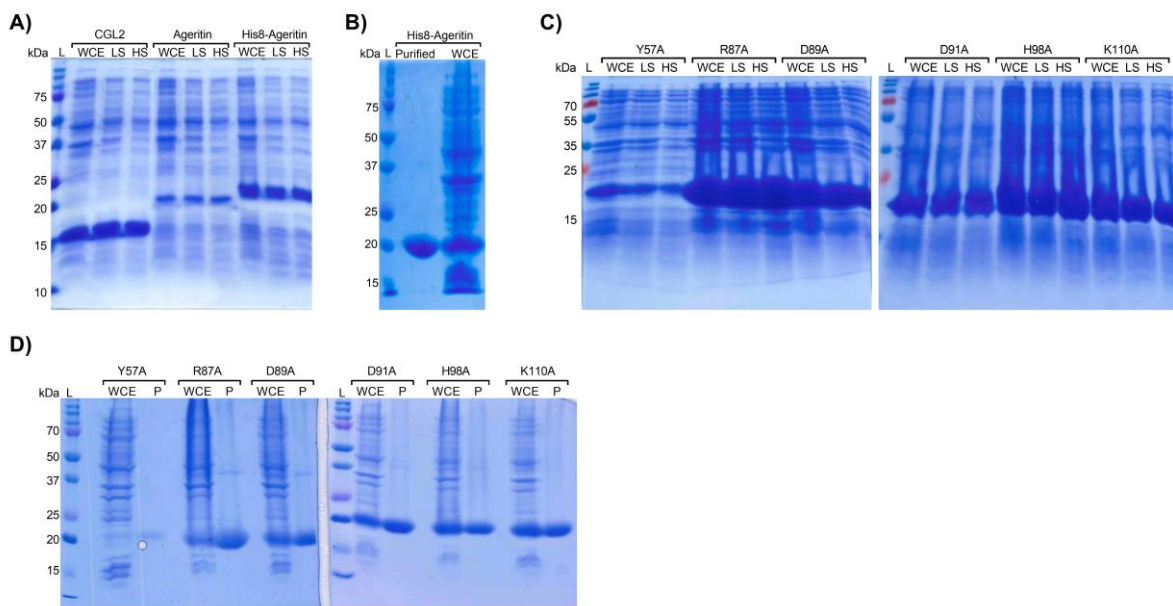


Figure S2: Expression analysis. **A)** Heterologous expression and solubility of ageritin and its His8-tagged version in *E. coli* BL21 cells. 20 µl of whole cell extract (WCE), supernatants of low spin (LS; 5 min. at 5000 × g) and high spin (HS; 30 min. at 16000 × g) of bacterial lysate were loaded on SDS-PAGE gel. Cgl2 was used as a positive control for IPTG-induced expression and solubility. **B)** His8-ageritin was produced in *E. coli* BL21 and 20 µl of Ni-NTA purified protein loaded onto the SDS-PAGE along with 20 µl of WCE. Ageritin single-site mutant constructs were produced in *E. coli* BL21 (**C**), and purified over Ni-NTA beads. **D)** 5 µl of purified protein (P) of each were loaded onto a SDS-PAGE along with 20 µl of its WCE.

Chapter 4

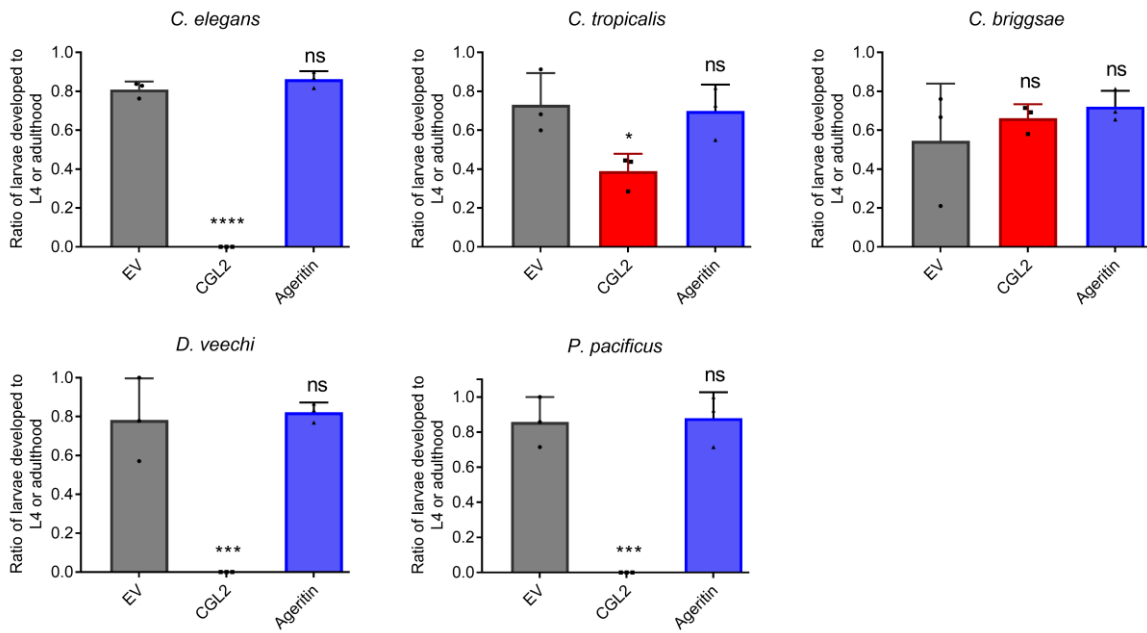


Figure S3: Nematotoxicity of ageritin. Nematotoxicity of ageritin was tested against five different bacterivorous nematodes species (*Caenorhabditis elegans*, *C. briggsae*, *C. tropicalis*, *Distolabrellus veechi* and *Pristionchus pacificus*). IPTG-induced *E. coli* BL21 expressing previously characterized nematotoxic protein Cgl2 or carrying 'empty' vector (EV) were used as positive and negative controls, respectively. Dunnett's multiple comparisons test was used for statistical analysis. Error bars represent standard deviation of three biological replicates. Symbols/abbreviations: ns: not significant, * $p < 0.05$, ** $p < 0.01$, *** $p < 0.001$, **** $p < 0.0001$ vs. EV.

Chapter 4

Table S1. Organisms used in this study.

Name	Strain	Source/Reference
<i>Caenorhabditis briggsae</i>	AF16	Caenorhabditis Genetics Center (CGC)
<i>Caenorhabditis elegans</i>	N2	Caenorhabditis Genetics Center (CGC)
<i>Caenorhabditis tropicalis</i>	JU1373	Caenorhabditis Genetics Center (CGC)
<i>Distolabrellus veechi</i>	environmental isolate	Luis Lugones, Utrecht university, Netherlands
<i>Pristionchus pacificus</i>	PS312	Iain Wilson, BOKU, Vienna, Austria
<i>Aedes aegypti</i>	Rockefeller	Pie Müller, Swiss Tropical and Public Health Institute, Basel, Switzerland
<i>Agrocybe aegerita</i>	AAE-3	Florian Hennicke, Senckenberg BiK-F, Frankfurt a.M., Germany; genome-sequenced (Gupta et al. 2018 BMC Genomics 19:48)
<i>Escherichia coli</i>	DH5α	
<i>Escherichia coli</i>	BL21(DE3)	Novagen
<i>Escherichia coli</i>	OP50	Hengartner laboratory, University of Zürich, Switzerland

Table S2. Primers used in this study.

Primer ^a	Sequence 5' - 3' ^b
pAGT1-Nd	ggcgcat <u>ATGTCGAGTCCTCTACCTCACCACTGC</u>
pAGT1-N	gtgcggccgc <u>T</u> CACGCCGGAGCCTTGC
pF_8His-Ag	CACCACCAC <u>ACGAGTCCTCTACCTCACCACTG</u>
pR_8His-Ag	ATGATGATGATGGGACATATGTATATCTCCTTCT
pF_8His-Ag(Y57A)	AAGTTGGTCACGGCCACCAGCCGCC
pR_8His-Ag(Y57A)	GGTCTTATCAATTTC <u>GTCCTTCCCCG</u>
pF_8His-Ag(R87A)	GTCGCGCTCGACATGGACAACACC
pR_8His-Ag(R87A)	GTAGGGCAC <u>GATGGAGCCCGCGGC</u>
pF_8His-Ag(D89A)	TGCCCTACGTCCGGCTGCCATGG
pR_8His-Ag(D89A)	CGATGGAGCCCGGGCCGTTGA
pF_8His-Ag(D91A)	GTCCGGCTCGACATGGCCAACACC
pR_8His-Ag(D91A)	GTAGGGCAC <u>GATGGAGCCCGCGGC</u>
pF_8His-Ag(H98A)	GGCAAGGGCATCGCTTCAA
pR_8His-Ag(H98A)	GGTGTGTC <u>CATGTCGAGCC</u>
pF_8His-Ag(K110A)	AGTTCCGCCGCGCTCGCCG
pR_8His-Ag(K110A)	GTCGGAGAGTTAGTCGCGTTGAAA
cds01767-f	TTCTTTCGCTACTCAGAACATCGTTG
cds01767-r	CAGAGCTCTCCCAACCACAG
02268_f	AGATGCGTATTCTGATGGTTGGTC
02268_r	CCCACACTGTGAATGAGATGTT
07769_f	ATTCCCTACGATCCTTGCCG
07769_r	GATCATATTGTTGGGAGTCCT
11594_f	TCTGATCTGACTGTCGGCAA
11594_r	ATCCTCGTCCTTATGCTCCTC
01767_f	AAGCCCCGCA <u>TATCAGAAG</u>
01767_r	CTGTCGGAGAGTTAGTCGC
01768_f	GAAAGACCCAGATTGACCCAG
01768_f	GTGAATTTAGGCCGACGC

^aPrimers used for qRT-PCR are labelled with forward (f) and reverse (r), respectively. Primers for cDNA generation start by coding sequence (cds) and end by forward (fw) or reverse (rv). ^bLowercase letters are primer extensions to create the underlined restriction sites.

Chapter 4

Table S3. qRT-PCR program for measuring *AaeAGT1* and *AaeAGT2* expression in this study

Programme step	Temperature	Time
Reverse transcription	50 °C	10 min
Initial denaturation (hot start)	95 °C	3 min
40 cycles		
Denaturation	95 °C	5 sec
Annealing	58 °C	10 sec
Extension	72 °C	10 sec
Melting curve	65 °C to 95 °C (resolution 0.5 °C)	5 min

Chapter 4

Table S4: Ageritin homologs used in this study. All proteins were retrieved from JGI database.

Hit Name JGI	EValue	% Hit Identity	Hit Start	Hit End	Organism	Dataset
jgi Amath1 68221	1.52E-61	72.59%	8	142	Amanita thiersii Skay4041 v1.0	Amath1_GeneCatalog_proteins_20120702.aa
jgi Rhiso1 11500	1.26E-53	61.31%	36	172	Rhizoctonia solani AG-1 IB	Rhiso1_GeneCatalog_proteins_20131028.aa
jgi Amath1 6987	2.94E-53	65.91%	6	137	Amanita thiersii Skay4041 v1.0	Amath1_GeneCatalog_proteins_20120702.aa
jgi Thacu1 248938	2.17E-51	62.41%	36	168	Thanatephorus cucumeris MPI-SDFR-AT-0096 v1.0	Thacu1_GeneCatalog_proteins_20170424.aa
jgi Monpe1_1 86336	2.18E-22	57.55%	91	221	Moniliophthora perniciosa FA553	Monpe1_1_GeneCatalog_proteins_20131213.aa
jgi Antsi1 786650	4.66E-41	60.00%	27	150	Antrodia sinuosa LB1 v1.0	Antsi1_GeneCatalog_proteins_20130416.aa
jgi Hexnit1 807338	6.04E-24	49.67%	10	144	Hexagonia nitida CIRM-BRFM 1802 v1.0	Hexnit1_GeneCatalog_proteins_20170619.aa
jgi Amath1 6990	1.03E-39	58.40%	105	227	Amanita thiersii Skay4041 v1.0	Amath1_GeneCatalog_proteins_20120702.aa
jgi Triab1_1 547334	1.96E-32	50.75%	31	160	Trichaptum abietinum v1.0	Triab1_1_GeneCatalog_proteins_20130513.aa
jgi Wolco1 152878	3.21E-36	56.91%	4	143	Wolfiporia cocos MD-104 SS10 v1.0	Wolco1_GeneCatalog_proteins_20100915
jgi Wolco1 164043	6.18E-36	61.26%	4	142	Wolfiporia cocos MD-104 SS10 v1.0	Wolco1_GeneCatalog_proteins_20100915
jgi Amath1 68223	2.36E-40	48.48%	126	257	Amanita thiersii Skay4041 v1.0	Amath1_GeneCatalog_proteins_20120702.aa
jgi Volvo1 116772	2.82E-29	53.78%	9	168	Volvariella volvacea V23	Volvo1_GeneCatalog_proteins_20130703.aa
jgi Stehi1 156399	9.54E-33	48.46%	3	139	Stereum hirsutum FP-91666 SS1 v1.0	Stehi1_GeneCatalog_proteins_20101026.aa
jgi Obbri1 798605	5.90E-30	52.25%	60	202	Obba rivulosa 3A-2 v1.0	Obbri1_GeneCatalog_proteins_20140615.aa
jgi Cersu1 87778	3.63E-27	50.47%	26	164	Ceriporiopsis (Gelatoporia) subvermispora B	Ceriporiopsis subvermispora gene models (protein)
jgi Bolvit1 445973	5.11E-23	47.01%	30	162	Bolbitius vitellinus SZMC-NL-1974 v1.0	Bolvit1_GeneCatalog_proteins_20160525.aa
jgi Boled1 941169	6.67E-25	75.41%	26	85	Boletus edulis v1.0	Boled1_GeneCatalog_proteins_20130211.aa
jgi Rigmic1 875498	7.69E-20	60.49%	26	143	Rigidoporus microporus ED310 v1.0	Rigmic1_GeneCatalog_proteins_20170307.aa
jgi CerAGI 557995	2.57E-23	33.33%	8	144	Ceratobasidium sp. (anastomosis group I, AG-I) v1.0	CerAGI_GeneCatalog_proteins_20150524.aa
jgi Obbri1 786721	1.28E-22	47.52%	20	160	Obba rivulosa 3A-2 v1.0	Obbri1_GeneCatalog_proteins_20140615.aa
jgi Boled1 941180	6.80E-23	68.25%	24	85	Boletus edulis v1.0	Boled1_GeneCatalog_proteins_20130211.aa
jgi Antsi1 778948	1.06E-22	49.04%	1	99	Antrodia sinuosa LB1 v1.0	Antsi1_GeneCatalog_proteins_20130416.aa
jgi Xenvag1 1670194	1.67E-22	48.15%	11	121	Xenasmatella vaga CBS212.54 v1.0	Xenvag1_GeneCatalog_proteins_20160511.aa
jgi Cersu1 99198	4.32E-22	52.00%	27	162	Ceriporiopsis (Gelatoporia) subvermispora B	Ceriporiopsis subvermispora gene models (protein)
jgi Rhiso1 11501	1.25E-21	34.56%	1	138	Rhizoctonia solani AG-1 IB	Rhiso1_GeneCatalog_proteins_20131028.aa
jgi Velabi1 321655	3.46E-17	48.96%	38	136	Veluticeps abietina OMC1657 v1.0	Velabi1_GeneCatalog_proteins_20180530.aa
jgi Pleery1 1455417	3.37E-16	44.76%	41	145	Pleurotus eryngii ATCC 90797 v1.0	Pleery1_GeneCatalog_proteins_20150629.aa
jgi Thacu1 633440	6.87E-20	33.82%	35	172	Thanatephorus cucumeris MPI-SDFR-AT-0096 v1.0	Thacu1_GeneCatalog_proteins_20170424.aa

Chapter 5

Toxicity of potential fungal defense proteins towards the fungivorous nematodes

Aphelenchus avenae and *Bursaphelenchus okinawaensis*

Annageldi Tayyrov^{a*}, Stefanie S. Schmieder^{a,b*}, Silvia Bleuler-Martinez^{a,c}, David F. Plaza^{a,d}, Markus Künzler^{a#}

^aInstitute of Microbiology, Department of Biology, ETH Zürich, Zürich, Switzerland

^bPresent address: Division of Gastroenterology, Boston Children's Hospital, Harvard Medical School, Boston, USA

^cPresent address: Roche Diagnostics International Ltd, Rotkreuz, Switzerland

^dPresent address: Molecular Biology and Immunology Department, Fundación Instituto de Inmunología de Colombia (FIDIC), Basic Sciences Department, School of Medicine and Health Sciences, Universidad del Rosario, Bogotá, Colombia

#Corresponding author, mkuenzle@ethz.ch

*Both authors contributed equally to this work

Manuscript accepted for publication in Applied and Environmental Microbiology (AEM).

DOI: 10.1128/AEM.02051-18

Contributions:

- *A. gossypii* transformation for CGL2 and MOA
- Confirming expression of FBDPs in *A. gossypii* transformants
- Testing toxicity of *A. gossypii* transformants for toxicity against fungivorous nematodes

Chapter 5

Abstract

Resistance of fungi to predation is thought to be mediated by toxic metabolites and proteins. Many of these fungal defense effectors are highly abundant in the fruiting body and not produced in the vegetative mycelium. The defense function of fruiting body-specific proteins however, including cytoplasmically localized lectins and antinutritional proteins such as biotin-binding proteins, is mainly based on toxicity assays using bacteria as heterologous expression system with bacterivorous/omnivorous model organisms as predators. Here, we present an ecologically more relevant experimental setup to assess the toxicity of potential fungal defense proteins towards the fungivorous, stylet-feeding nematodes, *Aphelenchus avenae* and *Bursaphelenchus okinawaensis*. As heterologous expression host, we exploited the filamentous fungus *Ashbya gossypii*. Using this new system, we assessed the toxicity of six previously characterized, cytoplasmically localized, potential defense proteins from fruiting bodies of different fungal phyla against the two fungivorous nematodes. We find that all of the tested proteins were toxic against both nematodes, albeit to varying degrees. The toxicity of these proteins against both, fungivorous and bacterivorous nematodes, suggests that their target(s) have been conserved between the different feeding groups of nematodes and that bacterivorous nematodes are valid model organisms to assess the nematotoxicity of potential fungal defense proteins.

Importance

Our results support the hypothesis that cytoplasmic proteins abundant in fungal fruiting bodies are involved in fungal resistance against predation. The toxicity of these proteins towards stylet-feeding nematodes, which are also capable of feeding on plants, and the abundance of these proteins in edible mushrooms, may open possible avenues for biological crop protection against parasitic nematodes e.g. by expression of these proteins in crops.

Keywords: Mycophagy, lectin, avidin, filamentous fungus, *Ashbya gossypii*, nematotoxicity

Chapter 5

Introduction

The fungal fruiting body is a relatively short-lived structure that, as a nutrient source, attracts many different predators as a nutrient source due to its high and readily available nutrient content (1-6). Its importance to the organism as sexual reproductive organ is reflected by the plethora of toxic molecules that are constitutively and specifically produced in this tissue at relatively high levels. These molecules have been discussed to reduce the negative impact of predators on the reproductive potential of the organism (7-9) by deterrence (10-15). While the role of many secondary metabolites in defense has been established over the years; the contribution of fruiting body-specific proteins such as lectins or biotin-binding proteins to defense remains still elusive. Similar to secondary metabolites (16, 17), the biosynthesis of these proteins is subject to spatiotemporal regulation during fungal fruiting body development (18, 19).

Lectins are defined as proteins possessing at least one non-catalytic domain that binds reversibly to a specific mono- or oligosaccharide (20). They act as recognition and effector molecules in the innate immune response of several phyla, including invertebrates, mammals and plants (21, 22). In fungi, lectins are abundant in fruiting bodies and sclerotia (19, 23-25). Their cytoplasmic expression, the absence of cytoplasmic ligands, as well as the lack of developmental phenotypes upon downregulation, argue against an endogenous function *e.g.* in fungal development (23, 26, 27). Recently, we tested the toxicity of different bacterially produced fungal fruiting body lectins for their toxicity against invertebrate and protozoan model organisms including *Caenorhabditis elegans*, *Acanthamoeba castellanii* and *Aedes aegypti* (28). Their toxicity towards these bacteriovorous and omnivorous organisms suggests that fruiting body lectins may mediate a constitutive protein-based resistance of the fruiting body against predators (28).

Biotin-binding proteins are another class of putative defense molecules expressed in fruiting bodies. The synthesis of biotin is restricted to plants and some microorganisms, making biotin an essential vitamin for most other organisms including herbivores and fungivorous. Biotin binding proteins are expressed by many different species. They are characterized by a very strong non-covalent binding to biotin and have been implicated as antimicrobial host defense factors that create a "biotin-free-zone" (29-32). The cytoplasmic biotin-binding proteins of the basidiomycete *Pleurotus cornucopiae*, Tamavidin 1 (Tam1) and 2 (Tam2), were shown to be toxic to *C. elegans*, *Acanthamoeba spp.* and *Drosophila melanogaster* (33).

The contribution of individual proteins to fungal resistance towards ecologically relevant fungivores has hardly been investigated in the past. To date, most studies determined the toxicity of individual, heterologously expressed proteins to model organisms (18, 28, 33-35). In contrast, for this study, we assessed the potential of different protein classes as resistance molecules against two fungivorous nematode species. Nematodes are one of the most abundant organisms in the soil ecosystem, and many of them include fungi in their diets or feed exclusively on fungi (36). Thus, nematodes represent an ecologically relevant phylum of fungal predators. Due to their feeding mechanism *i.e.* piercing the hyphal cell wall with a stylet, fungivorous nematodes can bypass many deterring secondary metabolites deposited in the cell wall (37-39). The

Chapter 5

cytoplasmic expression of nematotoxic proteins in fungi could therefore be a prime mechanism to defend against this type of predation. The fungivorous nematodes *Aphelenchus avenae* Bastian (40) and *Bursaphelenchus okinawaensis* strain SH1 (41) were used as model predators due to their ubiquitous presence in soils of temperate regions, co-habiting this ecosystem with most fungal species chosen for this study. These nematodes feed on mycelium and as well as fruiting body tissue, making them ideal candidate organisms to evaluate the toxicity of cytoplasmically expressed fruiting body defense proteins (FBDPs) (42, 43). Six different FBDPs belonging to the FBDP classes introduced earlier in this section were chosen for this study. We heterologously expressed these FBDPs individually in the cytoplasm of vegetative hyphae of the ascomycete *Ashbya gossypii*, thereby retaining the physiological context of the proteins.

The applied experimental system allowed a direct comparison of the toxicity between the individual proteins. The observed susceptibility of a fungal predator to different FBDPs supports the hypothesis that these proteins are produced to confer fruiting body resistance to predation. Similar toxicity against fungivorous and bacterivorous nematodes were found, suggesting that the respective targets of the toxins are conserved between different species/classes of nematodes.

Chapter 5

Table 1. Overview of the fruiting body defense proteins (FBDP) tested for toxicity against *A. avenae* and *B. okinawaensis*^a

Lectin/defense protein (FBDP) ^b	Molecular weight (kDa)	Origin	Protein Family	Carbohydrate specificity/activity	Toxicity		GenBank accession no.	References
					<i>A. aegypti</i>	<i>C. elegans</i>		
CGL2	16.7	<i>Coprinopsis cinerea</i>	Galectin	Galβ(1,4)Glc, Galβ(1,4)GlcNAc, Galβ(1,4)Fuc	toxic	toxic	AAF34732	(28, 44, 45)
CCL2	15.3	<i>Coprinopsis cinerea</i>	RicinB-type lectin	GlcNAcβ(1,4)[Fuca(1,3)]GlcNAc	non-toxic	toxic	EU659856	(18, 46)
TAP1	16.1	<i>Sordaria macrospora</i>	Actinoporin-like lectin	Galβ(1,3)GalNAc	toxic	toxic	CAH03681	(23, 28)
MOA	32.3	<i>Marasmius oreades</i>	Chimeric RicinB-type lectin	Galα(1,3)Gal	toxic	toxic	AY066013	(35, 47)
AAL	33.4	<i>Aleuria aurantia</i>	β-propeller lectin	Fucose	toxic	toxic	BAA12871	(28, 48-50)
Tam1	15.1	<i>Pleurotus cornucopiae</i>	Biotin-binding protein	Biotin	non-toxic	toxic	AB102784	(33, 51)

^aSix different FBDPs from five fungal species were cloned and expressed in *A. gossypii*, in order to test their toxicity towards fungal feeding nematodes *A. avenae* and *B. okinawaensis*. The six selected FBDPs, were previously shown to be toxic to at least one of the indicated bacterivorous or omnivorous model organisms.

^b CGL2, *Coprinopsis cinerea* galectin 2; CCL2, *Coprinopsis cinerea* lectin 2; AAL, *Aleuria aurantia* lectin; MOA, *Marasmius oreades* agglutinin; TAP1, *Sordaria macrospora* transcript associated with perithecial development 1; Tam1, tamavidin 1.

Results

We selected a panel of six previously characterized FBDPs, covering a wide spectrum of fungal species, protein folds and biochemical activities, to assess the biotoxicity of such proteins against the fungivorous nematodes *A. avenae* and *B. okinawaensis* (Table 1). The ascomycete *A. gossypii* was the expression host system of choice, because it can be easily modified genetically and expresses no orthologues of the FBDPs tested in this study. To obtain comparable results in a well-defined system and to maintain the physiological localization of the FBDPs during predation, we cloned and expressed each of the fungal FBDPs individually in the cytoplasm of *A. gossypii* and probed their expression (Fig. 1A). In immunoblots, we could detect all proteins at their calculated molecular weight, except for Tam1, which was detected via its tetrameric, biotin-bound form (see Materials and Methods) (Fig. 1B). This detection method for Tam1 was validated by assaying the heterologous expression of the protein in *E. coli* (Fig. 1C).

In the propagation rate assay, both nematodes grew at an exponential rate on *A. gossypii*, proving that it is a suitable food source for the fungivorous nematodes used in this study (Fig. 2A). Three times more *B. okinawaensis* was added to compensate the slow growth of this worm compared to that of *A. avenae* on *A. gossypii* plates (Fig. 2A).

The toxicity of the individual FBDPs to fungivorous nematodes was assessed by comparing propagation of the nematodes on *A. gossypii* transformants, constitutively expressing one of the defense proteins, relative to an *A. gossypii* vector control (VC) strain (Fig. 3). After 28 days of co-cultivation, the cultures were harvested and the size of the nematode population was assessed. This period corresponds, according to the determined propagation rates, to the exponential growth phase of the nematodes (Fig. 2A) We found that four out of six tested FBDPs expressed in *A. gossypii* (AAL, MOA, TAP1 and Tam1) conferred a significant inhibition of propagation for both nematodes (Fig. 2B and C). The two fruiting body lectins from *C. cinerea*, CGL2 and CCL2, exhibited significant toxicity for *B. okinawaensis*, while the effect on the propagation of *A. avenae* was not statistically significant and highly variable (Fig. 2B and C). Determination of the propagation rate of *A. avenae* nematodes fed with *A. gossypii* transformants expressing these two lectins was repeated with more biological replicates; however, the high variability among biological replicates was reproducible.

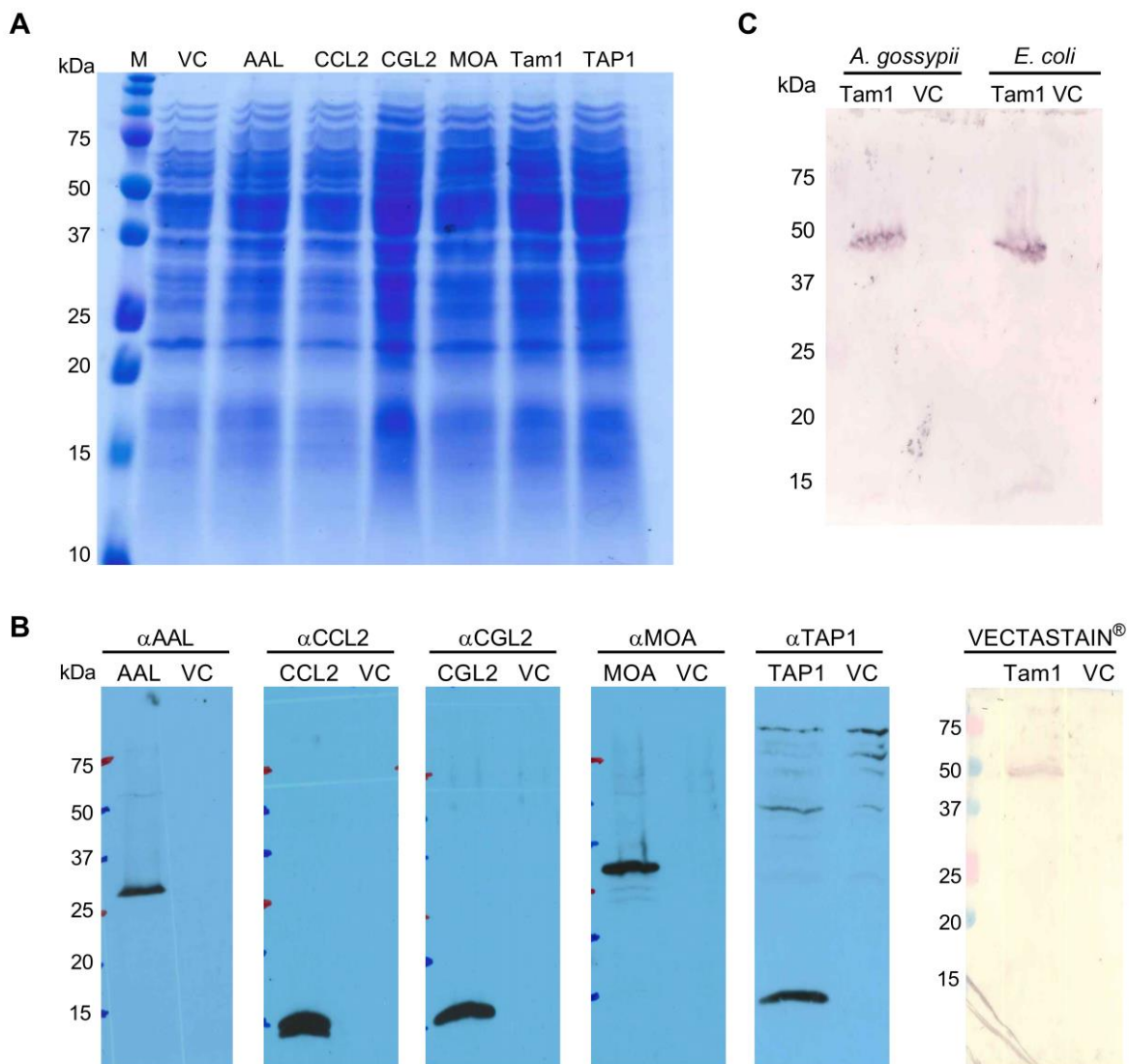


Figure 1. Expression analysis of *A. gossypii* transformants expressing different FBDPs. (A) Fungal lysate (20 μ l) were loaded on an SDS-PAGE and stained with Coomassie[®] brilliant blue. (B) Whole-cell protein extracts of *A. gossypii* transformants carrying the *A. gossypii* VC (VC) or one of the FBDP-encoding plasmids were analyzed by immunoblotting using an FBDP-specific polyclonal antibodies. For detection of tamavidin 1, the VECTASTAIN[®] ABC alkaline phosphatase system was used. Expected molecular weight of each protein is given in Table 1. (C) Expression of Tamavidin1 in *A. gossypii* and *E. coli* was detected using the VECTASTAIN[®] ABC alkaline phosphatase system. The sizes of the marker proteins are indicated. The sizes of the marker proteins are indicated.

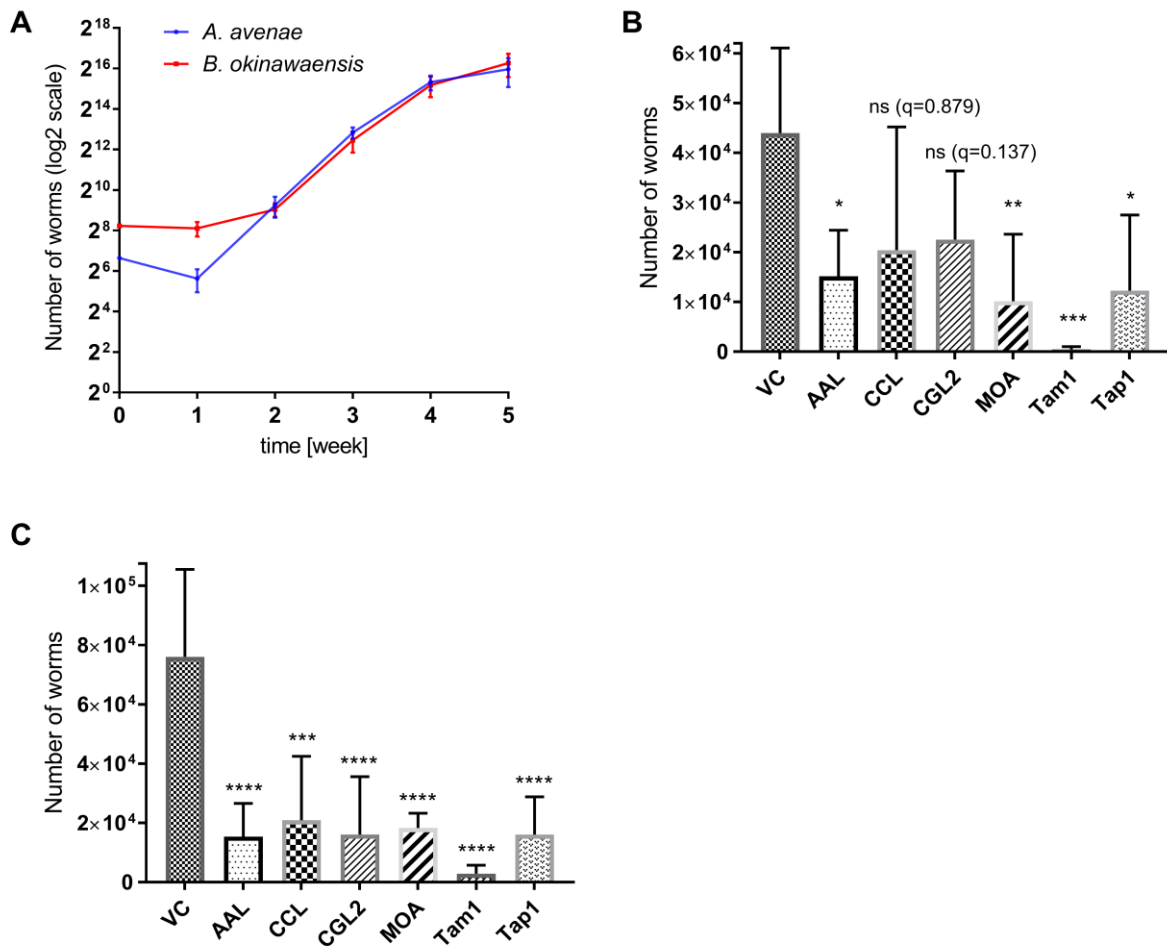


Figure 2. Propagation rate of fungivorous nematodes on different *A. gossypii* transformants. (A) 100 *A. avenae* or 300 *B. okinawaensis* were propagated on *A. gossypii*-VC. Nematodes were harvested and counted after the indicated times of incubation. (B) Indicated FBDPs were individually expressed in the vegetative mycelium of *A. gossypii*. 100 *A. avenae* were inoculated on individual *A. gossypii* transformants and incubated for 28 days at 20 °C. Thereafter, nematodes were harvested and counted. (C) Indicated FBDPs were individually expressed in the vegetative mycelium of *A. gossypii*. 300 *B. okinawaensis* were inoculated on individual *A. gossypii* transformants and incubated for 28 days at 20 °C. After this period, nematodes were harvested and counted. Error bars represent standard deviation of five biological replicates. Dunnett's multiple comparisons test was used for statistical analysis. ns: not significant, *p < 0.05, **p < 0.01, ***p < 0.001, ****p < 0.0001. Significance was measured versus VC.

Three of the toxic FBDPs were lectins (Fig. 2B). AAL, a fucose-binding lectin from *Aleuria aurantia*, MOA, a chimerolectin expressed in the fruiting bodies of *Marasmius oreades* and TAP1, an actinoporin-like lectin from perithecia of *Sordaria macrospora*, significantly slowed both *A. avenae* and *B. okinawaensis* propagation when constitutively expressed in *A. gossypii*. In these three treatments, the nematode populations were approximately a quarter of the size of the control. The most dramatic effect on nematode development was observed for treatments expressing the biotin-binding protein Tamavidin 1 (Fig. 2B and C). When this protein was expressed in *A. gossypii* very few nematodes (less than 4% compared to that of VC strain population) were retrieved from the co-cultures, indicating that expression of biotin-binding proteins strongly prevented the propagation of the fungivorous nematodes.

The toxicity of the tested FBDPs is similar to what was observed for the bacterivorous model organism *C. elegans* (Table 1), suggesting that the underlying target(s) are conserved among different nematode species.

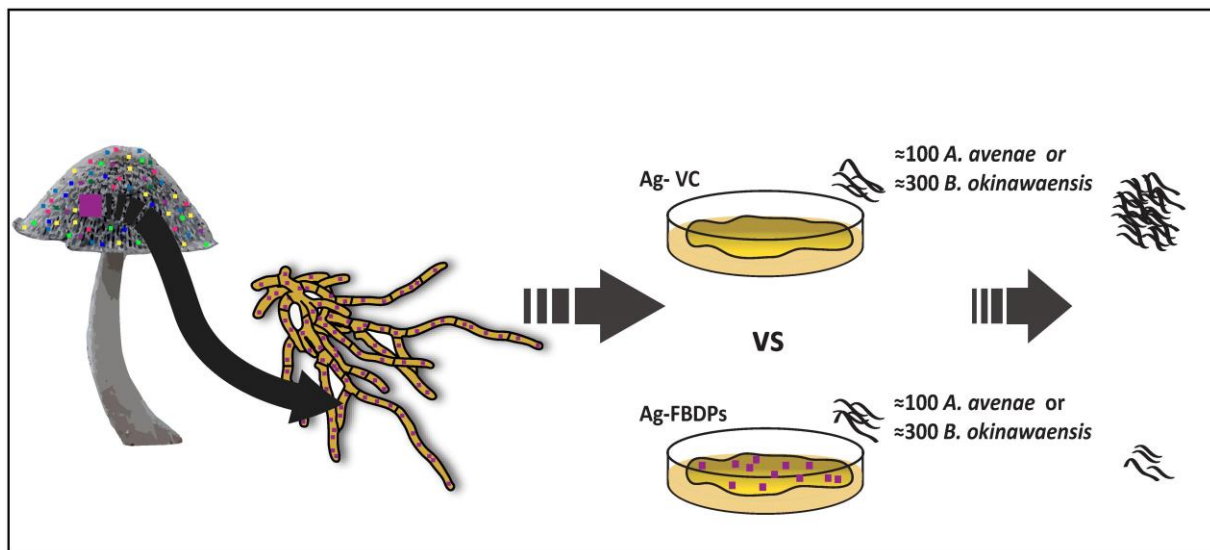


Figure 3. Schematic representation of the experimental setup. FBDPs from different fungal species were selected and individually expressed in *A. gossypii* vegetative mycelium. The indicated numbers of the each nematode were picked and placed onto an *A. gossypii* colony harboring a control plasmid or expressing a FBDP. After four weeks, the co-culture was harvested and nematodes counted.

Chapter 5

Discussion

Fungal fruiting and resting (sclerotia) bodies express multiple defense toxins against predators (17, 52). The functional redundancy of these molecules with regard to toxicity makes it difficult to study the contribution of an individual compound or protein to the fungal resistance towards a specific predator. Therefore, a synthetic approach is favored over the deletion of individual genes. We present here a heterologous fungal expression system that is similar to the physiological situation in the originating fungi and thus allows investigation of the role of an individual protein in fungal resistance towards fungivores.

The filamentous yeast *A. gossypii* appears to be an ideal tool for studying individual FBDPs and their contribution to the protein-mediated defense against a particular predatory species. The organism lacks orthologs of many FBDPs, possibly due to its phylogenetic relatedness to the yeast *Saccharomyces cerevisiae* and its adaptation to insects as ecological niche (53), but it is readily used as a prey by the model fungivorous nematodes (Fig. 2A). Expression analysis showed that all proteins are expressed and can be detected in *A. gossypii* (Fig. 1B). Due to the use of different antisera for the different FBDPs, no real quantitative statements about the expression levels of the various FBDPs can be made, however. The detection signal for Tamavidin 1 was very weak at the expected molecular weight (15.1 kDa) of the monomer and much stronger at 50 kDa (Fig. 1B and C). Previously, it was shown that Tamavidin 1 is a homotetramer in its native form. The molecular weight of the homotetramer was estimated to be around 50 kDa based on gel filtration chromatography (51) which agrees with our findings. We hypothesize that the denaturing conditions of the SDS-PAGE lead to dissociation of most of the Tam1 homotetramers into monomers, but since the native tetrameric form binds biotin with high affinity, it is much better detected by use of an avidin-based detection reagent. Resistance of homotetrameric Tam1 to SDS-PAGE denaturing conditions was confirmed by expressing the protein in *E. coli* (Fig. 1C).

The biotin-binding protein Tamavidin 1 was highly effective against both *A. avenae* and *B. okinawaensis* (Fig. 2B and C). Toxicity of this protein is thought to depend on the sequestration of free biotin, thus reducing the bioavailability for the predator of this essential nutrient (29, 33, 54). The sequestration of an essential vitamin by a proteolysis-resistant, high-affinity binding protein seems to be a powerful way to prevent predation. Our results confirm previous studies in which biotin-binding proteins have been implicated in fungal resistance and employed as effective repellents in plants for several different predators and parasites (33, 54). The lack of toxicity of Tamavidin 1 expression for the producing organisms *E. coli* (33) and *A. gossypii* (this study) suggests that there is no freely available biotin in the cytoplasm of these organisms.

Besides Tamavidin 1, three of the tested lectins AAL, MOA and TAP1, were clearly toxic for the both nematodes (Fig. 2B and C). In comparison to the biotin-binding protein, however, growth was not

Chapter 5

dramatically abolished and the extent to which the lectins attenuated population growth, varied. The *C. cinerea* fruiting body lectins CGL2 and CCL2 showed inconsistent effects on the *A. avenae* population size after 28 days, even though they were shown to be strongly toxic to the model nematode *C. elegans* (18, 28). The variable toxicity of these proteins towards *A. avenae* may be explained by the existence of specific mechanisms of this nematode to escape intoxication by these toxins e.g. through changes of the glycans in the digestive tract. Thus far, there is no report about such a mechanism but it has been shown in *C. elegans* that mutations in specific glycosyltransferases can confer resistance to both CGL2 and CCL2 (18, 45). The lower nematotoxicity of these proteins expressed in the *A. gossypii* (Fig. 1A) compared to *E. coli* (18, 28, 45) may be due to the lower expression levels of CGL2 and CCL2 in the fungus compared to the bacterium.

With this study we present the first experimental evidence that FBDPs are involved in the defense of fungi against fungivores. Based on our experiments, we cannot make a statement, however, about how the observed toxicity would protect the fungus from predation. Based on previous experiments with FBDP-expressing *E. coli* and *C. elegans*, we hypothesize that the nematodes would avoid feeding on the toxic fungus (28). The heterologous expression system for FBDPs implemented here, allows the comparison of many different candidate proteins and protein classes for their toxicity against the fungivorous nematodes *A. avenae*, *B. okinawaensis* and other fungivores. Since some of these proteins are abundant in edible mushrooms and the nematodes included in this study are known to also feed on plants, our results open possible avenues for crop protection e.g. by expression of FBDPs from edible mushrooms in crops.

3. Material and Methods

3.1 Strains and cultivation conditions

Escherichia coli strains DH5 α and BL21 were used for cloning and protein purification, respectively. Both strains were cultivated on LB medium as described (55). The nematodes *A. avenae* (Bastian, 1865) and *B. okinawaensis* (SH1) were maintained on a sporulation-deficient strain (BC-3) of *Botrytis cinerea* cultivated on malt extract agar medium (MEA) supplemented with additional 15 g/L agar and 100 μ g/ml chloramphenicol at 20 °C in the dark (41, 56). Nematodes were extracted from co-cultures by Baermann funneling (57, 58) and decontaminated on 1.5 % water-agar plates containing 200 μ M G418 (Geneticin) and 50 μ g/ml Kanamycin for 2 days at 20 °C (28). Toxicity assays were performed with *A. gossypii* ATCC 10895 and its transformants created in this study (Table 2) on solid AFM medium [1 % (w/v) yeast extract, 1 % (w/v) peptone, 1.5 % (w/v) agar, 2 % (w/v) glucose, 0.1 % (w/v) myo-inositol and 200 μ M G418] at 20 °C (59).

3.2 Cloning and expression of fungal lectins and other cytoplasmic defense proteins in *A. gossypii*

We selected a total of six previously characterized fruiting body-specific lectins and a biotin- binding protein from five different fungal species (Table 1). The primers and plasmids used to amplify the respective cDNAs from pET expression vectors as well as the plasmids generated in this study are listed in Tables 3 and 2, respectively.

Table 2. *A. gossypii* plasmids and strains generated and used for this study.

Plasmid	Markers	Insert	Source or reference	Resulting strain
pRS-AgTEFp-GFP ^a	<i>Amp</i> ^R , <i>GEN3</i>	GFP	(60)	AgGFP
pRS-AgTEF-VC	<i>Amp</i> ^R , <i>GEN3</i>	none	This study	AgVC
pRS-AgTEF-CGL-2	<i>Amp</i> ^R , <i>GEN3</i>	CGL2	This study	AgCGL2
pRS-AgTEF-CCL-2	<i>Amp</i> ^R , <i>GEN3</i>	CCL2	This study	AgCCL2
pRS-AgTEF-TAP-1	<i>Amp</i> ^R , <i>GEN3</i>	TAP1	This study	AgTAP-1
pRS-AgTEF-MOA	<i>Amp</i> ^R , <i>GEN3</i>	MOA	This study	AgMOA
pRS-AgTEF-AAL	<i>Amp</i> ^R , <i>GEN3</i>	AAL	This study	AgAAL
pRS-AgTEF-Tam1	<i>Amp</i> ^R , <i>GEN3</i>	Tam1	This study	AgTam1

^aGFP, green fluorescence protein.

As a general cloning strategy, the GFP-encoding sequence in the *A. gossypii* expression plasmid pRS-AgTEFp-GFP was replaced by FBDP-encoding sequences using the restriction sites SalI/Xhol and Ascl. The sequences of the resulting plasmids were verified by Sanger sequencing. Plasmids were transformed into *A. gossypii* by electroporation as described (61). Transformants were selected on

Chapter 5

Ashbya full medium (AFM) plates containing 200 µM G418. Homokaryons were produced by a second selection of spores isolated from transformants on AFM plates containing 200 µM G418.

Table 3. Primer sequences used for amplification of FBDP-coding sequences and their cloning into *A. gossypii* expression vector pRS-AgTEF.

Name	Sequence (5' to 3')	Parental plasmid	Reference
CGL2 fwd Sall	GGGGGGGTCGACATGCTCTACCACCTTTCGTCAAC	pET24b-CGL2	(62)
CGL2 rev Ascl	GGGGGGGGCGCGCCCTAACGAGGGGGAAAGTGGG		
CCL2 fwd Sall	GGGGGGGTCGACATGGACTCCCCAGCTGTGAC	pET24b-CCL2	(18)
CCL2 rev Ascl	GGGGGGGGCGCGCCCTAGACCTCTCGATGACCC		
TAP1 fwd Xhol	AAAAAACTCGAGGTGACATGTCTACACCCCTCACCTCCGT	pET24b-TAP1	(28)
TAP1 rev Ascl	AAAAAAGGCGCGCCTAAAGATACTCAACCGTAGCCCT		
MOA fwd Sall	GATGTCGTCGACCATATGTCCTGCGACGCCGAATTAC	pET22-MOA	(35)
MOA rev Ascl	GTATTAGGCGCGCCCTCAGTAGAAGGCCATGTAGCTGTC		
AAL fwd Sall	GGGGGGGTCGACATGCCTACCGAATTCTCTAC	pET28b-AAL	(28)
AAL rev Ascl	GGGGGCGCGCCTACCCTCCCAGGGAGTG		
Tam1 fwd Sall	TTTTTGTGACATGAAAGACGTCCAATCTCTCCTCACC	pET24b-Tam1	(33)
Tam1 rev Ascl	TTTTTGGCGCGCCTACTCGAACCTAACCGCGACG		

3.3 Protein expression analysis in *A. gossypii*

A. gossypii transformants were grown on AFM containing 200 µM G418 at 28 °C for 7 days. Protein expression was verified by harvesting the mycelium and preparing whole cell protein extracts of the *A. gossypii* transformant colonies as described (28). The prepared extracts were analyzed by immunoblotting using specific antisera (1:2500 dilutions) for detection of the various FBDPs, except for the extracts containing Tamavidin 1 where the blotted extract proteins were probed for bound biotin using the VECTASTAIN® ABC alkaline phosphatase system (Vector Laboratories) in combination with 1-Step NBT/BCIP (nitro-blue tetrazolium/5-bromo-4-chloro-3'-indolyl phosphate) solution (Thermo Scientific). Antisera against *Coprinopsis cinerea* galectin 2 (CGL2) and *Coprinopsis cinerea* lectin 2 (CCL2) have been described earlier (18, 28). The rabbit antisera against *Marasmius oreades* agglutinin (MOA), *Aleuria aurantia* lectin (AAL) and *Sordaria macrospora* transcript associated with perithecial development 1 (TAP1) were raised against the purified recombinant proteins by Pineda Antikörper-Service (Berlin, Germany). Expression and purification of these proteins from *E. coli* were carried out as previously described (28, 35, 49).

Chapter 5

3.4 Determination of propagation rates of fungivorous nematodes on *A. gossypii*

Propagation rates of *A. avenae* and *B. okinawaensis* on *A. gossypii* was determined by transferring 100 and 300 mixed-stage worms, respectively, onto a 7 days old *A. gossypii*-VC colony harboring the pRS-AgTEF-VC (Table 2) on AFM plates containing 200 µM G418. During subsequent incubation of the cocultures for 35 days at 20 °C, nematodes from five plates were harvested in parallel every week by Baermann-funneling overnight at room temperature. The funneled volume was adjusted to 0.5 to 30 ml based on the estimated number of nematodes and counted six times by taking different aliquots each time. The total number of nematodes extracted from each plate was determined by multiplying the average of the six counts by the appropriate conversion factor (see Table S1). Thus, for each time point, five biological replicates were analyzed.

3.5 Toxicity assays of FBDPs towards fungivorous nematodes

The toxicity of the individual toxins against fungivorous nematodes was assessed by cultivating *A. gossypii* transformants expressing the various FBDPs or carrying the expression vector control (VC) on AFM plates containing 200 µM G418 for 7 days at 28 °C before inoculating the plates with 100 or 300 mix staged *A. avenae* or *B. okinawaensis*, respectively. The co-cultivation plates were incubated at 20 °C for four weeks. Subsequently, the plates were harvested by Baermann-funneling overnight. The nematode population was assessed as described above. All assays were performed with five biological replicates. The individual counts and results of each biological replicate for both *A. avenae* and *B. okinawaensis* are listed in Table S2 and S3, respectively. Every data point in Fig. 2A, B and C corresponds to the mean of five biological replicates.

3.6 Statistical analysis

The statistical significance of the difference between the means of the nematode abundance for the various FBDPs and the respective controls were assessed using one-way analysis of variance followed by Dunnett's multiple comparisons test. All statistical analyses were conducted using GraphPad Prism 7 (GraphPad, San Diego, CA, USA).

Chapter 5

Acknowledgements

We thank Jürgen Wendland (Carlsberg Laboratory, Copenhagen, Denmark) and Peter Phillipson (Biozentrum Basel, Switzerland) for the plasmids, strains and protocols for heterologous expression of proteins in *A. gossypii*. We are grateful to Therese Wohlschlager and Niels van der Velden for the purification of recombinant TAP1 and MOA used for antibody production. We thank Markus Aeby for his continuing interest, helpful discussions and critical reading of the manuscript.

This work was supported by the Swiss National Science Foundation (Grant No. 31003A_173097) and ETH Zürich.

References

1. **Hanski I.** 1988. Fungivory: fungi, insects and ecology. Academic Press, London.
2. **Camazine S, Resch J, Eisner T, Meinwald J.** 1983. Mushroom chemical defense. *Journal of Chemical Ecology* **9**:1439-1447.
3. **Guevara R, Dirzo R.** 1999. Consumption of macro-fungi by invertebrates in a Mexican tropical cloud forest: do fruit body characteristics matter? *Journal of Tropical Ecology* **15**:603-617.
4. **Courtney SP, Kibota TT, Singleton TA.** 1990. Ecology of Mushroom-feeding Drosophilidae, p 225-274. In M. Begon AHF, Macfadyen A (ed), *Advances in Ecological Research*, vol Volume 20. Academic Press.
5. **Launchbaugh KL, Urness PJ.** 1992. Mushroom consumption (mycophagy) by North American cervids. *Western North American Naturalist* **52**:321-327.
6. **Martin MM.** 1979. Biochemical Implications of Insect Mycophagy. *Biological Reviews of the Cambridge Philosophical Society* **54**:1-21.
7. **Spiteller P.** 2008. Chemical defence strategies of higher fungi.
8. **Guevara R, Rayner ADM, Reynolds SE.** 2000. Effects of fungivory by two specialist ciid beetles (*Octotemnus glabriculus* and *Cis boleti*) on the reproductive fitness of their host fungus, *Coriolus versicolor*. *New Phytologist* **145**:137-144.
9. **Thomas N. Sherratt, David M. Wilkinson, Roderick S. Bain.** 2005. Explaining Dioscorides' "Double Difference": Why Are Some Mushrooms Poisonous, and Do They Signal Their Unprofitability? *The American Naturalist* **166**:767-775.
10. **Stadler M, Sterner O.** 1998. Production of bioactive secondary metabolites in the fruit bodies of macrofungi as a response to injury. *Phytochemistry* **49**:1013-1019.
11. **Demain A, Fang A.** 2000. The Natural Functions of Secondary Metabolites, p 1-39. In Fiechter A (ed), *History of Modern Biotechnology I*, vol 69. Springer Berlin Heidelberg.
12. **Rohlf M, Churchill ACL.** 2011. Fungal secondary metabolites as modulators of interactions with insects and other arthropods. *Fungal Genetics and Biology* **48**:23-34.
13. **Scheu S, Simmerling F.** 2005. Growth and reproduction of fungal feeding Collembola as affected by fungal species, melanin and mixed diets.
14. **Rohlf M, Albert M, Keller NP, Kempken F.** 2007. Secondary chemicals protect mould from fungivory. *Biology Letters* **3**:523-525.
15. **Wood WF, Archer CL, Largent DL.** 2001. 1-Octen-3-ol, a banana slug antifeedant from mushrooms. *Biochemical Systematics and Ecology* **29**:531-533.
16. **Doll K, Chatterjee S, Scheu S, Karlovsky P, Rohlf M.** 2013. Fungal metabolic plasticity and sexual development mediate induced resistance to arthropod fungivory. *Proc Biol Sci* **280**:20131219.
17. **Amon J, Keisham K, Bokor E, Kelemen E, Vagvolgyi C, Hamari Z.** 2018. Sterigmatocystin production is restricted to hyphae located in the proximity of hulle cells. *J Basic Microbiol* **58**:590-596.
18. **Schubert M, Bleuler-Martinez S, Butschi A, Walti MA, Egloff P, Stutz K, Yan S, Wilson IB, Hengartner MO, Aebi M, Allain FH, Kunzler M.** 2012. Plasticity of the beta-trefoil protein fold in the recognition and control of invertebrate predators and parasites by a fungal defence system. *PLoS Pathog* **8**:e1002706.
19. **Boulianane RP, Liu Y, Aebi M, Lu BC, Kues U.** 2000. Fruiting body development in *Coprinus cinereus*: regulated expression of two galectins secreted by a non-classical pathway. *Microbiology* **146 (Pt 8)**:1841-1853.

Chapter 5

20. **Peumans WJ, Vandamme EJM.** 1995. Lectins as Plant Defense Proteins. *Plant Physiology* **109**:347-352.
21. **Vasta G, Ahmed H, Tasumi S, Odom E, Saito K.** 2007. Biological Roles of Lectins in Innate Immunity: Molecular and Structural Basis for Diversity in Self/Non-Self Recognition, p 389-406. *In* Lambris J (ed), *Current Topics in Innate Immunity*, vol 598. Springer New York.
22. **De Hoff PL, Brill LM, Hirsch AM.** 2009. Plant lectins: the ties that bind in root symbiosis and plant defense. *Mol Genet Genomics* **282**:1-15.
23. **Nowrouzian M, Cebula P.** 2005. The gene for a lectin-like protein is transcriptionally activated during sexual development, but is not essential for fruiting body formation in the filamentous fungus *Sordaria macrospora*. *BMC Microbiol* **5**:64.
24. **Candy L, Van Damme EJM, Peumans WJ, Menu-Bouaouiche L, Erard M, Rougé P.** 2003. Structural and functional characterization of the GalNAc/Gal-specific lectin from the phytopathogenic ascomycete *Sclerotinia sclerotiorum* (Lib.) de Bary. *Biochemical and Biophysical Research Communications* **308**:396-402.
25. **Burrows PR, Barker ADP, Newell CA, Hamilton WDO.** 1998. Plant-derived enzyme inhibitors and lectins for resistance against plant-parasitic nematodes in transgenic crops. *Pesticide Science* **52**:176-183.
26. **Walti MA, Villalba C, Buser RM, Grunler A, Aebi M, Kunzler M.** 2006. Targeted gene silencing in the model mushroom *Coprinopsis cinerea* (*Coprinus cinereus*) by expression of homologous hairpin RNAs. *Eukaryot Cell* **5**:732-744.
27. **Li M, Rollins JA.** 2010. The development-specific ssp1 and ssp2 genes of *Sclerotinia sclerotiorum* encode lectins with distinct yet compensatory regulation. *Fungal Genet Biol* **47**:531-538.
28. **Bleuler-Martinez S, Butschi A, Garbani M, Walti MA, Wohlschlager T, Potthoff E, Sabotic J, Pohleven J, Luthy P, Hengartner MO, Aebi M, Kunzler M.** 2011. A lectin-mediated resistance of higher fungi against predators and parasites. *Mol Ecol* **20**:3056-3070.
29. **Mine Y.** 2000. Avidin, p 253–264. *Natural food antimicrobial systems* CRC Press, LLC, London, United Kingdom.
30. **Korpela J, Kulomaa M, Tuohimaa P, Vaheri A.** 1983. Avidin is induced in chicken embryo fibroblasts by viral transformation and cell damage. *The EMBO Journal* **2**:1715-1719.
31. **Michael Green N.** 1990. [5] Avidin and streptavidin, p 51-67. *In* Meir W, Edward AB (ed), *Methods in Enzymology*, vol Volume 184. Academic Press.
32. **Elo HA, Räisänen S, Tuohimaa PJ.** 1980. Induction of an antimicrobial biotin-binding egg white protein (avidin) in chick tissues in septicEscherichia coli infection. *Experientia* **36**:312-313.
33. **Bleuler-Martinez S, Schmieder S, Aebi M, Kunzler M.** 2012. Biotin-binding proteins in the defense of mushrooms against predators and parasites. *Appl Environ Microbiol* **78**:8485-8487.
34. **Sabotić J, Bleuler-Martinez S, Renko M, Avanzo Caglić P, Kallert S, Štrukelj B, Turk D, Aebi M, Kos J, Künzler M.** 2012. Structural Basis of Trypsin Inhibition and Entomotoxicity of Coprin, Serine Protease Inhibitor Involved in Defense of *Coprinopsis cinerea* Fruiting Bodies. *Journal of Biological Chemistry* **287**:3898-3907.
35. **Wohlschlager T, Butschi A, Zurfluh K, Vonesch SC, auf dem Keller U, Gehrig P, Bleuler-Martinez S, Hengartner MO, Aebi M, Kunzler M.** 2011. Nematotoxicity of *Marasmius oreades* agglutinin (MOA) depends on glycolipid binding and cysteine protease activity. *J Biol Chem* **286**:30337-30343.
36. **Ruess L, Lussenhop J.** 2005. Trophic interactions of Fungi and Animals, p 581–598. *In* J. D, White JF, Oudemans P (ed), *The Fungal Community: Its Organization and Role in the Ecosystems* doi:10.1201/9781420027891.ch28. CRC Press, Boca Raton.

Chapter 5

37. **Crowther TW, Boddy L, Jones TH.** 2011. Outcomes of fungal interactions are determined by soil invertebrate grazers. *Ecol Lett* **14**:1134-1142.
38. **Yeates GW, Bongers T, De Goede RG, Freckman DW, Georgieva SS.** 1993. Feeding habits in soil nematode families and genera—an outline for soil ecologists. *J Nematol* **25**:315-331.
39. **Ragsdale EJ, Crum J, Ellisman MH, Baldwin JG.** 2008. Three-dimensional reconstruction of the stomatostylet and anterior epidermis in the nematode *Aphelenchus avenae* (Nematoda: Aphelenchidae) with implications for the evolution of plant parasitism. *J Morphol* **269**:1181-1196.
40. **Townshend JL.** 1964. FUNGUS HOSTS OF APHELENCHUS AVENAE BASTIAN, 1865 AND BURSAPHELENCHUS FUNGIVORUS FRANKLIN & HOOPER, 1962 AND THEIR ATTRACTIVENESS TO THESE NEMATODE SPECIES. *Canadian Journal of Microbiology* **10**:727-737.
41. **Shinya R, Hasegawa K, Chen A, Kanzaki N, Sternberg PW.** 2014. Evidence of hermaphroditism and sex ratio distortion in the fungal feeding nematode *Bursaphelenchus okinawaensis*. *G3 (Bethesda)* **4**:1907-1917.
42. **Walker GE.** 1984. Ecology of the mycophagous nematode *Aphelenchus avenae* in wheat-field and pine-forest soils. *Plant and Soil* **78**:417-428.
43. **Okada H, Kadota I.** 2003. Host status of 10 fungal isolates for two nematode species, *Filenchus misellus* and *Aphelenchus avenae*. *Soil Biology and Biochemistry* **35**:1601-1607.
44. **Walser PJ, Pw H, M K, D S, U K, M A, Ban N.** 2004. Structure and functional analysis of the fungal galectin CGL2.
45. **Butschi A, Titz A, Walti MA, Olieric V, Paschinger K, Nobauer K, Guo X, Seeberger PH, Wilson IB, Aebi M, Hengartner MO, Kunzler M.** 2010. *Caenorhabditis elegans* N-glycan core beta-galactoside confers sensitivity towards nematotoxic fungal galectin CGL2. *PLoS Pathog* **6**:e1000717.
46. **Bleuler-Martinez S, Stutz K, Sieber R, Collot M, Mallet JM, Hengartner M, Schubert M, Varrot A, Kuzler M.** 2017. Dimerization of the fungal defense lectin CCL2 is essential for its toxicity against nematodes. *Glycobiology* **27**:486-500.
47. **Winter HC, K M, Goldstein IJ.** 2002. The mushroom *Marasmius oreades* lectin is a blood group type B agglutinin that recognizes the Galalpha 1,3Gal and Galalpha 1,3Galbeta 1,4GlcNAc porcine xenotransplantation epitopes with high affinity.
48. **Fujihashi M, Peapus DH, Nakajima E, Yamada T, Saito JI, Kita A, Higuchi Y, Sugawara Y, Ando A, Kamiya N, Nagata Y, Miki K.** 2003. X-ray crystallographic characterization and phasing of a fucose-specific lectin from *Aleuria aurantia*. *Acta Crystallogr D Biol Crystallogr* **59**:378-380.
49. **Olausson J, Tibell L, Jonsson BH, Pahlsson P.** 2008. Detection of a high affinity binding site in recombinant *Aleuria aurantia* lectin. *Glycoconj J* **25**:753-762.
50. **Wimmerova M, E M, Jf S, C G, Imbert A.** 2003. Crystal structure of fungal lectin: six-bladed beta-propeller fold and novel fucose recognition mode for *Aleuria aurantia* lectin.
51. **Takakura Y, Tsunashima M, Suzuki J, Usami S, Kakuta Y, Okino N, Ito M, Yamamoto T.** 2009. Tamavidins--novel avidin-like biotin-binding proteins from the Tamogitake mushroom. *FEBS J* **276**:1383-1397.
52. **Cary JW, Harris-Coward PY, Ehrlich KC, Di Mavungu JD, Malysheva SV, De Saeger S, Dowd PF, Shantappa S, Martens SL, Calvo AM.** 2014. Functional characterization of a veA-dependent polyketide synthase gene in *Aspergillus flavus* necessary for the synthesis of asparasone, a sclerotium-specific pigment. *Fungal Genet Biol* **64**:25-35.
53. **Dietrich FS, Voegeli S, Kuo S, Philippse P.** 2013. Genomes of ashbya fungi isolated from insects reveal four mating-type Loci, numerous translocations, lack of transposons, and distinct gene duplications. *G3 (Bethesda)* **3**:1225-1239.

Chapter 5

54. **Christeller JT, Markwick NP, Burgess EPJ, Malone LA.** 2010. The Use of Biotin-Binding Proteins for Insect Control. *Journal of Economic Entomology* **103**:497-508.
55. **Sambrook J, Fritsch EF, Maniatis T.** 1989. Molecular cloning : a laboratory manual, 2nd ed. ed. Cold Spring Harbor Laboratory Press, Cold Spring Harbor, N.Y. :.
56. **Kumar S, Khanna A, Chandel Y.** 2007. Effect of population levels of *Aphelenchoides swarupi* and *Aphelenchus avenae* inoculated at spawning on mycelial growth of mushrooms and nematode multiplication. *Nematologia Mediterranea* **35**:155.
57. **Hooper DJ, Hallmann J, Subbotin SA.** 2005. Methods for extraction, processing and detection of plant and soil nematodes. *Plant parasitic nematodes in subtropical and tropical agriculture* **2**:53-86.
58. **Walker JT, Wilson JD.** 1960. The separation of nematodes from soil by a modified Baermann funnel technique. *Plant Disease Reporter* **44**:94-97.
59. **Altmann-Jöhl R, Philippse P.** 1996. AgTHR4, a new selection marker for transformation of the filamentous fungus *Ashbya gossypii*, maps in a four-gene cluster that is conserved between *A. gossypii* and *Saccharomyces cerevisiae*. *Molecular and General Genetics MGG* **250**:69-80.
60. **Dunkler A, Wendland J.** 2007. Use of MET3 promoters for regulated gene expression in *Ashbya gossypii*. *Current Genetics* **52**:1-10.
61. **Wendland J, Philippse P.** 2000. Determination of cell polarity in germinated spores and hyphal tips of the filamentous ascomycete *Ashbya gossypii* requires a rhoGAP homolog. *J Cell Sci* **113** (Pt 9):1611-1621.
62. **Walti MA, Thore S, Aebi M, Kunzler M.** 2008. Crystal structure of the putative carbohydrate recognition domain of human galectin-related protein. *Proteins* **72**:804-808.

Chapter 5

Supplementary Information

Chapter 5

Table S1^a: Population growth assay for *A. avenae* and *B. okinawaensis* on *A. gossypii*-VC population

WEEK1										
Biological replicates	Count 1	Count 2	Count 3	Count 4	Count 5	Count 6	Mean	Final volume (µl)	Volume used for each counting (µl)	Final number
A. avenae_1	1	4	6	3	4	4	3.67	500	25	73
A. avenae_2	3	1	2	1	1	3	1.83	500	25	37
A. avenae_3	2	2	3	2	3	3	2.50	500	25	50
A. avenae_4	1	3	0	2	2	0	1.33	500	25	27
A. avenae_5	4	4	5	1	3	1	3.00	500	25	60
Biological replicates	Count 1	Count 2	Count 3	Count 4	Count 5	Count 6	Mean	Final volume (µl)	Volume used for each counting (µl)	Final number
B. okinawaensis_1	11	11	12	9	11	9	10.50	500	25	210
B. okinawaensis_2	20	26	12	16	17	13	17.33	500	25	347
B. okinawaensis_3	10	13	11	9	10	7	10.00	500	25	200
B. okinawaensis_4	19	19	15	22	11	12	16.33	500	25	327
B. okinawaensis_5	12	16	14	17	14	15	14.67	500	25	293
WEEK2										
Biological replicates	Count 1	Count 2	Count 3	Count 4	Count 5	Count 6	Mean	Final volume (µl)	Volume used for each counting (µl)	Final number
A. avenae_1	23	15	24	26	17	20	20.83	1000	25	833
A. avenae_2	13	9	14	8	15	8	11.17	1000	25	447
A. avenae_3	14	8	5	8	10	6	8.50	1000	25	340
A. avenae_4	12	15	17	14	15	23	16.00	1000	25	640
A. avenae_5	22	20	18	17	10	28	19.17	1000	25	767
Biological replicates	Count 1	Count 2	Count 3	Count 4	Count 5	Count 6	Mean	Final volume (µl)	Volume used for each counting (µl)	Final number
B. okinawaensis_1	8	16	9	11	9	16	11.50	1000	25	460
B. okinawaensis_2	10	14	15	10	7	7	10.50	1000	25	420
B. okinawaensis_3	23	21	14	18	14	9	16.50	1000	25	660
B. okinawaensis_4	12	7	16	8	13	10	11.00	1000	25	440
B. okinawaensis_5	24	14	15	12	17	16	16.33	1000	25	653

^aThe table continues on the next page

Chapter 5

WEEK3										
Biological replicates	Count 1	Count 2	Count 3	Count 4	Count 5	Count 6	Mean	Final volume (µl)	Volume used for each counting (µl)	Final number
A. avenae_1	12	17	18	8	13	12	13.33	15000		25 8000
A. avenae_2	7	16	11	11	9	13	11.17	15000		25 6700
A. avenae_3	8	15	16	16	11	6	12.00	15000		25 7200
A. avenae_4	12	19	9	21	12	19	15.33	15000		25 9200
A. avenae_5	8	9	11	5	14	8	9.17	15000		25 5500
Biological replicates	Count 1	Count 2	Count 3	Count 4	Count 5	Count 6	Mean	Final volume (µl)	Volume used for each counting (µl)	Final number
B. okinawaensis_1	7	10	5	16	9	14	10.17	15000		25 6100
B. okinawaensis_2	12	17	8	7	21	17	13.67	15000		25 8200
B. okinawaensis_3	9	17	7	15	8	8	10.67	15000		25 6400
B. okinawaensis_4	4	11	10	5	6	4	6.67	15000		25 4000
B. okinawaensis_5	6	8	8	4	5	3	5.67	15000		25 3400
WEEK4										
Biological replicates	Count 1	Count 2	Count 3	Count 4	Count 5	Count 6	Mean	Final volume (µl)	Volume used for each counting (µl)	Final number
A. avenae_1	13	16	23	21	19	37	21.50	30000		25 25800
A. avenae_2	37	41	35	39	41	36	38.17	30000		25 45800
A. avenae_3	35	39	42	34	45	43	39.67	30000		25 47600
A. avenae_4	37	41	37	33	56	47	41.83	30000		25 50200
A. avenae_5	36	38	33	24	30	21	30.33	30000		25 36400
Biological replicates	Count 1	Count 2	Count 3	Count 4	Count 5	Count 6	Mean	Final volume (µl)	Volume used for each counting (µl)	Final number
B. okinawaensis_1	38	44	45	49	51	43	45.00	30000		25 54000
B. okinawaensis_2	31	41	33	34	28	45	35.33	30000		25 42400
B. okinawaensis_3	35	30	23	41	32	27	31.33	30000		25 37600
B. okinawaensis_4	34	19	22	21	29	31	26.00	30000		25 31200
B. okinawaensis_5	13	14	21	17	17	20	17.00	30000		25 20400

^aThe table continues on the next page

Chapter 5

WEEKS										
Biological replicates	Count 1	Count 2	Count 3	Count 4	Count 5	Count 6	Mean	Final volume (µl)	Volume used for each counting (µl)	Final number
A. avenae_1	41	37	59	43	55	39	45.67	30000	25	54800
A. avenae_2	91	83	79	70	67	88	79.67	30000	25	95600
A. avenae_3	46	48	29	39	31	34	37.83	30000	25	45400
A. avenae_4	24	25	30	18	33	22	25.33	30000	25	30400
A. avenae_5	96	61	84	77	76	72	77.67	30000	25	93200
Biological replicates	Count 1	Count 2	Count 3	Count 4	Count 5	Count 6	Mean	Final volume (µl)	Volume used for each counting (µl)	Final number
B. okinawaensis_1	38	46	37	51	45	47	44.00	30000	25	52800
B. okinawaensis_2	83	63	71	97	92	88	82.33	30000	25	98800
B. okinawaensis_3	26	40	36	39	28	43	35.33	30000	25	42400
B. okinawaensis_4	67	74	77	59	79	83	73.17	30000	25	87800
B. okinawaensis_5	106	89	96	111	78	77	92.83	30000	25	111400

Chapter 5

Table S2: Toxicity of *A. gossypii* transformants against *A. avenae*

Constructs	BR ^a	Count 1	Count 2	Count 3	Count 4	Count 5	Count 6	Mean	Final volume (μl)	Used ^b volume (μl)	Final number
AAL	1	22	18	18	15	20	21	19	30000	25	22800
AAL	2	7	5	8	7	5	6	6.33	30000	25	7600
AAL	3	16	12	23	21	18	16	17.67	30000	25	21200
AAL	4	20	18	13	14	22	20	17.83	30000	25	21400
AAL	5	2	3	3	1	2	3	2.33	30000	25	2800
CCL2	1	35	52	38	46	40	41	42	30000	25	50400
CCL2	2	42	38	35	39	32	36	37	30000	25	44400
CCL2	3	2	6	4	7	5	2	4.33	30000	25	5200
CCL2	4	0	4	0	1	2	0	1.17	30000	25	1400
CCL2	5	0	0	2	0	0	1	0.5	30000	25	600
CGL2	1	13	5	7	14	7	6	8.67	30000	25	10400
CGL2	2	3	8	2	5	4	3	4.17	30000	25	5000
CGL2	3	35	23	28	29	32	22	28.17	30000	25	33800
CGL2	4	20	33	35	32	25	28	28.83	30000	25	34600
CGL2	5	22	23	23	32	27	17	24	30000	25	28800
MOA	1	4	4	5	3	4	1	3.5	30000	25	4200
MOA	2	0	0	1	1	0	0	0.33	5000	25	66.67
MOA	3	26	28	35	23	30	22	27.33	30000	25	32800
MOA	4	9	5	13	13	13	7	10	30000	25	12000
MOA	5	0	3	1	1	1	2	1.33	30000	25	1600
Tam1	1	0	2	0	0	0	0	0.33	5000	25	66.67
Tam1	2	0	1	0	0	0	1	0.33	30000	25	400
Tam1	3	1	1	1	1	2	1	1.17	30000	25	1400
Tam1	4	0	0	0	0	0	0	0	5000	25	0
Tam1	5	0	1	0	1	0	0	0.33	30000	25	400
TAP1	1	23	27	37	32	35	38	32	30000	25	38400
TAP1	2	12	17	5	8	9	3	9	30000	25	10800
TAP1	3	10	8	10	8	4	6	7.67	30000	25	9200
TAP1	4	0	0	1	0	2	2	0.83	30000	25	1000
TAP1	5	2	3	2	0	3	0	1.67	30000	25	2000
EV	1	28	20	18	21	29	32	24.67	30000	25	29600
EV	2	38	36	32	28	41	38	35.5	30000	25	42600
EV	3	52	48	52	38	65	59	52.33	30000	25	62800
EV	4	59	54	44	44	50	48	49.83	30000	25	59800
EV	5	22	23	25	16	24	16	21	30000	25	25200

^aBiological replicate.

^bVolume used for each counting (μl).

Chapter 5

Table S3: Toxicity of *A. gossypii* transformants against *B. okinawaensis*

Constructs	BR ^a	Count 1	Count 2	Count 3	Count 4	Count 5	Count 6	Mean	Final volume (μl)	Used ^b volume (μl)	Final number
AAL	1	31	29	33	26	27	21	27.83	30000	25	33400
AAL	2	12	12	9	11	16	9	11.5	30000	25	13800
AAL	3	4	5	3	6	5	2	4.17	30000	25	5000
AAL	4	10	4	11	3	3	6	6.17	30000	25	7400
AAL	5	11	18	10	20	15	12	14.33	30000	25	17200
CCL2	1	9	4	3	2	5	3	4.33	30000	25	5200
CCL2	2	8	11	13	11	9	11	10.5	30000	25	12600
CCL2	3	14	7	6	8	9	12	9.33	30000	25	11200
CCL2	4	46	61	55	35	35	62	49	30000	25	58800
CCL2	5	15	14	16	13	12	14	14	30000	25	16800
CGL2	1	5	3	1	2	1	2	2.33	30000	25	2800
CGL2	2	44	56	39	35	37	41	42	30000	25	50400
CGL2	3	7	12	12	7	6	10	9	30000	25	10800
CGL2	4	12	5	11	9	10	10	9.5	30000	25	11400
CGL2	5	6	4	7	2	4	2	4.17	30000	25	5000
MOA	1	15	16	14	12	15	13	14.17	30000	25	17000
MOA	2	12	14	15	11	12	14	13	30000	25	15600
MOA	3	13	17	24	13	24	22	18.83	30000	25	22600
MOA	4	20	23	23	17	16	22	20.17	30000	25	24200
MOA	5	12	11	12	10	7	9	10.17	30000	25	12200
Tam1	1	3	7	4	10	5	8	6.17	30000	25	7400
Tam1	2	0	0	0	1	0	1	0.33	30000	25	400
Tam1	3	1	0	0	1	1	0	0.5	30000	25	600
Tam1	4	2	3	2	2	4	2	2.5	30000	25	3000
Tam1	5	5	5	1	1	2	1	2.5	30000	25	3000
TAP1	1	24	19	30	29	31	24	26.17	30000	25	31400
TAP1	2	8	7	9	8	4	10	7.67	30000	25	9200
TAP1	3	3	3	2	6	4	5	3.83	30000	25	4600
TAP1	4	4	8	6	6	7	3	5.67	30000	25	6800
TAP1	5	31	19	21	17	34	20	23.67	30000	25	28400
EV	1	76	78	55	89	67	75	73.33	30000	25	88000
EV	2	62	54	50	49	33	60	51.33	30000	25	61600
EV	3	57	44	50	36	47	43	46.17	30000	25	55400
EV	4	46	48	39	45	46	40	44	30000	25	52800
EV	5	101	110	132	98	96	76	102.17	30000	25	122600

^aBiological replicate.

^bVolume used for each counting (μl).

Chapter 6

Induction of antibacterial proteins and peptides in the coprophilous mushroom *Coprinopsis cinerea* in response to bacteria

¹*Anja Kombrink, ¹*Annageldi Tayyrov, ¹*Andreas Essig, ¹°Martina Stöckli, ¹Sebastian Micheller, ¹^John Hintze, ¹Yasemin van Heuvel, ¹Natalia Dürig, ¹Chia-wei Lin, ¹Pauli T. Kallio, ¹Markus Aebi, ¹°Markus Künzler

¹Institute of Microbiology, Department of Biology, ETH Zürich, Vladimir-Prelog-Weg 4, CH-8093 Zürich, Switzerland

° Current address: rqmicro AG, Brandstrasse 24, 8952 Schlieren, Switzerland

^ Current address: Department of Cellular and Molecular Medicine, The Panum Institute, University of Copenhagen,
Blegdamsvej 3, DK-2200 Copenhagen, Denmark

° Corresponding author: +41 44 6324925, mkuenzle@ethz.ch

* Authors contributed equally to this work

Published in *The ISME Journal*.

DOI: 10.1038/s41396-018-0293-8

Contributions:

- Isolation and cloning of CPP2
- Expressing CPP2 in *P. pastoris* and confirming its antibacterial activity
- Reanalysis of RNA-seq data using improved annotations
- Part of qRT-PCR

Chapter 6

Abstract

Bacteria are the main nutritional competitors of saprophytic fungi during colonization of their ecological niches. This competition involves the mutual secretion of antimicrobials that kill or inhibit the growth of the competitor. Over the last years it has been demonstrated that fungi respond to the presence of bacteria with changes of their transcriptome, but the significance of these changes with respect to competition for nutrients is not clear as functional proof of the antibacterial activity of the induced gene products is often lacking. Here, we report the genome-wide transcriptional response of the coprophilous mushroom *Coprinopsis cinerea* to the bacteria *Bacillus subtilis* and *Escherichia coli*. The genes induced upon co-cultivation with each bacterium were highly overlapping, suggesting that the fungus uses a similar arsenal of effectors against Gram-positive and -negative bacteria. Intriguingly, the induced genes appear to encode predominantly secreted peptides and proteins with predicted antibacterial activities, which was validated by comparative proteomics of the *C. cinerea* secretome. Induced members of two putative antibacterial peptide and protein families in *C. cinerea*, the cysteine-stabilized $\alpha\beta$ -defensins (Cs $\alpha\beta$ -defensins) and the GH24-type lysozymes, were purified, and their antibacterial activity was confirmed. These results provide compelling evidence that fungi are able to recognise the presence of bacteria and respond with the expression of an arsenal of secreted antibacterial peptides and proteins.

Chapter 6

Introduction

Interactions between fungi and bacteria occur in many ecological contexts and can range from mutualistic to antagonistic (Deveau et al., 2018; Frey-Klett et al., 2011). As fungi and bacteria are the main decomposers of plant-derived dead organic matter, they are competitors for nutrients in such niches (Moller et al., 1999; Rousk and Baath, 2011). Fungi defend their niche mainly chemically i.e. by production and secretion of antibacterials (Boer et al., 2005). Such defense effectors range from secondary metabolites (natural products) to peptides and proteins and are not essential for the viability of the fungus under axenic conditions (Hoffmeister and Keller, 2007; Kempken and Rohlf, 2010; Kunzler, 2015). It is well established that the biosynthesis of these compounds in fungi is regulated in response to external and internal signals but the significance and the molecular mechanisms of this regulation are not well understood (Macheleidt et al., 2016). A deeper understanding of these issues will help to explore the hidden arsenal of fungal defense effectors e.g. for the discovery of new antibiotics (Adnani et al., 2017; Netzker et al., 2015; Wiemann and Keller, 2014).

In plants, whose primary defense is also chemical, the productions of defense effectors is either developmentally regulated, leading to tissue-specific expression patterns, or induced upon challenge with antagonists (Meldau et al., 2012). Whereas developmental regulation is thought to provide specific tissues with preventive protection against the most abundant antagonists, inducible defense enables the plant to save resources by omitting the production of defense effector molecules in the absence of antagonists and by tailoring its defense to a specific type of antagonist. Such an inducible defense system requires specific receptors for recognition of and differentiation between different antagonists and signalling pathways downstream of these receptors leading to transcriptional activation of genes coding for defense effectors against the respective antagonist (Choi and Klessig, 2016).

Tissue-specific production has been reported for fungal defense effectors. For example, production of a $\text{Cs}\alpha\beta$ -defensin, which is mainly active against Gram-positive bacteria, and two isolactonases cleaving typical quorum sensing molecules of Gram-negative bacteria, is restricted to vegetative mycelium and does not occur in the fruiting bodies of axenically cultivated mushroom *Coprinopsis cinerea* (Essig et al., 2014; Stockli et al., 2017). Conversely, various genes coding for nematotoxic lectins and insecticidal protease inhibitors are preferentially expressed in the fruiting body of *C. cinerea* and many other mushrooms (Plaza et al., 2014; Sabotic et al., 2016). The expression pattern of these defense effectors is in accordance with the ecology of *C. cinerea*, as the vegetative mycelium of this coprophilous fungus is mainly exposed to bacterial competitors and parasites, whereas the fruiting bodies are mainly under attack of animal predators (Kunzler, 2015). In addition to this constitutive defense of specific tissues, there is increasing evidence that fungi are also able to respond to the presence of specific antagonists through the upregulation of respective defense effectors. For example, upon challenge of the vegetative mycelium with a fungivorous nematode, *C. cinerea* induced the production of nematotoxic lectins that were not produced under axenic conditions or upon challenge

Chapter 6

with bacteria under the same condition (Bleuler-Martinez et al., 2011; Plaza et al., 2015). While these studies lack the experimental evidence that this response is physiologically significant for the fungus, other studies show that upregulation of secondary metabolite biosynthesis in the mold *Aspergillus nidulans* in response to grazing by a soil arthropod leads to deterrence of the arthropod (Doll et al., 2013; Rohlfs et al., 2007). These results suggest that fungi are able to respond to animal predators by mounting specific defense responses that directly affect the antagonist and are involved in securing fungal growth and propagation. Thus far, experimental evidence for an analogous, specific fungal defense response against bacterial competitors is poor. Although various interaction studies between fungi and bacteria report the induced expression of fungal genes coding for secondary metabolites and other putative defense effectors, the produced molecules either have not been characterized for antibacterial activity or did not show activity in such assays (Benoit et al., 2015; Deveau et al., 2015; Gkarmiri et al., 2015; Ipcho et al., 2016; Lamacchia et al., 2016; Mathioni et al., 2013; Mela et al., 2011; Schroeckh et al., 2009). The most compelling evidence for a specific defense response of fungi against bacteria comes from two recent reports on the induced production of antibacterial depsipeptides, in the marine-derived mold *Emericella* sp. upon cocultivation with a marine actinomycete (Oh et al., 2007) and in the fungal endophyte *Fusarium tricinctum* upon cocultivation with *B. subtilis* (Ola et al., 2013). These studies do not include any analysis of fungal gene expression, however.

In this study, we confronted the coprophilous model fungus *C. cinerea* with the Gram-negative and Gram-positive model bacteria, *Escherichia coli* and *Bacillus subtilis*, respectively, in a previously employed semi-liquid setup (Essig et al., 2014). We investigated the response of the fungus to the bacteria through comparative transcriptomics as well as comparative proteomics of the secretome. Analysis of the differentially expressed *C. cinerea* genes upon exposure to either of the bacteria revealed an overlapping set of highly induced genes. In line with a putative role in the extracellular interaction with bacteria, an overrepresentation of genes coding for secreted proteins was found among these induced genes. Moreover, for many induced genes, putative antibacterial activity could be attributed to the encoded proteins based on the *in silico* identification of conserved domains. These proteins included a paralog of the previously identified Csa β -defensin Copsin as well as members of a yet uncharacterized family of proteins containing a conserved defensin-like domain linked to a GH24-type lysozyme (phage lysozyme) domain (Essig et al., 2014; Wohlkönig et al., 2010). Importantly, the predicted antibacterial function of these proteins could be confirmed and characterized through antibacterial assays using heterologously produced proteins. Altogether, the presented results provide evidence for the presence of an inducible defense mechanism in *C. cinerea* against Gram-negative and Gram-positive bacteria.

2. Materials and Methods

2.1 Strains, culture media and chemicals

C. cinerea AmutBmut (A43mut B43mut pab1.2) (Swamy et al., 1984) and *Pichia pastoris* (NRRLY11430) were used for all experiments involving a fungus. *E. coli* (Nissle 1917) and *B. subtilis* (NCIB 3610) (Branda et al., 2001) were used as model bacterial competitors. *E. coli* (DH5 α) was used for cloning purposes throughout this study. *C. cinerea* was cultivated on YMG (0.4% (w/v) yeast extract (Oxoid), 1% (w/v) malt extract (Oxoid), 0.4% (w/v) glucose, 1.5% (w/v) agar), *P. pastoris* on YPD (1% (w/v) yeast extract, 2% (w/v) bacteriological peptone (Oxoid), 2% (w/v) glucose, 1.5% (w/v) agar) and the bacteria on Luria Bertani (LB) agar plates (0.5% (w/v) yeast extract, 1.0% (w/v) tryptone, 0.5% (w/v) sodium chloride, 1.5% (w/v) agar). Transformants of *P. pastoris* and *E. coli* DH5 α were selected and maintained on media containing either 100 mg/l or 30 mg/l of Zeocin (LabForce), respectively. The bacterial strains used for the antibacterial activity assays and their specific cultivation conditions are mentioned below. If not mentioned otherwise, all chemicals were bought at the highest available purity from Sigma-Aldrich.

2.2 *C. cinerea* co-cultivation with bacteria and preparation of RNA

Fungal-bacterial co-cultivation on glass beads was performed as previously described (Essig et al., 2014). In brief, the bottom of a Petri dish (10 cm diameter) was covered with borosilicate glass beads (5 mm diameter), submerged in 12 mL *C. cinerea* minimal medium (CCMM). Three plugs were cut from the margin of a *C. cinerea* mycelial colony, that had been previously cultivated on YMG agar plates at 28 °C for 3 days, and placed on top of glass beads. The fungal cultures were incubated in a humid chamber at 28 °C for 2.5 days in the dark. *E. coli* Nissle 1917 and *B. subtilis* NCIB 3610 (Branda et al., 2001), precultivated on LB agar plates, were cultivated in CCMM liquid medium to an optical density (OD_{600}) of 0.3. The cells were collected by centrifugation to remove the culture medium, resuspended in 0.5 ml culture medium taken from the individual *C. cinerea* plates and added to the respective *C. cinerea* glass beads plates at an OD_{600} of 0.1. *C. cinerea* cultures were also left untreated for axenic controls.

All cultivations were performed in triplicates and incubated at 28 °C for 8 h in the dark. Subsequently, the mycelium was harvested and flash frozen in liquid nitrogen. After lyophilizing the mycelium, 1 mL of Qiazol (Qiagen) and glass beads (0.5 mm diameter) were added and cells were lysed using a FastPrep (Thermo Scientific) device (three cycles for 30 sec at level 5.5 m/s with cooling the samples for 3 min on ice in between the cycles). Total RNA was extracted using the RNeasy Lipid Tissue Mini Kit (Qiagen) according to the manufacturer's protocol.

2.3 RNA library construction and sequencing

RNA quality control and concentration were assessed using the Bioanalyzer 2100 (Agilent) and Qubit (1.0) fluorometer (Life Technologies), respectively. Transcriptome library preparation (TruSeq Stranded RNA Kit),

Chapter 6

cDNA sequencing (Illumina HiSeq™ 2500), and data pre-processing were performed at the Functional Genomics Center Zurich (FGCZ) following manufacturers' protocols. Data analysis was performed using SUSHI (Hatakeyama et al., 2016), an NGS data analysis workflow management system developed by the FGCZ, which supports selected open source NGS data analysis packages. In detail, reads were aligned with STAR aligner (Dobin et al., 2013) with the additional options (--outFilterMatchNmin 30 --outFilterMismatchNmax 5 --outFilterMismatchNoverLmax 0.05 --outFilterMultimapNmax 50) which means that at least 30 bp matching was required, and accepted were at most 5 mismatches, and at most 5% of mismatches. Alignments were only reported for reads with less than 50 valid alignments with the genome. The *C. cinerea* AmutBmut pab1-1 genome (2013-07-19) and its annotation v1.0 (2016-09-12, filtered gene models) from the US Department of Energy (DOE) Joint Genome Institute (JGI) were used as reference (Muraguchi et al., 2015). Expression counts were computed using the featureCounts from the Bioconductor package subread (Liao et al., 2014). Differential expression was computed using the DESeq2 package (Love et al., 2014). The RNA data is deposited in the ArrayExpress database under the accession number E-MTAB-6876

2.4 Genome-wide analysis of differential gene expression

C. cinerea genes that displayed increased expression in the bacteria-treated samples compared to the control samples were considered significantly induced using criteria of a log₂ fold change (FC) ≥ 2, a P-value <0.005 and a false discovery rate < 0.005. In addition, a minimum raw reads of 10 was taken as a threshold for gene expression. The amino acid sequences encoded by the final set of 527 genes were used in conserved domain searches (CD-search NCBI) (Marchler-Bauer et al., 2015) and Gene Ontology (GO) database for functional annotation (Ashburner et al., 2000). A smaller set of highly induced genes was selected using a cut off of a log₂ FC ≥ 4. Their annotation was verified manually by comparing mapped reads to the predicted JGI gene models in the Integrative Genomics Viewer (IGV) (Robinson et al., 2011). The amino acid sequences of fifteen gene products were corrected and eight genes were excluded from the list due to wrong and currently not correctable (due to low read number) annotation (Supplementary Information SI2). The amino acid sequences of 108 genes and the entire *C. cinerea* AmutBmut proteome were investigated for the presence of predicted signal peptides by SignalP v4.1 (Petersen et al., 2011), and transmembrane domains by TMHMM v.2.0 (Krogh et al., 2001). Sequences with one predicted transmembrane domain were analysed for possible overlap with predicted signal peptides. Overrepresentation of secreted/membrane proteins encoded by induced genes vs the whole proteome was examined using the absolute numbers in a chi-square test with Yates' correction and two-sided P-values were obtained. An all-vs-all Blast search (NCBI) using an E-value of 1e-06 was performed to identify proteins encoded by duplicate genes. A cut off of minimal 60% coverage for the longest of the two sequences, at least 30% identity and a minimum bit score of 50 was used. To test the significance of the relative ratios between induced vs entire genome, a chi-square test was performed.

Chapter 6

2.5 qRT-PCR analysis of specific genes

To monitor the transcription level of specific *C. cinerea* genes, total cDNA was synthesized from total RNA (see above for extraction protocol) as described previously (Plaza et al., 2014). qRT-PCR of specific cDNAs and data analysis was performed as previously described (Plaza et al., 2015) using the primers listed in Table S2.

2.6 Alignment and phylogenetic analysis

The sequences of all 6 LYS, 10 DLP proteins and 7 Copsin paralogs were manually verified and corrected, if necessary, using IGV browser (Robinson et al., 2011). All the protein sequences that were used in this study are listed in Table S1. All the alignments were performed using the ClustalW algorithm (v2.1) (Thompson et al., 2002).

2.7 Cloning, production and purification of Copsin and CPP2

The codon-optimized prepro-Copsin (CPP1) insert and the native prepro-CPP2 insert were cloned into the pPICZA expression plasmid (Invitrogen) using the restriction enzymes *EcoRI/Sall* (Thermo Scientific) (Franzoi et al., 2017). Both constructs were linearized with *SacI* and transformed into *P. pastoris* by electroporation as described previously (Essig et al., 2014; Wu and Letchworth, 2004). The standard methanol-limited fed-batch procedure was performed in a 3.6 l Labfors 5 bioreactor (Infors) according to the *Pichia* fermentation process guidelines of Invitrogen (Thermo Scientific) and using the process parameters and feed-in strategy as described (Franzoi et al., 2017). The cells were removed by centrifugation (8000 x g, 20 °C, 20 min) and the resulting supernatant was vacuum filtered (0.22 µm rapid-Filtermax 500; Techno Plastic Products TPP). The solution was diluted to a conductivity of 9-11 mS/cm by adding ddH₂O and the pH was adjusted to 7 by adding ammonium hydroxide. After vacuum filtration (0.22 µm rapid-Filtermax 500; TPP), the solution was loaded on a self-made SP-Sephadex cation exchange column pre-equilibrated with binding buffer A (20 mM sodium phosphate pH 7, 10 mM NaCl). The column was washed with 17% buffer B (20 mM sodium phosphate pH 7, 1 M NaCl) and the peptide was eluted with 60% buffer B. The peptide elution was monitored at UV absorbance of 210 nm and 280 nm. Fractions containing either the Copsin or the CCP2 peptide were pooled and concentrated in a 2 kDa Spectra/Por dialysis membrane (Spectrum Laboratories) as previously described (Essig et al., 2014). The concentrated eluate was dialyzed against buffer C (2 mM sodium phosphate buffer pH 7.2, 70 mM NaCl) at 4 °C for 24 h. After further concentration in a 6-8 kDa Spectra/Por dialysis membrane (Spectrum Laboratories), the protein solution was again dialyzed against buffer C. The protein concentration was determined by a Pierce BCA protein assay, according to the manufacturer's instructions (Thermo Scientific).

2.8 Antimicrobial activity of Copsin and CPP2

MIC values were determined by the microdilution broth method according to the Clinical and Laboratory Standards Institute (CLSI) guidelines with minor modifications (Meskauskas et al., 1999). In brief, two-fold dilution series (0.12-64 µg/mL) of Copsin and CPP2 were prepared in 96-well polypropylene microtiter plates in cation-adjusted Mueller-Hinton broth (CAMHB; BD Diagnostics). The tested bacteria (see Figure 3) were grown in LB-Lennox medium to an OD₆₀₀ of 0.2 - 0.6 and added to the dilution series to 10⁵ - 10⁶ cfu/mL. For *Listeria monocytogenes* and *Corynebacterium diphtheriae*, CAMHB was supplemented with 3% laked horse blood (Oxoid). The plates were incubated at 37 °C for 20 h. Each strain was tested at least in duplicate. The cfu/mL was determined by plating dilutions of the growth control on LB-Lennox agar plates.

2.9 Cloning of GH24-type lysozyme genes

cDNA from RNA of induced co-cultures was synthesized using the Transcripter Universal cDNA Master kit (Roche) and used as template for the amplification of the DNA sequence encoding the protein of LYS1, LYS2 and LYS3 lacking the predicted signal sequences by PCR. Primers are listed in Table S2 and contained restriction sites for *Eco*RI at the 5' and for *Not*I at the 3' end. The PCR products were ligated into *P. pastoris* expression vector pPICZαA (Invitrogen) using the α-factor as secretion signal. The obtained plasmid containing LYS2 was subsequently used as template for the generation of LYS2His and LYS2HisΔN. The polyhistidine sequence was added to the reverse primer to obtain constructs with a C-terminal His6-tag and *Eco*RI and *Not*I restriction sites were used for ligation into pPICZαA. The pPICZαA-LYS2His plasmid was used as template for the generation of LYS2(D131A)His by targeted mutagenesis. Briefly, overlapping forward and reverse primers were designed with a single nucleotide change that results in the required amino acid change. The full plasmid was amplified and the PCR product was digested with *Dpn*I to remove the methylated template plasmid. After on-column cleaning, the plasmid with LYS2(D131A)His was transformed into *E. coli* DH5α for amplification.

2.10 GH24-type lysozyme production and purification

The GH24-type lysozyme-encoding plasmids were linearized with *Sac*I, or for pPICZαA_LYS1 with *Msp*I (*Pme*I), and transformed into *P. pastoris* (Essig et al., 2014; Wu and Letchworth, 2004). Approved *P. pastoris* transformants were used to inoculate 10 ml BMGY medium (1% (w/v) yeast extract, 2% (w/v) peptone, 1.3% (w/v) YNB without amino acids (BD Diagnostics), 100 mM potassium phosphate buffer pH 6, 1% (v/v) glycerol) and grown at 28 °C for 24 h at 180 rpm. The cells were pelleted by centrifugation (3000 x g, 5 min, RT (room temperature)), resuspended into a *P. pastoris* minimal medium (1.3% (w/v) YNB without amino acids, 100 mM potassium phosphate buffer pH 6, 0.4 g/mL biotin, 0.5% (w/v) NH4Cl, 1% (v/v) MeOH) and cultured further for 3 days at 28 °C and 180 rpm, during which MeOH was added to 1 % every 12 h.

Chapter 6

After centrifugation (3000 g, 10 min, 4 °C), the supernatant was filter sterilized and concentrated using Vivaflow 50R with a 5 kDa cut off filter membrane (Sartorius AG). For the purification of polyhistidine-tagged proteins, the concentrated medium was dialyzed in a dialysis membrane with a 2 kDa cut off (Spectrum Laboratories) against 2 x 4 L PBS at 4 °C for 24 h. For the non-tagged proteins, the solution was dialyzed against a 20 mM sodium phosphate pH 6.5, 50 mM NaCl buffer (buffer D). His6-tagged proteins were loaded on a PBS-calibrated Ni²⁺-NTA agarose column (Macherey-Nagel), washed with 10 mM imidazole and eluted with 250 mM imidazole in PBS. The non-tagged proteins were loaded on self-made SP-Sephadex cation exchange column equilibrated with buffer D. After washing with buffer D, the proteins were eluted at 200 mM NaCl in 20 mM Na-phosphate buffer pH 6.5. For all proteins, after elution from the column, the elution buffer was exchanged to PBS using PD-10 columns (GE Healthcare). Protein concentrations were determined using the Pierce BCA protein assay kit (Thermo Scientific).

2.11 Lysozyme activity assays

B. subtilis 168 (Kunst et al. 1997), *Staphylococcus aureus* 113 (DSMZ 4910) and *Staphylococcus carnosus* 361 (DSMZ 20501) were grown in LB medium at 37 °C to an OD₆₀₀ of 2. *Micrococcus luteus* (DSMZ 20030) was cultivated in nutrient broth (Difco, BD Diagnostics) at 28 °C to an OD₆₀₀ of 2. Cells were harvested by centrifugation (6000 rpm, 5 min, RT), washed with 66 mM potassium phosphate buffer pH 6.2 and resuspended in the same buffer to an OD₆₀₀ of 100 and frozen in small aliquots. Upon use, potassium phosphate buffer was added to obtain a starting OD₆₀₀ of 1 and aliquots of 100 µL of the cell suspension were transferred into a 96-well microtiter plate (Tissue culture test plate 96F; TPP). Lysozymes and BSA were added to a final concentration of 20 µg/mL in a total volume of 102 µL. The cells were incubated in the microplate reader (Infinite 200 PRO; Tecan), shaking (orbital, 4 mm amplitude) at 37 °C, and the OD₄₅₀ was measured in a time interval of 5 min, for 60 min (*B. subtilis* and *M. luteus*) or 120 min (*S. aureus* and *S. carnosus*).

3. Results

3.1 *C. cinerea* responds to *E. coli* and *B. subtilis* with induction of highly overlapping gene sets

The response of the fungus *C. cinerea* towards two different types of bacteria, Gram-positive and Gram-negative, was investigated exploiting a previously described experimental setup for cocultivation of fungi and bacteria (Droce et al., 2013; Essig et al., 2014), for comparative transcriptomics and proteomics. This setup involved cultivation of *C. cinerea* strain AmutBmut vegetative mycelium on glass beads submerged in liquid minimal medium to which either the Gram-negative bacterium *E. coli* Nissle 1917 or the Gram-positive species *B. subtilis* NCIB 3610 was added. *C. cinerea* mycelium was harvested for transcriptome analysis after 8 h of co-cultivation, during which time the OD₆₀₀ of *E. coli* increased from 0.1 at the time of bacterial inoculation, to 0.127 (± 0.017). The density of *B. subtilis* cells decreased during co-cultivation, probably due to the production of Copsin (Essig et al., 2014), resulting in an average OD₆₀₀ of 0.012 (± 0.001) at the time of mycelial harvesting. Differential expression of annotated protein-encoding *C. cinerea* genes was assessed by comparing DESeq2 normalized read values in *E. coli*- or *B. subtilis*-exposed mycelium to untreated mycelium. Comparing *E. coli*- and *B. subtilis*-induced genes ($\log_2 \text{FC} \geq 2$, FDR < 0.005) revealed that in the presence of *E. coli*, a higher number of *C. cinerea* genes (510 genes, 3.6% of the predicted proteome) were induced than in the presence of *B. subtilis* (165 genes, 1.2% of the predicted proteome) (Supplementary Information SI2). Interestingly, 90 % of the *B. subtilis*-induced genes are also induced by *E. coli*. This overlap comprises predominantly the *E. coli*-induced genes with the highest FC (Fig. S1). We selected a smaller set of highly induced genes, using a cut off of $\log_2 \text{FC} \geq 4$ and FDR < 0.005 for detailed analysis and identification and characterization of potential fungal defense genes (Table S3 and Supplementary Information SI2). The differential expression of five of these genes and one non-induced gene as control was confirmed by qRT-PCR (Fig. S6). Using the same cut off, $\log_2 \text{FC} \geq 4$ and FDR < 0.005, the expression of only ten and no genes was found to be downregulated in the presence of *E. coli* and *B. subtilis*, respectively. These genes were not further investigated.

3.2 *C. cinerea* genes with induced expression in response to bacteria tend to cluster and to occur in multi-gene families

Inspection of the genomic location of the bacteria-induced set of 108 genes ($\log_2 \text{FC} \geq 4$) revealed that many of these genes cluster. Although the incomplete assembly of the *C. cinerea* AmutBmut genome makes it difficult to perform a thorough analysis, we found that 62 of the 108 induced genes colocalize with one or more other induced gene(s) within a genomic region of maximum 100 kb.

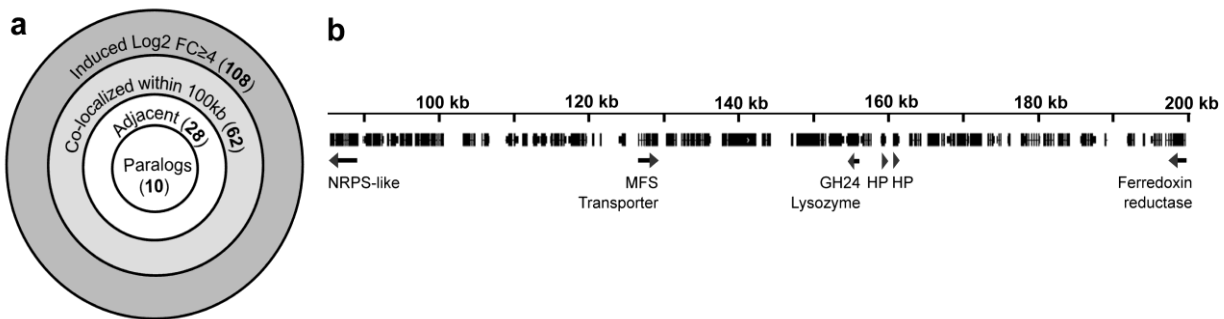


Figure 1 | Clustering of bacteria-induced genes in the *C. cinerea* genome. (a) Occurrence of different degrees of gene clustering. More than 50% of the 108 most highly induced genes were found to cluster; either within a larger chromosomal region of 100 kb or adjacent to each other (with a maximum of two genes in between). Paralogous genes are more likely to cluster and are therefore categorized separately. (b) Example illustrating the three degrees of clustering of bacteria-induced genes (marked with arrows), with the two hypothetical proteins (HPs) representing paralogs with 69% amino acid sequence identity. The respective JGI protein IDs are as follows: adenylate-forming reductase, 361483; MFS transporter, 559285; GH24-type lysozyme, 442447; HPs, 442449 and 559271; Ferredoxin reductase, 361411. Notion on the dimension of the indicated numbers of (protein-encoding) genes: The *C. cinerea* genome is predicted to encode 14242 proteins according to the JGI MycoCosm (May 2018) (Grigoriev et al., 2014). Thus, the proteins encoded by 142 genes roughly represent 1% of the predicted proteome.

Of these 62 genes, 28 genes are located adjacent to each other or separated by a maximum of two open reading frames and 10 genes represent pairs of paralogous genes that are adjacent to each other (Fig. 1A). Clustering of bacteria-induced genes is exemplified by a 120 kb genomic region containing 48 protein-encoding genes, in which six bacteria-induced genes were found (Fig. 1B). These genes encode an adenylate-forming reductase (Brandenburger et al., 2016), a ferredoxin reductase, a major facilitator superfamily (MFS) transporter, a lysozyme and two paralogous hypothetical proteins (HPs). Despite their clustering, these genes do not seem to constitute a classical gene cluster where the gene products function in the same (metabolic) pathway. Interestingly, however, we found an induced gene cluster where two bacteria-induced cytochrome P450 encoding genes flank a gene encoding a sesquiterpene synthase. The latter gene is the most highly induced gene in both *E. coli* and *B. subtilis*-exposed mycelium. This classical gene cluster has previously been functionally characterized and the encoded enzymes were proposed to be responsible for the production of the antimicrobial quinone sesquiterpenoid lagopodin (Agger et al., 2009).

Chapter 6

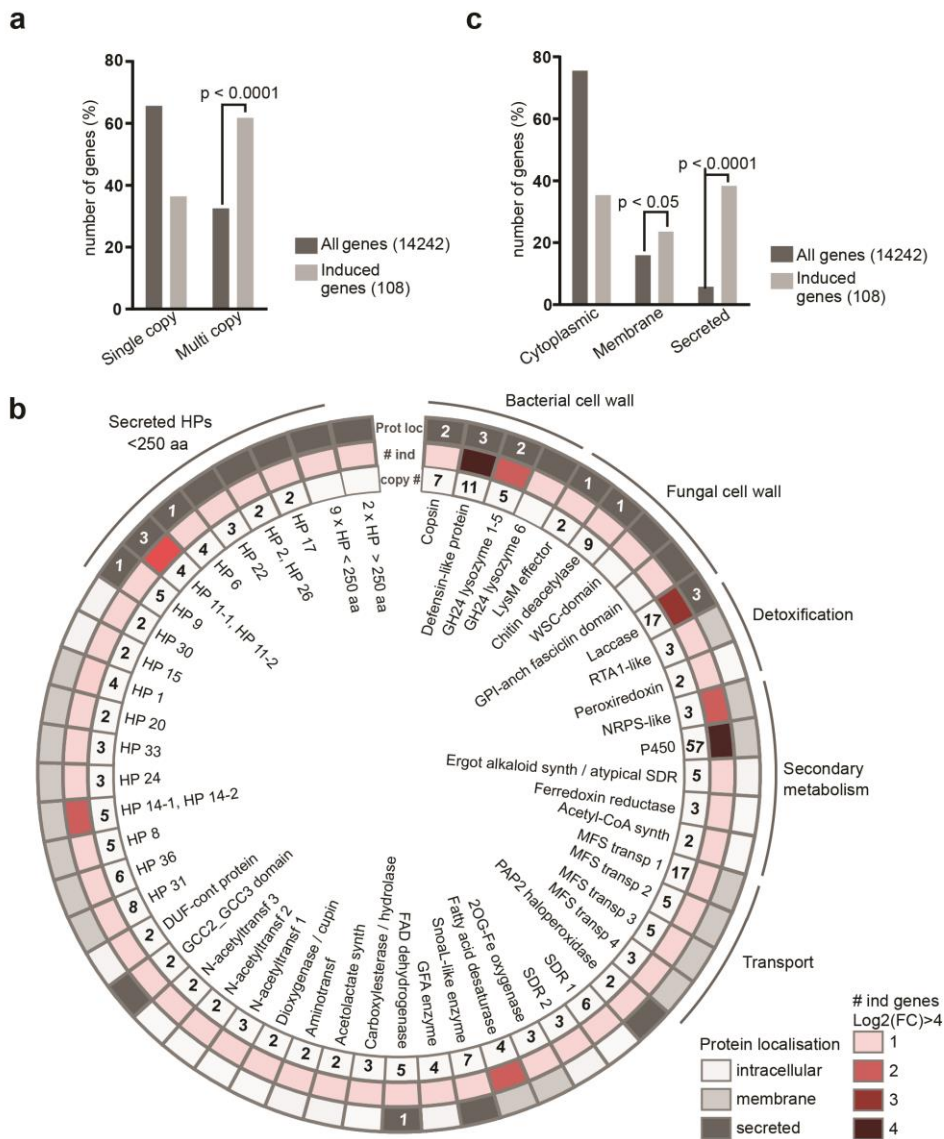


Figure 2 | Overrepresentation of multi-copy genes and genes encoding secreted proteins among bacteria-induced genes. **(a)** Relative numbers of single copy or duplicate genes among all *C. cinerea* genes or the bacteria-induced genes with a $\log_2 \text{FC} \geq 4$. **(b)** Representation of bacteria-induced genes being part of a multi-gene family and/or encoding predicted secreted proteins. Protein annotation is based on the identification of conserved domains (CD search NCBI) and putative functions related to bacterial-fungal interaction were assigned. The same annotation may occur multiple times in case multiple induced genes encode proteins with the same conserved domain but categorize in different gene families due to low overall similarity, e.g. GH24-type lysozyme 1-5 and 6. For bacteria-induced multi-copy genes, the total number of genes in the gene family is indicated in the inner circle (copy #). The colors in the second circle indicate how many genes of this family are bacteria-induced with a $\log_2 \text{FC} \geq 4$ (# ind). The predicted localization (Prot loc) of the encoded proteins is represented in the outer circle. The white numbers indicate the number of secreted proteins of the respective family that were identified in the *E. coli*-induced secretome. **(c)** Relative numbers of all *C. cinerea* proteins and the proteins encoded by bacteria-induced genes ($\log_2 \text{FC} \geq 4$) that are predicted to be cytoplasmic, membrane-bound (TMHMM2.0) or secreted (SignalP4.1). **(a and c)** P-values are calculated by chi-square tests using numerical values. FC stands for fold change, HP for hypothetical protein, MFS for major facilitator superfamily, DUF for domain of unknown function, GFA for glutathione-dependent formaldehyde-activating.

Chapter 6

We noticed that many bacteria-induced *C. cinerea* genes do not only cluster but also have paralogs. Since the *C. cinerea* genome is rich in gene duplications (Stajich et al., 2010), we investigated whether genes belonging to multi-copy gene families would be overrepresented in the bacteria-induced gene set. In an all-versus-all blast search (NCBI) we identified 4731 out of 14242 (33%) *C. cinerea* AmutBmut genes that have one or more duplicates, whereas a significant overrepresentation of 67 out of 108 (62%) of the bacteria-induced genes are part of multi-gene families ($P < 0.0001$) (Fig. 2A and Supplementary Information SI2). In some gene families, multiple members are induced by the presence of bacteria (Fig. 2B). For example, the genome of *C. cinerea* encodes for a gene family of three adenylate-forming reductases that might be involved in secondary metabolite synthesis (Brandenburger et al., 2016), and two of the(se) genes are induced in the presence of bacteria. Other induced genes might encode proteins that contain the same predicted conserved domain, but belong to different families (Fig. 2B) as the family classification is based on overall sequence similarity rather than the presence of a domain. For example, four induced genes encode for proteins that are all predicted to be MFS transporters but they belong to different gene families due to low sequence similarity with each other. MFS transporters may be involved in the export of antibiotics produced by *C. cinerea* or of antifungal compounds produced by bacteria out of the fungal cell (Coleman and Mylonakis, 2009). Taken together, we found that bacteria-induced *C. cinerea* genes are not randomly distributed in the genome and that multi-copy genes are overrepresented.

3.3 *C. cinerea* responds to bacteria by the secretion of proteins with predicted antibacterial activity

Induced *C. cinerea* genes encoding secreted proteins were of particular interest, as these proteins might directly interact with bacteria and possibly possess antibacterial activity (Kunzler, 2015). For this reason, the predicted localization of proteins, encoded by the set of the 108 most highly induced genes, was examined. A comparison with the predicted localization of all *C. cinerea* proteins revealed a significant overrepresentation of secreted proteins in the induced gene set ($P < 0.0001$) (Fig. 2C). Most of the 44 predicted secreted proteins do not contain a conserved domain (CD search, NCBI), and 20 of the proteins are smaller than 250 amino acids. These hypothetical proteins (HPs) resemble the small secreted proteins (SSP) that are produced by pathogenic and symbiotic fungi during host colonization as effectors to modulate the host and often lack homology to other proteins (Lo Presti et al., 2015; Plett et al., 2014). The induced expression of a significant number of genes coding for SSP-like proteins suggests that these proteins play a role as effectors in the interaction of *C. cinerea* with bacteria.

Interestingly, most secreted proteins containing a conserved domain (CD search NCBI) (Fig. 2B), could be assigned a putative function related to fungal or bacterial cell walls. For example, one protein (JGI protein ID, 422563) contains two Lysin motifs (LysM) and resembles LysM effectors of plant-pathogenic fungi which were demonstrated to bind fungal cell wall chitin (Sanchez-Vallet et al., 2015). Related to chitin is also the

Chapter 6

putative function of a chitin deacetylase (JGI protein ID, 440521), likely involved in conversion of chitin to chitosan.

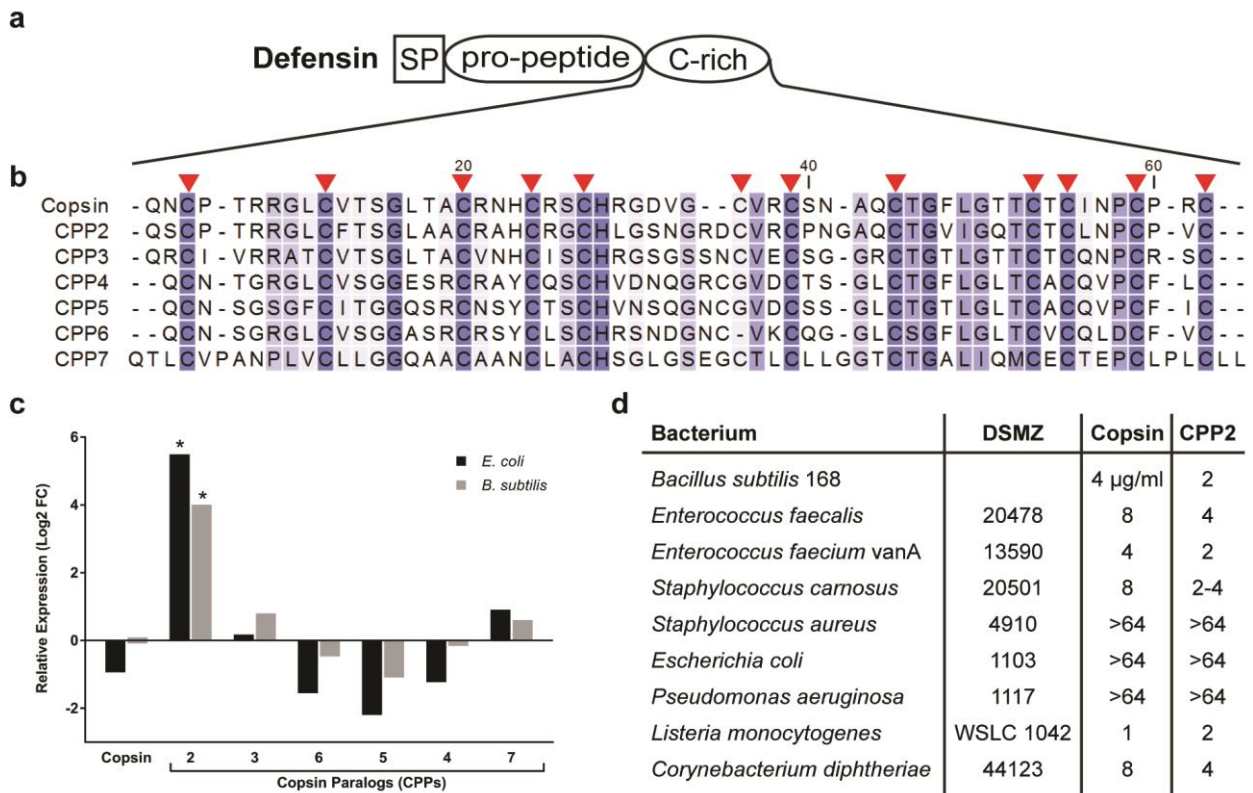


Figure 3 | Overview of Copsin-paralogous peptides (CPPs) encoded in the genome of *C. cinerea*. (a) Premature Copsin (CPP1) and its paralogs (CPP2-6) consist of a signal peptide (SP), a pro-peptide and a mature peptide of 57 to 65 amino acids. (b) The mature peptides show a conserved N-terminal glutamine and a characteristic cysteine pattern of 12 residues, which are indicated with red arrows. The sequences were aligned using the ClustalW algorithm (v2.1). (c) Relative expression of the genes coding for Copsin and its paralogs in the presence of *E. coli* or *B. subtilis* compared to the axenic control. Asterisks indicate $\log_2 FC \geq 2$ and FDR value < 0.005 . DeSeq2 normalized counts were placed in Fig. S3A. (d) Minimal inhibitory concentrations (MICs; µg/ml) of Copsin and its paralog CPP2 for different bacteria. The values were determined using the microdilution broth method (Meskauskas et al., 1999).

Furthermore, three laccase encoding genes (JGI protein IDs, 502564, 208308, 488706) were found to be induced; fungal laccases have been implicated in stress protection through their involvement in melanin synthesis, but also through degradation of antifungal compounds produced by bacteria (Baldrian, 2006) (Fig. 2B). The bacterial cell wall is the likely target of *C. cinerea* proteins containing a glycoside hydrolase 24 (GH24; PFAM 00959; phage lysozyme) domain (see below). Another family of ten genes, five of which are induced by bacteria, encode small secreted proteins with a length of around 100 amino acids with a conserved pattern

Chapter 6

of twelve cysteine residues. The amino acid sequence of these proteins do not indicate a conserved domain, but homology modeling using PHYRE2 (Kelley et al., 2015) predicts a defensin-like fold, consisting of an α -helix and two antiparallel β -strands stabilized by disulfide bonds. Based on previous studies of fungal Cs $\alpha\beta$ -defensins (Essig et al., 2014; Mygind et al., 2005; Zhu, 2008), we hypothesize that these proteins have antibacterial activity via interactions with the bacterial cell wall and designate these *C. cinerea* proteins defensin-like peptides (DLPs). Interestingly, the bacteria-induced gene set also was found to contain a paralog of a gene that encodes for the previously characterized antibacterial Cs $\alpha\beta$ -defensin Copsin (Essig et al., 2014). To verify whether the differential transcription of genes encoding secreted proteins is also reflected on protein level, we investigated the differential (cultivated with and without bacteria) secretome of *C. cinerea* on protein level by comparative proteomics (see Supplementary information for experimental details). To this end, the proteins in the culture supernatant of *C. cinerea* axenic cultures and co-cultures with *E. coli* were analyzed. Based on our analysis, a total of 23 *C. cinerea* proteins were more abundant in the presence of *E. coli* compared to the control ($FC \geq 4$) (Fig. 2B and S2), of which 13 proteins are encoded by genes that are bacteria-induced ($FC \geq 4$) (Supplementary Information SI3). In addition, four more proteins (three DLPs and one chitin deacetylase) that are encoded by family members of bacteria-induced genes, are more abundant by a $FC \geq 2$.

3.4 Bacteria-induced member of the *C. cinerea* Cs $\alpha\beta$ -defensin family has the same antibacterial activity profile as Copsin

To investigate the role of induced secreted proteins as antibacterial defense effectors of *C. cinerea*, bacteria-induced members of the Cs $\alpha\beta$ -defensin and GH24-type lysozyme families were produced in *P. pastoris* and the antibacterial activity of the recombinant peptides and proteins was evaluated.

We previously identified and characterized an antibacterial Cs $\alpha\beta$ -defensin, termed Copsin, produced by *C. cinerea* by activity-based fractionation of the fungal secretome (Essig et al., 2014). Copsin is active against Gram-positive bacteria and targets peptidoglycan biosynthesis via binding to the lipid II precursor (Franzoi et al., 2017). The production of Copsin in vegetative mycelium of *C. cinerea* was found to be constitutive i.e. not modulated by the presence of bacteria (Fig. S3A). In contrast, a Copsin paralog that was highly induced upon exposure to bacteria, was identified. This gene was found to be located adjacent to the Copsin-encoding gene and was termed Copsin-paralogous peptide 2 (*cpp2*). Additional BLAST search revealed that *C. cinerea* encodes for a family of 7 Copsin-paralogous peptides with a predicted Cs $\alpha\beta$ -defensin fold, of which only the gene encoding for CPP2 showed induced expression upon bacterial challenge (Fig. 3A-C; Fig. S3A). Determination of the minimal inhibitory concentrations (MICs) of recombinant CPP2 revealed an antibacterial activity profile that was highly similar to the profile of Copsin (Fig. 3D). These results suggest that *C. cinerea* is able to fortify the constitutive antibacterial activity of Copsin through induced production

Chapter 6

of a Copsin-paralog upon exposure to bacteria. Moreover, this finding demonstrates that the expression pattern of duplicated genes can significantly diversify while the function of the encoded proteins is preserved.

3.5 Bacteria-induced members of the *C. cinerea* GH24-type lysozyme family lyse bacterial cells

The genome of *C. cinerea* encodes for six paralogs of GH24-type lysozymes (Fig. 4, S3 and S4). The archetype of this type of lysozyme is the T4 lysozyme, also referred to as phage endolysin or lysis (Weaver and Matthews, 1987; Young, 1992). It hydrolyzes the β -1,4 glycosidic bond of peptidoglycan (PGN) in the bacterial cell wall for the release of the T4 phages (Kuroki et al., 1993). The expression of three *C. cinerea* GH24-type lysozyme-encoding genes, termed *lys1-3*, was found to be highly induced in the presence of bacteria (Fig. 4C). In agreement with this finding, LYS1 and LYS2 were also found in the *E. coli*-induced secreted proteome (Supplementary Information SI3).

Alignment of the sequences of all six *C. cinerea* GH24-type lysozymes revealed that five proteins contain a conserved cysteine-rich N-terminal domain, while the N-terminus of LYS6 is different and contains repetitive sequences (Fig. S4). Intriguingly, the amino acid sequence of this N-terminal domain, in particular the pattern of the twelve conserved Cys-residues, is homologous to the amino acid sequence of the DLPs described above and most likely adopts a defensin-like fold which is stabilized by up to six disulfide bridges (Fig. 4a and Fig. S3B). Thus, the *C. cinerea* genome encodes five GH24-type lysozymes (Table S1, LYS1-5) and ten DLPs (Table S1, DLP1-10) which share a defensin-like domain. These gene families have most likely arisen via gene fusion, multiplication and diversification. The bacteria-induced expression of several members of these gene families suggests a role of the encoded proteins and peptides in the interaction with bacteria.

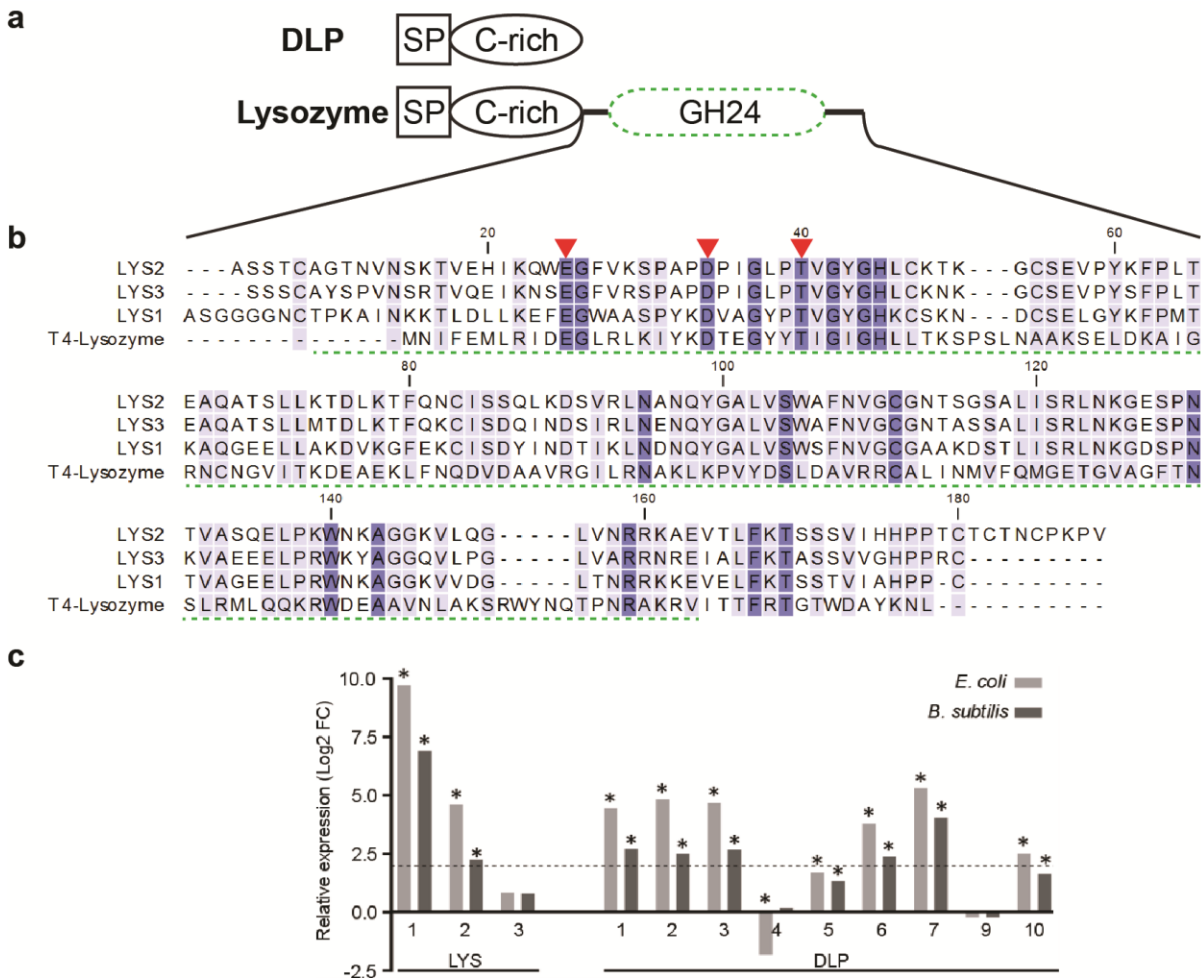


Figure 4 | *C. cinerea* encodes a family of GH24-type lysozymes (LYS) and defensin-like peptides (DLPs). (a) DLPs are composed of a signal peptide (SP) and a domain enriched with 12 cysteine residues as found in cypsin and paralogs (Fig. 3 and Fig. S3B). This cysteine-rich domain was also identified in secreted lysozymes, which is then attached over a linker-peptide to a C-terminal glycosyl hydrolase (GH24) domain (Fig. S3B and Fig. S4). (b) A sequence alignment of the lysozyme domain of LYS1-3 revealed conserved catalytic residues (red arrows) characteristic for the GH24-type lysozyme family with T4 lysozyme (PDB: 2LZM) as a founding member (Kuroki et al., 1993; Wohlkonig et al., 2010). The alignment was performed using the ClustalW algorithm (v2.1). The GH24 domain was assigned by the BlastP algorithm according to the LYS2 sequence and is marked with a green dashed line. (c) Relative expression of LYS- and DLP-encoding genes in the presence of *E. coli* or *B. subtilis* compared to the expression in the axenic control as determined by RNA sequencing. The dashed line and asterisks indicate the cut off of $\log_2 \text{FC} \geq 2$ and FDR value of < 0.005 , respectively. DeSeq2 normalized counts were placed in Figure S3C. *lys4*, *lys5* and *dlp8* are not included in the histograms due to their low level of expression (<10 reads/locus).

Chapter 6

In order to test the activity of defensin-like domain-containing lysozymes against bacteria, LYS1, LYS2 and LYS3 were produced in *P. pastoris*, purified (Fig. S5A) and tested for their ability to lyse bacterial cells. Analogous attempts to heterologously produce DLPs or isolated defensin-like domains of the identified fungal lysozymes were not successful. For the lysis assays, stationary bacterial cells were suspended in phosphate buffer in a 96-well microtiter plate and incubated with the recombinant lysozymes. Hen egg white lysozyme (HEWL) was used as positive and bovine serum albumin (BSA) as negative control. Optical density at 450 nm of the suspensions was measured over 60 to 120 min.

In case of *B. subtilis*, the three tested *C. cinerea* lysozymes showed lysis kinetics very similar to HEWL, with a rapid decrease in optical density between 10 and 20 min (Fig. 5A). In the assays with *M. luteus* (*lysodeikticus*), which is known for its susceptibility to lysozyme activity (Selsted and Martinez, 1980), LYS1 showed significantly reduced cell lysis activity compared to LYS2 and LYS3 (Fig. 5D). We further investigated this difference by incubating fluorescently labelled *M. luteus* cell wall preparations (EnzCheck, Thermo Scientific) with a concentration series of the lysozymes and subsequent measuring of released fluorescence due to cleavage of *M. luteus* PGN. In accordance with the cell-based assay, no fluorescence above background level was detected in this assay upon incubation with LYS1, whereas incubation with LYS2 and LYS3 resulted a concentration-dependent release of fluorescence (Fig. 5G). The inability of LYS1 to cleave *M. luteus* PGN and its drastically reduced *M. luteus* cell lysis activity suggested a significant difference in substrate specificity between this lysozyme and the other two paralogs. To further assess the lysozyme specificity for Gram-positive bacteria, we performed the bacterial cell lysis assays with *Staphylococcus carnosus* and *S. aureus* (Fig. 5C and 5F). In contrast to *S. carnosus*, *S. aureus* is known to O-acetylate its PGN, which contributes to resistance towards PGN cleavage by most lysozymes such as the HEWL-type (Bera et al., 2005). Although less rapidly than observed for *M. luteus* or *B. subtilis*, *S. carnosus* cells lysed in the presence of LYS2 and LYS3, but not in the presence of LYS1. In contrast, incubation with neither of the *C. cinerea* lysozymes resulted in *S. aureus* cell lysis. Taken together, these results demonstrate that *C. cinerea* lysozymes have the ability to lyse bacterial cells and that this activity is likely based on different modes of action on different bacterial species. The contribution of the defensin-like domain and the predicted active site residues to the bacterial cell lysis activity of the *C. cinerea* lysozymes was assessed by producing variants of LYS2. Full-length LYS2 (LYS2His), truncated LYS2 containing only the lysozyme domain (LYS2His Δ N) and a presumptive LYS2 catalytic mutant (D131A) (Fig. S5) were produced with a C-terminal His6-tag in *P. pastoris* and purified using metal chelate chromatography. LYS2His Δ N lysed *B. subtilis* and *M. luteus* cells as efficiently as full length LYS2His (Fig. 5B and 5E). In contrast, the LYS2(D131A)His mutant did not cause lysis of *B. subtilis* or *M. luteus* (Fig. 5B and 5E). In agreement with these results, LYS2His and LYS2His Δ N cleaved *M. luteus* PGN in the EnzChek lysozyme assay, whereas the LYS2(D131A)His mutant did not (Fig 5G). In conclusion, the results indicate that the N-terminal DLP domain of the lysozyme does not contribute to bacterial lysis and peptidoglycan hydrolysis activity of LYS2 whereas the predicted active site residue D131 was critical for these activities.

Chapter 6

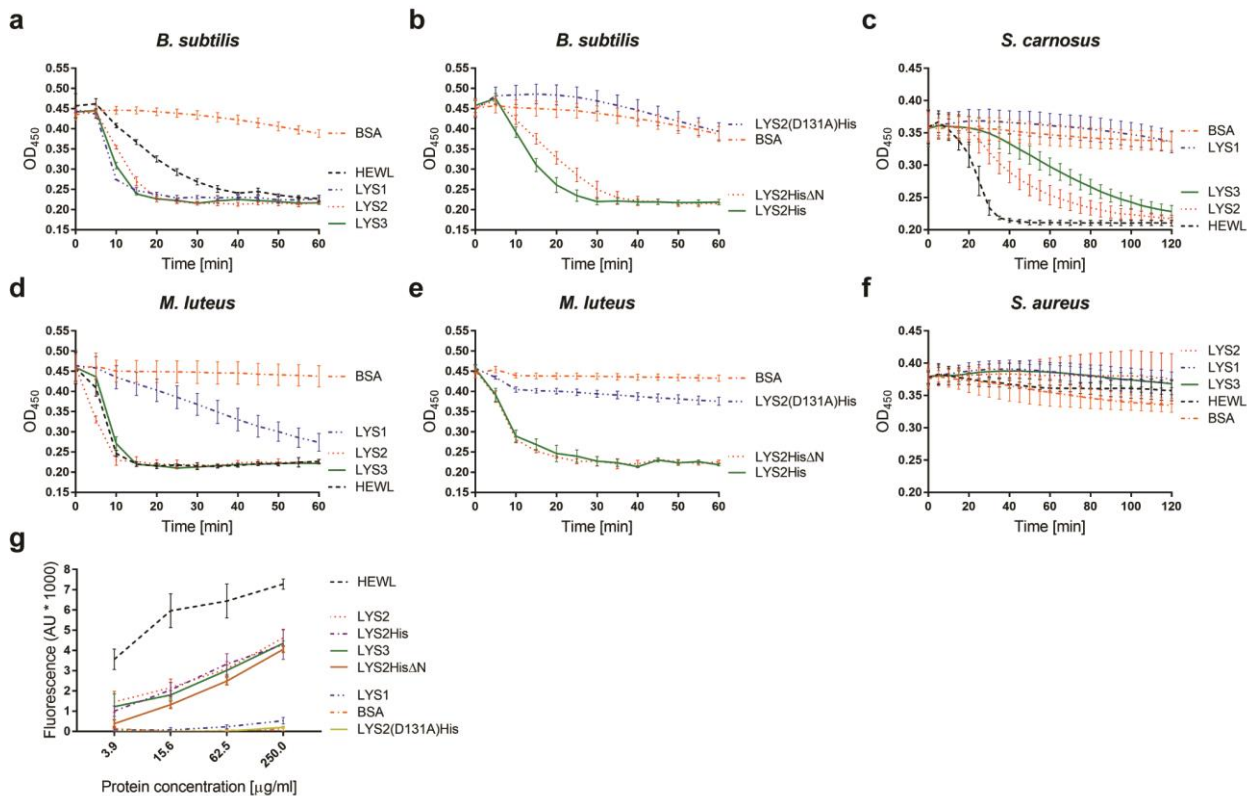


Figure 5 | Activity of *C. cinerea* GH24-type lysozymes on Gram-positive bacteria. (a-f) Bacterial cell lysis activity was determined in a microtiter plate turbidity assay for *B. subtilis*, *M. luteus*, *S. carnosus* and *S. aureus*. Cells were treated with the following proteins at a concentration of 20 $\mu\text{g/ml}$: Untagged recombinant lysozymes (LYS1-3), His6-tagged LYS2 (LYS2His), His6-tagged lysozyme domain of LYS2 (LYS2His Δ N), His6-tagged catalytic mutant LYS2 (LYS2(D131A)His), hen egg white lysozyme (HEWL) as positive and bovine serum albumin (BSA) as negative control. The bacterial suspensions were incubated at 37 °C and data points were acquired at an optical density of 450 nm in 5 min time intervals. The average of three biological replicates is shown together with the standard deviation. (g) Lysozyme activity was determined using the EnzChek Lysozyme assay kit (Thermo Scientific). 4-fold dilution series of the proteins listed above were incubated with *M. luteus* fluorescein-labelled cell wall. The release of fluorescein due to hydrolysis of cell wall was measured after 30 min of incubation at 37 °C with excitation and emission wavelengths of 485 nm and 535 nm, respectively. Each data point represents the average of three replicates. Error bars indicate standard deviation.

Discussion

The defense mechanisms employed by fungi to cope with competing or antagonistic bacteria are poorly understood. While fungi are notorious producers of antibacterial compounds, it is not clear whether these compounds can be produced as part of a specific defense response against bacteria. In the present study, results of transcriptome and secretome analyses demonstrate that bacteria induce an antibacterial response in the fungus *C. cinerea*. This response predominantly relies on secreted proteins, of which many are predicted or shown to have antibacterial activity. The majority of the secreted proteins found in the induced secretome or encoded by bacteria-induced genes are smaller than 250 amino acids and lack annotated domains, which complicates functional predictions. These characteristics are reminiscent of effector proteins that are produced by fungal pathogens and endophytes as well as mycorrhizal fungi during plant colonization to establish fungal growth in the host (Jones and Dangl, 2006; Rovenich et al., 2014; Zeilinger et al., 2016). An overrepresentation of genes encoding small secreted proteins (SSPs) was also found among *P. anserina* genes that were induced upon exposure to two bacterial *Serratia* species, one of which kills the fungus (Lamacchia et al., 2016). Therefore, it appears that the secretion of SSPs plays a significant role in the interaction of fungi with plants and bacteria, including mutualistic, pathogenic or competitive interactions. In previous interaction studies, the confrontation between fungi and bacteria was mostly done on agar plates, often without physical contact of the organisms (Deveau et al. 2014; Gkarmiri et al. 2015; Lamacchia et al. 2016). In this study we used a semi-liquid setup, in which we cultivated *C. cinerea* on submerged glass beads (Essig et al. 2014; Droce et al. 2013). This setup allowed motile bacteria, when added to the liquid phase, to interact with the mycelium in a dynamic and intimate manner. Moreover, this experimental system allowed us to analyze the gene expression of *C. cinerea* in response to bacteria on both transcriptome and secreted proteome level as secreted proteins could be easily retrieved from the liquid phase. These analyses revealed a relatively large number of genes with a high level of induction under these conditions.

Many of the bacteria-induced genes in the genome of *C. cinerea* are clustered. On the one hand, this is explained by tandem gene duplications. Gene duplication resulting in expansion of (effector) gene families has been described for fungal pathogens and may facilitate evolution of new protein functions due to functional redundancy (Duplessis et al., 2011; Powell et al., 2008). One prominent example is the bacteria-induced gene *cpp2* which is localized next to the paralogous gene *cpp1* coding for the previously described antibacterial C $\alpha\beta$ -defensin Copsin (Essig et al., 2014). On the other hand, clustering of non-homologous but functionally related genes is known from secondary metabolite biosynthesis in fungi (Martin and Liras, 2016). It is hypothesized that clustering minimizes meiotic recombination between and/or facilitates coregulation of these genes (Batada et al., 2007; Hurst et al., 2004). The above mentioned example of the *cpp2* and *cpp1* gene tandem, however, shows that duplicated genes can differ considerably in their expression pattern since *cpp1* is expressed constitutively under the applied conditions. Since CPP2 and Copsin are functionally redundant regarding their antibacterial activity, this special regulation pattern implies a mechanism where a

Chapter 6

Cs $\alpha\beta$ -defensin-mediated, constitutive defense of *C. cinerea* against bacteria is fortified in response to bacterial challenge. Genes coding for Cs $\alpha\beta$ defensins (of different classes) have recently been identified in a wide range of fungal genomes and, based on characterized antibacterial activities thus far, might be part of a general defense of fungi against bacteria (Mygind et al., 2005; Oeemig et al., 2012; Wu et al., 2018; Wu et al., 2017; Zhu, 2008). Accordingly, structural modelling predicts additional defensin-like proteins among our set of bacteria-induced, non-annotated *C. cinerea* proteins. These predictions are currently tested by heterologous expression of these proteins and analysis of their structure and function.

Bacteria-induced genes in *C. cinerea* also tend to belong to expanded gene families. This phenomenon is exemplified by the identification of a family of Copsin paralogs in *C. cinerea* (Fig. 3). Other examples are two families of *C. cinerea* proteins containing a defensin-like domain, either as single domain in defensin-like proteins (DLPs) or N-terminal of a GH24-type lysozyme domain. Both DLPs and GH24-type lysozymes are encoded by expanded gene families of ten and five genes, respectively. Detailed analysis of the expression and the function of individual family members suggests that these proteins play a significant role in the interaction with bacteria. Lysozymes with a GH24 domain belong to the phage lysozyme family and supposedly have muramidase activity, i.e. hydrolysis of the glycosidic bond between GlcNAc and MurNAc (Schmelcher et al., 2012). Despite the predicted muramidase activity, heterologously produced *C. cinerea* LYS1 was, in contrast to LYS2 and LYS3, not able to hydrolyse fluorescently labelled *M. luteus* cell wall material (Fig. 5G). In agreement with this observation, LYS1 was also less efficient in lysing *M. luteus* (Fig. 5D) and failed to lyse *S. carnosus* cells (Fig. 5C). These differences in activity suggests that *C. cinerea* lysozymes have functionally diverged. The activity of LYS2 appears to be dependent on its enzymatic function as mutation of the predicted active site residue (D131A) abolishes all activities (Fig. 5B, E and G). In addition, the cell lysis activity of the three *C. cinerea* lysozymes appears to be dependent on the acetylation of PGN since *S. aureus* cells could not be lysed by any of the analysed recombinant proteins (Fig. 5F). The function of the defensin-like domain of the lysozymes remains unclear as deletion of this domain did not have a significant effect on the activity of LYS2 in the cell lysis or cell wall material hydrolysis assays (Fig. 5B, E and G). Although we could not assess the antibacterial activity of the DLPs, the identification of four *dlp*s in bacteria-induced transcriptome and three DLPs in the *E. coli*-induced secretome strongly suggests that these proteins play a significant role in the interaction of *C. cinerea* with bacteria. To our knowledge, there is no precedence for such a dual appearance of a defensin-like domain in any organism. Conversely, although the distribution of proteins that consist of a defensin-like domain fused to a lysozyme domain is restricted to a few fungal species, the occurrence of the GH24-type lysozyme domain is widespread in the fungal kingdom. Therefore, it is hypothesized that, in other fungal species, proteins with similar (catalytic) functions as the characterized *C. cinerea* LYS proteins, but with a different domain organization, play a similar role in antibacterial defense. The overlap between the induced *C. cinerea* genes upon challenge with either Gram negative *E. coli* or Gram positive *B. subtilis* was particularly evident among the most highly induced genes. Overlapping responses of

Chapter 6

the fungal plant pathogenic basidiomycete *Rhizoctonia solani* as well as of the coprophilous ascomycete *Podospora anserina* to bacterial *Serratia* species of different levels of antagonism, were reported recently (Gkarmiri et al., 2015; Lamacchia et al., 2016). These results suggest that fungi do not differentiate between different bacteria and mount a rather general defense response that leads to the secretion of an arsenal of molecules affecting the growth of different types of bacteria e.g. by targeting conserved bacterial structures. Accordingly, two of the characterized defense effectors, Cs $\alpha\beta$ -defensins and GH24-type lysozymes fused to a defensin-like domain, affect peptidoglycan, a conserved constituent of the bacterial cell wall. The induction of genes with putative antifungal functions (LysM, chitinase, chitin deacetylase) in this study may indicate though that the fungus cannot differentiate between bacteria and fungi. Despite the apparent lack of specificity of the fungal defense response with regard to different types of microbial competitors, the lack of significant overlap between the transcriptional response of *C. cinerea* to fungivorous nematodes and to bacterial competitors on agar plates (Plaza et al., 2015) suggests that this fungus is able to discriminate between these two types of antagonists and to induce an antagonist-specific transcriptional response. It is currently not clear, however, how widespread this capability is in the fungal kingdom. Also the physiological significance of the antibacterial response of the fungus upon bacterial challenge is not clear since the fungus could use the secreted antibacterial proteins either as defense molecules to protect itself from damage or as predatory molecules to gain additional nutrients.

The molecular basis of the antagonist-specific responses of the fungus is currently unknown. Future experiments will address the questions whether the antibacterial response of *C. cinerea* is elicited by a single or multiple signals, whether the signal(s) is(are) of bacterial or fungal (produced by bacterial enzymes) origin, whether the signal(s) is (are) on the surface of the microbial cells or shed into the culture supernatant and, finally, whether Gram-positive and Gram-negative bacteria are recognized via the same signal(s) and respective fungal receptor(s) or whether specific recognition pathways exist that lead to activation of the same response. Candidate microbe-associated molecular patterns (MAMPs) that are common between the two types of bacteria, are peptidoglycan fragments (muropeptides). These compounds have been shown to be steadily shed into the medium during bacterial growth and to elicit responses in bacteria, animals and plants and even fungi via cell surface or intracellular receptors (Bertsche et al., 2015; Xu et al., 2008). Comparative genomics suggests that fungi lack cell surface Toll-Like Receptors (TLRs) and rely entirely on intracellular Nucleotide oligomerization domain-Like Receptors (NLRs) for defense (Uehling et al., 2017). The experimental evidence for this hypothesis, however, is rather weak so far and it remains to be seen whether the antibacterial response of *C. cinerea* is mediated via such receptors. Elucidation of these molecular details will help to advance the general knowledge about the innate defense system of fungi which lags far behind the one of plants and animals.

Chapter 6

Acknowledgements

We would like to thank the Functional Genomics Center Zürich, in particular Dr. Weihong Qi, for technical support. We are grateful to Dr. Andrea Sánchez-Vallet for proofreading and discussions and to Dr. Jerome Collemare for technical assistance and proofreading. This work was supported by ETH Zürich (ETH Zürich Postdoctoral Fellowship to A.K. and Grant ETH-45 16-1) and the Swiss National Science Foundation (Grant 31003A_149512).

Chapter 6

References

- Adnani, N., Rajski, S.R., and Bugni, T.S.** (2017). Symbiosis-inspired approaches to antibiotic discovery. *Nat Prod Rep* 34, 784-814.
- Agger, S., Lopez-Gallego, F., and Schmidt-Dannert, C.** (2009). Diversity of sesquiterpene synthases in the basidiomycete *Coprinus cinereus*. *Mol Microbiol* 72, 1181-1195.
- Ashburner, M., Ball, C.A., Blake, J.A., Botstein, D., Butler, H., Cherry, J.M., et al.** (2000). Gene ontology: tool for the unification of biology. The Gene Ontology Consortium. *Nat Genet* 25, 25-29.
- Baldrian, P.** (2006). Fungal laccases - occurrence and properties. *FEMS Microbiol Rev* 30, 215-242.
- Batada, N.N., Urrutia, A.O., and Hurst, L.D.** (2007). Chromatin remodelling is a major source of coexpression of linked genes in yeast. *Trends Genet* 23, 480-484.
- Benoit, I., van den Esker, M.H., Patyshakulyeva, A., Mattern, D.J., Blei, F., Zhou, M., et al.** (2015). *Bacillus subtilis* attachment to *Aspergillus niger* hyphae results in mutually altered metabolism. *Environ Microbiol* 17, 2099-2113.
- Bera, A., Herbert, S., Jakob, A., Vollmer, W., and Gotz, F.** (2005). Why are pathogenic staphylococci so lysozyme resistant? The peptidoglycan O-acetyltransferase OatA is the major determinant for lysozyme resistance of *Staphylococcus aureus*. *Mol Microbiol* 55, 778-787.
- Bertsche, U., Mayer, C., Gotz, F., and Gust, A.A.** (2015). Peptidoglycan perception-Sensing bacteria by their common envelope structure. *Int J Med Microbiol* 305, 217-223.
- Bleuler-Martinez, S., Buttschi, A., Garbani, M., Walti, M.A., Wohlschlager, T., Potthoff, E., et al.** (2011). A lectin-mediated resistance of higher fungi against predators and parasites. *Mol Ecol* 20, 3056-3070.
- Boer, W., Folman, L.B., Summerbell, R.C., and Boddy, L.** (2005). Living in a fungal world: impact of fungi on soil bacterial niche development. *FEMS Microbiol Rev* 29, 795-811.
- Branda, S.S., Gonzalez-Pastor, J.E., Ben-Yehuda, S., Losick, R., and Kolter, R.** (2001). Fruiting body formation by *Bacillus subtilis*. *P Natl Acad Sci USA* 98, 11621-11626.
- Brandenburger, E., Braga, D., Kombrink, A., Lackner, G., Gressler, J., Kunzler, M., et al.** (2016). Multi-genome analysis identifies functional and phylogenetic diversity of basidiomycete adenylate-forming reductases. *Fungal Genet Biol*.
- Choi, H.W., and Klessig, D.F.** (2016). DAMPs, MAMPs, and NAMPs in plant innate immunity. *BMC Plant Biol* 16, 232.
- Coleman, J.J., and Mylonakis, E.** (2009). Efflux in fungi: la piece de resistance. *PLoS Pathog* 5, e1000486.
- Deveau, A., Barret, M., Diedhiou, A.G., Leveau, J., de Boer, W., Martin, F., et al.** (2015). Pairwise transcriptomic analysis of the interactions between the ectomycorrhizal fungus *Laccaria bicolor* S238N and three beneficial, neutral and antagonistic soil bacteria. *Microb Ecol* 69, 146-159.
- Deveau, A., Bonito, G., Uehling, J., Paoletti, M., Becker, M., Bindschedler, S., et al.** (2018). Bacterial-fungal interactions: ecology, mechanisms and challenges. *FEMS Microbiol Rev* 42, 335-352.
- Dobin, A., Davis, C.A., Schlesinger, F., Drenkow, J., Zaleski, C., Jha, S., et al.** (2013). STAR: ultrafast universal RNA-seq aligner. *Bioinformatics* 29, 15-21.
- Doll, K., Chatterjee, S., Scheu, S., Karlovsky, P., and Rohlf, M.** (2013). Fungal metabolic plasticity and sexual development mediate induced resistance to arthropod fungivory. *Proc Biol Sci* 280, 20131219.
- Droce, A., Sorensen, J.L., Giese, H., and Sondergaard, T.E.** (2013). Glass bead cultivation of fungi: combining the best of liquid and agar media. *J Microbiol Methods* 94, 343-346.
- Duplessis, S., Cuomo, C.A., Lin, Y.C., Aerts, A., Tisserant, E., Veneault-Fourrey, C., et al.** (2011). Obligate biotrophy features unraveled by the genomic analysis of rust fungi. *Proc Natl Acad Sci U S A* 108, 9166-9171.

Chapter 6

- Essig, A., Hofmann, D., Munch, D., Gayathri, S., Kunzler, M., Kallio, P.T., et al.** (2014). Copsin, a novel peptide-based fungal antibiotic interfering with the peptidoglycan synthesis. *J Biol Chem* 289, 34953-34964.
- Franzoi, M., van Heuvel, Y., Thomann, S., Schurch, N., Kallio, P.T., Venier, P., et al.** (2017). Structural Insights into the Mode of Action of the Peptide Antibiotic Copsin. *Biochemistry* 56, 4992-5001.
- Frey-Klett, P., Burlinson, P., Deveau, A., Barret, M., Tarkka, M., and Sarniguet, A.** (2011). Bacterial-fungal interactions: hyphens between agricultural, clinical, environmental, and food microbiologists. *Microbiol Mol Biol Rev* 75, 583-609.
- Gkarmiri, K., Finlay, R.D., Alstrom, S., Thomas, E., Cubeta, M.A., and Hogberg, N.** (2015). Transcriptomic changes in the plant pathogenic fungus *Rhizoctonia solani* AG-3 in response to the antagonistic bacteria *Serratia proteamaculans* and *Serratia plymuthica*. *BMC genomics* 16, 630.
- Grigoriev, I.V., Nikitin, R., Haridas, S., Kuo, A., Ohm, R., Otiillar, R., et al.** (2014). MycoCosm portal: gearing up for 1000 fungal genomes. *Nucleic Acids Res* 42, D699-704.
- Hatakeyama, M., Opitz, L., Russo, G., Qi, W., Schlapbach, R., and Rehrauer, H.** (2016). SUSHI: an exquisite recipe for fully documented, reproducible and reusable NGS data analysis. *BMC Bioinformatics* 17, 228.
- Hoffmeister, D., and Keller, N.P.** (2007). Natural products of filamentous fungi: enzymes, genes, and their regulation. *Nat Prod Rep* 24, 393-416.
- Hurst, L.D., Pal, C., and Lercher, M.J.** (2004). The evolutionary dynamics of eukaryotic gene order. *Nat Rev Genet* 5, 299-310.
- Ipcho, S., Sundelin, T., Erbs, G., Kistler, H.C., Newman, M.A., and Olsson, S.** (2016). Fungal Innate Immunity Induced by Bacterial Microbe-Associated Molecular Patterns (MAMPs). *G3 (Bethesda)* 6, 1585-1595.
- Jones, J.D., and Dangl, J.L.** (2006). The plant immune system. *Nature* 444, 323-329.
- Kelley, L.A., Mezulis, S., Yates, C.M., Wass, M.N., and Sternberg, M.J.** (2015). The Phyre2 web portal for protein modeling, prediction and analysis. *Nat Protoc* 10, 845-858.
- Kempken, F., and Rohlf, M.** (2010). Fungal secondary metabolite biosynthesis - a chemical defence strategy against antagonistic animals? *Fungal Ecology* 3, 107-114.
- Krogh, A., Larsson, B., von Heijne, G., and Sonnhammer, E.L.** (2001). Predicting transmembrane protein topology with a hidden Markov model: application to complete genomes. *J Mol Biol* 305, 567-580.
- Kunst, F. et al.** (1997). The complete genome sequence of the gram-positive bacterium *Bacillus subtilis*. *Nature* 390, 249– 256.
- Kunzler, M.** (2015). Hitting the sweet spot-glycans as targets of fungal defense effector proteins. *Molecules* 20, 8144-8167.
- Kuroki, R., Weaver, L.H., and Matthews, B.W.** (1993). A covalent enzyme-substrate intermediate with saccharide distortion in a mutant T4 lysozyme. *Science* 262, 2030-2033.
- Lamacchia, M., Dyrka, W., Breton, A., Saupe, S.J., and Paoletti, M.** (2016). Overlapping *Podospora anserina* Transcriptional Responses to Bacterial and Fungal Non Self Indicate a Multilayered Innate Immune Response. *Front Microbiol* 7, 471.
- Liao, Y., Smyth, G.K., and Shi, W.** (2014). featureCounts: an efficient general purpose program for assigning sequence reads to genomic features. *Bioinformatics* 30, 923-930.
- Lo Presti, L., Lanver, D., Schweizer, G., Tanaka, S., Liang, L., Tollot, M., et al.** (2015). Fungal effectors and plant susceptibility. *Annu Rev Plant Biol* 66, 513-545.
- Love, M.I., Huber, W., and Anders, S.** (2014). Moderated estimation of fold change and dispersion for RNA-seq data with DESeq2. *Genome Biol* 15, 550.
- Macheleidt, J., Mattern, D.J., Fischer, J., Netzker, T., Weber, J., Schroeckh, V., et al.** (2016). Regulation and Role of Fungal Secondary Metabolites. *Annu Rev Genet* 50, 371-392.
- Marchler-Bauer, A., Derbyshire, M.K., Gonzales, N.R., Lu, S., Chitsaz, F., Geer, L.Y., et al.** (2015). CDD: NCBI's conserved domain database. *Nucleic Acids Res* 43, D222-226.

Chapter 6

- Martin, J.F., and Liras, P.** (2016). Evolutionary formation of gene clusters by reorganization: the meleagrin/roquefortine paradigm in different fungi. *Applied microbiology and biotechnology* *100*, 1579-1587.
- Mathioni, S.M., Patel, N., Riddick, B., Sweigard, J.A., Czymmek, K.J., Caplan, J.L., et al.** (2013). Transcriptomics of the rice blast fungus Magnaporthe oryzae in response to the bacterial antagonist Lysobacter enzymogenes reveals candidate fungal defense response genes. *PLoS One* *8*, e76487.
- Mela, F., Fritsche, K., de Boer, W., van Veen, J.A., de Graaff, L.H., van den Berg, M., et al.** (2011). Dual transcriptional profiling of a bacterial/fungal confrontation: Collimonas fungivorans versus Aspergillus niger. *ISME J* *5*, 1494-1504.
- Meldau, S., Erb, M., and Baldwin, I.T.** (2012). Defence on demand: mechanisms behind optimal defence patterns. *Ann Bot* *110*, 1503-1514.
- Meskauskas, A., Novak Frazer, L., and Moore, D.** (1999). Mathematical modelling of morphogenesis in fungi: a key role for curvature compensation ('autotropism') in the local curvature distribution model. *New Phytol* *143*, 387-399.
- Moller, J., Miller, M., and Kjoller, A.** (1999). Fungal-bacterial interaction on beech leaves: influence on decomposition and dissolved organic carbon quality. *Soil Biol Biochem* *31*, 367-374.
- Muraguchi, H., Umezawa, K., Niikura, M., Yoshida, M., Kozaki, T., Ishii, K., et al.** (2015). Strand-Specific RNA-Seq Analyses of Fruiting Body Development in Coprinopsis cinerea. *PLoS One* *10*, e0141586.
- Mygind, P.H., Fischer, R.L., Schnorr, K.M., Hansen, M.T., Sonksen, C.P., Ludvigsen, S., et al.** (2005). Plectasin is a peptide antibiotic with therapeutic potential from a saprophytic fungus. *Nature* *437*, 975-980.
- Netzker, T., Fischer, J., Weber, J., Mattern, D.J., Konig, C.C., Valiante, V., et al.** (2015). Microbial communication leading to the activation of silent fungal secondary metabolite gene clusters. *Front Microbiol* *6*, 299.
- Oeemig, J.S., Lynggaard, C., Knudsen, D.H., Hansen, F.T., Norgaard, K.D., Schneider, T., et al.** (2012). Eurocin, a New Fungal Defensin: STRUCTURE, LIPID BINDING, AND ITS MODE OF ACTION. *J Biol Chem* *287*, 42361-42372.
- Oh, D.C., Kauffman, C.A., Jensen, P.R., and Fenical, W.** (2007). Induced production of emericellamides A and B from the marine-derived fungus *Emericella* sp. in competing co-culture. *J Nat Prod* *70*, 515-520.
- Ola, A.R., Thomy, D., Lai, D., Brotz-Oesterhelt, H., and Proksch, P.** (2013). Inducing secondary metabolite production by the endophytic fungus *Fusarium tricinctum* through coculture with *Bacillus subtilis*. *J Nat Prod* *76*, 2094-2099.
- Petersen, T.N., Brunak, S., von Heijne, G., and Nielsen, H.** (2011). SignalP 4.0: discriminating signal peptides from transmembrane regions. *Nat Methods* *8*, 785-786.
- Plaza, D.F., Lin, C.W., van der Velden, N.S., Aebi, M., and Kunzler, M.** (2014). Comparative transcriptomics of the model mushroom *Coprinopsis cinerea* reveals tissue-specific armories and a conserved circuitry for sexual development. *BMC Genomics* *15*, 492.
- Plaza, D.F., Schmieder, S.S., Lipzen, A., Lindquist, E., and Kunzler, M.** (2015). Identification of a Novel Nematotoxic Protein by Challenging the Model Mushroom *Coprinopsis cinerea* with a Fungivorous Nematode. *G3 (Bethesda)* *6*, 87-98.
- Plett, J.M., Daguerre, Y., Wittulsky, S., Vayssieres, A., Deveau, A., Melton, S.J., et al.** (2014). Effector MiSSP7 of the mutualistic fungus *Laccaria bicolor* stabilizes the *Populus JAZ6* protein and represses jasmonic acid (JA) responsive genes. *Proc Natl Acad Sci U S A* *111*, 8299-8304.
- Powell, A.J., Conant, G.C., Brown, D.E., Carbone, I., and Dean, R.A.** (2008). Altered patterns of gene duplication and differential gene gain and loss in fungal pathogens. *BMC genomics* *9*, 147.
- Robinson, J.T., Thorvaldsdottir, H., Winckler, W., Guttman, M., Lander, E.S., Getz, G., et al.** (2011). Integrative genomics viewer. *Nat Biotechnol* *29*, 24-26.

Chapter 6

- Rohlf, M., Albert, M., Keller, N.P., and Kempken, F.** (2007). Secondary chemicals protect mould from fungivory. *Biol Lett* 3, 523-525.
- Rousk, J., and Baath, E.** (2011). Growth of saprotrophic fungi and bacteria in soil. *Fems Microbiol Ecol* 78, 17-30.
- Rovenich, H., Boshoven, J.C., and Thomma, B.P.** (2014). Filamentous pathogen effector functions: of pathogens, hosts and microbiomes. *Curr Opin Plant Biol* 20, 96-103.
- Sabotic, J., Ohm, R.A., and Kunzler, M.** (2016). Entomotoxic and nematotoxic lectins and protease inhibitors from fungal fruiting bodies. *Appl Microbiol Biotechnol* 100, 91-111.
- Sanchez-Vallet, A., Mesters, J.R., and Thomma, B.P.** (2015). The battle for chitin recognition in plant-microbe interactions. *FEMS Microbiol Rev* 39, 171-183.
- Schmelcher, M., Waldherr, F., and Loessner, M.J.** (2012). Listeria bacteriophage peptidoglycan hydrolases feature high thermostability and reveal increased activity after divalent metal cation substitution. *Applied microbiology and biotechnology* 93, 633-643.
- Schroeckh, V., Scherlach, K., Nutzmann, H.W., Shelest, E., Schmidt-Heck, W., Schuemann, et al.** (2009). Intimate bacterial-fungal interaction triggers biosynthesis of archetypal polyketides in *Aspergillus nidulans*. *Proc Natl Acad Sci U S A* 106, 14558-14563.
- Selsted, M.E., and Martinez, R.J.** (1980). A simple and ultrasensitive enzymatic assay for the quantitative determination of lysozyme in the picogram range. *Anal Biochem* 109, 67-70.
- Stajich, J.E., Wilke, S.K., Ahren, D., Au, C.H., Birren, B.W., Borodovsky, et al.** (2010). Insights into evolution of multicellular fungi from the assembled chromosomes of the mushroom *Coprinopsis cinerea* (*Coprinus cinereus*). *Proc Natl Acad Sci U S A* 107, 11889-11894.
- Stockli, M., Lin, C.W., Sieber, R., Plaza, D.F., Ohm, R.A., and Kunzler, M.** (2017). *Coprinopsis cinerea* intracellular lactonases hydrolyze quorum sensing molecules of Gram-negative bacteria. *Fungal Genet Biol* 102, 49-62.
- Swamy, S., Uno, I., and Ishikawa, T.** (1984). Morphogenetic Effects of Mutations at the a and B Incompatibility Factors in *Coprinus-Cinereus*. *J Gen Microbiol* 130, 3219-3224.
- Thompson, J.D., Gibson, T.J., and Higgins, D.G.** (2002). Multiple Sequence Alignment Using ClustalW and ClustalX. *Current Protocols in Bioinformatics*; 00(2.3):2.3.1–2.3.22.
- Uehling, J., Deveau, A., and Paoletti, M.** (2017). Do fungi have an innate immune response? An NLR-based comparison to plant and animal immune systems. *PLoS Pathog* 13, e1006578.
- Weaver, L.H., and Matthews, B.W.** (1987). Structure of bacteriophage T4 lysozyme refined at 1.7 Å resolution. *J Mol Biol* 193, 189-199.
- Wiemann, P., and Keller, N.P.** (2014). Strategies for mining fungal natural products. *J Ind Microbiol Biotechnol* 41, 301-313.
- Wohlkonig, A., Huet, J., Looze, Y., and Wintjens, R.** (2010). Structural relationships in the lysozyme superfamily: significant evidence for glycoside hydrolase signature motifs. *PLoS One* 5, e15388.
- Wu, J., Liu, S., and Wang, H.** (2018). Invasive fungi-derived defensins kill drug-resistant bacterial pathogens. *Peptides* 99, 82-91.
- Wu, S., and Letchworth, G.J.** (2004). High efficiency transformation by electroporation of *Pichia pastoris* pretreated with lithium acetate and dithiothreitol. *Biotechniques* 36, 152-154.
- Wu, Y., Gao, B., and Zhu, S.** (2017). New fungal defensin-like peptides provide evidence for fold change of proteins in evolution. *Biosci Rep* 37, BSR20160438
- Xu, X.L., Lee, R.T., Fang, H.M., Wang, Y.M., Li, R., Zou, H., et al.** (2008). Bacterial peptidoglycan triggers *Candida albicans* hyphal growth by directly activating the adenylyl cyclase Cyr1p. *Cell Host Microbe* 4, 28-39.
- Young, R.** (1992). Bacteriophage lysis: mechanism and regulation. *Microbiol Rev* 56, 430-481.

Chapter 6

- Zeilinger, S., Gupta, V.K., Dahms, T.E., Silva, R.N., Singh, H.B., Upadhyay, R.S., et al.** (2016). Friends or foes? Emerging insights from fungal interactions with plants. *FEMS Microbiol Rev* *40*, 182-207.
- Zhu, S.** (2008). Discovery of six families of fungal defensin-like peptides provides insights into origin and evolution of the CSalpha/beta defensins. *Mol Immunol* *45*, 828-838.

Chapter 6

Supplementary Information

Chapter 6

Supplementary Materials and Methods

Differential analysis of the *C. cinerea* secreted proteome

C. cinerea was cultivated as described for the RNA preparation with some modifications: Glass petri dishes with a diameter of 18.5 cm containing 200 g glass beads and 70 ml CCMM were inoculated with eight mycelial plugs and incubated at 28°C in the dark. After 3 days of incubation two plates were inoculated with *E. coli* Nissle 1917 to an OD₆₀₀ of 0.1. Two cultures were left for the control. After 22 h of co-cultivation at 28°C in the dark, the culture broth was extracted, centrifuged (3680 × g, 4°C, 20 min) and filter sterilized (0.22 µm PES filter, TPP) for the samples that contained bacteria. The culture broth was shock frozen in liquid nitrogen and concentrated to 1.5 ml by lyophilization. To precipitate the proteins, 300 µl of 100% trichloroacetic acid was added and the suspension was incubated at 4°C for 20 min. After centrifugation (16000 × g, 4°C, 15 min), the pellet was washed three times with 100% cold acetone (16000 × g, 4°C, 10 min) and dissolved in 75 µl denaturing buffer (8 M urea, 0.1 M ammonium bicarbonate buffer pH 8). The proteins were reduced by adding dithiothreitol (DTT) to 10 mM (37°C, 900 rpm, 30 min) and alkylated by adding iodoacetamide to 30 mM (25°C, 900 rpm, 30 min, in the dark). After addition of 300 µl 0.1 M ammonium bicarbonate buffer, the proteins were digested with 500 ng trypsin (35°C, 900 rpm, 16 h). The reaction was stopped by lowering the pH to 2-3 with formic acid and the peptides were desalted on C18 ZipTip columns (Millipore, MA). The mass spectrometry analyses were performed on a Velos LTQ Orbitrap mass spectrometer (Thermo Scientific) coupled to an Eksigent-nano-HPLC system (Eksigent Technologies). Separation of peptides was done on a self-made column (75 µm x 150 mm) packed with C18 ReproSil-Pur 120 C18-AQ, 1.9 µm (Dr. Maisch GmbH). Peptides were eluted with a linear gradient from 2% to 31% acetonitrile in 53 min at a flow rate of 300 nL/min. Full mass spectrometry data were acquired in the Orbitrap unit in a mass range of with a mass to charge ratio (*m/z*) of 300–1800, with an automatic gain control setting of 1e6, at a resolution of 60,000 at 400 *m/z* and a maximum injection time of 250 ms. CID-MS/MS spectra were acquired in the data dependent mode with up to 20 CID spectra recorded in the linear ion trap. A minimal signal threshold of 1000 was required to trigger the MS/MS acquisition and the automatic gain control value was set at 1e4 with a maximum injection time of 40 ms. All measurements were performed with one microscan. Data was analyzed using Progenesis QI as described in Plaza et al., 2014 with some modifications and normalized to all proteins, where *Cc_Ec2* was used as reference run. Briefly; data were searched against the *C. cinerea* AmutBmut pab1-1 v1.0 predicted proteome hosted at JGI (Copci_AmutBmut1_GeneCatalog_ proteins_20130522) where some protein sequences were corrected based on the transcriptome data (Supplementary Information SI2) using the Mascot search engine v2.4 considering carbamidomethylation on cysteine and oxidation on methionine as modifications and allowing one missed-cleavage. The tolerance of mass accuracy of MS and MS/MS was 5 ppm and 0.6 Da, respectively. The false discovery rate was 1%. Non-unique peptides were assigned to all proteins containing this peptide. The secretome of *C. cinerea* AmutBmut was determined by considering proteins with a predicted signal peptide (SigP v4.1) (Petersen et al., 2011). Proteins identified in the mascot

Chapter 6

search with a signal peptide were included in the further analysis. As a cut off for differentially produced proteins a fold change bigger than 4 was considered. The calculation was based on the total MS1 peak area under the curve (AUC) obtained by summing up all peptide peaks of a protein. CD search (NCBI) (Marchler-Bauer et al., 2015) was used to annotate the proteins. A list of the identified peptides is given in the supplementary dataset (Supplementary Information SI3).

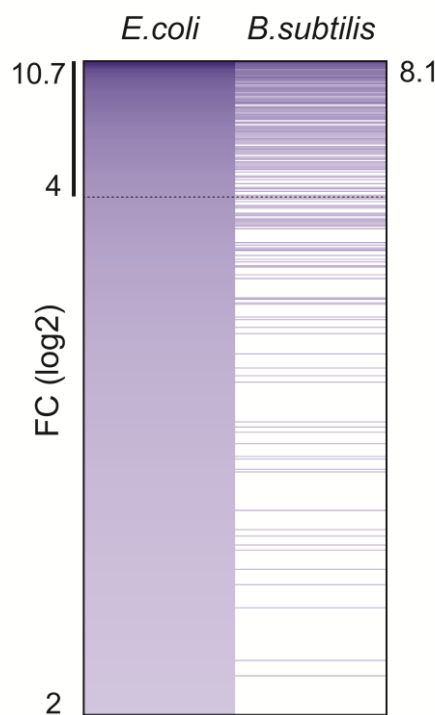


Figure S1 | Representation of *E. coli*-induced *C. cinerea* genes and the overlap with genes induced by the presence of *B. subtilis*. All 510 *E. coli*-induced genes that are expressed with a $\log_2 \text{FC} \geq 2$ ($\text{FDR} < 0.005$) compared to expression in the control samples, are presented as a colored line according to their level of induction. Out of a total of 165 *B. subtilis*-induced genes ($\log_2 \text{FC} \geq 2$ ($\text{FDR} < 0.005$)), 148 overlap with *E. coli*-induced genes and are represented on the panel on the right-hand side colored according to the scale as set for *E. coli*-induced genes. The black line on the left and the dashed line indicate the set of 108 genes that are *E. coli*-induced with a $\log_2 \text{FC} \geq 4$ and which were used for further qualitative analysis. FC stands for fold change. Notion on the dimension of the indicated numbers of (protein-encoding) genes: The *C. cinerea* genome is predicted to encode 14242 proteins according to the JGI mycocosm (May 2018). Thus, the proteins encoded by 142 genes roughly represent 1% of the predicted proteome.

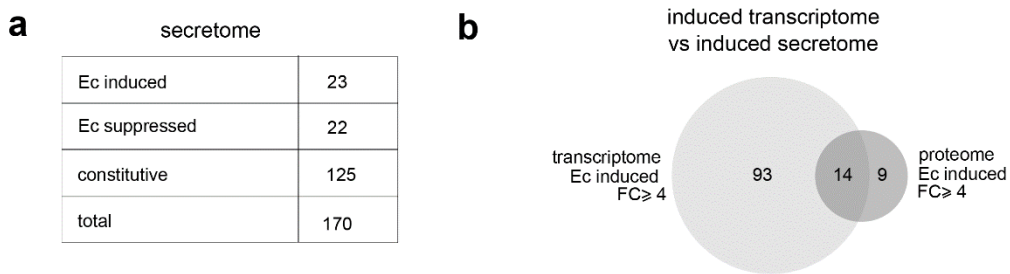


Figure S2 | Comparison between the proteome and the transcriptome of induced secreted proteins. (a) List of the number of secreted proteins that were induced, suppressed or present constitutively. Secreted proteins are defined as annotated proteins containing a predicted signal sequence according to SignalP 4.0. (b) Area-proportional Venn diagram representing the number of induced secreted proteins found on transcriptome and proteome level. FC is fold change. A list of the proteins identified in the secretome is given in the Supplementary Information SI2 and SI3. Notion on the dimension of the indicated numbers of (protein-encoding) genes: The *C. cinerea* genome is predicted to encode 14242 proteins according to the JGI mycocosm (May 2018). Thus, the proteins encoded by 142 genes roughly represent 1% of the predicted proteome.

Chapter 6

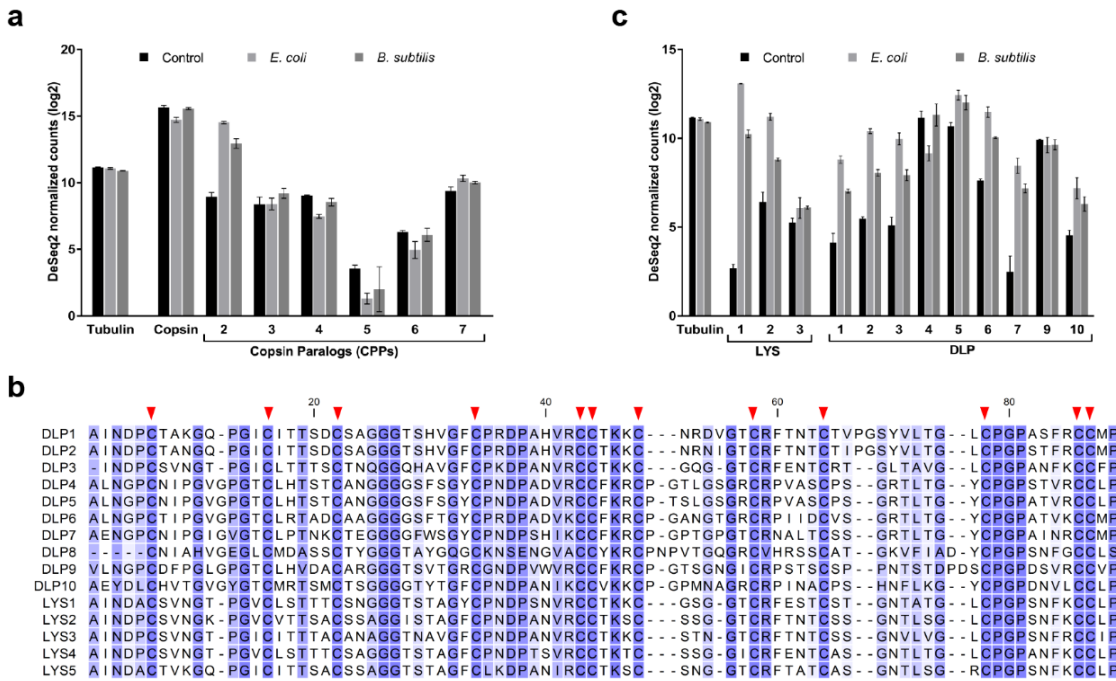


Figure S3 | Normalized transcript levels of copsin paralogous peptides (CPPs), lysozymes (LYS) and defensin-like peptides (DLPs) as determined by RNAseq. (a) DeSeq2-normalized counts of the axenic control and bacterial challenges are shown for copsin (CPP1) and its paralogs CPP2-7 together with the tubulin control. **(b)** Alignment of the cysteine-rich domain of DLP 1-10 and lysozymes 1-5 with their conserved cysteine pattern indicated with red arrows. **(c)** Normalized counts are displayed for LYS 1-3, DLP 1-10 and tubulin.

Chapter 6

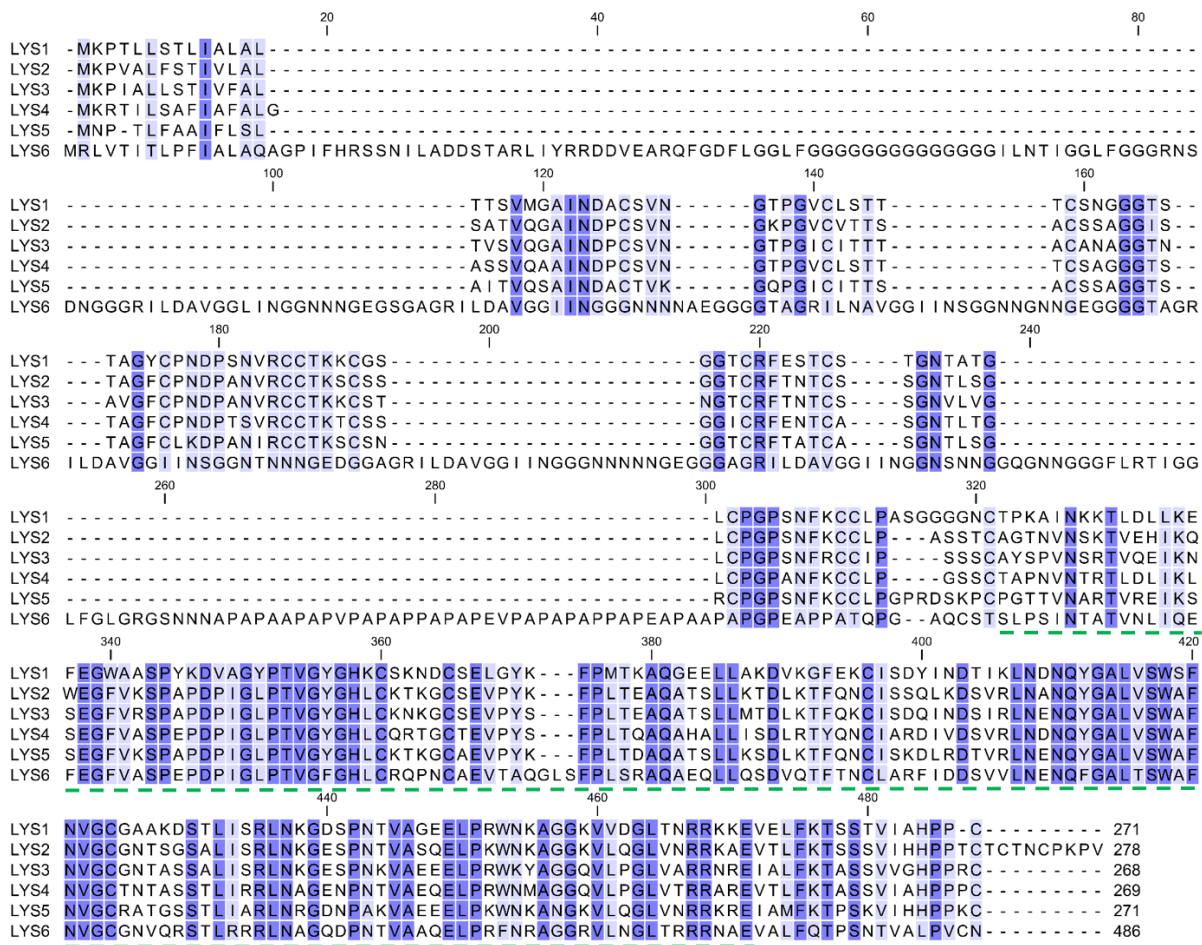


Figure S4 | Alignment of the amino acid sequences of all six *Coprinopsis cinerea* GH24-type lysozymes. The GH24-type lysozyme domain is indicated by a dashed green line below the sequences. LYS1-LYS5 display high overall similarity and share a cysteine-rich N-terminal domain, whereas LYS6 does not contain this domain.

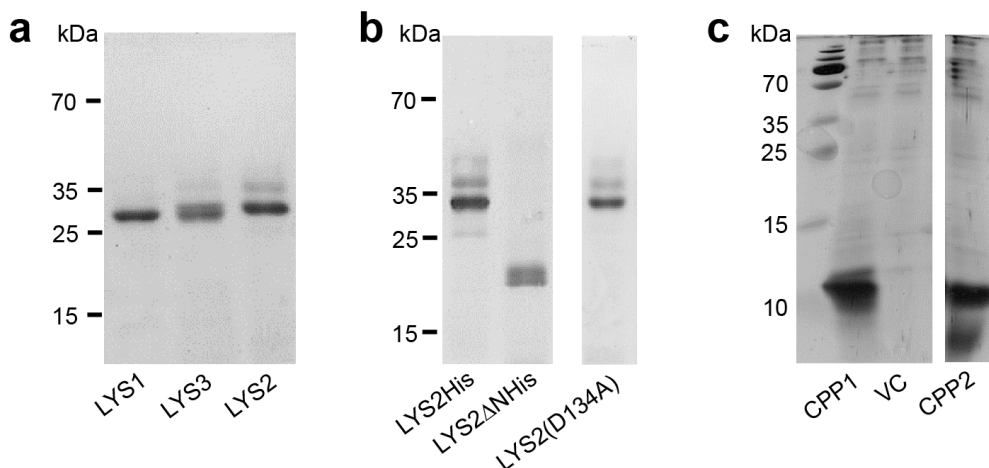


Figure S5 | Heterologous production and purification of *Coprinopsis cinerea* GH24-type lysozymes and Csa β -defensins. (a) Coomassie-stained SDS-PAGE of wild-type untagged LYS1, LYS2 and LYS3 that were produced in *P. pastoris* and purified over Sephadex cation exchange columns. (b) Coomassie-stained SDS-PAGE of His6-tagged LYS2, LYS2 Δ N and LYS2(D134A) that were produced in *P. pastoris* and affinity purified over Ni²⁺-NTA agarose columns. 5 μ g of the different proteins were loaded on the SDS-PAGE. The sizes of the marker proteins are indicated. (c) Silver-stained SDS-PAGE of 5x concentrated supernatants of *P. pastoris* cultures expressing untagged Copsin (CPP1) or CPP2 or containing the respective vector control (VC).

Chapter 6

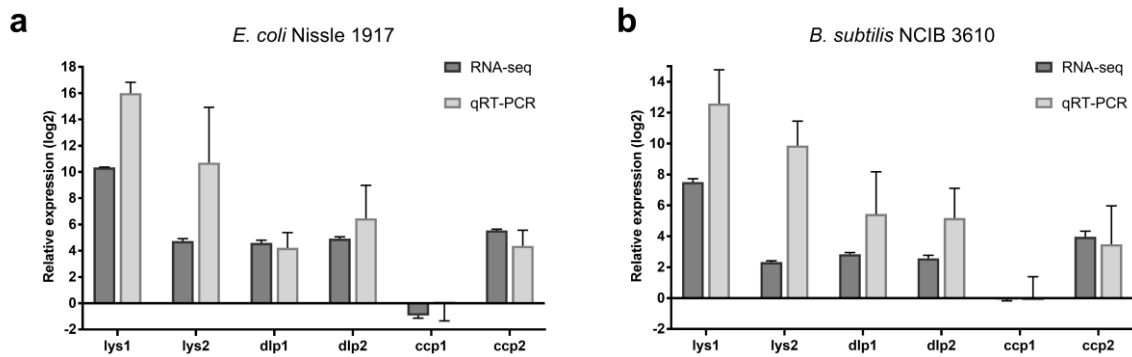


Figure S6 | Independent confirmation of RNA-seq-based differential gene expression data. The RNA-seq-based differential expression of six genes was validated by qRT-PCR. For this experiment, *C. cinerea* was challenged with either *E. coli* Nissle 1917 (a) or *B. subtilis* NCIB 3610 (b) on glass beads for 12 hours. Thereafter, total RNA was extracted and cDNA was synthesized to perform qRT-PCR with gene specific primers listed in Table S2. The Y-axis shows the gene expression relative to unchallenged *C. cinerea* determined by RNA-seq and qRT-PCR. Error bars represent standard deviation of three biological replicates.

Chapter 6

Table S1. JGI protein IDs of proteins used in this study

Name	JGI Protein ID
LYS1	432813
LYS2	112978
LYS3	377192
LYS4	377203
LYS5	482075
LYS6	442447
DLP1	464767
DLP2	481478
DLP3	377219
DLP4	448242
DLP5	541708
DLP6	433115
DLP7	378260
DLP8	501838
DLP9	481141
DLP10	488448
Copsin (CPP1)	559348
CPP2	559260
CPP3	559349
CPP4	437532
CPP5	400893
CPP6	559350
CPP7	559264
Tubulin	393528

Chapter 6

Table S2. Primers used in this study.

Primer name	Sequence 5' - 3'
pF_LYS1	CGGTATGAATTGCCATTACGATGCCTGCTC
pR_LYS1	CGGTATCGGCCGCCTAGCAAGGAGGATGGCGATG
pF_LYS2	CGGTATGAATTGCCATCAATGACCCCTGC
pR_LYS2	CGTCTAGCGGCCGCTTAGACAGGCTTAGGGCAGTTG
pF_LYS3	CGGTATGAATTGCCATCAACGATCCCTGCT
pR_LYS3	CGGTATGCGGCCGCCTAGCACCTGGGAGGATGCC
pR_LYS2His	GTCTAGCGGCCGCTCAATGATGATGATGGACAGGCTTAGGGCAGTTG
pF_LYS2HisΔN	CGGTATGAATTGTAACCTCAAACCGTCGAAC
pF_42HIS(D131A)	GCACCAGCCCCAATCGGTCTCCCCAC
pR_42HIS(D131A)	CGATTGGGGCTGGTGCBBBBBATTGAC
pF_CPP2	CCGGAATTCATGAAATTACACATCTGTTCG
pR_CPP2	ACCGCTCGACTAACAAACAGGGCACGGATT
qRT- LYS1_F	CTGGGAACACCGCTACAGGACTATG
qRT- LYS1_R	GACGTCTTGTAGGGCGAAGCG
qRT- LYS2_F	GAAACACGCTATCAGGCCTTGCC
qRT- LYS2_R	TTGGGTCTGGTGCBBBBBATTGA
qRT- DLP1_F	TGTATCACCACCTCCGACTGCTCAG
qRT- DLP1_R	CAGGGCAAAGGCCGGTCAAACATA
qRT- DLP2_F	CTGCATCACCACTCTGACTGCTCA
qRT- DLP2_R	GCAGAGGCCAGTCAAGACATAGCTT
qRT- CCP1_F	TCAGGCCACCAACCGTCCCCGGAT
qRT- CCP1_R	AAGCCGAGCCAGGAGAAAGTCAGT
qRT- CCP2_F	GATGCTACGCTGAATGCCTCGAGAA
qRT- CCP2_R	CGGGCAAGACGCGACTCAAACCG
qRT- Tub_F	CCGATACCGTCGTTGAGCCTTAC
qRT- Tub_R	ATGACGATGGAGACGAGGTGGTTG

Chapter 6

Table S3: List of the bacteria-induced gene set with $\log_2 \text{FC} \geq 4$ and $\text{FDR} < 0.05$. HP is hypothetical protein and the number corresponds to the number in Figure 3b. Full version of this table can be found online.

JGI ID Protein	$\log_2 \text{FC}$ <i>E. coli</i>	FDR <i>E. coli</i>	$\log_2 \text{FC}$ <i>B. subtilis</i>	FDR <i>B. subtilis</i>	Annotation based on CD search (NCBI)	SignalP	TM	Length (aa)
394772	10.7	0	8.137	4.569E-293	terpene cyclase/synthase	No	0	326
420898	10.06	0	7.804	0	P450	No	1	527
		6.176E-						
432813	9.965	265	6.715	1.599E-143	GH24 lysozyme LYS1	Yes	0	272
502564	9.455	0	6.96	0	ascorbate, laccase adenylate-forming	Yes	0	534
361483	9.032	0	6.247	0	reductase	No	5	1050
488706	8.547	0	6.416	3.794E-197	ascorbate, laccase	No	1	526
371150	8.096	0	4.437	6.63E-255	aminotransferase	No	0	444
471478	8.018	0	5.434	4.181E-164	fatty acid desaturase	No	4	397
372220	7.991	0	5.659	2.554E-249	P450	No	0	474
		3.667E-			short chain dehydrogenase			
441645	7.658	258	5.498	3.504E-118	reductase (SDR)	No	0	344
559271	7.625	0	5.499	1.411E-198	MFS transporter	Yes	0	162
422976	7.457	0	4.513	1.667E-110	fatty acid desaturase	No	0	434
426342	7.379	0	6.498	9.973E-301	HP 2	Yes	0	213
		4.148E-			GPI-anchored fascilin			
500405	7.128	41	4.834	1.419E-28	domain-containing	Yes	0	382
201523	6.998	0	5.13	9.405E-165	p450	No	1	516
		1.462E-						
405832	6.927	296	4.134	3.019E-67	HP 4	Yes	0	114
		5.259E-						
443013	6.884	97	3.35	4.02E-20	HP 5	Yes	0	339
		3.825E-						
442447	6.842	179	5.065	5.754E-125	GH24 lysozyme LYS6	Yes	0	487
243699	6.721	0	2.834	6.185E-82	MFS transporter	No	12	496
		5.489E-						
559272	6.662	67	3.303	9.019E-42	HP 26	Yes	0	117
490004	6.619	0	4.436	8.677E-119	carboxylesterase/hydrolase	No	0	327
		6.433E-						
41230	6.51	226	4.822	2.894E-99	HP 6	Yes	0	185
					adenylate-forming			
468140	6.448	0	4.332	2.851E-181	reductase	No	5	1091
		8.103E-						
559274	6.393	83	4.447	3.519E-58	HP 14-1	No	7	350
		1.769E-			ergot alkaloid			
374282	6.328	235	2.842	3.964E-49	synthase/atypical SDR	No	0	187
		5.59E-						
499485	6.292	107	4.277	1.938E-58	HP 8	No	6	273
442000	6.275	0	4.207	6.636E-132	HP 7	Yes	0	61
		4.053E-						
442161	6.274	35	2.466	1.659E-07	HP 13	No	0	316
		1.217E-						
442931	6.241	109	2.938	8.767E-26	HP 9	Yes	0	172
280527	6.188	0	4.191	1.157E-109	DUF-containing protein	No	0	194
		4.951E-						
462661	6.145	175	3.821	4.057E-66	HP 10	Yes	0	124

Chapter 6

442449	6.087	176 6.027E-	4.214	2.324E-107	HP 11-1	Yes	0	163
151024	6.019	213	5.308	6.036E-211	HP 12	Yes	0	194
438642	6	0	3.507	2.26E-127	acetyl-CoA synthase	No	0	146
462454	5.98	0 9.122E-	1.993	7.139E-15	HP 15	No	0	551
543443	5.935	107 3.719E-	4.112	3.249E-46	NmrA-like SDR	No	0	358
9990	5.86	219 7.892E-	4.347	8.329E-105	PAP2 haloperoxidase	Yes	0	412
382592	5.703	217	2.862	1.206E-31	HP 16	Yes	0	51
254167	5.678	0	3.581	1.178E-91	N-acetyltransferase	No	0	224
361411	5.634	0 1.636E-	3.271	5.429E-81	ferredoxin reductase	No	6	663
484084	5.613	62 4.049E-	2.243	2.577E-08	HP 18	Yes	0	145
496557	5.611	211 7.145E-	3.979	2.201E-74	HP 17	Yes	0	125
441612	5.591	154 3.766E-	3.483	2.216E-62	HP 19	No	1	361
378260	5.504	52 6.528E-	3.847	5.966E-33	defensin-like protein DLP7	Yes	0	104
442015	5.5	178	3.812	2.522E-99	HP 21	No	0	183
559260	5.492	0 3.158E-	3.838	8.863E-92	Copsin homolog	Yes	0	189
559279	5.487	186 1.71E-	1.685	1.223E-12	HP 33	No	1	203
467052	5.303	103 9.233E-	3.81	3.071E-55	HP 11-2	Yes	0	165
363038	5.302	137 2.266E-	3.276	1.011E-49	P450	No	1	555
490975	5.267	71 5.378E-	1.524	0.0002196	SnoaL-like enzyme	Yes	0	166
559282	5.173	112 5.857E-	3.18	4.791E-41	MFS transporter	No	0	615
380312	5.122	234 6.914E-	3.066	7.803E-66	glutathione S-transferase	No	0	320
208308	5.035	230	3.735	1.852E-145	ascorbate, laccase	Yes	0	519
449056	4.994	0 1.42E-	2.776	1.069E-80	peroxiredoxin	No	0	171
421349	4.991	194 7.915E-	3.96	4.74E-131	HP 22	Yes	0	92
482270	4.973	50 2.518E-	2.909	2.763E-16	HP 24	No	6	365
39973	4.967	214 1.965E-	2.763	1.893E-53	GCC2_GCC3 domain containing	Yes	0	318
438924	4.958	62 1.417E-	2.646	8.555E-14	HP 23	Yes	0	97
559285	4.954	252 2.512E-	2.403	5.26E-48	HP 1	No	12	441
406666	4.916	43 9.659E-	2.396	5.119E-10	acetyl-CoA synthetase	No	0	611
559296	4.901	38 1.364E-	3.64	5.755E-27	HP 20	No	0	162
436043	4.864	103	2.835	6.905E-37	HP 25	No	5	211

Chapter 6

		2.948E-							
481478	4.855	178	2.469	8.054E-34	defensin-like protein DLP2	Yes	0	116	
		1.945E-							
443904	4.849	45	2.715	1.265E-13	HP 27 short chain dehydrogenase	Yes	0	215	
		6.551E-			reductase (SDR)	No	0	259	
61180	4.83	302	2.507	3.207E-68		No	7	376	
		3.029E-				No	0	153	
448067	4.808	133	1.925	2.563E-21	HP 14-2	No	0	113	
		2.304E-				No	0	354	
491480	4.772	142	2.771	3.427E-30	HP 30	No	7	300	
		4.198E-				No	7	364	
377219	4.753	93	2.6	1.386E-24	defensin-like protein DLP3	Yes	0	252	
		2.211E-				No	0	202	
468158	4.744	241	3.775	2.3E-85	N-acetyltransferase	No	0	144	
		7.065E-				No	0	434	
432263	4.739	61	2.411	2.841E-12	RTA1-like	No	7	273	
		7.054E-				No	7	68	
559290	4.72	26	2.8	6.325E-12	HP 28	No	7	322	
		4.399E-				No	7	184	
440521	4.715	107	2.474	4.424E-23	chitin de-acetylase	Yes	0	116	
						No	0	259	
559286	4.706	0	2.846	2.345E-121	HP 34	No	0	202	
		1.878E-				No	0	364	
496393	4.687	243	1.539	1.933E-22	HP 29	No	0	144	
		4.905E-				No	0	472	
112978	4.655	117	2.206	2.106E-23	GH24 lysozyme LYS2	Yes	0	279	
		1.162E-				No	0	322	
559287	4.651	260	2.225	3.899E-56	dioxygenase / cupin glutathione-dependent formaldehyde-activating	Yes	0	136	
		5.395E-			(GFA) enzyme	No	0	259	
273741	4.621	232	3.811	1.356E-74	HP 3	No	4	179	
		1.053E-				No	1	68	
559292	4.607	36	1.934	3.471E-07	WSC-domain containing	Yes	0	235	
		5.515E-			protein	No	0	322	
489010	4.578	27	3.292	9.038E-19	2OG-Fe oxygenase	Yes	0	144	
		4.026E-				No	0	202	
443942	4.553	287	2.239	2.702E-36	defensin-like protein DLP1	Yes	0	364	
		5.612E-				No	0	259	
559284	4.522	188	2.17	1.74E-43	HP 31	No	0	184	
						No	1	68	
466335	4.501	0	2.221	1.843E-56	HP 32	No	0	322	
		2.458E-				No	0	273	
475201	4.49	121	2.743	2.233E-38	Ytp1-domain containing	Yes	0	116	
		3.978E-			acetolactate synthase	No	0	259	
464767	4.48	73	2.584	3.328E-21	HP 43	Yes	0	144	
		2.056E-			adenine	No	0	364	
431038	4.398	11	3.096	1.877E-11	phosphoribosyltransferase	Yes	0	202	
		5.905E-				No	0	322	
355044	4.364	200	1.484	1.769E-24	HP 36	No	0	184	
		1.708E-			FAD-containing	No	0	130	
445367	4.334	109	2.2	5.489E-20	dehydrogenase	Yes	5	608	
		2.135E-				No	11	614	
559300	4.317	20	1.743	0.0003217	Ytp1-domain containing	No	0	472	
		4.38E-			acetolactate synthase	No	0	116	
365455	4.268	144	1.838	4.404E-18	MFS transporter	No	13	259	
		1.882E-				No	7	364	
421528	4.259	145	2.615	1.746E-84	RTA1-like	Yes	0	184	
		9.836E-			defensin-like protein DLP3	No	0	202	
377150	4.226	97	2.727	2.425E-25	HP 28	No	0	322	

Chapter 6

467082	4.224	5.115E-08	1.145		HP 44		No	7	384
437942	4.218	5.076E-164	2.228	2.578E-32	HP 38		No	0	359
445129	4.209	3.56E-200	1.517	2.486E-17	HP 39		No	0	482
403889	4.202	5.883E-245	1.668	3.07E-33	aldolase		No	0	242
198404	4.201	7.877E-194	2.946	6.26E-90	N-acetyltransferase		No	0	336
279184	4.192	5.597E-36	1.638	0.00006823	HP 37		No	0	83
442673	4.179	1.855E-226	1.944	3.477E-42	hemerythrin-like		No	0	174
498956	4.158	1.347E-119	2.612	2.126E-35	methyltransferase		No	0	585
490529	4.124	1.131E-41	3.26	1.85E-27	HP 41		No	0	151
559298	4.115	1.777E-126	1.65	1.44E-15	HP 40		No	12	461
369380	4.079	1.024E-238	2.903	6.387E-17	ergot alkaloid biosynthetic protein A		No	0	302
376388	4.063	2.998E-236	1.949	2.554E-38	FMN-dependent dehydrogenase		No	0	436
440168	4.062	4.241E-223	1.962	2.958E-31	FAD-dependent dehydrogenase		No	0	449
479963	4.052	4.883E-25	2.286	8.595E-09	HP 45		No	1	217
546528	4.019	8.518E-257	2.43	2.949E-59	glutathione S-transferase		No	0	216
372943	4.009	1.618E-216	2.059	8.209E-67	HP 42		No	3	525
422563	3.543	103	4.241	3.382E-99	LysM domain containing		Yes	0	132

Chapter 6

The following two supplementary excel files are available in the electronic version of this thesis:

Supplementary Information SI2 contains:

Sheet 1: Absolute expression values for 14242 genes of *C. cinerea* together with their Pfam domains and GO terms.

Sheet 2: List of *E. coli* and *B. subtilis* induced genes with \log_2 fold change ≥ 2 AND FRD < 0.05 .

Sheet 3 : List of *E. coli* and *B. subtilis* induced genes with \log_2 fold change ≥ 4 AND FRD < 0.05 together with their Pfam domains and GO terms.

Supplementary Information SI3 contains:

Sheet 1: Peptide list of *E. coli* induced secreted proteins.

Sheet 2: Peptide list of *E. coli* suppressed secreted proteins.

Sheet 3: Peptide list of constitutive produced secreted proteins.

Chapter 6

Supplementary references

- Marchler-Bauer, A., Derbyshire, M.K., Gonzales, N.R., Lu, S., Chitsaz, F., Geer, L.Y., et al.** (2015). CDD: NCBI's conserved domain database. *Nucleic Acids Res* 43, D222-226.
- Petersen, T.N., Brunak, S., von Heijne, G., and Nielsen, H.** (2011). SignalP 4.0: discriminating signal peptides from transmembrane regions. *Nat Methods* 8, 785-786.

Chapter 7

Concluding remarks and future perspectives

Chapter 7

This Ph.D. thesis aimed at the characterization of novel types of inducible defense effectors of basidiomycetous fungi in order to expand our understanding of the antagonistic interactions of these organisms with animal predators and bacterial competitors. In each section below, I first summarize the main findings of each chapter and then formulate interesting questions that arise based on these findings.

Assessing *C. cinerea* anti-nematode defense response using microfluidics-based RNA sequencing

Previous studies have shown that production of defense proteins can be induced in *C. cinerea* upon predation by foraging nematodes such as *A. avenae* [1]. The induction of defense genes was found to be mostly restricted to the regions of the mycelia where the nematodes had foraged (Schmieder et al. in revision). Thus, conventional agar plate-based methods, where the mycelia are spread out over the plate, would be unfeasible to precisely extract the induced part of the mycelia to assess the defensome of fungi against nematodes. This limitation is addressed in this thesis by using tailor-made microfluidic devices, where the fungal-nematode interaction occurs within a confined area, making it possible to extract mostly induced mycelia from the interaction zone for subsequent RNA-seq-based gene expression analysis. Transcriptome analysis of the *C. cinerea* defensome against *A. avenae* performed in the microfluidic device revealed that a substantially high number of genes were differentially expressed compared to the nematode-challenge assays using agar plates. One of the induced genes (JGI ID: P450139) of *C. cinerea* was characterized further. We showed that P450139 has structural similarity to bacterial β-pore-forming toxins, and demonstrated its strong nematotoxicity against several bacterivorous nematodes and its lack of toxicity against *A. aegypti* larvae. We also found that a considerable number of genes were induced in response to both nematodes and bacteria. Hence, we profiled the bacteria present in the microbiome of the fungivorous nematode *A. avenae*.

The findings of this thesis contribute to previous knowledge on fungal defense against predators such as nematodes. However, these findings also lead to several interesting questions, as explained in the following paragraphs.

The molecular basis of the fungal defense response is still unclear: it is not clear which factors induce the defense response of fungi against nematodes, and which receptors are involved in the recognition and further propagation of the signal. Until very recently, gene knockout procedures in *C. cinerea* were difficult involving the transformation of protoplasts generated from the vegetative mycelium of a ku70-knockout strain [2]. However, very recently, CRISPR/Cas9-mediated knockout of *C. cinerea* genes was achieved [3]. Thus, it is now possible to conduct knockout experiments on candidate receptor genes in order to assess their involvement in the recognition of nematodes and subsequent induction of inducible defense response. In our experiments, we assessed the defense response of only one fungus against one species of fungivorous

nematode. However, for a more comprehensive description of fungal response towards their antagonists, the study should be extended to the analysis of gene expression of another fungal species in response to *A. avenae*. In preliminary experiments, we showed that an ascomycetous fungus *Sordaria macrospora* behaves in a similar way to *C. cinerea* in the microfluidic device. Thus, the similar nematode-challenge experiment can be performed using this fungus. The findings would help us to understand the evolution and conservation of the fungal defense response across different fungal phyla against the same predators. Further, challenging *C. cinerea* with other fungivorous nematodes such as *B. okinawaensis* [4] could provide additional insight into the defense response of this particular fungus species against different but related predators.

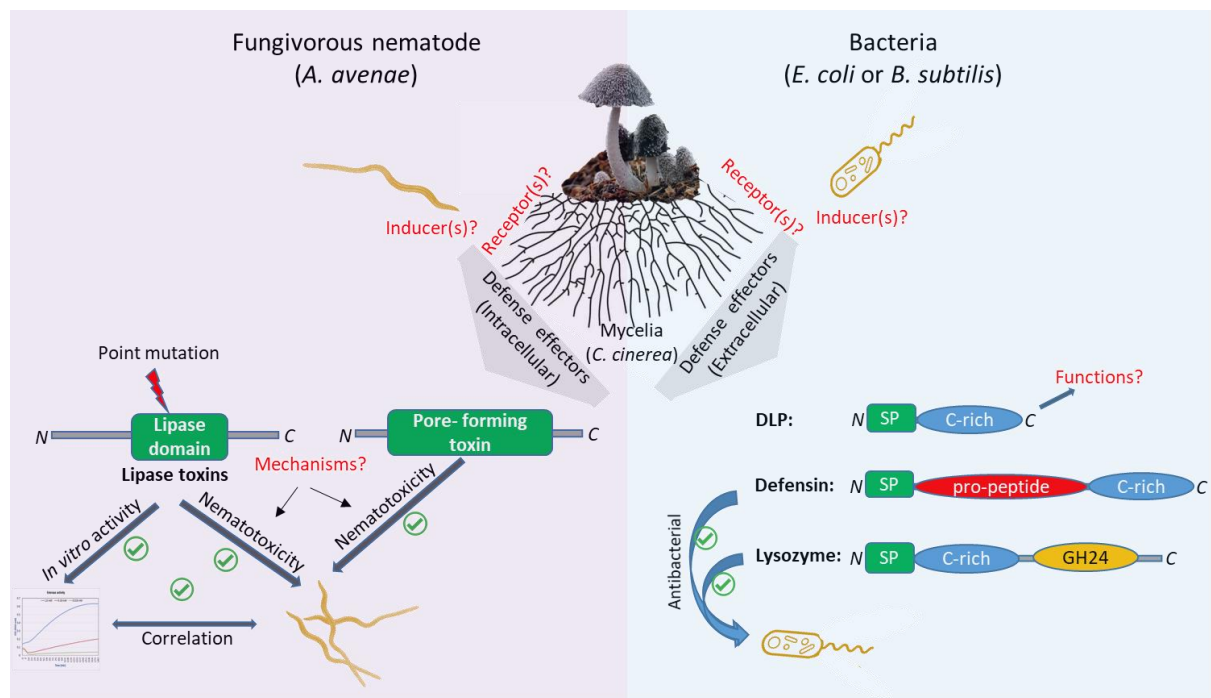


Figure 1. An overview of the *C. cinerea* effectors studied in this thesis

(Left) *C. cinerea* vegetative mycelium was challenged with the fungivorous nematode *A. avenae* in tailor-made microfluidic devices. Three of the most highly induced genes that belong to two different toxin classes, i.e., lipase toxins and pore-forming toxin, were identified and characterized. Both of the lipase toxins (CLT1 and CLT2) and the pore-forming toxin (P450139) showed toxicity against nematodes. The molecular basis of the actions of toxins and fungal self-protection against these intracellular toxins remain unknown. **(Right)** Likewise, the defense response of *C. cinerea* mycelium was assessed in the presence of either *E. coli* or *B. subtilis*. In the set of induced and secreted genes, we identified phage-like lysozymes and an inducible paralog (CCP2) of the previously characterized and constitutively expressed antibacterial defensin copsin. The antibacterial activity of both CCP2 and the lysozymes was confirmed against gram-positive bacteria. Fungal defense-inducing signals for both nematodes and bacteria and the binding of these inducers by fungi still need to be studied in future.

Chapter 7

The inducible defense response of *C. cinerea* against more distant predators such as insects should also be studied, as this could provide some insight into the defense response against more distantly related fungal predators. However, previous fungal insect challenge experiments were performed in agar-plate based assays [5], which have their limitations (as mentioned earlier), and the microfluidics platform that we used in this study is designed explicitly for nematodes. Thus, new microfluidic devices need to be designed to perform fungi-insect challenge experiments. Given the flexibility in the design and manufacture of microfluidic devices, making such a device should be feasible.

The identified putative-pore forming toxin P450139 showed potent toxicity against four of the five tested nematode species. It would be interesting to understand what makes these nematode species susceptible while other nematode species and *A. aegypti* show resistance to the toxin. Furthermore, the receptors and mechanisms of the toxin need to be elucidated. In *in vitro* hemolysis assays, the lytic activity of the P450139 protein could not be demonstrated despite its structural similarity to bacterial hemolysins. This could mean that the toxin is activated via posttranslational modifications such as proteolytic cleavage, or that it may require host-specific cofactors for its activation, as observed for other fungal and bacterial toxins [6, 7]. Likewise, information about the mechanism of activation and the following action of the toxin would help clarify the self-protection mechanism of the producer fungus against this intracellularly produced effector protein.

16S rRNA analysis revealed that *A. avenae* contains several different bacterial species as a part of its microbiome. We identified several antibacterial peptides, such as CPP2 (copsin paralog peptide 2), that were strongly induced in *C. cinerea* upon nematode challenge; thus, nematode predation of a fungus is likely a tripartite interaction. It would be interesting to investigate whether some of the induced genes show antibacterial activity against identified bacterial species in the *A. avenae* microbiome. Furthermore, since the whole worm was used as starting material for microbiome analysis of the worm, it would be highly interesting to study the location of these bacterial species within the nematode.

Lipases as a novel class of fungal defense proteins against nematodes

The RNA-seq-based defensome of *C. cinerea* was further analyzed to identify novel fungal defense effector proteins. As a result, two highly induced genes with similar expression dynamics to previously known nematotoxic proteins were identified. Homology search engines showed that these two genes possess a lipase domain. The lipase domain-containing proteins were named CLT1 and CLT2, and they showed strong nematotoxicity against several tested nematode species. Further, *in vitro* lipase activity assays with synthetic para-nitrophenyl substrates demonstrated the lipase activates of these lipases. In addition, putative catalytic site mutant constructs of both CLT1 and CLT2 showed that the observed nematotoxicity is dependent on

Chapter 7

their lipase activities. The activity of the lipases was demonstrated using synthetic substrates. However, to gain more insight into the mechanism of action and specificity of these lipase toxins, it is important to identify the natural lipid substrates of these toxins.

The lipase toxins identified here (CLT1 and CLT2) are intracellularly produced. Thus, the producing fungus probably has a mechanism in place to protect itself against these toxins. There are three ways toxin-producing organisms protect themselves against their own toxins: (a) they coproduce antitoxins against the toxins within their cells [8, 9], (b) they synthesize and release the toxin as a prototoxin that is activated only after it leaves the producer organism either by secondary modifications such as proteolytic cleavage [6] or by host-specific activating cofactors [10], and (c) the target molecule of a toxin is only present in host organisms [11]. These lipase toxins were heterologously expressed in a fully soluble manner in *E. coli*, which means that they were not toxic against *E. coli*. Thus, it is unlikely that the toxins are co-produced with an antitoxin. Host organism-specific activation was also not supported by our experiments, since the heterologously produced lipase toxins were active against synthetic substrates and addition of the host cell lysate did not change their activity. This means that the toxins have specific target molecules in nematodes that are either absent or inaccessible in fungus. This could eventually be demonstrated by treating fungal and nematode lipid extracts with the lipase toxins and conducting pre- and post-treatment lipidome analysis to narrow down the potential target lipids of these toxins. We are currently investigating the substrate specificity of the lipase toxins in collaboration with the lab of Prof. Laura Nyström (ETHZ, Department of Food Science).

Ageritin as a novel type of ribotoxin

We identified the gene coding for ageritin from the recently published genome of the edible mushroom *A. aegerita* [12]. Ageritin is the first ribotoxin discovered in the phylum Basidiomycota, and its amino acid sequence differs from the previously identified Ascomycota ribotoxins. Furthermore, ageritin does not carry any known signal sequence, making it the first discovered cytoplasmic ribotoxin so far. Ageritin cDNA was cloned and heterologously expressed in *E. coli*. Toxicity assays toward *A. aegypti* larvae and several bacterivorous nematode species showed that it had exclusive toxicity against the mosquito larvae. For the rRNA cleavage assay, ageritin was purified using Ni-NTA beads. Ageritin showed ribonucleolytic cleavage activity specific to ribotoxins, which resulted in the release of the α -fragment from the 28S rRNA subunit of ribosomes. By mutating several conserved catalytic residues, we confirmed that ageritin toxicity was dependent on its rRNA cleavage activity.

Ribotoxins are known to act on the well-conserved SRL loop located in the large subunit of all known ribosomes [13]. The alignment of the 23S/28S rRNA of the species across different phyla revealed a complete

Chapter 7

sequence conservation at the GAGA-tetraloop while sequences at the SRL region and beyond showed sequence variations (Figure 2). Thus, producer fungi need to protect their ribosomes against their own ribotoxins. Since all the ribosomes discovered before ageritin were extracellular, it was assumed that the toxins were excreted via secretory pathways in order for the producer fungi to avoid self-toxicity [14]. However, protection against intracellularly produced ageritin may involve a different strategy, since it does not possess any known signal sequence. Currently, we are collaborating with the lab of Prof. Ute Krengel (University of Oslo, Norway) to elucidate the crystal structure of ageritin. The structure would help us address the specificity of ageritin, for instance, by docking it onto the solved structures of ribosomes [15]. So far, there are no known cell surface receptors for ribotoxins that facilitate their recognition and entry into target cells. It is believed that they bind to target membranes with the help of the high number of basic residues and subsequently diffuse through the cell membrane due to their small size [16].

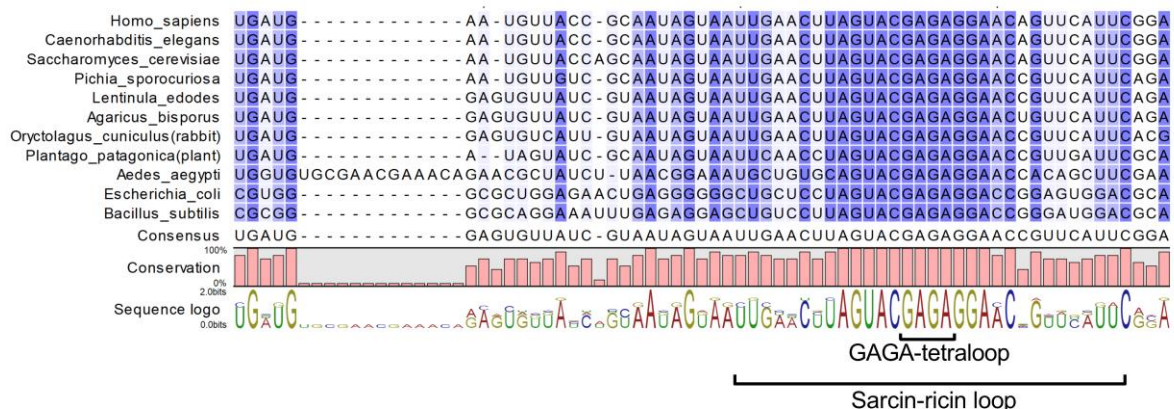


Figure 2. Alignment of 23S/28S rRNA nucleotide sequences.

23S/28S rRNA nucleotide sequences of several species across different kingdoms were aligned. The GAGA-tetraloop, a region where RIPs and ribotoxins act on, and the SRL region are labeled. Alignment of the complete sequences is available in the electronic version of this thesis. The sequences used in this alignment were retrieved from SILVA ribosomal RNA gene database [17].

Ageritin is a very basic and small protein. It remains unclear whether ageritin uses the same strategy to reach its target ribosomes as other ribotoxins. A paralog of ageritin with a significantly lower pI than ageritin did not show toxicity against *A. aegypti* larvae; thus, the basic pI of ageritin may indeed play a role in its toxicity. Whether the paralog possesses *in vitro* RNase activity like ageritin remains to be addressed in the future. An overview of the findings and the remaining questions within the scope of the ageritin project are summarized in Figure 3.

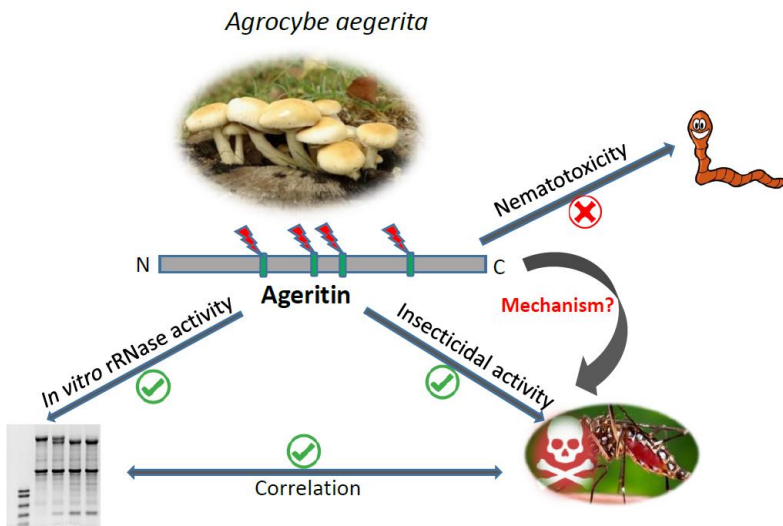


Figure 3. An overview of the *in vivo* and *in vitro* activities of ageritin

The ageritin-encoding gene was amplified from the primordia of *A. aegerita* and cloned into *E. coli* for expression. Ageritin showed strong toxicity against *A. aegypti* larvae, but it did not show activity against nematodes. Ageritin was purified over Ni-NTA beads, and its 28S rRNA cleavage activity was confirmed using ribosomes from rabbit reticulocyte lysate. Six conserved residues of ageritin were individually mutated, and the dependency of its insecticidal activity on its *in vitro* rRNase activity was confirmed. The molecular basis of the mechanism by which ageritin reaches its target and its subsequent action on ribosomes are currently under investigation. Furthermore, the self-defense strategy of the fungus still needs to be addressed in future experiments.

***A. gossypii* as a fungal expression system for potential fungal defense proteins**

Until now, the toxicity of putative fungal defense proteins had been tested by heterologously expressing them in *E. coli* and feeding the bacteria to bacterivorous nematodes such as *C. elegans*. In this study, we developed an alternative heterologous expression method using a filamentous fungus, *A. gossypii*, as an expression host. With the help of this novel expression system, the toxicity of previously characterized nematotoxic proteins was confirmed against two fungivorous nematodes, *A. avenae* and *B. okinawaensis*. The system offers an easy approach to test the toxicity of putative fungal defense proteins in a more ecologically relevant context, i.e., expression in fungi rather than in bacteria and toxicity testing of putative defense proteins against fungivorous nematodes rather than bacterivorous nematodes. The next step would be to clone and express the putative pore-forming toxin (P450139) and lipase toxins (CLT1 and CLT2) in this system and test their toxicity against real fungal foragers such as *A. avenae* and *B. okinawaensis*.

Antibacterial response of *C. cinerea* against gram-positive and gram-negative bacteria

In the course of this thesis, the genome-wide transcriptional response of *C. cinerea* to the bacteria *E. coli* and *B. subtilis* was assessed using the RNA-sequencing approach. The fungi responded by inducing a similar set

Chapter 7

of genes against both bacteria, although the response was much stronger in the case of *E. coli*. Within the set of highly induced genes, two putative antibacterial peptides were cloned and purified for further characterization. These two antibacterial proteins, CPP2 (copsin paralog peptide 2) and LYS1 (lysozyme 1), belong to the $\alpha\beta$ -defensin and GH24-type lysozyme families, respectively, and they show antibacterial activity against gram-positive bacteria. Another group of induced genes called defensin-like proteins (DLPs) was found in the highly induced set of genes. However, the functions of DLPs need to be elucidated in future experiments. Similar to the fungal-nematode interactions, the molecular basis and the nature of bacterial signal elicitors and fungal signal recognition receptors that are involved in bacteria-fungi interactions are largely unknown.

As a general conclusion, this thesis contributes to the better understanding of inducible fungal defense strategies against their predators and bacterial competitors. The discovered nematotoxic and insecticidal fungal toxin proteins may open possible avenues for biological strategies to protect crops and animals against parasitic nematodes and insects.

References

1. Plaza DF, Schmieder SS, Lipzen A, Lindquist E, Künzler M: **Identification of a Novel Nematotoxic Protein by Challenging the Model Mushroom *Coprinopsis cinerea* with a Fungivorous Nematode.** *Genes/Genomes/Genetics* 2016, **6**:87-98.
2. Nakazawa T, Ando Y, Kitaaki K, Nakahori K, Kamada T: **Efficient gene targeting in Delta Cc.ku70 or Delta Cc.lig4 mutants of the agaricomycete *Coprinopsis cinerea*.** *Fungal Genet Biol* 2011, **48**(10):939-946.
3. Sugano SS, Suzuki H, Shimokita E, Chiba H, Noji S, Osakabe Y, Osakabe K: **Genome editing in the mushroom-forming basidiomycete *Coprinopsis cinerea*, optimized by a high-throughput transformation system.** *Sci Rep-Uk* 2017, **7**.
4. Shinya R, Hasegawa K, Chen A, Kanzaki N, Sternberg PW: **Evidence of Hermaphroditism and Sex Ratio Distortion in the Fungal Feeding Nematode *Bursaphelenchus okinawaensis*.** *G3 (Bethesda, Md)* 2014, **4**:1907-1917.
5. Fohgrub U, Kempken F: **Molecular Analysis of Fungal Gene Expression upon Interkingdom Competition with Insects.** In: *Fungal Secondary Metabolism: Methods and Protocols*. Edited by Keller NP, Turner G. Totowa, NJ: Humana Press; 2012: 279-286.
6. Gordon VM, Klimpel KR, Arora N, Henderson MA, Leppla SH: **Proteolytic activation of bacterial toxins by eukaryotic cells is performed by furin and by additional cellular proteases.** *Infect Immun* 1995, **63**(1):82-87.
7. Nagamune K, Yamamoto K, Naka A, Matsuyama J, Miwatani T, Honda T: **In vitro proteolytic processing and activation of the recombinant precursor of El Tor cytolsin/hemolysin (Pro-HlyA) of *Vibrio cholerae* by soluble hemagglutinin/protease of V-cholerae, trypsin, and other proteases.** *Infect Immun* 1996, **64**(11):4655-4658.
8. Muñoz-Gómez AJ, Lemonnier M, Santos-Sierra S, Berzal-Herranz A, Díaz-Orejas R: **RNase/anti-RNase activities of the bacterial parD toxin-antitoxin system.** *Journal of Bacteriology* 2005, **187**(9):3151-3157.
9. Campos PC, de Melo LA, Dias GLF, Fortes-Dias CL: **Endogenous phospholipase A(2) inhibitors in snakes: a brief overview.** *J Venom Anim Toxins* 2016, **22**.
10. Anderson DM, Feix JB, Frank DW: **Cross Kingdom Activators of Five Classes of Bacterial Effectors.** *Plos Pathogens* 2015, **11**(7).
11. Butschi A, Titz A, Walti MA, Olieric V, Paschinger K, Nobauer K, Guo XQ, Seeberger PH, Wilson IBH, Aeby M et al: ***Caenorhabditis elegans* N-glycan Core beta-galactoside Confers Sensitivity towards Nematotoxic Fungal Galectin CGL2.** *Plos Pathogens* 2010, **6**(1).
12. Gupta DK, Rühl M, Mishra B, Kleofas V, Hofrichter M, Herzog R, Pecyna MJ, Sharma R, Kellner H, Hennicke F et al: **The genome sequence of the commercially cultivated mushroom *Agrocybe aegerita* reveals a conserved repertoire of fruiting-related genes and a versatile suite of biopolymer-degrading enzymes.** *Bmc Genomics* 2018, **19**.
13. Wool IG: **Structure and mechanism of action of the cytotoxic ribonuclease α-sarcin.** *Ribonucleases: Structures and Functions* 1997:131-162.
14. Lamy B, Davies J: **Isolation and Nucleotide-Sequence of the Aspergillus-Restrictus Gene Coding for the Ribonucleolytic Toxin Restrictocin and Its Expression in Aspergillus-Nidulans - the Leader Sequence Protects Producing Strains from Suicide.** *Nucleic Acids Research* 1991, **19**(5):1001-1006.
15. Ben-Shem A, Jenner L, Yusupova G, Yusupov M: **Crystal structure of the eukaryotic ribosome.** *Science* 2010, **330**(6008):1203-1209.
16. Álvarez-García E, Martínez-del-Pozo A, Gavilanes JG: **Role of the basic character of alpha-sarcin's NH₂-terminal beta-hairpin in ribosome recognition and phospholipid interaction.** *Archives of Biochemistry and Biophysics* 2009, **481**(1):37-44.
17. Quast C, Pruesse E, Yilmaz P, Gerken J, Schweer T, Yarza P, Peplies J, Glockner FO: **The SILVA ribosomal RNA gene database project: improved data processing and web-based tools.** *Nucleic Acids Research* 2013, **41**(D1):D590-D596.

Curriculum Vitae

Annageldi Tayyrov

Date of Birth 07.02.1991
Place of Birth Garabekewül, Türkmenistan

Education:

- 08/2014 – present PhD in Microbiology and Immunology, Institute of Microbiology, ETH Zürich, Zürich, Switzerland
- 08/2012 – 06/2014 MSc in Bioscience, Computational Bioscience Research Center, King Abdullah University of Science and Technology, Jeddah, Saudi Arabia
- 10/2008 – 06/2012 BSc in Biology, Focus: Molecular biology and Genetics.
Double Major: BSc in Genetics and Bioengineering
Istanbul/Fatih University, Istanbul, Turkey.

Publications:

- 2018 **Tayyrov A***, Schmieder SS*, Bleuler-Martinez S, Plaza DF, Künzler M: Toxicity of potential fungal defense proteins towards the fungivorous nematodes *A. avenae* and *B. okinawaensis*. *AEM*, in press. *Equally contributed.
- 2018 Kombrink A*, **Tayyrov A***, Essig A*, Stöckli M, Micheller S, *et al*: Induction of antibacterial proteins and peptides in the coprophilous mushroom *Coprinopsis cinerea* in response to bacteria. *ISME J*, in press. *Equally contributed.
- 2015 Woo, Y. H., ... **Tayyrov, A.**, ... Pain, A. (2015). Chromerid genomes reveal the evolutionary path from photosynthetic algae to obligate intracellular parasites. *eLife*, 4, e06974.
- 2012 Şakalar E., Abasiyanik M.F., Bektik E., **Tayyrov A.** Effect of heat processing on DNA quantification of meat species. *J. Food Science*, 2012. 77(9): p. N40-4.